Technische Universität München

Lehrstuhl für Mikrobiologie

Characterization of dehydrogenase mutants in continuous cultures of *Clostridium acetobutylicum*

Zheng Xu

Vollständiger Abdruck der von der Fakultät Wissenschaftszentrum Weihenstephan für Ernährung, Landnutzung und Umwelt der Technischen Universität München zur Erlangung des akademischen Grades eines

Doktors der Naturwissenschaften

genehmigten Dissertation.

Vorsitzender: Univ.-Prof. Dr. Erwin Grill

Prüfer der Dissertation:
1. Univ.-Prof. Dr. Wolfgang Liebl
2. Univ.-Prof. Dr. Rudi F. Vogel

Die Dissertation wurde am 14.08.2014 bei der Technischen Universität München eingereicht und durch die Fakultät Wissenschaftszentrum Weihenstephan für Ernährung, Landnutzung und Umwelt am 07.11.2014 angenommen.

Content list

Abbreviations

a	Antisense
AA	Amino acid
ABC (transporter)	ATP-binding cassette (transporter)
ABE	Acetone/butanol/ethanol
ad	Fill up tothe specified volume
ATCC	American Type Culture Collection
ATP	Adenosine-5'-triphosphate
BLAST	Basic Local Alignment Search Tool
bp	Basepair
°C	Degree centigrade
cDNA	Complementary deoxyribonucleic acid
CDS	Coding sequence
Cm	Chloramphenicol/thiamphenicol
cm	Centimeter
CoA	Coenzyme A
CT	ClosTron
DMF	Dimethylformamide
DNA	Deoxyribonucleic acid
DNase	Deoxyribonuclease
dNTP	Deoxyribonucleoside-5'-triphosphate
DTT	Dithiothreitol
EDTA	Ethylene diamine tetraacetic acid
EMS	Ethyl methanesulfonate
ErmB	Erythromycin resistant cassette
et al.	And more (*et alii*)
EtBr	Ethidium bromide
EtOH	Ethanol
FAD	Flavin adenine dinucleotide
Fig.	Figure
FMN	Flavin mononucleotide
g	Gram
GSP	Gene-specific primers
h	Hour
HEPES	4-(2-Hydroxyethyl)-1-piperazineethanesulfonic acid
HTH	Helix-turn-helix (structural motif)
IPTG	Isopropyl β-D-1-thiogalactopyranoside
k	Kilo (10^3)
kb	Kilobases
L	Liter
LB (medium)	Luria Bertani (medium)
log	Logarithm
m	Milli (10^{-3})/meter
M	Molar (mol/L), mega (10^6)
min	Minute
mRNA	Messenger ribonucleic acid

n	Nano (10^{-9})
NaAc	Sodium acetate
NAD	Nicotinamide adenine dinucleotide
NADP	Nicotinamide adenine dinucleotide phosphate
NCBI	National Center for Biotechnology Information
NMNG	*N*-methyl-*N'*-nitro-*N*-nitrosoguanidine
OD_{600}	Optical density at a wavelength of 600 nm
ORF	Open reading frame
ox	Oxidative
p	Pico (10^{-12})
P	Phosphate
PCR	Polymerase chain reaction
PEP	Phosphoenolpyruvate
pH	Negative decimal logarithm of the proton concentration
Pi	Inorganic phosphate
PTS	Phosphotransferase system
r	Resistant/resistance
RAM	Retrotransposition-Activated Marker
red	Reductive
RLM-RACE	RNA ligase-mediated rapid amplification of 5' and 3' cDNA ends
RNA	Ribonucleic acid
RNase	Ribonuclease
rpm	Revolutions per minute
rRNA	Ribosomal ribonucleic acid
RT	Room temperature/reverse transcription
s	Second/sense
SAM	*S*-adenosyl methionine
SDS	Sodium dodecyl sulfate
SOE (PCR)	Splicing with overlap extensions (PCR)
sp.	Species
SSC	Saline sodium citrate
TAE buffer	Tris-acetate-EDTAbuffer
TCA cycle	Tricarboxylic acid cycle
THF	Tetrahydrofolic acid
Tm	Melting temperature
TPR	Tetratricopeptide repeat(structural motif)
Tris	Tris-hydroxymethyl-aminomethane
tRNA	Transfer ribonucleic acid
U	Unit of the enzyme activity
V	Volt
Vol.	Volume
v/v	Ratio of volumeto volume
WT	Wildtype
w/v	Ratio of weightto volume
µ	Micro (10^{-6})

Nucleotide bases

A	Adenine (purine)	G	Guanine (purine)
C	Cytosine (pyrimidine)	T	Thymidine (pyrimidine)

Amino acids

A	Alanine	M	Methionine
C	Cysteine	N	Asparagine
D	Aspartic acid	P	Proline
E	Glutamic acid	Q	Glutamine
F	Phenylalanine	R	Arginine
G	Glycine	S	Serine
H	Histidine	T	Threonine
I	Isoleucine	V	Valine
K	Lysine	W	Tryptophan
L	Leucine	Y	Tyrosine

1 Introduction

1.1 Overview

Acetone/butanol/ethanol (ABE) fermentation was started at the beginning of the twentieth century in the United Kingdom and peaked in the 1950s, but declined afterwards due to vigorous development of the petroleum industry and the price increase of the feedstocks (Jones and Woods, 1986). However, the availability of fossil fuels could last only a limited period, and it was assumed that the price of this substance was supposed to increase constantly. Besides, the greenhouse gas CO_2 emission on the climate of the world, caused by burning of petroleum-based diesel and gasoline, was another aspect of concern of the people. Consequently, utilizing reproducible resources for the sustainable production of biofuel was a wisdom choice to replace fossil-based energy and compensate the continuous increase of CO_2 in the atmosphere (Dürre, 2007).

The development of the production of biofuels experienced several phases. First-generation biofuels focused on the production of biodiesel and bioethanol from animal fats, vegetable oil, or recycled restaurant greases, and sugar-containing feedstock, respectively. Second-generation biofuels employed lignocellulosic biomass as the material, yielding mainly diesel. However, this process used wood as the base material, instead of other biomass, e.g. leaves, stalks and grass, bringing a possibility of destroying ecology. Several years ago, the biobutanol formation strategy was initiated with the utilization of solvent-producing clostridia, e.g., *Clostridium beijerinckii* and *Clostridium acetobutylicum* (Dürre, 2007).

In comparison to ethanol, butanol shows a number of superior characteristics. This substance possesses higher energy content, it is safer to cope with and can be blended in any concentration with gasoline and requires no modification of car engines. Moreover, it is convenient for distribution using existing infrastructure owing to its properties of non-hygroscopicity and low corrosivity. Besides, the dibutyl ether derivative has the potential for a diesel fuel (Dürre, 2007). As a result, biobutanol is an alternative fuel with tremendous potential (Dong *et al.*, 2010) and meanwhile the interest of research on fermentation of biobutanol by *C. acetobutylicum* has regained (Lehmann and Lütke-Eversloh, 2011; Lehmann *et al.*, 2012a, 2012b; Cooksley *et al.*, 2012; Jang *et al.*, 2012; Ventura *et al.*, 2013; Hou *et al.*, 2013).

C. acetobutylicum, an obligate anaerobe isolated from soil, is Gram-positive, rod-shaped and endospore-forming (Fig. 1). It features the ABE fermentation during solventogenic growth after a transition from acidogenesis (Jones and Woods, 1986). Most research on *C. acetobutylicum* focused on batch fermentation, in which hydrogen, carbon dioxide, acetic acid and butyric acid were formed in the exponential phase (acidogenesis), followed by the stationary growth where previously produced acids were re-assimilated and the formation of neutral solvents acetone, butanol, ethanol was initiated (solventogenesis). The pH of the culture medium dropped continuously when acids were produced during the exponential growth and the pH was increased afterwards by the shift of the metabolism of cells to solvent production where carbohydrate was consumed concomitantly. Besides, the ratio of ABE generated under standard batch conditions was 3:6:1. Due to the property of acetone, however, it could not be used as a fuel (Jones and Woods, 1986; Dürre, 2007). Consequently, maximization of biobutanol yields and minimization or elimination of acetone formation are the ultimate aims of the research on ABE fermentation of *C. acetobutylicum*. Accordingly,

best understanding of the metabolic pathways and physiological characteristics of *C. acetobutylicum* are obviously the prerequisites for engineering this bacterium.

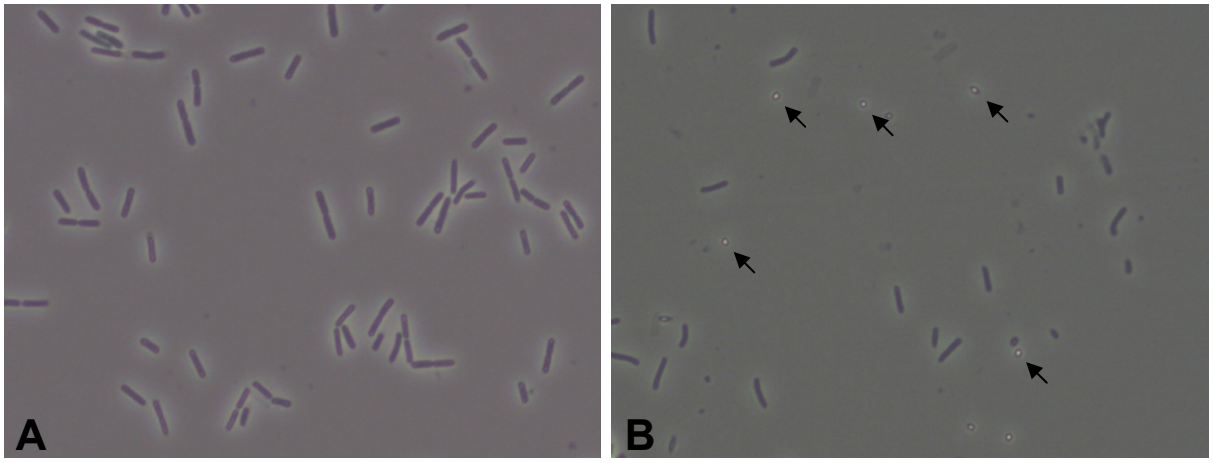

Fig. 1. Microscopic images of *C. acetobutylicum*. It is rod-shaped during exponential growth (A) and forms free spores in late stationary phase, as indicated in arrows in (B).

1.2 Central metabolic pathways of *C. acetobutylicum*

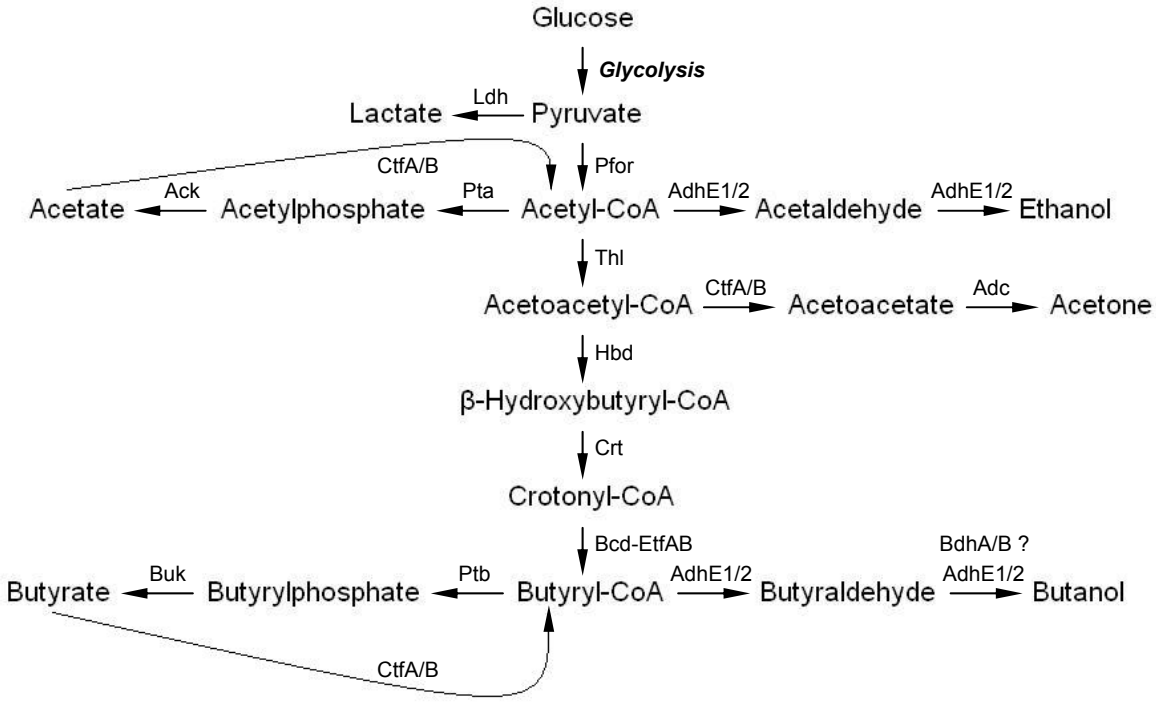

Fig. 2. Schematic diagram of the central metabolic pathways of *C. acetobutylicum*. Abbreviations: Ldh, lactate dehydrogenase; Pfor, pyruvate:ferredoxin oxidoreductase; AdhE1/2, aldehyde/alcohol dehydrogenases 1/2; Pta, phosphotransacetylase; Ack, acetate kinase; CtfA/B, acetoacetyl-CoA:acyl-CoA transferase; Thl, thiolase; Adc, acetoacetate decarboxylase; Hbd, β-hydroxybutyryl-CoA dehydrogenase; Crt, crotonase; Bcd-EtfAB, butyryl-CoA dehydrogenase-electron transfer flavoprotein complex; Ptb, phosphotransbutyrylase; Buk, butyrate kinase; BdhA/B, butanol dehydrogenases A/B.

C. acetobutylicum utilizes hexose (e.g. glucose) and pentose (e.g. xylose and arabinose) as substrates with a preference of glucose (Ezeji and Blaschek, 2008). *C. acetobutylicum* carries all enzymes for the glycolysis route (Nölling *et al.*, 2001) and glucose is catabolised via this pathway. By glycolysis, 1 mol of glucose is converted to 2 mol of pyruvate, with generation of 2 mol of ATP and 2 mol of reduced NADH. The pyruvate formed from glycolysis is then converted to carbon dioxide, reduced ferredoxin and acetyl-CoA by a pyruvate:ferredoxin oxidoreductase (PFOR). Acetyl-CoA is the core intermediate in the C_4 metabolism pathways for production of both acids and solvents (Fig. 2). The pentose phosphate pathway exists in many bacteria, where pentoses (i.e., ribulose-5-phosphate, ribose-5-phosphate, xylulose-5-phosphate) are converted to fructose-6-phosphate and glyceraldehyde-3-phosphate, both of which are connected to the glycolytic pathway towards pyruvate formation. In *C. acetobutylicum*, however, homologues of enzymes for the oxidative pentose phosphate pathway are absent (Nölling *et al.*, 2001). As a result, ribose-5-phosphate and erythrose-4-phosphate were produced predominantly via transketolase (~80%), a nonoxidative pentose phosphate pathway (Amador-Noguez *et al.*, 2010).

The production of acetate, butyrate, acetone, butanol and ethanol by *C. acetobutylicum* relies on the central metabolic pathways. In this C_4 pathway, ThlA (thiolase A), Hbd (β-hydroxybutyryl-CoA dehydrogenase), Crt (crotonase or enoyl-CoA hydratase), Bcd (butyryl-CoA dehydrogenase) and EtfA/B (electron transferring flavoprotein α and β subunits) serve as the key catalysts for the conversion of acetyl-CoA to butyryl-CoA (Fig. 2), and this is responsible for formation of both acids and solvents (Jones and Woods, 1986). By primer extension experiments, it was confirmed that *crt*, *bcd*, *etfB*, *etfA* and *hbd* consisted of an operon corresponding to a regulatory unit of associated functions and upstream of *crt*, the only transcriptional start site was identified (Boynton *et al.*, 1996). In eukaryotes, the β oxidation of fatty acids was concerned with a similar arrangement of enzymes: 3-hydroxyacyl-CoA dehydrogenase (HAD), enoyl-CoA hydratase (ECH), and acyl-CoA dehydrogenase (ACD), which suggested a set of functionally and structurally conserved elements (Youngleson *et al.*, 1989; Boynton *et al.*, 1996). In addition, a similar enzyme structure was also found in *Escherichia coli* which contained thiolase, HAD, ECH, epimerase, and isomerase. They were involved in fatty acid degradation (Yang *et al.*, 1991; Yang and Elzinga, 1993).

In detail, *C. acetobutylicum* ThlA converts acetyl-CoA to acetoacetyl-CoA, the first step of the route to butyryl-CoA formation, and acetoacetyl-CoA is the direct precursor of acetone. Hbd in *C. acetobutylicum* catalyzes the reduction of acetoacetyl-CoA by NAD(P)H to β-hydroxybutyryl-CoA which is subsequently converted to crotonyl-CoA by crotonase. Afterwards, an EtfA/B-Bcd complex makes the metabolic flux go towards butyryl-CoA, the branch point for formation of both butyrate and butanol (Fig. 2).

In addition, phosphotransacetylase (Pta) and acetate kinase (Ack) are responsible for the acetate formation from acetyl-CoA, and phosphotransbutyrylase (Ptb) and butyrate kinase (Buk) are for the generation of butyrate from butyryl-CoA. In terms of production of solvents, aldehyde/alcohol dehydrogenases (AdhE1 and AdhE2) are believed to function in the last two steps of biosynthesis process of ethanol and butanol (Dürre *et al.*, 1995), while acetoacetate decarboxylase (Adc) and acetoacetyl-CoA:acyl-CoA transferase (CtfA/B) are responsible for the production of acetone. CtfA/B is involved in acid re-assimilation when metabolism of *C. acetobutylicum* transits from acidogenesis to solventogenesis (Jones and Woods, 1986).

As described above, the central metabolism pathways of *C. acetobutylicum* are of significance for production of both acids and solvents. Among the gene products responsible

for these routes, an electron transfer system (EtfA/B-Bcd complex) functions at the last node of the C_4 route (Fig. 2) and is important for the generation of C_4 products of *C. acetobutylicum*. In the next section, more information about the electron transfer complex is introduced.

1.3 Electron transferring flavoprotein and its dehydrogenase

As indicated above (section 1.2), *C. acetobutylicum* butyryl-CoA dehydrogenase (BCD) serves as a catalyst for the conversion from crotonyl-CoA to butyryl-CoA and butyryl-CoA is the key intermediate for the synthesis of both butyrate and butanol.

Bacterial BCD possessed characteristics similar to those of the corresponding enzymes from mammalian mitochondria, i.e., short-chain acyl-CoA dehydrogenase (SACD). In addition, the *bcd* coding sequence showed a high similarity to its mammalian counterpart (Boynton *et al.*, 1996). Acyl-CoA dehydrogenase (ACD) needed flavin adenine dinucleotide (FAD) as the cofactor and required an electron transfer flavoprotein (ETF; α, β subunits) as the electron donor-acceptor for function (Kelly *et al.*, 1987; Matsubara *et al.*, 1987, 1989; Naito *et al.*, 1989). *C. acetobutylicum* BCD functioned in the reverse direction from the degradation of fatty acid to form reduced butyryl-CoA, but the characterization of this enzyme had not been reported (Boynton *et al.*, 1996). BCD was purified from *Megasphaera elsdenii* (Engel, 1981) and the apoprotein of BCD showed high reconstitutability (50-80%) and reconstituted >80% of the original specific activity (Van Berkel *et al.*, 1988).

In addition, ETF transferred electrons between NAD(H) and Bcd, and the Bcd activity was found to require ETF (Boynton *et al.*, 1996; Inui *et al.*, 2008). Accordingly, Bcd is an EtfA/B-dependent dehydrogenase.

The genes coding for two different subunits of an ETF have been identified from *M. elsdenii* through a partial genomic DNA library. The sequence of the gene for the β-subunit was located upstream of the gene for the α-subunit. The amino acid sequence of *M. elsdenii* ETF showed homology with the mitochondrial ETF and bacterial ETF, and the greatest similarity occurred with the putative ETF from clostridia and with *fixAB* gene products from nitrogen-fixing bacteria. *M. elsdenii* ETF served as an electron donor to butyryl-CoA dehydrogenase, and it also had NADH dehydrogenase activity. It functioned to transfer electrons from D-lactate dehydrogenase and NADH to butyryl-CoA dehydrogenase (O'Neill *et al.*, 1998).

ETF and its related dehydrogenase had been reported from several species. In *Clostridium propionicum*, an acryloyl-CoA reductase was identified. This enzyme complex consisted of a propionyl-CoA dehydrogenase (α2) and two ETF subunits, and it contained 90% FAD and 10% FMN (flavin mononucleotide). *C. propionicum* acryloyl-CoA reductase catalysed the irreversible NADH-dependent generation of propionyl-CoA from acryloyl-CoA. It exhibited acyl-CoA dehydrogenase activity with propionyl- or butyryl-CoA as the electron donor and ferricenium hexafluorophosphate as the acceptor. The enzyme complex also had diaphorase activity and NADH oxidase activity, catalysing oxidation of NADH by iodonitrosotetrazolium chloride, thus leading to formation of H_2O_2. The N-terminus of the dimeric propionyl-CoA dehydrogenase subunit showed up to 55% of similarity to those of butyryl-CoA dehydrogenases from several clostridia and related anaerobes. The N-termini of the subunits of ETF shared ~40% sequence identities with those of the ETF subunits from

butyrate-producing anaerobe *M. elsdenii*, and up to 60% with those of assumed ETFs from other anaerobes (Hetzel *et al.*, 2003).

A three-component flavoprotein electron transfer system catalyzed the oxidation of lactate and the reduction of crotonyl-CoA. Reduced D-lactate dehydrogenase could reduce Bcd only when the electron transferring flavoprotein component B was present, whereas component A did not have this property. Moreover, component A and B reduced Bcd via reduced nicotinamide adenine dinucleotide (NAD). It was also demonstrated that ETF was the mediator of the oxidation of D-lactate dehydrogenase and the reduction of Bcd (Brockman, 1971).

Generally, FAD or FMN serves as a coenzyme of flavoproteins which function as moderators of electron transfer (Satomura *et al.*, 2002). A typical binding motif for FAD was GXGXXG (Reed *et al.*, 1999). The function of ETF was to generate short chain fatty acids by linking the oxidation of NADH to the reduction of butyryl-CoA dehydrogenase (BCD). Bcd was a flavoprotein which reduced short chain α, β unsaturated fatty acids. The electron transport process is as follows (Baldwin and Milligan, 1964):

$NADH + H^+ + ETF\ (ox) \longrightarrow NAD^+ + ETF\ (red)$

ETF (red) + butyryl-CoA dehydrogenase (ox) —> ETF (ox) + butyryl-CoA dehydrogenase (red)

Butyryl-CoA dehydrogenase (red) + crotonyl-CoA —> butyryl-CoA dehydrogenase (ox) + butyryl-CoA

In the above mentioned example, it was shown that the ETF served as the electron donor to its related dehydrogenases, and with electron transfer by ETF, electrons were transferred from one dehydrogenase to another.

In *Clostridium kluyveri*, the EtfA/B-Bcd complex was found to function in the endergonic ferredoxin reduction with NADH, in addition to the exergonic crotonyl-CoA reduction with NADH (Li *et al*., 2008). The reaction is as follows:

$2\ NADH + crotonyl\text{-}CoA + Ferredoxin\ (Fd_{ox}) \longrightarrow 2\ NAD^+ + butyryl\text{-}CoA + Fd_{red}^{2-}$

CA_C2542 (*fcd*), *CA_C2543* (*etfA*) and *CA_C2544* (*etfB*) are clustered genes on the chromosome of *C. acetobutylicum*, but no reports about this cluster are available. *fcd* was annotated to be the coding-gene for a FAD/FMN-containing dehydrogenase (FCD) and *CA_C2543* and *CA_C2544* coded for EtfA and EtfB, respectively. Consequently, the product of this cluster was an EtfA/B-dependent dehydrogenase complex which was the second one in *C. acetobutylicum* (the other one is EtfA/B-Bcd, CA_C2709-CA_C2711). From a microarray analysis, it was shown that the transcript levels of these clustered genes were elevated at least 5.6-fold during the steady-state solventogenic growth as compared to that during acidogenesis, suggesting this cluster plays a role during solventogenesis (Grimmler *et al.*, 2011). Besides, during the pH shift of the chemostat culture from the steady-state acidogenic growth (pH 5.7-pH 4.5) the expression of this cluster started to increase from

pH 4.9 and it kept highly expressed until the steady-state solventogenic growth (Grimmler *et al.*, 2011).

1.4 pSOL1 megaplasmid and genes on it

In addition to chromosomal genes which are responsible for the C_4 pathways, *adhE1*, *ctfA* and *ctfB* (*sol* operon), *adhE2* and *adc* are central metabolism genes located on the pSOL1 megaplasmid of *C. acetobutylicum* (Fig. 2, 3). pSOL1 megaplasmid is 192 kb in size and in total contains 178 annotated open reading frames (ORFs) (Nölling *et al.*, 2001). Apart from biochemically known genes for formation of solvents, it was also found that pSOL1 possessed other physiologically-important genes coding for, e.g., transcription factors and amylases, the latter are now the main indicator for detection of the presence of the pSOL1 megaplasmid in the bacterial cell (section 2.5.1, 2.9.4).

Lots of studies have been carried out concerning the role of the pSOL1 megaplasmid. In 1989, a *C. acetobutylicum* mutant strain, M5, was generated from the wild type strain through *N*-methyl-*N*′-nitro-*N*-nitrosoguanidine (NMNG) treatment (Clark *et al.*, 1989). The resulting mutant was asporogenous and deficient in the formation of butanol and acetone (degenerate) owing to loss of four indispensable genes *adhE*, *ctfA*, *ctfB* and *adc* (Cornillot *et al.*, 1997). In addition, the M5 mutant strain could be complemented for butanol (Nair and Papoutsakis, 1994) and acetone (Mermelstein *et al.*, 1993) formation by expressing *adhE*, and *adc* plus *ctfA* and *ctfB*, respectively. Moreover, by serial subculturing of *C. acetobutylicum* wild type for numerous passages, a spontaneous degenerate strain DG1 was obtained with the same deficiency as the M5 mutant (Nair, 1995). It was found that these two mutants did not harbor the pSOL1 megaplasmid (Cornillot *et al.*, 1997). These studies demonstrated, for the first time, that genes encoding enzymes for the last steps of the synthesis routes for butanol and acetone resided on the pSOL1 megaplasmid and its loss resulted in degeneration of the strain (Cornillot *et al.*, 1997). However, the degenerate strains M5 and DG1 of *C. acetobutylicum* had not been re-sequenced to eliminate possibilities of the mutation in the chromosome. As a result, it was necessary to establish a new method for direct deletion of the pSOL1 megaplasmid of *C. acetobutylicum* in order to understand the physiological role of this plasmid as a whole and the metabolic effects pSOL1 exerts on the organism.

Several studies concerning genetic modification of *C. acetobutylicum* had been conducted based on the DG1 and M5 mutant strains because of their deficiency in solvent production. The recombinant DG1 with the pSPD5 plasmid, carrying the NADH-consuming 1,3-propanediol pathway genes from *Clostridium butyricum* VPI 3266, could grow on glycerol without glucose, and form 1,3-propanediol (González-Pajuelo *et al.*, 2005, 2006; Mendes *et al.*, 2011). Besides, complementation of *adhE2* gene was performed in the DG1 mutant by expression of this gene from the thiolase promoter. The production of butanol was restored in the recombinant strain as compared to the plasmid control strain and a protein product for AdhE2 was detected via SDS-PAGE analysis (Fontaine *et al.*, 2002).

Moreover, several efforts to increase the butanol yield have been undertaken with the M5 mutant as the background. It has been demonstrated that the mutant M5 could be restored to a normal butanol producer with a plasmid-coded *adhE1* gene under the control of the *ptb* promoter, but establishment of a superb butanol producer without acetone formation was difficult. It was suggested that the pSOL1-free M5 strain became more preferable to the acid formation pathways, especially the butyrate synthesis route (Sillers *et al.*, 2008). Moreover,

with *adhE1-ctfAB* gene complementation in the M5 strain, the resultant strain had restored the butanol formation and increased the butanol selectivity (a molar ratio of butanol to total solvents) to 0.84 at pH 5.5, which was much higher than that (0.61 at pH 5.5; or 0.57 at pH 5.0) of the wild type strain (Lee *et al.*, 2009).

In addition, because of the similar phenotype in terms of the production of solvents, transcription analysis was carried out for the M5 mutant, together with a SKO1 mutant whose *spo0A* gene (*CA_C2071*) had been inactivated. The DNA microarray chips used covered 1,019 genes (about 25%) of the whole genome of *C. acetobutylicum*, including all 178 genes from the pSOL1 megaplasmid. The results showed that *spo0A* was repressed when pSOL1 was removed, indicating this gene was positively influenced by the megaplasmid-coding gene(s) (Tomas *et al.*, 2003).

In addition to the investigations on the pSOL1 megaplasmid as a single function unit, individual genes on it have also been studied. For instance, *adhE2* was characterized in terms of biochemistry and molecular biology (Fontaine *et al.*, 2002). In *C. acetobutylicum*, there were two aldehyde/alcohol dehydrogenases (AADHs), i.e., AdhE1 and AdhE2, making this species the only example with two AADHs (Fontaine *et al.*, 2002). It has been demonstrated that *adhE1* gene was responsible for the two final steps of butanol production in solventogenic cultures (Dürre *et al.*, 1995), while *adhE2* gene was in charge of butanol production only under alcohologenic conditions (Fontaine *et al.*, 2002) at a high $NADH/NAD^+$ ratio. *E. coli adhE* gene was also proposed to be controlled by the $NADH/NAD^+$ ratio (Leonardo *et al.*, 1993).

Research on *C. acetobutylicum* has been accelerated since the sequence of its whole genome became available (Nölling *et al.*, 2001; Bao *et al.*, 2011; Hu *et al.*, 2011). Several genes on the pSOL1 megaplasmid were found to be significantly regulated at the onset of solventogenesis, showing they might play roles during solventogenic growth (Alsaker and Papoutsakis, 2005).

Among these, *CA_P0129* was of great interest. This gene encodes a glycogen-binding regulatory subunit (GBRS) of Serine/Threonine protein phosphatase I, and it is 744 bp in size, containing two fragments for putative phosphatase regulatory subunits. Besides, *CA_P0129* is located in reverse direction on the pSOL1 megaplasmid. DNA microarray results from chemostat cultures showed that the expression of *CA_P0129* was significantly induced (~4.5-fold or ≥5.6-fold) during the steady-state solventogenic growth (pH 4.5) (Janssen *et al.*, 2010; Grimmler *et al.*, 2011), and that its expression had reached the mentioned level at pH 5.1 during the dynamic pH shift from acidogenesis (pH 5.8) (Grimmler *et al.*, 2011). The data indicated that *CA_P0129* might play a role in solvent production. In DNA microarray studies of batch fermentation, Alsaker *et al.* found that the transcript level of *CA_P0129* was strongly elevated at least 10-fold when the fermentation entered solventogenesis (Alsaker and Papoutsakis, 2005), which was in agreement with results from continuous cultures although different cultivation methods were employed. This further suggested the significance of the function of *CA_P0129* for solventogenesis. Unfortunately, no further study about the role of this gene had been reported so far, leaving a promising field.

CA_P0036 and *CA_P0037* are two ORFs located on the pSOL1 megaplasmid and consist of a ~1.4 kb transcription unit (Janssen *et al.*, 2010). Both genes were observed to be significantly induced only during the steady-state acidogenic growth (144.9- and 217.7-fold, respectively) via DNA microarray experiments, and the data was further verified by 2D gel electrophoresis analyses of the identical samples (Janssen *et al.*, 2010). A similar phenomenon was found in

another microarray analysis based on the chemostat culture and it was also shown that during the dynamic pH shift of the culture the expression of this operon was noticeable (logarithmic ratio >4) (Grimmler *et al.*, 2011). However, previous research on *C. acetobutylicum* under batch conditions revealed that the expression of this operon hardly changed during the whole course of the fermentation as compared to that in mid-exponential phase (Alsaker and Papoutsakis, 2005; Jones *et al.*, 2008).

CA_P0059 is annotated as a gene coding for a putative alcohol dehydrogenase which was proposed to be related to alcohologenic metabolism (Nölling *et al.*, 2001) and its function remained unknown. It was reported that the transcript level of *CA_P0059* was up-regulated after the onset of solventogenesis under batch conditions (Alsaker and Papoutsakis, 2005), but not obviously changed during the course of a continuous culture (Grimmler *et al.*, 2011). Besides, it was suggested that this gene was responsible for the formation of ethanol and butanol (Papoutsakis, 2008). However, inactivation of this gene resulted in enhanced production of all three solvents (Cooksley *et al.*, 2012), which was opposite to what was expected. What mentioned above indicates that the role of this gene could be complex.

To sum up, several studies had been conducted concerning the physiological roles of genes on pSOL1 megaplasmid. However, none of these genes have been characterized in detail due to the previous unavailability of methodology for mutagenesis of *C. acetobutylicum*. The consequence was that only general information about these genes could be obtained, e.g., as mentioned above, expression patterns and transcript levels, leaving a promising field for further elucidation of the gene functions.

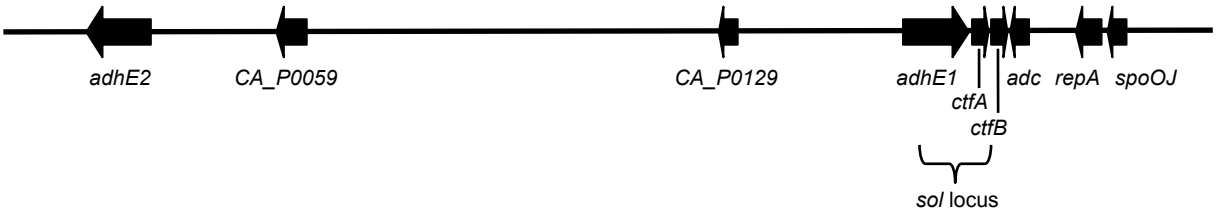

Fig. 3. Schematic map of the pSOL1 genes relevant for solventogenesis (also including those studied in this dissertation). The 192-kb pSOL1 megaplasmid contains a *sol* locus, *adhE2* and *adc* genes which function in central metabolic pathways of *C. acetobutylicum* (Fig. 2). *repA* encodes a replication protein and *spoOJ* codes for a Soj/ParA protein related to DNA partitioning.

1.5 ClosTron-mediated mutagenesis in *C. acetobutylicum*

1.5.1 The ClosTron system

Stable mutants of *C. acetobutylicum* could not be obtained until the ClosTron technology was developed (Heap *et al.*, 2007, 2010a, 2010b). On the basis of group II intron retro-homing (replication and insertion) mechanism (Mills *et al.*, 1997), the ClosTron technology opened a new window for mutagenesis of *Clostridium* spp. and allowed the generation of mutants within 10 days. The ClosTron mutagenesis system was used widely in this study. The Ll.LtrB intron from *Lactococcus lactis ltrB* gene was ligated into the shuttle vector pMTL007 backbone. The resultant pMTL007 plasmid contained a *catP* gene, which made

chloramphenicol- and thiamphenicol-resistance available for *E. coli* and *C. acetobutylicum* host cells after they were transformed with the vector. The constructed vector needed to be introduced into *E. coli* competent cells harbouring pAN2 methylation plasmid. Methylated plasmid was ready to be used for electroporation of *C. acetobutylicum* with methylations protecting against digestion by a restriction system in *C. acetobutylicum*. When the pMTL007 plasmid was introduced into clostridial cells, the Group I intron moved out of the erythromycin resistance gene located within the Group II intron, thus making previously split resistance coding sequence reunion. As a result, positive clones could be screened on an agar plate containing erythromycin when Group II intron retro-homing occurred.

Nowadays, a derivative of pMTL007 plasmid, pMTL007C-E2, was available, which was much more suitable for mutagenesis of *C. acetobutylicum* (Heap *et al.*, 2010b). This second generation ClosTron plasmid contains a constitutive promoter of the ferredoxin gene *fdx*, allowing intron insertion to happen as soon as the plasmid is introduced into the host cells, thus avoiding a step of IPTG induction for the previously used IPTG-inducible *fac* promoter on pMTL007 plasmid. Because of the advantages that pMTL007C-E2 possesses, this plasmid is now widely utilized for mutant generation in *C. acetobutylicum* (Table 7, section 2.4).

1.5.2 Application of the ClosTron technology

By using the ClosTron technology, numerous mutants of *C. acetobutylicum* have been generated (Cooksley *et al.*, 2012; Kuit *et al.*, 2012; Lehmann and Lütke-Eversloh, 2011; Lehmann *et al.*, 2012a, 2012b; Vasileva *et al.*, 2012). Among them, a set of 10 mutants of genes involved in central metabolism pathways was described in a study (Cooksley *et al.*, 2012). This brought a comprehensive view of the physiology of *C. acetobutylicum* under batch fermentation conditions. The results of this study are as follows:

Genes for *sol* locus consist of *adhE1*, *ctfA* and *ctfB*. Mutations of *ctfA* or *ctfB* resulted in deficiency in re-utilization of the acids and inability to produce acetone, and an *adc* mutant formed only ~2 mM acetone. Acetate, butyrate and lactate formation were raised by these three mutants, while butanol and ethanol concentrations were decreased (Cooksley *et al.*, 2012).

The *adhE1* mutant formed a tiny amount of acetone (1.7 mM), butanol (2.5 mM) and ethanol (2.5 mM) after 96 h of cultivation, suggesting that the *adhE1* gene was the key gene for the production of solvents during batch fermentation and AdhE1 was the principle dehydrogenase responsible for butanol and ethanol formation under this condition (Cooksley *et al.*, 2012).

The *ack* mutant produced at most ~5 mM acetate and the normal amount of butyrate and acetone. The ethanol concentration formed by the *ack* mutant was 4-fold higher than the wild type level and the butanol concentration was increased by ~20% (Cooksley *et al.*, 2012).

The *ptb* mutant generated did not produce butyrate, as expected. Instead, it produced huge amounts of acetic and lactic acid. During solventogenic growth, this mutant did not produce acetone and formed a very low concentration of butanol. Interestingly, 113 mM ethanol, as the major fermentation product, was produced. Nevertheless, the phenotype of the *ptb* mutant could not be complemented by the expression of a plasmid-borne *ptb*. The reason was a frameshift in the gene *CA_C2783* (*thlA*) which mediates the reaction from acetyl-CoA to

acetoacetyl-CoA, the branch point for production of acetone, butyrate and butanol (Cooksley *et al.*, 2012). Another *ptb* mutant was generated by Lehmann *et al.* (2012b). It produced a high level of lactate and acetate and low concentrations of all three solvents in MS-MES batch cultures without pH control (Lehmann *et al.*, 2012b). When cultivating this mutant in a pH-controlled (≥5.0) medium, acetone and butanol concentrations were decreased, while the ethanol concentration reached ~280 mM, at least 8-fold higher than the wild type control. As a result, production of ethanol of this *ptb* mutant relied on the fermentation conditions. Butyrate was never detected under both conditions and butyrate utilization was not affected by disruption of the *ptb* gene (Lehmann *et al.*, 2012b). Complementation of this *ptb* mutant (Lehmann *et al.*, 2012b) was not reported.

From the schematic diagram of the central metabolic routes of *C. acetobutylicum* (Fig. 2), it was widely assumed that *bdhA* and *bdhB* were both involved in butanol formation in the last step of the butanol synthesis pathway from butyraldehyde to butanol. After disruption of these two genes, however, the production of solvents remained the normal level. This revealed that these two genes had minor contributions to butanol production in batch cultures (Cooksley *et al.*, 2012).

An *adhE2* mutant strain did not show any changes in the generation of metabolites under batch culture conditions, which was unexpected because it encodes the second bifunctional alcohol/aldehyde dehydrogenase that catalyzes the last steps of biosynthesis of ethanol and butanol. This observation suggested that *adhE2* hardly exerted influences on the product formation (Cooksley *et al.*, 2012). However, under alcohologenic conditions, AdhE2 was demonstrated to be the main enzyme responsible for alcohol production owing to high NAD(P)H availability at near neutral pH (Fontaine *et al.*, 2002).

The *CA_P0059* gene coding for a putative alcohol dehydrogenase, which was proposed to have a potential role in butanol and ethanol formation (Papoutsakis, 2008), was not investigated until a ClosTron-mediated single mutant was generated. A decreased production of solvents was expected for the *CA_P0059* mutant. However, an enhancement of all three solvents (acetone, butanol and ethanol) was observed under standard batch fermentation conditions. The reason behind this observation was unclear, but the data suggested that *CA_P0059* was an interesting candidate for further study on regulation of solvent production (Cooksley *et al.*, 2012).

In addition to the above results from the literature (Cooksley *et al.*, 2012), several other mutants of *C. acetobutylicum* had been generated and characterized using batch culture conditions.

Jang *et al*. disrupted the *pta* and *buk* genes (encoding phosphotransacetylase and butyrate kinase, respectively; Fig. 2), resulting in a strain with the maximal flux for butanol formation through central C_4 channel (Jang *et al.*, 2012). To further enhance the butanol production via the acetyl-CoA/butyryl-CoA route of this *pta/buk* double mutant, Jang *et al*. overexpressed *adhE1* gene with its 485th amino acid residue, Asp, altered (to Gly) for higher affinity for NADPH. In earlier literature, the replacement of Asp (38th amino acid residue) with Gly in the ADH2 of *Zymomonas mobilis* displayed an enhanced affinity for NADPH (Rellos *et al.*, 1997).

An *hbd* mutant (Lehmann and Lütke-Eversloh, 2011) was generated using the ClosTron technology (Heap *et al.*, 2010b). β-Hydroxybutyryl-CoA dehydrogenase (HBD) is responsible for the conversion from acetoacetyl-CoA to β-hydroxybutyryl-CoA (Fig. 2). The

hbd mutant produced more than 700 mM of ethanol, and decreased concentration of acetone (~40 mM) as compared to the wild type. The production of butyrate and butanol was completely abolished when *hbd* was deleted. The phenotype of the *hbd* mutant indicated that the butanol/butyrate fermentative route was not essential (Lehmann and Lütke-Eversloh, 2011).

A *pta* mutant (Lehmann *et al.*, 2012a) formed a wild type level of acetate no matter whether acetate was added before inoculation or not. The *adc* and *ctfA* mutants (Lehmann *et al.*, 2012a) produced higher concentrations of acetate but a lower amount of butanol and ethanol. The *ctfA* mutant did not produce acetone, while the *adc* mutant formed strongly lower concentration of acetone. These aspects were similar with the results mentioned above (Cooksley *et al.*, 2012). A *pta-adc* double mutant (Lehmann *et al.*, 2012a) reduced the production of acetate, ethanol and butanol, and hardly formed acetone. However, this mutant produced much higher concentration of butyrate without re-assimilation during the transition from acidogenesis to solventogenesis. A *pta-ctfA* mutant (Lehmann *et al.*, 2012a) formed a small amount of acetate and butanol, lower concentration of ethanol (comparable with the *pta-adc* mutant), no acetone and a similar concentration of butyrate as the *pta-adc* mutant. To sum up, enhanced butanol production was not observed within 5 mutants with disruption of competing metabolic pathways, which showed complicated causal relationships in the metabolism of *C. acetobutylicum* (Lehmann *et al.*, 2012a).

In CGM medium, an *ack* mutant produced a slightly higher concentration of butanol and a much lower concentration of lactate, although the lactate production in the wild type strain employed was much higher than that of wild type in other studies. In CM1 medium containing acetate, acetate production as well as OD_{600} was decreased and the solvents produced were comparable to the wild type level (Kuit *et al.*, 2012).

The gene coding for a putative ferric uptake regulator (FUR) was inactivated and the resulting strain was characterized. Phenotypically, it grew slower and was more sensitive to oxygen than the wild type strain. In addition to formation of solvents at a normal level, the *fur* mutant overproduced riboflavin. In microarray experiments, the *rib* operon, a lactate dehydrogenase gene and a flavodoxin gene were significantly up-regulated. The genes affected by *fur* inactivation were not completely the same as those in the wild type under iron-limitation conditions. To sum up, *C. acetobutylicum* sensed and responded to availability of iron on multiple levels using a sophisticated system, and that Fur played an important role in this process (Vasileva *et al.*, 2012).

1.5.3 Issues remaining from ClosTron mutagenesis

The inactivation of *hydA* and *thlA* were attempted respectively at least two times and were not successful, which suggested the disruption of these two genes might be lethal under the conditions used (Cooksley *et al.*, 2012). As a result, it was not possible to study the physiological roles of these two genes in *C. acetobutylicum*.

1.6 Other attempts for enhanced butanol production

1.6.1 Recombinant strains with gene over-expression

In parallel with the mutagenesis using ClosTron system, many other recombinant strains had been constructed for the purpose of elevated butanol yields.

Ventura *et al*. constructed a recombinant strain with the overexpression of both 6-phosphofructokinase (*pfkA*) and pyruvate kinase (*pykA*) genes. This strain produced higher concentrations of butanol and ethanol (29.4% and 85.5%) as compared to the wild type, but the acetone production was comparable under the batch fermentation conditions. In addition, 19.12 g/L and 28.02 g/L butanol and total solvent (acetone, butanol, and ethanol) was reached in fed-batch fermentations. The reason of the above mentioned phenotype suggested by the authors was increased ATP and NADH concentrations and raised tolerance to butanol in the double-overexpressed strain of *C. acetobutylicum* (Ventura *et al.*, 2013).

An engineered strain was developed by first disrupting the *adc* gene to reduce the acetone production, because acetone was not a desired product for biofuel. And then, *gshAB* genes of *E. coli* were expressed in the resulting strain for glutathione biosynthetic capability to improve the robustness of the strain. Afterwards, *thl*, *hbd*, *crt*, *bcd*, *adhE1* and *ctfAB* genes were introduced into the strain. The engineered strain formed 14.86±0.26 g/L of butanol and 18.11±0.66 g/L alcohol, respectively (Hou *et al.*, 2013).

Several attempts have been conducted and recombinant strains showed improved performances. However, positive effects on butanol yields are limited, indicating further efforts are necessary.

1.6.2 Inhibition of hydrogenase activity

In addition to the expression of genes in *C. acetobutylicum*, other ways like iron limitation and carbon monoxide sparge have been carried out to increase the ratio of butanol to acetone.

The production of butanol-acetone-ethanol with a ratio of 10:1:1 was achieved when whey filtrate and 0.5% yeast extract were used (Maddox, 1980). Furthermore, when whey was utilized for the fermentation of *C. acetobutylicum*, butanol and acetone were generated in a ratio of ~100:1 and the amount of acetone formed increased when citrate in the whey was removed and minerals were supplemented (Bahl *et al.*, 1986). In iron-limited continuous fermentation, the ratio of butanol to acetone was 8:1, as compared with the ratio by continuous cultures where phosphate was the limiting factor (2:1). Either lactic acid or butanol was the main fermentation product under the iron-limiting conditions according to the pH value. Instead of production of butyrate and acetate at pH above 5, lactic acid was generated, whereas lactate was replaced by butanol formation at low pH (Bahl *et al.*, 1986).

Butanol was reported to become the main end product when the culture of *C. acetobutylicum* was under iron limitation conditions in batch fermentation, though a small amount of acetate was formed. Under this limitation condition, the activity of hydrogenase and acetoacetate decarboxylase (ADC) was reduced by 40% and 25%, respectively (Junelles *et al.*, 1988).

Carbon and electrons were redirected from generation of H_2, CO_2, acetate, and butyrate towards production of ethanol and butanol when CO was present. The butanol concentration and productivity was increased by 63% and 31% when 85% N_2 and 15% CO were constantly sparged versus N_2 alone (Kim BH *et al.*, 1984). The reason was that CO is a potent inhibitor of hydrogenase, thereby redirecting the electrons to reduced products. The enhanced butanol production was particularly obvious when butyric acid, which served as the electron sink, was added. Moreover, no acetone was generated with CO regulation (Datta and Zeikus, 1985). Besides, the glucose-limited continuous culture sparged with CO exhibited a phenotype in which no acetone and little or no acetic/butyric acids were produced while ethanol/butanol and lactate were generated specifically (Meyer *et al.*, 1986).

Based on the assumption that methyl viologen was a better substrate for a presumed ferredoxin-$NAD(P)^+$ reductase than the original ferredoxin, an artificial electron transport system might be generated: pyruvate:ferredoxin oxidoreductase-methyl viologen-ferredoxin-$NAD(P)^+$ reductase-NAD(P) (Peguin *et al.*, 1994b). Meanwhile, simultaneous application of iron limitation and addition of methyl viologen revealed additive effects on the culture, suggesting that these two operations played their roles independently in the metabolic routes (Peguin and Soucaille, 1995).

In summary, the *in vivo* hydrogenase activity can be reduced through the following methods: (a) a raise of partial hydrogen pressure (Doremus *et al.*, 1985; Yerushaimi and Volesky, 1985); (b) sparging with carbon monoxide (Datta and Zeikus, 1985; Kim BH *et al.*, 1984; Meyer *et al.*, 1986); (c) iron limitation (Bahl *et al.*, 1986; Junelles *et al.*, 1988); and (d) addition of an artificial electron carrier, e.g. methyl viologen (Kim TS and Kim BH *et al.*, 1988; Peguin *et al.*, 1994a, 1994b; Rao and Mutharasan, 1986, 1987).

1.7 Fermentation methodology

Fermentation of *C. acetobutylicum* was conducted by either batch cultures or continuous cultures. During batch fermentations, the status of cells during both exponential and stationary growth phases were not uniform, bringing bad reproducibility and difficulties to the study concerning gene regulatory networks of metabolism and physiology. Besides, endospore formation was another interfering factor. It was initiated along with the solvent production in batch cultures during transition from acidogenesis to solventogenesis, which disturbed the research with a preference to enhance the butanol yields. More importantly, acid crash (Maddox *et al.*, 2000) frequently happened in batch cultures but the reason behind was still unclear. In spite of these disadvantages of batch fermentation, this cultivation way is still widely used because it is quick, cheap and easy-to-operate. However, in a phosphate-limited continuous culture, cells were able to remain during the steady-state at pH 5.7 (acidogenesis) and pH 4.5 (solventogenesis) by adjusting the external pH (Bahl *et al.*, 1986). During the steady-states, the OD_{600} of the culture and the level of metabolites in the medium, as well as the condition of intracellular gene expression were stable, which provided a favourable background for research of the phenotypes and gene regulatory networks of *C. acetobutylicum* strains. More importantly, after approximately three days of cultivation, all spores formed had been washed out and sporulation did not occur afterwards when cells started to exhibit stable production of metabolites, making studies with only emphasis on the events related to production of solvents became possible and feasible. As a result, in the present study the phosphate-limited continuous fermentation was employed as the main

methodology for characterization of *C. acetobutylicum* strains and cells growing during steady-states of continuous cultures were used as the materials for transcriptome analyses.

1.8 Aims of this study

According to the above descriptions about the solvent formation of *C. acetobutylicum*, it is found that several disadvantages may exist: (a) limited knowledge about the metabolic pathways and gene regulatory networks of this bacterium; and (b) wide usage of batch fermentations for characterization of mutant strains of *C. acetobutylicum*.

In order to provide novel insights into the physiology of the solvent production of *C. acetobutylicum*, ten genes, which form an EtfA/B-dependent dehydrogenase system or are located on the pSOL1 megaplasmid, were studied in this dissertation. The set of ten resultant mutants were characterized in continuous cultures and by transcriptome analyses to elucidate the physiological and regulatory influences that the disrupted genes exerted. The genes analyzed in this dissertation are listed in the Table 1.

Table 1. Genes studied in this dissertation

Mutated genes	Reasons for targeting
etfB-etfA-fcd gene cluster (*CA_C2544-CA_C2543-CA_C2542*)	Highly expressed during solventogenic growth in continuous cultures of the wild type
htpG (*CA_C3315*)	Mutated in the first try for knockout of *fcd* gene (generation of a *fcd/htpG* double mutant, section 3.2.5)
repA (*CA_P0175*)	Encodes the replication protein of pSOL1 megaplasmid. Hypothesized knockout of this gene lead to loss of the pSOL1
spoOJ (*CA_P0177*)	Encodes a protein related to DNA partitioning. Hypothesized knockout of this gene lead to loss of the pSOL1
CA_P0129	Highly expressed during solventogenic growth in continuous cultures of the wild type
adhE1 (*CA_P0162*)	AdhE is responsible for the last two steps of alcohol formation
CA_P0059	Proposed to be responsible for production of alcohol. Knockout of this gene, unexpectedly, led to enhanced production of all three solvents under batch culture contidions

2 Methods and materials

2.1 Chemicals and devices

Chemicals, regents and devices used in this study are listed in the tables below. Chemicals were dissolved at room temperature (RT) in deionized water of appropriate volume with stirring on magnetic stirrers (JAK Werk, Staufen, Germany/Variomag, Daytona Beach, USA). Biochemical kits and enzymes were employed according to the instruction of the manufacturer and some hazardous regents were utilized in the ventilation hood. Devices were used based on official manuals.

Table 2. Chemicals used in this study

Chemical	Company
KH_2PO_4	Carl roth, Karlsruhe, Germany
K_2HPO_4	Carl roth, Karlsruhe, Germany
$K_2HPO_4 \times 3H_2O$	Merck, Darmstadt, Germany
$(NH_4)_2SO_4$	AppliChem, Darmstadt, Germany
$MgSO_4 \times 7H_2O$	Merck, Darmstadt, Germany
$MnSO_4 \times H_2O$	Merck, Darmstadt, Germany
NaCl	AppliChem, Darmstadt, Germany
$Na_2MoO_4 \times 2H_2O$	AppliChem, Darmstadt, Germany
$CaCl_2 \times 2H_2O$	Carl roth, Karlsruhe, Germany
$FeSO_4 \times 7H_2O$	Fluka, Steinheim, Germany
Thiamine hydrochloride	Applichem, Darmstadt, Germany
p-Aminobenzoic acid	Applichem, Darmstadt, Germany
Biotin	Sigma-Aldrich, Steinheim, Germany
Glucose $\times H_2O$	AppliChem, Darmstadt, Germany
Yeast extract	Becton Dickinson, Heidelberg, Germany
Tryptone	Becton Dickinson, Heidelberg, Germany
Bacteriological Agar No. 1	Oxoid, Hampshire, UK
Reinforced Clostridial Agar (RCA)	Fluka, Steinheim, Germany
Thiamphenicol	Molecula, Shaftesbury, UK
Erythromycin	Sigma-Aldrich, Steinheim, Germany
Chloramphenicol	Sigma-Aldrich, Steinheim, Germany
Tetracycline hydrochloride	Sigma-Aldrich, Steinheim, Germany
Lysozyme	Sigma-Aldrich, Steinheim, Germany
Proteinase K	Sigma-Aldrich, Steinheim, Germany
RNase A	AppliChem, Darmstadt, Germany
LE Agarose	Biozym Scientific GmbH, Hessisch Oldendorf, Germany
IPTG	Sigma-Aldrich, Steinheim, Germany
Blocking reagent	Roche, Mannheim, Germany
SDS	AppliChem, Darmstadt, Germany
Tris	AppliChem, Darmstadt, Germany
HCl (37%)	AppliChem, Darmstadt, Germany

Table 2. (continued)

Chemical	Company
Acetic acid	AppliChem, Darmstadt, Germany
Ethanol absolute	AppliChem, Darmstadt, Germany
Phenol	Carl roth, Karlsruhe, Germany
Chloroform	Carl roth, Karlsruhe, Germany
Potassium iodine solution (Lugol)	Carl roth, Karlsruhe, Germany
pH buffer (pH 4.01, pH 7.00)	WTW, Weilheim, Germany

Table 3. Enzymes and reagents used in this study

Enzyme and reagent	Company
*Eco*RV-HF® (20 U/µL)	NEB, Frankfurt am Main, Germany
*Bsr*GI (10 U/µL)	NEB, Frankfurt am Main, Germany
*Hin*dIII (20 U/µL)	NEB, Frankfurt am Main, Germany
RNase-free DNase I (10 U/µL)	Roche, Mannheim, Germany
Random hexamers $p(dN)_6$ (5 µg/µL)	Roche, Mannheim, Germany
dATP, dTTP, dCTP, dGTP (100 mM)	Roche, Mannheim, Germany
dNTP mix (10 mM each)	Thermo Scientific, Schwerte, Germany
Phire Hot-Start DNA Polymerase	Finnzymes, Espoo, Finnland
Qiagen OneStep RT-PCR Kit	Quiagen, Hilden, Germany
Cy™3-dCTP, Cy™5-dCTP	GE Healthcare Europe GmbH, Munich, Germany
T4 DNA ligase (10 U/µL)	Thermo Scientific, Schwerte, Germany
6× DNA loading dye	Thermo Scientific, Schwerte, Germany
1 kb DNA ladder	Thermo Scientific, Schwerte, Germany
50× Denhart's solution	Invitrogen GmbH, Karlsruhe, Germany

Table 4. Biochemical kits used in this study

Kit	Company
AxyPrep™ Plasmid Miniprep Kit	Serva Electrophoresis, Heidelberg, Germany
Wizard® SV Gel and PCR Clean-Up System	Promega GmbH, Mannheim, Germany
Master Pure DNA Purification Kit	Epicentre, Madison, USA
RNeasy Midi Kit	Qiagen, Hilden, Germany
QIAquick PCR Purification Kit	Qiagen, Hilden, Germany
OneStep RT-PCR Kit	Qiagen, Hilden, Germany
SuperScript III Reverse Transcriptase	Invitrogen GmbH, Karlsruhe, Germany
Biotin DecaLabel DNA Labeling Kit	Thermo Scientific, Schwerte, Germany
Biotin Chromogenic Detection Kit	Thermo Scientific, Schwerte, Germany
D-Glucose Assay (GOPOD) Kit	Megazyme International, Wicklow, Ireland
Acetate Assay (K-ACETRM) Kit	Megazyme International, Wicklow, Ireland
TURBO DNA-*free*™ Kit	Ambion, Huntington/Austin, USA

Table 5. Devices used in this study

Device	Company
Anaerobic chamber	Coy Laboratory Products Inc., Michigan, USA
2.5 L Anaerobic jar/sachet	Oxoid Ltd., Basingstoke, England
Vortex Genie 2™	Bender & Hobein AG, Zürich, Switzerland
Electrophoresis device	Bio-Rad Laboratories, California, USA
Benchtop centrifuge Micro 200R/Universal 320R	Hettich, Tuttlingen, Germany
Magnetic stirrer	JAK Werk, Staufen, Germany
Benchtop Stirrer Mobio 60	Variomag, Daytona Beach, USA
Phase-contrast microscope	Zeiss, Göttingen, Germany
UV/VIS-Spectrometer Ultrospec®3300pro	Amersham Pharmacia Biotech
Alpha Imager Mini	Biozym, Hessisch Oldendorf, Germany
Micro-Dismembrator U	Sartorius, Göttingen, Germany
Eppendorf Mastercycler gradient	Eppendorf, Hamburg, Germany
ThermoCycler Primus 96	Aviso Mechatronic Systems, Jena, Germany
Primus HT cycler	MWG Biotech, Ebersberg, Germany
FlexCycler	Jena Analytik, Jena, Germany
Tecan Hybridization Station HS400Pro	Tecan Austria GmbH, Grödig/Salzburg, Austria
Scanner GenePix 4000B	Axon Instruments, Union City, USA
Bio-flow superclean bench	Heraeus Instruments GmbH, Hanau, Germany
Biostat B plus Fermentor	Sartorius, Göttingen, Germany
Peristaltic Pump 101 U/R	Watson-Marlow Pumps Group, Wilmington, USA
NanoDrop ND-1000 Spectrophotometer	PeqLab, Erlangen, Germany
Electronical scales	Sartorius, Göttingen, Germany
Cuvettes	Ratiolab, Dreieich, Germany
Positively charged nylon membrane	Roche, Mannheim, Germany
Vacuum blotter	Bio-Rad Laboratories, California, USA
20-L Ilmabor Boro 3.3 glass jar	TGI GmbH, Ilmenau,Germany
Screw caps for glass bottles	Schott AG, Mainz, Germany
MasterFlex peroxide-cured silicone tubing	Cole-Parmer, Vernon Hills, USA
Electroporation cuvettes	PeqLab, Erlangen, Germany
Electroporation device	Bio-Rad Laboratories, California, USA
Gas Chromatography	Shimadzu GmbH, Duisburg, Germany
Stabilwax-DA column	Restek Corporation, Bellefonte, USA
Parafilm M® laboratory film	Bemis Flexible Packaging, Oshkosh, USA
Steritop™ filter units	EMD Millipore, Billerica, USA
ScanMaker 1000Xl	Microtek, Willich, Germany
pH electrochemical sensor	Hamilton, Bonaduz, Switzerland

2.2 Anaerobic handling of bacteria

The anaerobic manipulation was carried out in an anaerobic chamber (Coy Laboratory Products Inc., Michigan, USA) containing an atmosphere of 90% nitrogen and 10% hydrogen (Air Liquide, Düsseldorf, Germany). The 2.5 L AnaeroJar Assembly together with the AnaeroGen sachet placed inside (Oxoid Ltd., Basingstoke, England) were utilized for cultivation of *C. acetobutylicum* on agar plates.

Anaerobic Hungate-type tubes or Balch-type serum bottles (Müller+Krempel AG, Bülach, Switzerland) were prepared in a container filled with deionized water. First, they were placed below the water surface and filled with water to make oxygen leave, and then reversed and simultaneously injected with nitrogen until all water was discharged. Afterwards, they were sealed by rubber stoppers plus plastic screw caps for Hungate-type tubes or by aluminum crimp seals for Balch-type serum bottles with a crimper. Prepared Hungate-type tubes and Balch-type serum bottles were autoclaved for 20 min at 121 °C.

2.3 Bacterial strains

In this study, *C. acetobutylicum* and *E. coli* were employed and several insertional mutants of *C. acetobutylicum* were generated. All used and constructed strains are listed in table 6.

Table 6. Strains used in this study

Strains	Genotype	Origin
Clostridium acetobutylicum ATCC 824	Wild type strain	American Type Culture Collection (ATCC)
Escherichia coli TOP10	F^-, *mcr*A, Δ(*mrr-hsd*RMS-*mcr*BC), φ80*lac*ZΔM15, Δ*lac*X74, *rec*A1, *ara*D139, Δ(ara-leu)7697, *gal*U, *gal*K, *rps*L, (Str^R), *end*A1, *nup*G	Invitrogen GmbH, Karlsruhe, Germany
Cac-repA-273a::CT	*C. acetobutylicum* ATCC 824 *repA* (*CA_P0175*) mutant (pSOL1-free)	This study
Cac-fcd-1065a::CT	*C. acetobutylicum* ATCC 824 *fcd* (*CA_C2542*) mutant	This study
Cac-etfA-1128a::CT	*C. acetobutylicum* ATCC 824 *etfA* (*CA_C2543*, from the *etfB-etfA-fcd* cluster) mutant	This study
Cac-etfB-523s::CT	*C. acetobutylicum* ATCC 824 *etfB* (*CA_C2544*, from the *etfB-etfA-fcd* cluster) mutant	This study
Cac-GbRs-303a::CT	*C. acetobutylicum* ATCC 824 *GbRs* (*CA_P0129*) mutant	This study
Cac-adhE1-468s::CT	*C. acetobutylicum* ATCC 824 *adhE1* (*CA_P0162*) mutant	Cooksley *et al.* (2012)
Cac-0059-261s::CT	*C. acetobutylicum* ATCC 824 *CA_P0059* mutant	Cooksley *et al.* (2012)
Cac-spoOJ-257s::CT	*C. acetobutylicum* ATCC 824 *spoOJ* (*CA_P0177*) mutant (pSOL1-free)	This study

Table 6. (continued)

Strains	Genotype	Origin
Cac-htpG-266a::CT	*C. acetobutylicum* ATCC 824 *htpG* (*CA_C3315*) mutant	This study
Cac-fcd/htpG::CT	*C. acetobutylicum* ATCC 824 *fcd/htpG* (*CA_C2542/CA_C3315*) double mutant	This study

The number appearing in the name of the strains represents the insertion site of the intron, and adjacent "s" or "a" was short for sense and antisense (insertion direction of the intron), respectively.

2.4 Plasmids

Table 7. Plasmids used in this study

Plasmid	Characteristic[a]	Origin
pMTL007	Clostridial expression vector for expression of ClosTron containing Erm RAM, Cm^R, IPTG-inducible *fac* promoter	Heap *et al.* (2007)
pMTL007C-E2	Clostridial expression vector for expression of ClosTron containing Erm RAM, Cm^R, constitutive *fdx* promoter	Heap *et al.* (2010b)
pAN2	Plasmid harboring φ3T I methyltransferase gene of *B. subtilis* phage φ3*t*I to methylate shuttle plasmids before their introduction into *C. acetobutylicum*	Heap *et al.* (2007)
pMTL007::cac-fcd-1065a	ClosTron plasmid retargeted to *C. acetobutylicum fcd* (*CA_C2542*) gene (1^{st} try)	This study
pMTL007C-E2::cac-fcd-1065a	ClosTron plasmid retargeted to *C. acetobutylicum fcd* (*CA_C2542*) gene (2^{nd} try)	This study
pMTL007C-E2::cap-repA-273a	ClosTron plasmid retargeted to *C. acetobutylicum repA* (*CA_P0175*) gene	This study
pMTL007C-E2::cac-etfA-1128a	ClosTron plasmid retargeted to *C. acetobutylicum etfA* (*CA_C2543*) gene of the *etfB-etfA-fcd* cluster	This study
pMTL007C-E2::cac-etfB-523s	ClosTron plasmid retargeted to *C. acetobutylicum etfB* (*CA_C2544*) gene of the *etfB-etfA-fcd* cluster	This study
pMTL007C-E2::cap-GbRs-303a	ClosTron plasmid retargeted to *C. acetobutylicum GbRs* (*CA_P0129*) gene	This study
pMTL007C-E2::cap-spoOJ-257s	ClosTron plasmid retargeted to *C. acetobutylicum spoOJ* (*CA_P0177*) gene	This study
pMTL007C-E2::cac-htpG-266a	ClosTron plasmid retargeted to *C. acetobutylicum htpG* (*CA_C3315*) gene	This study

The number appearing in the name of the plasmids represents the insertion site of the target gene by the intron, and adjacent "s" or "a" was short for sense and antisense (insertion direction of the intron), respectively.

[a] Cm^R, chloramphenicol/thiamphenicol resistance gene.

2.5 Bacterial cultivation

2.5.1 Media used for cultivation

Clostridial growth medium (CGM) (Hartmanis and Gatenbeck, 1984a) or CGM agar plate was utilized for general cultivation, mutant generation and recovery of *C. acetobutylicum* strains. When testing the presence of the pSOL1 megaplasmid in mutant cells, the Reinforced Clostridial Agar (RCA) (Fluka, Steinheim, Germany) plates were used. Agar plates of clostridium basal medium (CBM) (O'Brien and Morris, 1971) were employed to test the capability of production of granulose by a *C. acetobutylicum* mutant (*CA_P0129* mutant). For the pre-cultures and main continuous cultures of *C. acetobutylicum* wild type and its mutant derivatives, MMVK (minimal medium for pre-culture) (Bahl *et al.*, 1982) and PLMM (phosphate-limited minimal medium) (Bahl *et al.*, 1982) media were utilized, respectively, with differences in the absence of $K_2HPO_4 \times 3H_2O$ and a lower KH_2PO_4 concentration in PLMM. *E. coli* strains were routinely cultivated in Luria Bertani (LB) (Sambrook, 2001) liquid medium or LB agar plates. The ingredients of each medium are listed below.

Clostridial growth medium (CGM) (Hartmanis and Gatenbeck, 1984a)	
KH_2PO_4	0.75 g
K_2HPO_4	0.75 g
$(NH_4)_2SO_4$	2 g
$MgSO_4 \times 7H_2O$	0.71 g
$MnSO_4 \times H_2O$	0.01 g
NaCl	1 g
Yeast extract	5 g
Asparagine	2 g
$FeSO_4 \times 7H_2O$	0.01 g
Glucose$\times H_2O$	50 g
Deionized water	*ad* 1000 mL

The last three components were dissolved independently and added after autoclaving using a 0.45 μm sterile filter, followed by sparging with nitrogen to ensure the anaerobic condition.

RCA (Fluka, Steinheim, Germany)	
Casein enzymatic hydrolysate	10 g/L
Beef extract	10 g/L
Yeast extract	3 g/L
Dextrose	5 g/L
Sodium chloride	5 g/L
Sodium acetate	3 g/L
Starch soluble	1 g/L
L-Cysteine hydrochloride	0.5 g/L
Agar	13.5 g/L

The pH value of the RCA is 6.8±0.2 (at 25 °C). According to the manual of the manufacturer, 51 g of RCA powder was suspended in 1 L deionized water and then autoclaved for 15 min at 115 °C. Sterile RCA media was directly poured into Petri dishes.

Solidified clostridium basal medium (CBM) (O'Brien and Morris, 1971)	
KH_2PO_4	0.5 g
K_2HPO_4	0.5 g
$MgSO_4 \times 7H_2O$	0.2 g
$MnSO_4 \times H_2O$	7.6 mg
Casein hydrolysate	4 g
p-aminobenzoic acid	1 mg
Biotin	0.002 mg
Thiamine×HCl	1 mg
$FeSO_4 \times 7H_2O$	0.01 g
Glucose×H_2O	50 g
Agar	15 g
Deionized water	*ad* 1000 mL

Vitamins, ferric iron and glucose were dissolved independently and added after autoclaving using a 0.45 μm sterile filter. Sterile CBM medium was directly poured into Petri dishes.

Minimal medium for pre-culture (MMVK) (Bahl *et al.*, 1982)	
$CaCO_3$	1 g
KH_2PO_4	1 g
$K_2HPO_4 \times 3H_2O$	1 g
$(NH_4)_2SO_4$	2 g
$MgSO_4 \times 7H_2O$	0.1 g
$MnSO_4 \times H_2O$	0.01 g
$FeSO_4 \times 7H_2O$	0.015 g
NaCl	0.01 g
$Na_2MoO_4 \times 2H_2O$	0.01 g
$CaCl_2 \times 2H_2O$	0.01 g
p-aminobenzoic acid	2 mg
Biotin	0.1 mg
Thiamine×HCl	2 mg
Resazurin (0.1%, w/v)	1 mL
Glucose×H_2O	20 g
$Na_2S_2O_4$	0.035 g
Deionized water	*ad* 1000 mL

Vitamins, ferric iron and glucose were dissolved independently and added after autoclaving using a 0.45 μm sterile filter. Resazurin and sodium dithionite were used exclusively in media in the fermenter (they were not used for pre-cultures).

Phosphate-limited minimal medium (PLMM) (Bahl *et al.*, 1982)	
KH_2PO_4	1.4 g
$(NH_4)_2SO_4$	40 g
$MgSO_4 \times 7H_2O$	2 g
$MnSO_4 \times H_2O$	0.3 g
$FeSO_4 \times 7H_2O$	0.3 g
NaCl	0.2 g
$Na_2MoO_4 \times 2H_2O$	0.2 g
$CaCl_2 \times 2H_2O$	0.2 g
p-aminobenzoic acid	0.04 g
Biotin	2 mg
Thiamine×HCl	0.04 g
Glucose×H_2O	800 g
Deionized water	*ad* 20 L
	Adjust pH to 2.0 with H_2SO_4

Total volume of this medium was scaled up than what was described in the reference (Bahl *et al.*, 1982) because of extended fermentation duration needed in this study. Vitamins, ferric iron and glucose were dissolved independently in 4 L deionized water and adjusted to pH 2.0. They were then sterilized using a Steritop filter unit (EMD Millipore, Billerica, USA) and added into 16 L autoclaved saline solution.

Luria Bertani (LB) medium (Sambrook, 2001)	
Yeast Extract	5 g
Sodium Chloride	10 g
Tryptone	10 g
Agar (when solid medium was needed)	15 g
Deionized water	*ad* 1000 mL

2.5.2 Media supplements

2.5.2.1 Antibiotics

Stock solutions of antibiotics used in this study were prepared in 70% ethanol or DMF (N,N-dimethylformamide). After complete dilution, each stock solution was dispensed into several 1.5 mL centrifuge tubes by sterile filtration and then stored at -20 °C. The appropriate volume of antibiotic stock solution was added to the liquid or agar medium whose temperature was below 50 °C.

Antibiotic	Stock solution (menstruum)	Final concentration
Chloramphenicol	10 mg/mL (70% EtOH)	12.5 μg/mL in liquid, 25 μg/mL in solid
Tetracycline	10 mg/mL (70% EtOH)	10 μg/mL
Thiamphenicol	15 mg/mL (DMF)	7.5 μg/mL in liquid, 15 μg/mL in solid
Erythromycin	20 mg/mL (70% EtOH)	40 μg/mL

2.5.2.2 IPTG

IPTG (isopropyl β-D-1-thiogalactopyranoside) was employed for the 1st generation of ClosTron system. pMTL007 plasmid contained a *fac* promoter whose expression required IPTG induction. 100 mM (24 mg/mL) of IPTG stock solution was prepared in deionized water and dispensed into 1.5 mL centrifuge tubes with sterile filtration, followed by photophobic storage at -20 °C. The working concentration of IPTG in this study was 1 mM, which meant IPTG stock solution had to be diluted 100-fold when used.

2.5.3 Media preparation for *E. coli*

LB liquid media for *E. coli* were prepared in 500 mL storage bottles in room temperature and autoclaved for 20 min at 121 °C. Agar was premixed (1.5%, w/v) before autoclaving when solidified plates were needed. When the temperature of media decreased below 50 °C after autoclaving, they were supplemented with appropriate antibiotics when necessary. Media for agar plates were poured into Petri dishes in the Bio-flow bench (Heraeus Instruments GmbH, Hanau, Germany). The prepared LB liquid media and agar plates were stored in the 4 °C chamber.

2.5.4 Cultivation of *E. coli* strains

E. coli was routinely cultivated aerobically in test tubes or on agar plates at 37 °C, and appropriate antibiotics were used when necessary. Colonies of *E. coli* grew on LB agar plates which were incubated upside down. For liquid cultures of *E. coli*, colonies were picked using sterile toothpicks and inoculated in test tubes containing 5 mL of LB medium, followed by overnight cultivation on a 180 rpm shaker.

2.5.5 Media preparation for *C. acetobutylicum*

Liquid media (CGM and MMVK) were prepared in 500 mL serum flasks with deionized water and sterilized by autoclaving. Agar was premixed (1.5%, w/v) before autoclaving when solidified plates were needed, except for RCA (Fluka, Steinheim, Germany) which already contained agar. Autoclaving conditions for liquid and solid media were always the same (121 °C, 20 min), apart from that for RCA where requiring 15 min at 115 °C according to the

instruction of the manufacturer. Thermolabile substances, i.e., vitamins, ferrous iron, glucose, as well as antibiotics when necessary, were supplemented after autoclaving with a sterile 0.45 μm filter when temperature of media was below 50 °C. Thereafter, the prepared liquid media was sealed by sterile rubber stoppers and metal screw caps, followed by sparging with nitrogen using needles to make it free of oxygen. Prepared agar media (including RCA) were directly poured into Petri dishes which were then placed in the Bio-flow bench (Heraeus Instruments GmbH, Hanau, Germany) for about two days for complete evaporation of surface water. Subsequently, plates were stored in the anaerobic chamber (Coy Laboratory Products Inc., Michigan, USA).

Liquid media for continuous cultures, i.e. PLMM media, were prepared in a different manner. Salt components of this medium were first dissolved in 16 L deionized water in a 20 L glass storage jar and the pH of this solution was adjusted to 2.0. Afterwards, the jar was autoclaved for 20 min at 121 °C. The solution of ferrous iron, vitamins and glucose was prepared separately in 4 L deionized water and then adjusted to pH 2.0. After sterilization with 500 mL Steritop^{TM} filter units (EMD Millipore, Billerica, USA), it was subsequently added to the autoclaved saline solution whose temperature had been below 80 °C. The resultant PLMM medium was connected and sparged with nitrogen for 30 min to make the media free of oxygen.

2.5.6 Cultivation of *C. acetobutylicum* strains

C. acetobutylicum strains were cultivated in anaerobic conditions at 37 °C in Hungate-type tubes, 100-, 200-mL sealed serum bottles, or a 1 L fermenter (Sartorius, Göttingen, Germany).

For routine cultivation, *C. acetobutylicum* mutants were recovered from stock solutions on CGM agar plates. About 100 μL stock solution of mutant strains was streaked on a CGM agar plate in the anaerobic chamber (Coy Laboratory Products Inc., Michigan, USA) and then plates were cultivated upside down in a 2.5 L anaerobic jar (Oxoid Ltd., Basingstoke, England) for 1-2 days at 37 °C. Subsequently, colonies were picked and inoculated in 5 mL CGM liquid medium in Hungate tubes.

The spore suspension cells of *C. acetobutylicum* wild type were heated for 10 min at 80 °C to kill all vegetative cells and allow germination. Afterwards, 5 mL fresh CGM liquid medium was inoculated with heated spore suspension at a percentage of 10%, followed by cultivation for ~2 days. Cultures that grew in CGM were transferred to another Hungate tube or a serum bottle containing fresh CGM at a percentage of 10%.

For cultivation of *C. acetobutylicum* strains in the fermenter (Sartorius, Göttingen, Germany), mutants and wild type strain were transferred from CGM culture (from stock solutions or spore suspension cells) to 20 mL MMVK medium at a percentage of ~5% and cultivated overnight at 37 °C on a 150 rpm shaker, followed by a second transfer to 90 mL fresh MMVK medium (10%) in the next morning. The well-growing pre-culture was then inoculated into the fermenter vessel containing 650 mL MMVK medium and cultivated overnight under conditions of pH 5.7, 37 °C and 150 rpm of stirring. As soon as the 20 L PLMM medium was connected in the next morning (cultures were well-growing at this time), the growth conditions of *C. acetobutylicum* cultures in the fermenter were set to pH 5.7, 37 °C and 200 rpm of stirring. Afterwards, nutrient conditions gradually became phosphate-limited, consequently cultures were able to enter steady-states acidogenic growth

(pH 5.7) and solventogenic growth (pH 4.5, shifted from pH 5.7). Detailed description concerning continuous cultures is in section 2.6.

2.5.7 Growth measurement

Growth of *C. acetobutylicum* strains was monitored by measuring the OD_{600} of the culture using a UV/VIS-Spectrometer Ultrospec®3300pro (Amersham Pharmacia Biotech). A ~200 µL culture sample was taken from Hungate tubes or serum bottles by a 1-mL syringe and placed in a 1.5 mL centrifuge tube. 100 µL sample was then transferred to a new 1.5 mL centrifuge tube using a pipette and diluted 10-fold with distilled water, followed by measurement against water in disposable plastic cuvettes. The reading was then multiplied by 10 and the resultant value was recorded.

2.5.8 Strain maintenance

After successful transformation of plasmids into *E. coli* competent cells, plates with colonies on were sealed with Parafilm M® laboratory film (Bemis Flexible Packaging, Oshkosh, USA) and stored upside down at 4 °C. Besides, *E. coli* cultures containing plasmids which had been verified and sequenced were transferred to a 2 mL tube equipped with a screw cap (rubber ring inside) and added with glycerol at a final percentage of 25%. After tightly closing the tube, the culture stock solution was well mixed and stored at -80 °C.

C. acetobutylicum wild type strain was maintained as the spore suspension in CGM liquid medium in a Hungate-type tube at room temperature. *C. acetobutylicum* mutant strains generated in this study were maintained in Hungate-type tubes which were supplemented with glycerol (to a final concentration of 25%) and then stored at -80 °C.

2.6 Continuous Fermentation

2.6.1 Fermentation devices

A Biostat B plus fermenter system equipped with a 1 L fermenter (Sartorius, Göttingen, Germany), a 20 L Ilmabor Boro 3.3 glass jar (TGI GmbH, Ilmenau, Germany), MasterFlex peroxide-cured silicone tubing (Cole-Parmer, Vernon Hills, USA) and a peristaltic pump 101 U/R (Watson-Marlow Pumps Group, Wilmington, USA) were utilized for the continuous fermentation of *C. acetobutylicum* strains.

Fermenter was assembled according to the instructions of the manufacturer (Sartorius, Göttingen, Germany). A pH electrochemical sensor (Hamilton, Bonaduz, Switzerland) was employed for real-time monitoring pH, and it was adjusted (pH 7.00 and pH 4.01) by standard pH buffer (WTW, Weilheim, Germany) before use.

2.6.2 Preparation of pre-cultures of strains

C. acetobutylicum type strain and mutants were recovered as described previously (section 2.5.6). Several recovered colonies of mutant strains were picked and inoculated in 5 mL CGM liquid medium using toothpicks in the anaerobic chamber (Coy Laboratory Products Inc., Michigan, USA), followed by cultivation overnight at 37 °C (150 rpm). In the following morning, 1 mL of well-growing culture was sampled, followed by isolation of chromosomal DNA (section 2.7.1.2) for confirmation of the mutation and the presence of pSOL1 megaplasmid using PCR with appropriate primers (Table 39-40, Appendix section). In the evening, 20 mL fresh MMVK medium was inoculated with 1 mL CGM culture of a mutant strain, followed by cultivation overnight at 37 °C (150 rpm). In the next morning, 10 mL of this overnight mutant culture was inoculated in a new anaerobic serum bottle containing 90 mL fresh MMVK medium and the culture was cultivated at 37 °C (150 rpm) until its OD_{600} reached ~2.0 (~10 h after the second transfer in MMVK). It was the pre-culture of *C. acetobutylicum* mutant strains ready for inoculation into the fermenter.

The pre-culture of *C. acetobutylicum* wild type was prepared as that for mutants, except for that CGM inoculum came from heated spore suspension cells (section 2.5.6) and PCR was carried out exclusively for verification of the pSOL1 presence.

2.6.3 Inoculation of pre-cultures into the fermenter

620 mL of MMVK medium (saline components) prepared in a glass cylinder was directly added into the fermenter vessel which was then autoclaved for 20 min at 121 °C. Afterwards, the vessel was connected to the control unit of the Biostat B plus fermenter system (Sartorius, Göttingen, Germany) according to the instruction of the manufacturer. When the temperature of the medium dropped below 40 °C, 30 mL of vitamin solution, ferric iron and glucose was sterilely supplemented via the inoculation well with a 0.45 μm filter. Before inoculating the pre-culture, the inoculation well of the fermenter was flame-treated to ensure sterile condition. 100 mL pre-culture was then injected into the fermenter vessel using a rubber tubing equipped with manual switches at both ends. Pressure in the serum bottle containing the pre-culture drove the injection. Subsequently, the inoculation well was flame-treated again and covered with a cap. pH was then set to 5.7 and stirring was set to 150 rpm.

2.6.4 Start of continuous fermentation

After cultivation overnight, the density of the culture in the fermenter had been appropriate for initiation of continuous fermentation. Therefore, the hose of the jar containing 20 L PLMM medium was connected with the import tubing of the fermenter, thus starting supply of fresh medium whose rate was regulated by a peristaltic pump (Watson-Marlow Pumps Group, Wilmington, USA). To keep the volume of the culture constant, the export of the excess culture was also started by connecting according tubing of the vessel with that of the waste container. This was controlled by a pump on the control unit of the fermenter. Stirring was set to 200 rpm and it was the zero hour of the continuous culture.

2.6.5 Process of the continuous fermentation

After inoculation of the pre-culture of *C. acetobutylicum* strains, fermenter settings were as follows: 150 rpm, pH 5.7 and 37 °C. The pH was controlled by automatic addition of 2 M KOH because acids were produced by the culture. When the culture in the vessel was well-growing after inoculation, acidic PLMM medium was connected and pumped into the vessel. The drainage was also started to keep the volume of the culture constant. Once the continuous fermentation was initiated, stirring was adjusted to 200 rpm, as the only variable. And the culture was growing acidogenically (pH 5.7). About 3~6 days after initiation of the continuous fermentation, cultures entered the steady-state acidogenic growth. This was determined by the OD_{600} of the culture, which was supposed to be hardly changed. And 40 h to ~48 h later, pH was set to 4.5 and accordingly addition of KOH was automatically stopped. The pH of the culture started to decrease due to formation of acids. When pH dropped to 4.5, KOH pump restarted working to keep acidity and the culture grew under more acidic conditions (solventogenesis). Gradually, the OD_{600} of cells became stable at this pH in 1-2 days, and additional 2-3 days later, continuous fermentation was able to be finished and the whole fermentation process was successful.

The dilution rate of the continuous culture was 0.075 h^{-1}, which was equal to the fact that the culture in the fermenter was able to be completely washed out in 13.33 h and 40 h was for 3 rounds of replacement. As a result, at least extra 40 h was necessary before starting the dynamic pH shift (from acidogenesis to solventogenesis) when the culture entered the steady-state acidogenic growth, so was for steady-state solventogenic growth before stopping continuous fermentation.

2.6.6 Sampling from the continuous culture

Samples were taken from the continuous culture every day for the measurement of the OD_{600} and collection of supernatant which was then analyzed by gas chromatography (Shimadzu GmbH, Duisburg, Germany) for detection of concentrations of metabolites. For this, cold 15 mL Falcon centrifuge tubes were used to take samples. 100 µL of sample was then transferred to a 1.5 mL centrifuge tube by a pipette and diluted 10-fold with deionized water, followed by measurement of the OD_{600} against water (section 2.5.7). Centrifugation was simultaneously performed at 4 °C for the tube containing 2 mL culture and supernatant was subsequently transferred to a new 2 mL tube with a screw cap (rubber ring inside). The supernatant was stored at -20 °C.

On the other hand, samples were taken in both steady-states acidogenic growth and solventogenic growth for RNA preparation and subsequent microarray analysis. To this end, 15 mL Falcon centrifuge tubes filled with 3 mL methanol were pre-cooled on ice. After well mixing 10 mL of the culture with methanol, centrifugation was immediately conducted (-20 °C, 9000 rpm) for 10 min. Supernatant was then discarded and the pellet was frozen in liquid nitrogen. Samples for RNA isolation were stored at -80 °C.

In addition, the actual pH shift from acidogenesis to solventogenesis (pH 5.7-pH 4.5) generally lasted ~14 h or more, in these cases time-points at pH 4.5 during a dynamic pH shift were omitted and the last sample taken during the shift was at pH 4.7 or even at pH 4.9, which was dependent on the shift speed. Thereafter, the first sample after the shift was taken 24 h after start of pH shift to measure the OD_{600} and collect the supernatant.

2.7 Technologies for DNA manipulation

2.7.1 DNA isolation

2.7.1.1 Regents for DNA isolation

Stock solutions of Tris-HCl (1 M, pH 8.0) and EDTA (0.5 M, pH 8.0) were used to prepare TE buffer (pH 8.0, containing 10 mM Tris-HCl and 1 mM EDTA). This buffer was then autoclaved for 20 min at 121 °C for inactivation of DNase. 2× T&C buffer and MPC protein precipitation buffer were from Master Pure DNA Purification Kit (Epicentre, Madison, USA). Lysozyme and proteinase K (both from Sigma-Aldrich, Steinheim, Germany) were dissolved with deionized water to a concentration of 20 mg/mL. 70% ethanol (v/v) was prepared by mixing absolute ethanol (molecular biology grade) (AppliChem, Darmstadt, Germany) with deionized water. RNase A (AppliChem, Darmstadt, Germany) was dissolved in deionized water to a concentration of 10 mg/mL, followed by incubation at 95 °C for 10 min to inactivate contained DNase. SDS (sodium dodecyl sulfate) was carefully prepared in deionized water at a percentage of 10%, and phenol and chloroform were utilized in a ventilation hood. Recipe of TE buffer is listed below, which is the same for RNA isolation (section 2.8).

Tris-HCl (1 M, pH 8.0)	
Tris	121.14 g
Deionized water	*ad* 1 L

EDTA (0.5 M, pH 8.0)	
$Na_2EDTA \times 2H_2O$	46.5 g
Deionized water	*ad* 250 mL

TE buffer (pH 8.0)	
Tris-HCl (1 M, pH8.0)	1 mL
EDTA (0.5 M, pH 8.0)	200 µL
Deionized water	*ad* 100 mL

2.7.1.2 Isolation of chromosomal DNA with Master Pure DNA Purification Kit

2 mL fresh overnight culture of *C. acetobutylicum* was centrifugated (12,000 rpm, 2 min) at room temperature and the pellet was re-suspended with 150 µL TE buffer, followed by addition of 30 µL lysozyme (20 mg/mL). After well mixing, the blend was incubated for 30 min at 37 °C and then supplemented with 180 µL 2× T&C buffer and 1 µL proteinase K (20 mg/mL) for cell lysis and protein degradation. After incubation for 15 min at 65 °C during which vortex was performed every 5 min, 210 µL of MPC protein precipitation buffer was added to the sample and mixed for protein precipitation. Subsequently, the sample was centrifugated (12,000 rpm, 10 min) and the supernatant was transferred to a new centrifuge tube. Afterwards, 900 µL cold absolute ethanol was added for precipitation of nucleic acids,

followed by additional centrifugation (12,000 rpm, 10 min). Supernatant was discarded and 70% ethanol was added for washing the pellet. Afterwards, the pellet was dried at room temperature for 10 min and then dissolved with 500 µL-1 mL DNase-free water based on the size of precipitate. 1 µL RNase A (10 mg/mL) was subsequently added in the sample which was then incubated for 30 min at 37 °C for RNA degradation. Finally, chromosomal DNA sample was stored at -20 °C.

2.7.1.3 Isolation of chromosomal DNA using phenol:chloroform method

The methodology for DNA isolation described in section 2.7.1.2 was unsuitable for the chromosomal DNA used for Southern hybridization, probably due to the activity of residual endo-nuclease. Consequently, the phenol:chloroform method (Sambrook and Russell, 2006) was employed for extraction of chromosomal DNA from *C. acetobutylicum* when resultant DNA sample would be used for Southern hybridization.

2 mL fresh culture was centrifugated (12,000 rpm, 2 min) at room temperature and the pellet was washed with 1 mL TE buffer twice. Afterwards, the pellet was re-suspended in 600 µL TE buffer, followed by addition of 200 µL lysozyme (20 mg/mL). After well mixing, the blend was incubated for 1 h at 37 °C and then supplemented with 70 µL 10% SDS for cell lysis, as well as 65 µL EDTA (0.5 M, pH 8.0), 3 µL Tris-HCl (1 M, pH 7.5) and 8 µL proteinase K (20 mg/mL). The sample was then gently mixed by reversion. After additional incubation for 1 h at 37 °C, 180 µL of 5 M $NaClO_4$ was added to the sample and mixed mildly. The mixture was subsequently centrifugated (11,000 rpm, 10 min) and the supernatant (~800 µL) was transferred to a new 2 mL centrifuge tube followed by addition of 500 µL phenol and 500 µL chloroform in the ventilation hood. After reversion for several times, the sample was centrifugated (11,000 rpm, 10 min) and the resultant upper phase was transferred again to a new centrifuge tube and added with cold absolute ethanol for precipitation of nucleic acids. The sample was then centrifugated (11,000, 10 min) at 4 °C and supernatant was discarded. And then, 70% ethanol was added for washing the sample and this step was performed twice. The pellet was dried at room temperature and dissolved in 60 µL DNase-free water. RNase A (10 mg/mL, 2 µL) treatment was performed for 30 min at 37 °C as the last step.

2.7.2 Polymerase chain reaction (PCR)

2.7.2.1 System and program of standard PCR

When several procedures were necessary, e.g., amplifying DNA fragment, screening transformants and integrants, as well as confirming mutation, PCR was an optimal choice. It allowed *in vitro* amplification of specific DNA sequence. In this work, PCR was carried out with Phire Hot Start DNA Polymerase (Finnzymes, Espoo, Finland) in a thermal cycler. dNTP mix (10 mM each) used was from Thermo Scientific (Schwerte, Germany). The composition of the reaction system was according to the instruction of the manufacturer. The reaction program was also based on the manual. Sequences of oligonucleotides (primers) were listed in Appendix section (Table 38-40). The PCR reaction system and program are listed below.

Standard PCR reaction system	
Chromosomal DNA/plasmid DNA	at most 100 ng/10 ng
5× Phire reaction buffer	4 μL
Forward primer (10 μM)	1 μL
Reverse primer (10 μM)	1 μL
dNTP mix (10 mM each)	0.4 μL
Phire Hot Start DNA Polymerase	0.4 μL
Deionized water	*ad* 20 μL

Steps	PCR program	Temperature	Time
1	Denaturation	94 °C	5 min
2	Denaturation	94 °C	45 s
3	Annealing	55-60 °C	45 s
4	Extention	72 °C	1 kb/min
5	Back to 2 (×30)		
6	Extention	72 °C	5 min

Annealing temperature depended on the Tm value of each corresponding primer pair.

2.7.2.2 Splicing by overlap extension (SOE) PCR

In this study, SOE (splicing by overlap extension) PCR (Ho *et al.*, 1989) was employed when mutating retargeting regions of pMTL007 series plasmids. Detailed description concerning this technology was described in section 2.7.3.1.

2.7.2.3 Purification of DNA fragments

After excising desired bands from the agarose gel (section 2.7.4), PCR products and digested plasmid fragments were purified using Wizard® SV Gel and PCR Clean-Up System (Promega GmbH, Mannheim, Germany) strictly based on the instruction of the manufacturer. The purified products was free of primers, buffers, enzymes, etc., which was of importance for the subsequent biochemical reaction, e.g., ligation and labelling. Purified products were directly used or stored at -20 °C.

2.7.3 Plasmid construction

2.7.3.1 Construction of plasmids for targeting *C. acetobutylicum* genes

pMTL007 series plasmids (Heap *et al.*, 2007, 2010a, 2010b) were used for targeting genes of interest in *C. acetobutylicum*, allowing the plasmid-borne Ll.LtrB intron insert into the specified region of the specified gene. Considering the original Ll.LtrB intron on pMTL007 series plasmids was not able to recognize any DNA region (gene) of *C. acetobutylicum* (different origin), several sequences of the intron had to be modified to cope with the requirements for retro-homing (replication and insertion). As the first step, intact DNA

sequence of the gene of interest was used on the ClosTron site (http://www.clostron.com/) to calculate the sites in this gene to which the Ll.LtrB intron was able to be targeted (Perutka *et al.*, 2004; Heap *et al.*, 2007, 2010a, 2010b). Afterwards, one of these sites, usually the one with highest score (strongest possibility of intron retro-homing) by the computer algorithm, was selected and input in another assigned window. As a result, the retargeting region of the intron was designed which was specific for the recognition of the gene of interest by base-pairing. In addition, the primers (EBS2 and EBS1d) for altering the retargeting sequences of the intron were given, together with the IBS primer responsible for splicing. The common EBS Universal primer was also given from the ClosTron website. In addition, the sequence of the retargeting region of the intron was also predicted accordingly (~350 bp).

SOE (splicing by overlap extension) PCR

After four primers were synthesized from Eurofins Genomics (Ebersberg, Germany), the second step of the plasmid construction was to perform a SOE PCR (splicing by overlap extension PCR) (Ho *et al.*, 1989) with the purpose of mutation of three DNA sequences (EBS1d, EBS2 and IBS regions) of the retargeting region of the intron which would insert into the gene of interest in *C. acetobutylicum*. Initially, two independent PCR reactions were carried out using a mixture of IBS/EBS Universal primers and EBS2/EBS1d primers, respectively. The pMTL007 plasmid was utilized as the DNA template. Thereafter, a mixture of these two PCR products was employed as the template in the second round of PCR together with IBS/EBS1d primers. This PCR was to combine two fragments (two PCR products from the first round PCR) of the retargeting region in the intron, because 22 bp of sequences of the EBS Universal primer and the EBS2 primer overlapped. The resultant PCR product (~350 bp) was the intron retargeting region containing three mutated sequences responsible for the recognition of the gene of interest by the intron. The composition and program of these two PCR reactions are listed below. Sequence information of primers (EBS1d, EBS2, IBS) for each gene of interest and of EBS Universal primer are listed in Appendix section (Table 38).

Composition of the 1st PCR	
pMTL007	10 ng
5× Phire reaction buffer	10 μL
IBS or EBS2 primer (5 μM)	2 μL, respectively
EBS Universal or EBS1d primer (5 μM)	2 μL, respectively
dNTP mix (10 mM each)	1 μL
Phire Hot Start DNA Polymerase	1 μL
Deionized water	*ad* 50 μL

Steps	1st PCR program	Temperature	Time
1	Denaturation	94 °C	2 min
2	Denaturation	94 °C	15 s
3	Annealing	55 °C	15 s
4	Extention	72 °C	45 s
5	Back to 2 (×30)		
6	Extention	72 °C	2 min

Composition of the 2nd PCR	
Products of the 1st PCR	1 µL+1 µL
5× Phire reaction buffer	10 µL
IBS primer (5 µM)	2 µL
EBS1d primer (5 µM)	2 µL
dNTP mix (10 mM)	1 µL
Phire Hot Start DNA Polymerase	1 µL
Deionized water	*ad* 50 µL

Steps	2nd PCR	Temperature	Time
1	Denaturation	94 °C	2 min
2	Denaturation	94 °C	15 s
3	Annealing	58 °C	15 s
4	Extention	72 °C	45 s
5	Back to 2 (×30)		
6	Extention	72 °C	2 min

Double digestion of plasmids and inserts

The PCR product of the second round reaction was then separated in 1% agarose gel (section 2.7.4) and the ~350 bp DNA fragment was subsequently excised and purified, as describe in section 2.7.2.4. The retargeting region of the intron (this ~350 bp DNA fragment) harboured recognition sites for both *Bsr*GI and *Hin*dIII restriction enzymes (introduced by EBS1d and IBS primers, respectively; Table 38, Appendix section), so did the pMTL007 series plasmids. Therefore, double digestion with *Bsr*GI and *Hin*dIII (NEB, Frankfurt am Main, Germany) was conducted for both plasmids and the purified DNA fragments (inserts) to form compatible cohesive ends. The digestion reaction lasted 4 h at 37 °C. The ingredients of the digestion reaction are listed below.

Composition of double digestion reaction	
Plasmids or inserts	2 µg
10× NEbuffer 2	5 µL
*Bsr*GI (10 U/µL)	2 µL
*Hin*dIII (20 U/µL)	1 µL
Deionized water	*ad* 50 µL

After digestion with *Bsr*GI and *Hin*dIII restriction enzymes, pMTL007 series plasmids and inserts were visualized using agarose gel electrophoresis (section 2.7.4), followed by excising and purifying the gel, as describe in section 2.7.2.4. When analyzing double-digested pMTL007 series plasmids by electrophoresis, two bands were given. One was ~350 bp (~250 bp for pMTL007C-E2), the other was ~11.5 kb (~8.7 kb for pMTL007C-E2). The ~11.5 kb or ~8.7 kb plasmid backbone was excised and purified.

Ligation of plasmids and inserts

The purified inserts was subsequently ligated into the pMTL007 or pMTL007C-E2 backbone to generate a new plasmid which contained retargeting region specific for the gene of interest. The ligation reaction lasted 16 h at 14 °C with T4 DNA ligase (Thermo Scientific, Schwerte, Germany) and the components of the reaction are listed below.

Composition of ligation reaction	
Plasmids	100 ng
Inserts	Molar ratio 3:1 to plasmids
10× Ligase buffer	3 µL
T4 DNA ligase (10 U/µL)	1 µL
Deionized water	*ad* 30 µL

Transformation of constructed retargeting plasmids into *E. coli*

After incubation for 16 h at 14 °C, the ligation reaction mixture was transformed into *E. coli* TOP 10 competent cells (Invitrogen GmbH, Karlsruhe, Germany; Table 6, section 2.3) by heat shock, and the transformed cells were screened on a LB agar plate (section 2.5.1) supplemented with 25 µg/mL chloramphenicol (Sigma-Aldrich, Steinheim, Germany). Detailed manipulation process of transformation were described in Section 2.9.1.2.

Verification of constructed retargeting plasmids

Approximate 20 h of cultivation allowed *E. coli* chloramphenicol-resistant colonies (transformants) grow on a LB agar plate (section 2.5.1). Several transformants were picked and inoculated in 5 mL LB liquid medium containing 12.5 µg/mL chloramphenicol (Sigma-Aldrich, Steinheim, Germany). After overnight cultivation, 4 mL culture was centrifugated (10,000 rpm, 1 min) and plasmid purification was carried out according to the instruction of the manufacturer, as described in section 2.7.3.2. Plasmids were then digested with *Bsr*GI and *Hin*dIII restriction enzymes (NEB, Frankfurt am Main, Germany) for verification (double digestion, section 2.7.3.1). Correct plasmids result in two bands in agarose gel (Biozym Scientific GmbH, Hessisch Oldendorf, Germany), one was at ~350 bp, the other was at ~11.5 kb (~8.7 kb for pMTL007C-E2). These corresponded to sizes of the insert and the plasmid backbone. In addition, culture PCR was also conducted using primers specific for pMTL007(C-E2) plasmid (pMTL007 check primers or pMTL007C-E2 check primers; Table 40, Appendix section) and 1 µL culture as the template (section 2.7.2.1). A

specific PCR product would be obtained for a plasmid fragment. After these two confirmation steps, correct plasmids were sent for sequencing (Eurofins Genomics, Ebersberg, Germany) using pMTL007 check primer (Forward) or pMTL007C-E2 check primer (Forward). And sequence information obtained were subsequently aligned against predicted sequences of intron retargeting region which was given by the ClosTron site (http://www.clostron.com/).

Re-transformation of retargeting plasmids

Due to the restriction system of *C. acetobutylicum* cells, retargeting plasmids which were transformed into *C. acetobutylicum* had to be methylated to avoid degradation of the plasmid by the endonuclease. Thus, constructed pMTL007 series plasmids were subsequently re-transformed into another *E. coli* recombinant strain containing pAN2 plasmids (Heap *et al.*, 2007) which possessed the gene of a DNA methylase from *Bacillus* phage Φ3T. The transformation process was the same as described in section 2.9.1.2, so was the subsequent bacterial cultivation and plasmid purification (section 2.7.3.2). pMTL007 series plasmids purified after this step was the ultimate retargeting plasmids harbouring specific recognition region to genes of interest. The process of electroporation of plasmids into *C. acetobutylicum* was described below (section 2.9.2).

2.7.3.2 Purification of plasmids

Purification of plasmids was conducted strictly according to the instruction of the manufacturer for AxyPrep^{TM} Plasmid Miniprep Kit (Serva Electrophoresis, Heidelberg, Germany) in which all buffers as well as the silica membrane column were supplied. The methodology employed in this kit was based on the alkaline lysis of bacterial cells. When the lysate was applied to the column, only plasmid DNA could be specifically bound in the column. Chromosomal DNA and proteins were in the flow-through and RNA was degraded in the first step of purification by RNase A (50 mg/mL) supplemented in Buffer S1.

2.7.4 Agarose electrophoresis

DNA or RNA electrophoresis was performed in 1% agarose gel (Biozym Scientific GmbH, Hessisch Oldendorf, Germany) in 1× TAE buffer for ~40 min. Voltage of electrophoresis was generally set to 120 V. Before running the gel, the nucleic acid samples were well mixed with 6× DNA loading dye (Thermo Scientific, Schwerte, Germany) and 1 kb DNA ladder (Thermo Scientific, Schwerte, Germany) was used as the molecular standard. The gel was then soaked in an ethidium bromide (EtBr) bath (10 µg/mL) and visualized under UV light at 302 nm in a Alpha Mini Imager (Biozym, Hessisch Oldendorf, Germany).

50× TAE buffer (pH 8.0)	
Tris	242 g
EDTA (0.5 M, pH 8.0)	100 mL
Acetic acid	57 mL
Deionized water	*ad* 1000 mL

Prepared buffer was autoclaved for 20 min at 121 °C, followed by dilution of 50-fold in a container.

2.7.5 DNA hybridization

2.7.5.1 Digestion of chromosomal DNA

Chromosomal DNA of *C. acetobutylicum* was isolated by the phenol:chloroform method, as previously described (section 2.7.1.3). 30 µg of chromosomal DNA was digested with *Eco*RV-HF® (NEB, Frankfurt am Main, Germany) or *Hin*dIII (NEB, Frankfurt am Main, Germany) enzyme at 37 °C for 16 h, and 2 µL of the digested sample was checked by electrophoresis (section 2.7.4) to ensure complete digestion which was able to be visualized as a smear pattern in a lane of the agarose gel (Biozym Scientific GmbH, Hessisch Oldendorf, Germany). The composition of the digestion reaction was as previously described (section 2.7.3.1), with the only difference in the amount of enzyme used. 3 µL of *Eco*RV-HF® or *Hin*dIII was added into the reaction system.

2.7.5.2 DNA probe labelling

The probe for DNA hybridization was PCR amplified (section 2.7.2.1) using intron specific primers (ISP, Forward and Reverse primers; Table 40, Appendix section) and pMTL007 plasmid the agarose gel (Biozym Scientific GmbH, Hessisch Oldendorf, Germany) containing the PCR product fragment (probe) was purified with Wizard® SV Gel and PCR Clean-Up System (Promega GmbH, Mannheim, Germany) (section 2.7.2.4). The concentration of the probes was determined using a NanoDrop ND-1000 Spectrophotometer (PeqLab, Erlangen, Germany). Afterwards, 1 µg of the probe was biotin-labelled using Biotin DecaLabel DNA Labelling Kit strictly based on the official manual (Thermo Scientific, Schwerte, Germany).

2.7.5.3 Hybridization of probes with digested DNA

Digested chromosomal DNA was separated in 0.8% agarose gel (Biozym Scientific GmbH, Hessisch Oldendorf, Germany) for ~2.5 h at 80 V voltage. Afterwards, the gel was placed on a vacuum blotter (Bio-Rad Laboratories, California, USA) with a piece of positively charged nylon membrane (~100 cm^2; Roche, Mannheim, Germany) under the gel. The rest bare area of the vacuum blotter surface was covered with a plastic cloth to avoid escaping air when vacuuming. Depurination, denaturation and neutralization of DNA were carried out by starting the vacuum pump and pouring the according solution directly on the gel. Depurination and denaturation respectively lasted 30 min, and neutralization was for 20 min. After neutralization, 2 h of DNA transfer from the gel to the positively charged nylon membrane was conducted using a transfer solution (20× SSC solution) and during DNA

transfer 20× SSC solution was supplemented on the gel every 30 min. The positively charged nylon membrane with DNA attached was then rinsed in deionized water shortly, followed by drying in sterile tissues. Afterwards, UV fixation was performed to the nylon membrane for 1 min at 302 nm. Thereafter, the DNA-attached nylon membrane was placed into a hybridization glass tube and pre-hybridization was subsequently performed for 2 h at 42 °C using 10 mL hybridization buffer without probes. And hybridization step was finally carried out with fresh 20 mL hybridization buffer containing biotin-labelled probes (50 ng/mL) for ~16 h at 42 °C. Solutions used in these steps are listed below.

Depurination solution	
HCl (37%)	16.66 mL
Deionized water	*ad* 800 mL

Solution was then autoclaved for 20 min at 121 °C.

Denaturation solution	
NaCl	70.13 g
NaOH	16 g
Deionized water	*ad* 800 mL

Solution was then autoclaved for 20 min at 121 °C.

Neutralization solution	
Tris-HCl	48.46 g (pH 7.5)
NaCl	140.26 g
Deionized water	*ad* 800 mL

Tris was first dissolved in appropriate volume of deionized water and adjusted to pH 7.5 with HCl. Thereafter, NaCl was added and dissolved. Solution was then autoclaved for 20 min at 121 °C.

Transfer solution (20× SSC, pH 7.0)	
NaCl	140.26 g
Trisodium citrate	70.58 g
Deionized water	*ad* 800 mL

Solution was then autoclaved for 20 min at 121 °C.

Maleic acid buffer (pH 7.5)	
Maleic acid	9.29 g
NaCl	7.01 g
NaOH	5.6 g
Deionized water	*ad* 800 mL

This buffer was prepared for dissolving blocking reagent (Roche, Mannheim, Germany).

10% Blocking stock solution	
Blocking reagent (Roche, Mannheim, Germany)	10 g
Maleic acid buffer (pH 7.5)	*ad* 100 mL

Blocking reagent suspension was boiled shortly in a microwave oven and well mixed. Afterwards, it was stored at -20 °C.

Hybridization buffer	
20× SSC (pH 7.0)	12.5 mL
10% Blocking stock solution	5 mL
10% N-lauryl sarcosine	0.5 mL
10% SDS	0.1 mL
Deionized water	*ad* 50 mL

Hybridization buffer was stored at -20 °C when prepared. 10% N-lauryl sarcosine and 10% SDS were prepared in advance (w/v).

2.7.5.4 Detection of hybridization signals

The detection procedure of the positively charged nylon membrane (after hybridizing probes with genomic DNA attached) was conducted in the next morning and strictly based on the instruction of the manufacturer for Biotin Chromogenic Detection Kit (Thermo Scientific, Schwerte, Germany). The hybridized nylon membrane was first washed twice with washing buffer 1 for 10 min at 42 °C, followed by washing two times with washing buffer 2 for 10 min at 65 °C. Thereafter, the hybridized nylon membrane was detected with the reagents supplied in the Biotin Chromogenic Detection Kit. When detection procedure was completed, i.e., desired bands were visible, the hybridized nylon membrane was rinsed with deionized water to stop reactions and subsequently scanned in gray scale using a ScanMaker 1000Xl (Microtek, Willich, Germany). The resultant image was stored in a tagged image file format (TIFF). The ingredients of washing buffers are listed below.

Washing buffer 1	
20× SSC (pH 7.0)	80 mL
10% SDS	8 mL
Deionized water	*ad* 800 mL

Washing buffer 2	
20× SSC (pH 7.0)	4 mL
10% SDS	8 mL
Deionized water	*ad* 800 mL

2.8 RNA technologies

2.8.1 RNA preparation

2.8.1.1 Reagents and implements for RNA preparation

All self-prepared solutions, i.e., TE buffer (pH 8.0), deionized water, DNase buffer, sodium acetate (3.3 M, pH 5.0), and centrifuge tubes (1.5 mL and 0.2 mL), tips and towels were all autoclaved twice for 20 min at 121 °C to completely inactivate RNase. The composition of solutions is listed below and the recipe of TE buffer (pH 8.0) was described previously (section 2.7.1.1).

NaAc (3.3 M, pH 5.0)	
NaAc × $3H_2O$	408.1 g
Deionized water	*ad* 1 L

pH of this solution was adjusted to pH 5.0 using acetic acid (AppliChem, Darmstadt, Germany) in a ventilation hood.

5× DNase Buffer (pH 5.0)	
$MgSO_4$ × $7H_2O$	0.62 g
NaAc (3.3 M, pH 5.0)	15.2 mL
Deionized water	*ad* 100 mL

2.8.1.2 RNA preparation

RNA preparation was carried out based on RNeasy Midi Kit (Qiagen, Hilden, Germany). Samples for RNA isolation was collected as described previously (section 2.6.6). Cell pellets of *C. acetobutylicum* were washed with 1 mL cold TE buffer (pH 8.0) and centrifugated (9000 rpm, 10 min) at -10 °C. After this washing step, the pellet was re-suspended with 500 µL cold TE buffer and subsequently disrupted in a liquid nitrogen-containing shaking flask assembled in a dismembrator (Micro-Dismembrator U, Sartorius, Göttingen, Germany) for 3 min at 1600 rpm. Afterwards, the resultant frozen powder was re-suspended again with 4 mL supplied RLT lysis buffer which had been supplemented with 40 µL mercaptoethanol and transferred to a new 15 mL Falcon tube. After centrifugation (9,000 rpm, 10 min) of the lysate at room temperature, the supernatant was transferred again to a new Falcon tube, followed by addition of 2.8 mL cold absolute ethanol (molecular biology grade; Applichem, Darmstadt, Germany) and shaking the tube for ~5 s. The solution was then transferred to the supplied RNeasy Midi column using a pipette, followed by centrifugation (9,000 rpm, 10 min) at room temperature and three washing steps with supplied washing buffers. The nucleic acid sample bound in the RNeasy Midi column was subsequently eluted by 300 µL of RNase-free water (50 °C). In the next step, nucleic acid sample was transferred to a new 1.5 mL centrifuge tube and DNase treatment was then performed for 3 h at 28 °C using 15 µL RNase-free DNase (10 U/µL; Roche, Mannheim, Germany) and self-prepared RNase-free DNase Buffer (pH 5.0). Afterwards, phenol:chloroform extraction was carried out for inactivation of DNase and extraction of RNA (Sambrook and Russell, 2006). 500 µL phenol was added to the DNase-treated sample and mixed well, followed by centrifugation (12,000 rpm, 3 min) at 4 °C. The upper phase after centrifugation was transferred to a new

centrifuge tube and 500 µL chloroform was then added and mixed well, followed by another centrifugation (12,000 rpm, 3 min) at 4 °C. Upper phase after this step was transferred to a new centrifuge tube and added with 2.5 volume of cold absolute ethanol (molecular biology grade) for RNA precipitation which lasted overnight at -20 °C. Precipitated RNA was centrifugated (13,000 rpm, 30 min, 4 °C) in the next morning and RNA pellet was washed twice with 70% ethanol before it was dried in a towel-contained beaker for 1 h at 37 °C. Thereafter, the RNA sample was dissolved in 20 µL of cold RNase-free water and stored at -80 °C.

2.8.2 Determination of RNA integrity and concentration

To determine the integrity of the RNA sample, routine agarose gel electrophoresis was employed as previously described (section 2.7.4). After staining with ethidium bromide (10 µg/mL), three bands for ribosomal RNA (23S, 16S, 5S) were supposed to be bright and sharp under UV light at 302 nm, which was regarded as the indicator of the RNA sample free of RNase contamination. On the other hand, the concentration of RNA sample was also measured using a NanoDrop ND-1000 Spectrophotometer (PeqLab, Erlangen, Germany). For this, 1 µL RNA sample was transferred to a new centrifuge tube by a pipette and diluted with 9 µL of RNase-free water. And then, 1 µL diluted sample was used for measurement against RNase-free water. In this way, accuracy of measurement was able to achieved because the read for the diluted sample was generally lower than 1000 ng/µL, which was in the accurate measurement range.

2.8.3 Verification of complete removal of chromosomal DNA in RNA samples

RNA samples treated by RNase-free DNase (10 U/µL; Roche, Mannheim, Germany) were confirmed by PCR for absolute elimination of genomic DNA. For this, 600 ng of RNA sample was directly used as the template for amplification of *C. acetobutylicum atpB* gene (*atpB* Forward and Reverse primers, Table 39, Appendix section) and the chromosomal DNA of *C. acetobutylicum* wild type was utilized as a positive control. Only the positive control was supposed to give a band if chromosomal DNA in RNA samples had been completely degraded. The composition and program of PCR was described previously (section 2.7.2.1).

2.8.4 Elimination of residual chromosomal DNA after DNase treatment

In case of chromosomal DNA was not completely degraded by the routine strategy of DNA elimination as described previously (section 2.8.1.2), an additional DNase treatment had to be carried out using TURBO DNA-*free*™ Kit (Ambion, Huntington/Austin, TX, USA). Phenol:chloroform extraction (Sambrook and Russell, 2006) was not applicable when using this kit, thus allowing minimization of RNA loss. The kit was used according to the instruction of the manufacturer. Briefly, supplied 10× TURBO DNase buffer and 1 µL TURBO DNase (2 U/µL) were added to the RNA sample and mixed well, followed by incubation for 30 min at 37 °C. Thereafter, 0.1 volume of the supplied DNase Inactivation Reagent was added and well mixed. After 5 min of incubation at room temperature, centrifugation (12,000 rpm, 2 min) was conducted and upper phase (RNA) was transferred to

a new 1.5 mL centrifuge tube. Precipitating, washing and dissolving RNA was then performed as described previously (section 2.8.1.2).

2.8.5 Reverse Transcription PCR (RT-PCR)

In this work, a RT-PCR was conducted for the quality detection of RNA after its isolation. For this, a OneStep RT-PCR Kit (Qiagen, Hilden, Germany) was employed. Through this RT-PCR reaction system, the original two-step reaction was accomplished in a single tube where the mRNA was reverse-transcribed into the first strand of its complement DNA which was then the template for the *in vitro* amplification reaction. *atpBH* operon was selected as the target for this series of reactions (*atpB* Forward primer and *atpH* Reverse primer, Table 39, Appendix section). After visualization by agarose gel electrophoresis (section 2.7.4), the specificity and sharpness of the resultant PCR product was the quality indicator of the corresponding RNA sample which was subsequently used for transcriptome analysis. The composition and program of the reaction system are shown below.

RT-PCR reaction system	
RNA	600 ng
5× OneStep RT-PCR buffer	5 µL
atpB-Forward (10 µM)	3 µL
atpH-Reverse (10 µM)	3 µL
dNTP mix (supplied in the kit)	1 µL
OneStep RT-PCR Enzyme Mix	1 µL
RNase-free water	*ad* 25 µL

Steps	**RT-PCR reaction program**	**Temperature**	**Time**
1	Reverse transcription	50 °C	30 min
2	Activation of DNA polymerase	95 °C	15 min
3	Denaturation	96 °C	2 min
4	Denaturation	96 °C	30 s
5	Annealing	55 °C	30 s
6	Extention	72 °C	3.5 min
7	Back to 4 (×30)		
8	Extention	72 °C	10 min

2.9 Transformation and mutagenesis

2.9.1 Transformation of plasmids into *E. coli*

2.9.1.1 Preparation of *E. coli* competent cells

E. coli TOP10 competent cells were re-streaked on a LB agar plate without antibiotics. After an overnight cultivation, one clone was picked and inoculated into 5 mL LB medium (without antibiotics) and cultivated for ~15 h at 37 °C. In the next morning, 100 mL fresh LB

medium (without antibiotics) was inoculated with 1 mL overnight culture and cultivated at 37 °C until its OD_{600} reached 0.5-0.6. Culture was then poured into a 50 mL Falcon tube and incubated on ice for 10 min. Collection of cells was then carried out by centrifugation (4,000 rpm, 10 min) at 4 °C, followed by addition of 10 mL cold $CaCl_2$ (100 mM) to re-suspend cells and incubation on ice for 30 min. After another centrifugation (4,000 rpm, 10 min) at 4 °C, supernatant was discarded and fresh 2 mL cold $CaCl_2$ (100 mM) was added and the pellet was re-suspended gently. Afterwards, 2 mL 30% glycerol was supplemented to a final glycerol concentration of 15%. The resultant culture was the competent cells which were dispensed into 1.5 mL centrifuge tubes (50 µL each) and immediately frozen in liquid nitrogen. *E. coli* competent cells prepared were stored at -80 °C.

2.9.1.2 Transformation of ligation mixture or plasmids into *E. coli* competent cells

15 µL ligation reaction mixture (section 2.7.3.1) or purified plasmids (100 ng; section 2.7.3.2) was transformed into *E. coli* TOP 10 competent cells by heat shock. They were added to 50 µL of *E. coli* TOP10 competent cells which had been placed on ice for ~3 min in a Bio-flow bench (Heraeus Instruments GmbH, Hanau, Germany). This mixture was gently blended and incubated on ice for 30 min. Afterwards, it was heat shocked for 90 s at 42 °C and then immediately placed on ice for 2-3 min, followed by addition of 900 µL LB liquid medium without antibiotics and incubation at 37 °C (150 rpm) for 1 h for recovery. Recovered cells were then collected by centrifugation (6,000 rpm, 5 min) at room temperature and re-suspended with fresh 100 µL LB medium. Thereafter, the cells were plated on LB agar plates supplemented with 25 µg/mL chloramphenicol to screen for *E. coli* cells in which retargeting plasmids harbouring a chloramphenicol-resistance gene (*catP*) had been transformed, or on LB plates simultaneously containing 25 µg/mL chloramphenicol and 10 µg/mL tetracycline for screening of methylated pMTL007 series plasmids.

2.9.2 Electroporation of plasmids into *C. acetobutylicum*

2.9.2.1 Early preparation for electroporation

Spore suspension cells of *C. acetobutylicum* wild type strain were recovered as previously described (section 2.5.6). 500 µL fresh wild type culture was transferred to a new Hungate tube containing 5 mL CGM medium for the following overnight cultivation. 50 mL fresh CGM medium was inoculated in the next morning with 1 mL overnight culture and cultivated for ~5 h at 37 °C. As soon as the OD_{600} of the growing culture reached 0.6, electroporation could be started.

2.9.2.2 Preparation of *C. acetobutylicum* competent cells

The following manipulation was conducted in a anaerobic chamber (Coy Laboratory Products Inc., Michigan, USA). And a Falcon tube containing fresh culture or suspended cells was tightly closed when it was under aerobic conditions, i.e., during centrifugation. 40 mL of *C. acetobutylicum* fresh culture was poured into a 50 mL Falcon tube and centrifugated (5000 rpm, 10 min) at 4 °C. Afterwards, the pellet was re-suspended with

20 mL ETM buffer and centrifugated again under the same conditions as above. The resultant pellet was washed (re-suspended) using 10 mL ET buffer and centrifugated again (5000 rpm, 10 min) at 4 °C. The pellet after this process was finally re-suspended with 3 mL ET buffer. The competent cells of *C. acetobutylicum* were now ready for the subsequent electroporation. Recipes of ETM and ET buffers are listed below.

ETM buffer	
Sucrose	9.2 g
$Na_2HPO_4 \times H_2O$	0.001 g
$NaH_2PO_4 \times H_2O$	0.06 g
$MgCl_2 \times 6H_2O$	4.3 g
Deionized water	*ad* 100 mL

This buffer was autoclaved for 20 min at 121 °C.

ET buffer	
Sucrose	9.2 g
$Na_2HPO_4 \times H_2O$	0.001 g
$NaH_2PO_4 \times H_2O$	0.06 g
Deionized water	*ad* 100 mL

This buffer was autoclaved for 20 min at 121 °C.

2.9.2.3 Electroporation of plasmids into *C. acetobutylicum* competent cells

About 8 μg methylated plasmids (section 2.7.3.1, 2.7.3.2, 2.9.1.2) were added to the Falcon tube containing 3 mL *C. acetobutylicum* competent cells. After gently mixing plasmids and cells, 600 μL blend was transferred into a cold electroporation cuvette (4 mm gap; PeqLab, Erlangen, Germany). Conditions of 50 μF, 600 Ω and 1.8 kV were set for the electroporation device (Bio-Rad Laboratories, California, USA). The cold electroporation cuvette was then fixed in the electroporation racket (Bio-Rad Laboratories, California, USA) which was connected with the device. Subsequently, plasmids were electro-transformed into competent cells by starting the device (keeping to press two red buttons simultaneously until a sound 'beep' coming) and the duration time of electroporation was ~15 ms. Thereafter, 5 mL fresh CGM medium was inoculated with 600 μL transformed cells and cultivated at 37 °C for recovery. About 3 h later, cells were centrifugated (9,000 rpm, 10 min) at room temperature and re-suspended with 150 μL fresh CGM medium, followed by plating on a CGM agar plate containing thiamphenicol at a concentration of 15 μg/mL for screening of transformants.

2.9.3 Screening of mutants (integrants) of *C. acetobutylicum*

One to two days after electroporation, colonies (transformants) were visible on agar plates. To screen colonies (integrants, in case when pMTL007C-E2 was used) containing the intron which had inserted at the specific site on the chromosome, transformants were directly transferred to new CGM agar plates containing erythromycin (40 μg/mL) using toothpicks. After an additional day, integrants carrying the mutation of the gene of interest appeared on

the plate. These colonies were overnight cultivated in CGM liquid media and subsequently verified by PCR (section 2.7.2.1) using gene-specific primers (GSP; Table 39, Appendix section) after their chromosomal DNA was isolated (section 2.7.1.2). Correct insertion of the intron into the desired site resulted in a PCR product 1,781 kb (size of the intron) larger than that amplified using wild type chromosomal DNA as template, because GSP flanked the insertion sites. Confirmed culture was then re-spread on a CGM agar plate without antibiotics and in the following day several colonies were picked and inoculated into fresh CGM media. Afterwards, well-growing cultures were verified again by PCR using the chromosomal DNA isolated and corresponding GSP, followed by storage at -80 °C after being supplemented with 30% glycerol in Hungate-type tubes.

When the 1st generation of the ClosTron plasmid pMTL007 was used (only for mutagenesis of *CA_C2542* (*fcd*) gene in the first try), an IPTG induction process had to be carried out after obtaining transformants because an IPTG-inducible *fac* promoter was located on pMTL007 for intron expression. For this step, 5 mL fresh CGM medium (7.5 μg/mL thiamphenicol) was inoculated with a transformant clone and cultivated overnight at 37 °C. On the following morning, 900 μL of fresh CGM medium (7.5 μg/mL thiamphenicol) was inoculated with 100 μL of the overnight culture, followed by cultivation at 37 °C until there was visible growth (generally in 2 h). Afterwards, IPTG stock solution (100 mM; section 2.5.2.2) was added to the culture to a final concentration of 1 mM and culture was then incubated for 1 h at 37 °C for induction. Subsequently, cells were washed with CGM medium, and re-suspended with 1 mL CGM medium without antibiotics, followed by recovery for 3 h at 37 °C. Thereafter, recovered cells were plated on CGM agar plates containing 40 μg/mL erythromycin to select for integrants. Following manipulation was the same as described in the last paragraph.

2.9.4 Confirmation of mutants of *C. acetobutylicum*

The ClosTron mutants generated in this study were verified by three methods. First, standard PCR (section 2.7.2.1) was used to detect the correct insertion of the intron into the chromosome with corresponding gene-specific primers (Table 39, Appendix section) flanking the insertion sites. Second, Southern blotting (section 2.7.5) was employed to confirm that there was only one copy of the intron on the chromosome. An intron-specific probe which was PCR amplified and biotin-labelled was utilized for this DNA hybridization, and in case of pSOL1-free mutants, biotin-labelled gene-specific probes were also employed (section 2.7.5.2). Last but not the least, the presence of the pSOL1 megaplasmid in *C. acetobutylicum* mutant cells was tested using a starch plate test. pSOL1-containing colonies degraded surrounding starch and formed halos when exposed with potassium iodine solution (Lugol) (Carl roth, Karlsruhe, Germany). To this end, Reinforced Clostridial Agar (RCA, Fluka, Steinheim, Germany; section 2.5.1) plates were used and dozens of colonies of a mutant were transferred from a CGM (clostridia growth medium, section 2.5.1) agar plate to a RCA plate using sterile toothpicks. The RCA plate was then cultivated overnight at 37 °C under anaerobic conditions. Lugol solution was directly poured on the RCA plate where mutant colonies grew and was discarded ~1 min later. Halos formed were documented using a Coolpix E5200 digital camera (Nikon, Guangdong, China).

Granulose production was tested for the *GbRs* (*CA_P0129*) mutant and agar-solidified CBM (clostridium basal medium, section 2.5.1) was used (Robson *et al.*, 1974; Steiner *et al.*, 2011a, 2011b). For this, the *GbRs* mutant culture (OD_{600}≈1.0) was spread on a CBM agar plate (half

area), along with the wild type culture (OD_{600}≈1.0) which was plated on the other half section. After cultivation under anaerobic conditions for 24, 48 and 90 h, plates were treated with iodine vapor (potassium iodine solution (Carl roth, Karlsruhe, Germany)) in a ventilation hood. Potassium iodine solution was poured in the cover lid of the plate and the other part of the plate (with colonies growing) was placed on top of the cover lid. About 10 min later, colonies producing granulose became dark blue, while the color was unchanged for non-granulose-forming colonies.

2.10 Transcriptional analysis

2.10.1 RNA labelling

To study the metabolic effects brought by a mutated gene at the transcriptional level, a series of transcriptome analyses were conducted using the microarray platform in our laboratory (Janssen *et al.*, 2010, 2012; Grimmler *et al.*, 2010, 2011; Vasileva *et al.*, 2012; Schwarz *et al.*, 2012). For this, total RNA had to be reverse-transcribed into its complement DNA containing cyanine dye-labelled dCTP (GE Healthcare Europe GmbH, Munich, Germany) whose amount was used as an indicator for the detection of gene expression intensity when slides with hybridized probes and labelled cDNA were subjected to a scanning process. Reverse-transcription was employed using a SuperScript III Reverse Transcriptase Kit (Invitrogen GmbH, Karlsruhe, Germany), random hexamers $p(dN)_6$ (5 μg/μL; Roche, Mannheim, Germany) and dNTPs (Roche, Mannheim, Germany). Ingredients of the reaction are listed below.

Composition of labelling reaction system	
RNA	25 μg
Random hexamers $p(dN)_6$ (5 μg/μL)	4 μL
RNase-free water	*ad* 10 μL

The above ingredients were mixed well in a 0.2 mL centrifuge tube and incubated for 10 min at 70 °C to allow denaturation of RNA and annealing of hexamers and RNA. As soon as the time was up, the sample was immediately placed on ice for ~3 min, followed by a short spin for 3 s. Afterwards, the rest components for RNA labelling were added to the reaction system, and this process was carried out on ice.

Composition of labelling reaction system (continued)	
5× First-strand buffer	4 μL
0.1 M DTT (supplied)	2 μL
dNTP mix (10 mM dATP, dTTP, dGTP; 4 mM dCTP)	2 μL
dCTP ($Cy3^{TM}$ or $Cy5^{TM}$ dye-labelled nucleotide)	1 μL (1,600 pmol)
SuperScript III reverse transcriptase (200 U/μL)	1 μL
	In total 20 μL

The Cy3™ or Cy5™ dye-labelled dCTP, as the last ingredient, was added in dark. Thereafter, the sample was incubated in a thermo cycler for at least 3 h at 42 °C to allow mRNA reverse transcription during which the cyanine dye-labelled dCTP was integrated into the resultant cDNA.

For every RNA sample from a mutant or wild type, both Cy3™ and Cy5™ dye-labelled dCTP were employed. This meant that both Cy3™ dye-labelled and Cy5™ dye-labelled cDNA samples were prepared for every mutant as well as wild type, which was to eliminate influences on gene expression intensity caused by dye bias of certain gene(s).

When reverse transcription of RNA was accomplished (at least 3 h of incubation), samples were taken out of the thermo cycler and immediately placed on ice for ~3 min. Thereafter, a short spin was performed for ~3 s and 2 µL of NaOH (2.5 M) was added to each reaction tube for hydrolyzing the mRNA. Well-mixed samples were placed back in a thermo cycler and incubated for 15 min at 37 °C. Subsequently, samples were placed on ice and 10 µL of 2 M HEPES (4-(2-hydroxyethyl)-1-piperazineethanesulfonic acid) solution was added to each sample for neutralization of reaction. The ultimate reaction product (32 µL) was temporarily stored on ice for subsequent purification.

2.10.2 Purification of labelled cDNA

Labelled cDNA was purified using a QIAquick PCR Purification Kit (Qiagen, Hilden, Germany). 400 µL of supplied PB buffer was added into the supplied column and the labelled cDNA was subsequently added and well-mixed using a pipette. After centrifugation (12,000 rpm, 1 min) at room temperature, the flow-through was transferred back to the column, followed by additional centrifugation (12,000 rpm, 1 min) at room temperature. Thereafter, the column was washed two times with the supplied washing buffer and the cDNA bound in the column was finally eluted with 40 µL supplied EB buffer. The purified cDNA samples in EB buffer was temporarily stored on ice and directly analyzed through microarray experiments.

The concentration of purified labelled cDNA was then determined by a NanoDrop ND-1000 Spectrophotometer (PeqLab, Erlangen, Germany) using a program named “microarray” where concentrations of cDNA and cyanine dye (Cy3™ and Cy5™) were measured. EB buffer supplied in the QIAquick PCR Purification Kit (Qiagen, Hilden, Germany) was used as the control. Ideal concentration of labelled cDNA was ~200 ng/µL and at least 10 pmol/µL was optimal for cyanine dyes.

2.10.3 Preparation of labelled cDNA samples for loading on microarray device

Cy3™- and Cy5™-labelled cDNA samples of wild type were utilized as the reference in microarray experiments. Therefore, labelled cDNA samples of mutants were combined with that of wild type before analysis. Precisely speaking, Cy3™-labelled mutant cDNA was combined with Cy5™-labelled wild type cDNA, and Cy5™-labelled mutant cDNA was combined with Cy3™-labelled wild type cDNA. Two dyes displayed different fluorescence during scanning process (Cy3 for green fluorescence and Cy5 for red). At least 80 pmol of

each cyanine dye was used for one analysis (chip). Mixed cDNA samples (two cyanine dyes) were incubated for 5 min at 100 °C to eliminate any possible second structure. Tom-Freeman (TF) buffer was also incubated for 1 min under the same condition to dissolve the contained SDS. Samples and TF buffer were immediately placed on ice afterwards. Around 3 min later, both samples and TF buffer were centrifugated shortly and TF buffer was added to heat-treated samples to a final volume of 150 µL. This denatured sample in TF buffer was ready for hybridization using a Tecan Hybridization Station HS400Pro (Tecan Austria GmbH, Grödig/Salzburg, Austria).

Tom-Freeman hybridization buffer (Fitzpatrick *et al.*, 2005)	
Deionized formamide	20 mL
50× Denhart's solution	5 mL
20× SSC	12.5 mL
Sodium pyrophosphate (100 mM)	0.5 mL
Tris-HCl (1 M, pH 7.4)	2.5 mL
10% SDS	0.5 mL
Water for HPLC (Sigma-Aldrich, Steinheim, Germany)	*ad* 50 mL

Sterilized by a 0.22 µm filter and did aliquots to 1.5 mL centrifuge tubes. Prepared buffer was stored at -20 °C.

2.10.4 Hybridization of labelled cDNA with probes on slides

Tecan Hybridization Station HS400Pro (Tecan Austria GmbH, Grödig/Salzburg, Austria) was subjected to a washing step by Channel 4 (0.1× SSC) after start of the device. Thereafter, 150 µL denatured sample in TF buffer was injected using a pipette into the hybridization chamber of the device after slides fixed with probes were placed inside (positive side up) and the chamber was clamped. Four slides could be hybridized at the same time. The constitutive program of Tecan Hybridization Station HS400Pro was started subsequently as listed below (including washing and injection steps).

Step	**Description**	**Condition and setting**
1	Washing	45 °C, 30 s; Channel 4
2	Injection of samples	45 °C; Agitation
3	Hybridization	45 °C, 15 h; Agitation frequency: Low High Viscosity Mode: No
4	Washing	25 °C, 2.5 min; Channel 3; Soak time: 30 s
5	Washing	25 °C, 1.17 min; Channel 3
6	Washing	25 °C, 1.17 min; Channel 4; 3 times
7	Drying	30 °C, 3 min; Channel 1; Final Manifold Cleaning

Channels used	Composition
Channel 1	Water
Channel 3	1× SSC/0.2% SDS
Channel 4	0.1× SSC

2.10.5 Quantification of microarray data

Around 16 h later, hybridization and cleaning steps were finished and slides had to be scanned for further analysis. Quantification of slides and normalization of data were performed using a GenePix 4000B Scanner and a GenePix 4.0 or 6.0 software (Axon Instruments, Union City, USA). Pre-scanning was first carried out for determination of irradiation strength of photomultiplier tube (PMT; PMT at 635 nm for Cy5, PMT at 532 nm for Cy3). Irradiation strength was determined by the fluorescence intensity of array spots of housekeeping genes whose expression levels were supposed to be constant and would give an expression ratio of 1:1 when comparing mutant to wild type. Therefore, spots of these genes would show bright yellow colour when scanning during which Cy5 displayed red colour and green fluorescence was for Cy3. When all housekeeping genes showed yellow colour during pre-scanning, according PMT (at 635 nm and 532 nm) irradiation strength could be determined. After this pre-scanning process, main scanning was conducted using the previously-determined PMT irradiation strength and the settings listed below.

Pixel size	10 μm
Lines to average	1
Focus position	0 μm
Scan area	approx. 2000×7000 Pixel

The scanner produced two images for the fluorescence at 532 nm and 635 nm, respectively. And they were stored in a tagged image file format (TIFF).

Image analysis was subsequently performed with GenePix Pro 6.0 software (Axon Instruments, Union City, USA). Two TIFF images were imported in this software and automatically overlapped each other to become a single image. A GenePix array list (.gal) file (Ehrenreich, unpublished data), like a “mask”, was covered on this image to identify features on the image and assign their annotations. This “mask” file contained 32 blocks which matched with the probes spotted on a slide. Each block contained rows of circles surrounding the spots (feature indicators) and placement of feature indicators was automatically controlled by the algorithm of the software. As a result, manually slight adjustment of placement of feature indicators had to be carried out for each spot, because to some extent spots were irregular and might contain impurities. All pixels inside a feature indicator were regarded as the foreground and the local background was defined as entire adjoining pixels within a 3-fold radius of the feature diameter (Ehrenreich, 2006). After identification of all features, the image information was quantified by clicking “analysis” button of the software. The fluorescence signal of each spot was automatically calculated into values which contained the feature foreground, local background and standard deviation for each spot and both dyes, as well as the ratio of medians, ratio of means and regression ratio of red and green channels for each spot. Normalization was conducted by setting the arithmetic mean of the ratios equal to

one. The ratio of medians, ratio of means and regression ratio were three different methods for calculation of expression ratios that were based on different mathematical methods. Each pixel in a spot had intensity values at two wavelengths (PMT 635 nm and PMT 532 nm), so did the background pixel surrounding the spot. The mean fluorescence intensity ratio of a spot (the ratio of median and the ratio of mean) was calculated from the individual pixel intensity where the background pixel intensity had been subtracted. The regression ratio was the linear regression between pixel intensities within a 2-fold radius of the feature diameter and it was independent from strictly defining the background or foreground pixels (Ehrenreich, 2006). The set of data of a microarray experiment was exported in a text (.txt) file format which was then opened with the Excel working sheet (Microsoft, Redmond, USA).

2.10.6 Analysis of transcriptional data

To obtain the actual data from a microarray experiment, fluorescence values of local background plus one standard deviation for two channels (PMT at 635 nm and PMT at 532 nm) had to be subtracted from that of the foreground intensity (background correction) to ensure the signal quality and to prevent artefacts. The resultant strength values were only considered when they were larger than zero, which was the first filtering criterion during data analysis (Ehrenreich, 2006).

The other filtering criterion was the difference between the ratio of medians, the ratio of means and the regression ratio of each spot. Only those features could be taken into account where the deviation of these ratios was less than 30%.

Afterwards, logarithmic ratios (to the basis of 2) of features were selected to represent values of expression ratios due to its convenience of discriminating up- and down-regulated genes. Positive values in logarithmic ratios represent induced genes and repressed genes result in a negative ratio. In addition, fluorescence signals whose logarithmic ratios were greater than 1.60 were regarded as significantly induced, whereas values less than -1.60 indicate significant repression.

For a complete transcriptional analysis, duplicate microarray experiments had to be performed with reverse-labelled samples (dye-flip). This was to prevent dye bias caused by organization of certain nucleotides. The methodology of the dye-flip experiment was identical as what had been described (section 2.10). However, expression ratios obtained in dye-flip experiments had to be reversed to their opposite numbers, becoming actual expression ratios. From two microarray experiments, the average of two expression ratios of one gene was the final ratio of this gene as compared to wild type.

2.11 Determination of concentrations of components in supernatant

2.11.1 Quantitative determination of glucose

The amount of residual glucose in the culture supernatant was measured using D-Glucose Assay (GOPOD) Kit (Megazyme International, Wicklow, Ireland). Supernatant samples were first diluted 40-fold to fulfil the measurement requirement for accuracy (less than 1 mg/mL). By the reaction with glucose oxidase/peroxidase (GOPOD) at 45 °C, D-glucose that remained

in the supernatant was converted with stoichiometric amounts of quinine imine whose absorbance was measured at a wavelength of 510 nm against control (using water instead of sample). According to the absorbance of the glucose standard (1 mg/mL) supplied in the kit, concentrations of glucose in samples could be calculated. The manipulation of measurement and subsequent calculation were done according to the instructions of the manufacturer.

2.11.2 Gas Chromatography (GC) for detection of metabolites in supernatant

To measure fermentation products qualitatively and quantitatively, a Shimadzu GC-2010 gas chromatography (Shimadzu GmbH, Duisburg, Germany) was utilized. It was equipped with a Stabilwax-DA column (Restek Corporation, Bellefonte, USA) and nitrogen was used as the carrier gas.

To calibrate this device before measurement, substances with various known concentrations (0.000001-0.1 g/L) were utilized and their correspondingly measured concentrations were within the calibration limits. Besides, a set of standards (acetone, ethanol, butanol and butyrate) were prepared and quantified at the beginning of the measurement process to check accuracy of assays because concentrations of standards were known. 0.05% 1-propanol was employed in each sample as the internal standard to ensure the accuracy of the metabolite quantification. Its peak area should vary less than 10% between each sample.

For preparation of samples, 100 μL of culture supernatant was blended with 350 μL deionized water (pH 2.5, acidified with HCl) in a glass vessel, followed by addition of 50 μL 1-propanol stock solution (0.5%, w/w) to a final volume of 500 μL. The glass vessel was then tightly closed with a plastic cap. In addition, known concentrations of acetone, ethanol, butanol and butyrate (standards) were mixed and prepared as samples in the same way and their final concentrations were 0.0005%, 0.005% and 0.05%, respectively. Shimadzu GC Solution program (version 2.3; Shimadzu GmbH, Duisburg, Germany) was employed for measurement processes and subsequent data analyses. Concentrations of samples measured were determined by the formula: $((X \times 5 \times 10)/MW) \times 1000$ (mM), where X was the sample percentage obtained during measurement and MW was short for molecular weight. The method used for measurement processes of gas chromatography is listed below.

Time	Temperature
0 min	70 °C
5 min	98 °C
25 min	250 °C

2.11.3 Quantitative determination of acetic acid

The amount of acetic acid produced in the culture was measured using Acetate Assay (K-ACETRM) Kit (Megazyme International, Wicklow, Ireland). The manipulation of measurement and subsequent calculation were done according to the instructions of the manufacturer. Supernatant samples were first diluted 12.5-fold with deionized water to be within the measurement range (0.3-25 μg acetate in a reaction). All reactions were

accomplished in plastic cuvettes (1 cm light path) (Ratiolab, Dreieich, Germany) and at room temperature.

3 Results

In this study, in total 8 mutants were generated using the ClosTron technology (Heap *et al.*, 2007, 2010a, 2010b). They were mutants of *CA_C2542* (*fcd*), *CA_C2543* (*etfA*), *CA_C2544* (*etfB*), *CA_C3315* (*htpG*), *CA_P0175* (pSOL1-free), *CA_P0177* (pSOL1-free), *CA_P0129* (*GbRs*), and a *CA_C2542/3315* (*fcd/htpG*) double mutant. Three genes mutated resides on the pSOL1 megaplasmid of *C. acetobutylicum* (*CA_P0129*, *CA_P0175* and *CA_P0177*), whereas the rest were chromosomal genes. All of these mutants were verified through different methods, i.e., PCR (section 2.7.2.1) confirmation of intron insertion using corresponding gene-specific primers (Table 39, Appendix section) flanking insertion sites, Southern hybridization (section 2.7.5) for testing that there was only one copy of the intron inserted in chromosome, and the starch-containing plate test (section 2.5.1, 2.9.4) for verification of presence of the pSOL1 megaplasmid in *C. acetobutylicum* cells. Thereafter, each mutant was characterized via continuous fermentation (section 2.6). On the other hand, *CA_P0059* and *CA_P0162* (*adhE1*) mutants were obtained from the group of Prof. Nigel P. Minton, University of Nottingham (Cooksley *et al.*, 2012) and they were confirmed by PCR using corresponding gene-specific primers (Table 39, Appendix section) for correct insertion of the intron when conducting their chemostat cultures. Majority of these mutants (6 out of 10) mentioned above were analyzed at the transcriptional level employing a microarray technology (section 2.10) with cell samples from steady-states acidogenic and solventogenic growth of continuous cultures.

3.1 Continuous fermentation of *C. acetobutylicum* wild type strain

The continuous culture of *C. acetobutylicum* features separation of acidogenesis and solventogenesis by adjusting the external pH. The continuous culture of *C. acetobutylicum* wild type was first conducted in this study to understand fermentation profiles of this solvent-producing clostridium. Methods for continuous fermentation were described in detail previously (section 2.6).

During the steady-state acidogenic growth where pH was kept at 5.7, the OD_{600} of the wild type chemostat culture was ~3.9, and main products were acetic acid and butyric acid. The concentration of acetate was ~45 mM and butyrate concentration was ~60 mM. Solvents acetone, butanol and ethanol were also slightly produced during this growth phase with concentrations of ~0.8 mM, ~4.6 mM and ~4 mM, respectively (Fig. 4).

During solventogenesis, pH of the continuous culture of wild type was kept at 4.5 and the OD_{600} of the culture was ~3.8. Acetone and butanol were predominant metabolites with concentrations of ~24 mM and ~39 mM, respectively. Ethanol was also generated (~3.8 mM), which was similar to that during acidogenesis. Concentrations of acids were ~11 mM for acetate and ~13 mM for butyrate, both of which were decreased significantly as compared to acidogenic growth (Fig. 4).

Between acidogenesis (pH 5.7) and solventogenesis (pH 4.5), a dynamic pH shift was carried out by stopping addition of external KOH. pH of the culture declined due to formation of acids by cells and continuous supplementation of PLMM media (phosphate-limited minimal media, section 2.5.1). The pH shift lasted ~14 hours for the wild type strain (see 2.6.6). At the beginning of the pH shift (pH 5.7 to ~5.2), pH value dropped swiftly. However, then it fell

slower and slower afterwards owing to gradual decrease of the acid production, which was caused by a metabolism shift from acidogenesis to solventogenesis. Glucose was utilized as the sole carbon source and it was consumed at a higher level during acidogenesis than during solventogenesis of the wild type chemostat culture, and residual glucose amounts in these two phases were ~64 mM and ~95 mM, respectively (Fig. 4).

3.2 Functional analysis of the *etfB-etfA-fcd* cluster of *C. acetobutylicum*

C. acetobutylicum contains two EtfA/B-dependent dehydrogenases (Nölling *et al.*, 2001). One is the butyryl-CoA dehydrogenase (BCD, CA_C2711), the other is the FAD/FMN-containing dehydrogenase (FCD, CA_C2542). BCD was studied previously and it was demonstrated that *bcd*, *etfA* (*CA_C2709*) and *etfB* (*CA_C2710*) consisted of a *bcs* operon together with *crt* (crotonase coding gene, *CA_C2712*) and *hbd* (β-hydroxybutyryl-CoA dehydrogenase gene, *CA_C2708*) (Boynton *et al.*, 1996).

FCD is the second EtfA/B-dependent dehydrogenase in *C. acetobutylicum* of 467 amino acid length. *fcd* was coupled with the second set of *etfA* (*CA_C2543*) and *etfB* (*CA_C2544*) and the transcription direction of this cluster was *etfB-etfA-fcd* (Nölling *et al.*, 2001). Reports about this cluster are rare, therefore, its roles in physiological metabolism of *C. acetobutylicum* remain unclear. Expression patterns of *fcd*, *etfA* (*CA_C2543*) and *etfB* (*CA_C2544*) clustered genes were shown in a global transcriptional analysis of *C. acetobutylicum* wild type (Grimmler *et al.*, 2011), suggesting they functioned during solventogenic growth of a chemostat culture. In contrast to the *bcs* operon product which plays a role in central C_4 metabolism (Boynton *et al.*, 1996), where EtfA/B-Fcd complex functions is not detected. As a result, mutagenesis of these genes (for the second EtfA/B-dependent dehydrogenase complex) and subsequent analyses of the transcriptome of the mutants were necessary to establish a genome-wide view for functions of the *etfB-etfA-fcd* cluster.

On the other hand, the role of the *bcs* operon is also less understood although a primer extension experiment concerning this has been carried out (Boynton *et al.*, 1996). Therefore, mutagenesis of the *bcd* gene was attempted for numerous times in this study to get insights into functions of this EtfA/B-dependent dehydrogenase (BCD). In total ~500 clones (putative integrants) with retargeted pMTL007 or pMTL007C-E2 plasmid had been screened using identical strategies (section 2.9.3) to other successful mutagenesis. Unfortunately, none of colonies was a mutant with the intron inserted into *bcd* gene, implying mutation in *bcd* was probably lethal. Therefore, the only possibility to study the EtfA/B-dependent dehydrogenase in *C. acetobutylicum* was to analyze a mutant of the second EtfA/B-dependent dehydrogenase complex (EtfA/B-Fcd) by respectively inactivating *fcd* gene (*CA_C2542*) and accompanying *etfA* (*CA_C2543*) and *etfB* (*CA_C2544*) genes.

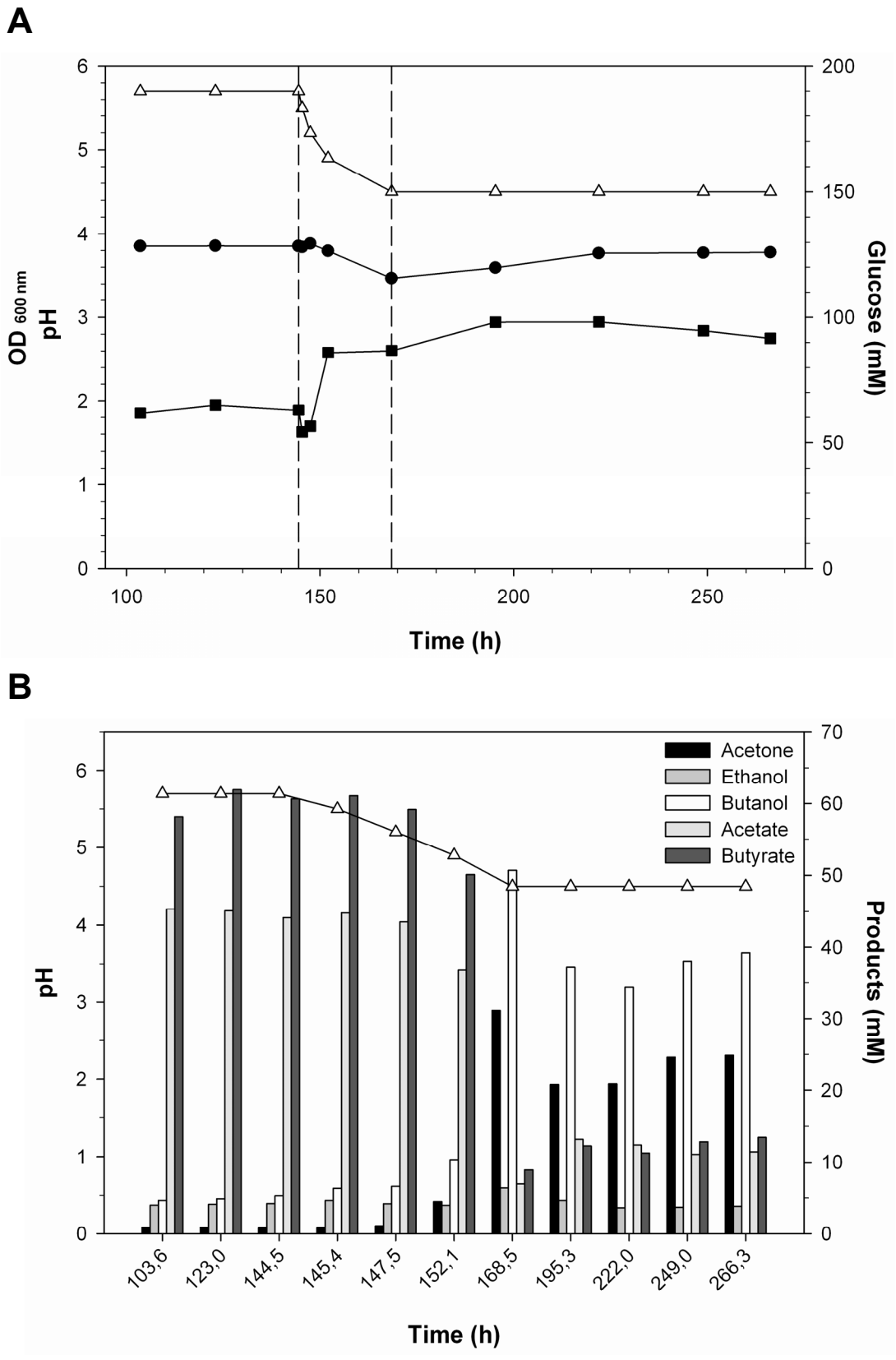

Fig. 4. Fermentation profile of a phosphate-limited continuous culture of *C. acetobutylicum* wild type strain. (A) Growth, glucose consumption and pH in the course of fermentation. Dashed lines indicate the dynamic pH shift. (B) Fermentation products from the steady-state acidogenic growth to solventogenic growth. Each grouped bar set corresponds to each time-point. The experiment was duplicated and the figure represents one exemplary fermentation. Quantification of metabolites was done with an internal standard of known concentration (section 2.11.2). Symbols: *triangles*, pH; *circles*, OD at 600 nm; *squares*, residual glucose concentration

3.2.1 Characterization of the *fcd* mutant

3.2.1.1 Generation of the *fcd* mutant using the ClosTron system

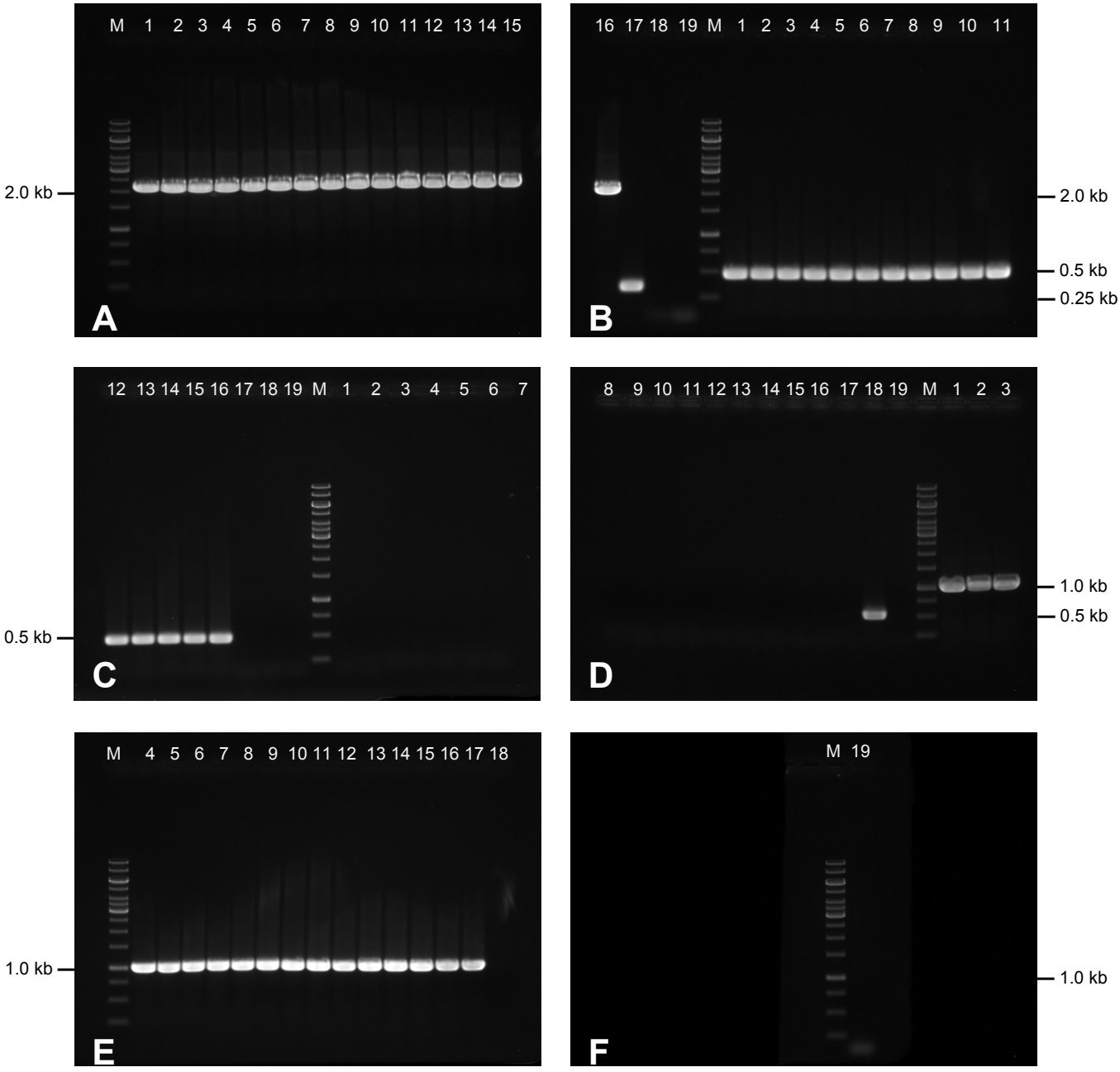

Fig. 5. PCR verification of the *fcd* mutant. (A-B) *fcd* gene-specific primers; (B-C) EBS universal primer and *fcd*-Reverse primer; (C-D) pMTL007C-E2 specific primers; (D-F) *CA_P0175* (*repA*) gene-specific primers. M, marker; lane 1-16, genomic DNA samples from different clones of the *fcd* mutant; lane 17, wild type genomic DNA; lane 18, pMTL007C-E2 plasmid; lane 19, deionized water as the negative control.

The methodology for generation of a ClosTron mutant was introduced in detail previously (section 2.7.3.1, 2.9). Target sites (where the intron could insert) in *fcd* gene (*CA_C2542*)

were predicted using a web-based intron targeting and design tool (www.clostron.com) and a target site with the highest score (9.212) was selected. Consequently, the target site in the *fcd* gene was determined at 1065/1066 bp (the length of the *fcd* gene is 1401 bp) and the intron was predicted to insert into this site at an antisense direction according to information given. In addition, four primers for SOE (splicing by overlap extension) PCR (section 2.7.3.1) (Ho *et al.*, 1989) were simultaneously designed (*fcd*-IBS, *fcd*-EBS1d, *fcd*-EBS2 and EBS universal; Table 38, Appendix section). They were used for the mutation of recognition sites of the intron retargeting region in pMTL007C-E2 whose intron was able to insert into the predicted *fcd* target site by a specific recognition of *fcd* gene with its mutated retargeting region. SOE PCR produced the mutated intron retargeting region which was then ligated with pMTL007C-E2 backbone to generate retargeted intron expression vector specific for *fcd* (pMTL007C-E2::cac-*fcd*-1065a, Table 7, section 2.4). This vector was subsequently transformed into *E. coli* containing pAN2 for *in vivo* methylation (section 2.9.1). Retargeted and methylated pMTL007C-E2::cac-*fcd*-1065a was electroporated into *C. acetobutylicum* (section 2.9.2), followed by screening of thiamphenicol- and erythromycin-resistant colonies (section 2.9.3).

Erythromycin-resistant clones (putative *fcd* mutant) were verified by standard PCR (section 2.7.2.1) using four different primers. *fcd* gene-specific primers (*fcd*-Forward and -Reverse primers, Table 39, Appendix section) were used first. Wild type genomic DNA gave a band at 345 bp, while the correct mutants exhibited products of 2,126 bp, ~1.8 kb larger than that of the wild type, which corresponded to the size of the intron inserted into the target gene (Fig. 5A-B). Another set of primers, an intron specific primer (EBS universal, Table 38, Appendix section) and an *fcd*-Reverse primer, were employed to verify an exon-intron junction part of the mutated gene, leading to a product of 493 bp, whereas the wild type was not supposed to result in a product (Fig. 5B-C). Besides, a primer pair specific for pMTL007C-E2 plasmid (pMTL007CE2check-Forward and -Reverse primers, Table 40, Appendix section) was used for confirmation of the loss of this shuttle vector from mutant cells and only pMTL007C-E2 plasmid control gave a band at 517 bp (Fig. 5C-D). Moreover, *CA_P0175* (*repA*) gene-specific primers (*repA*-Forward and -Reverse primers, Table 39, Appendix section) were used to verify the presence of the pSOL1 megaplasmid which carried key genes for solventogenesis, and products were visible (1,003 bp) in both the *fcd* mutant and the wild type (Fig. 5D-F). Confirmation of the presence of the pSOL1 was necessary when conducting mutagenesis in *C. acetobutylicum*, because several transfers of cultures or colonies were performed before electroporation and during screening, respectively. It was reported that serial subculturing led to loss of the pSOL1 which resulted in a degenerate strain incapable of producing solvents (Nair, 1995; Cornillot *et al.*, 1997). And in case of pSOL1 loss, the constructed strain would in fact be a double mutant with the *fcd* gene and the pSOL1 as a whole mutated.

To further confirm correct insertion of the intron, i.e., that only one copy of the intron had inserted into the *fcd* gene, Southern hybridization was carried out with the intron-specific probe. Detailed methods of the hybridization were described in detail previously (section 2.7.5). 590 bp of intron-specific probe was PCR amplified using intron specific primers (ISP; ISP-Forward and -Reverse primers, Table 40, Appendix section) and pMTL007 plasmid was used as the template. The intron-specific probe (fragment) was located at an intron-erythromycin gene junction section (339-928 bp) in the intron (1,781 bp in length) where 774 bp of erythromycin gene resided (710-1,483 bp). Genomic DNA of the *fcd* mutant as well as that of the wild type were digested with *Eco*RV-HF at 37 °C for 16 hours before they were transferred from an agarose gel to a positively charged nylon membrane which was

then hybridized overnight with the biotin-labeled intron-specific probe at 42 °C. Genomic DNA of the *fcd* mutant exhibited a single band at ~3.6 kb, demonstrating that the *fcd* mutant possessed only one copy of the intron on the chromosome and thus only the *fcd* gene was mutated. No hybridization signal was observed for wild type genomic DNA, as expected, because the intron-specific probe used did not hybridize to any original DNA sequence in *C. acetobutylicum*. Restricted pMTL007C-E2 with *Hin*dIII was used as a positive control, showing a signal at 8.9 kb which was equal to the size of linear pMTL007C-E2 plasmid (Fig. 6A). Consequently, after confirmation by PCR and Southern hybridization, it was proved that a single *fcd* mutant had been generated.

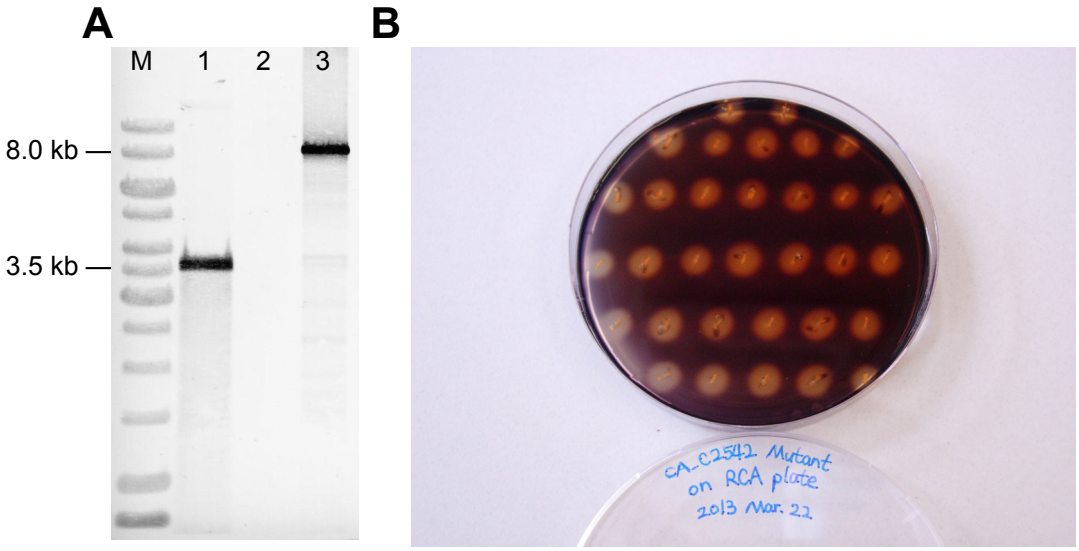

Fig. 6. Southern hybridization and starch plate test of the *fcd* mutant. *Eco*RV-digested genomic DNA samples of the *fcd* mutant and wild type were hybridized with the biotin-labelled intron-specific DNA probe (A). M, marker; lane 1, genomic DNA of the *fcd* mutant; lane 2, wild type genomic DNA; lane 3, pMTL007C-E2 plasmid digested with *Hin*dIII as a positive control. (B) The *fcd* mutant colonies were re-streaked on an agar plate containing starch, colonies still carrying the pSOL1 megaplasmid formed halos when staining with potassium iodine solution

The pSOL1 megaplasmid contains two amylase-coding genes (Nölling *et al.*, 2001) and the presence of these two genes is detected via an iodine-exposed starch plate test (section 2.5.1, 2.9.4). As a result, colonies of a strain which degraded starch in solidified media (forming halos when exposed with iodine) were the ones possessing pSOL1 megaplasmid. About 30 colonies of the *fcd* mutant strain were re-streaked on a RCA (reinforced clostridial agar) solidified plate which contained 1% starch. After 24 h of incubation at 37 °C under anaerobic conditions, colonies still containing pSOL1 degraded the surrounding starch and formed halos when the starch-containing plate was stained with potassium iodine solution (Lugol) solution (Fig. 6B). Through this test, it was demonstrated that the *fcd* mutant strain generated by the ClosTron system still carried the pSOL1 megaplasmid.

3.2.1.2 Continuous fermentation of the *fcd* mutant

After confirming the *fcd* mutant at molecular and phenotypical levels, continuous fermentation was conducted to characterize this strain (Fig. 7) and correct insertion of the intron in the *fcd* gene was monitored by PCR using *fcd* gene-specific primers (*fcd*-Forward and -Reverse primers, Table 39, Appendix section) which flanked the intron insertion site. The chemostat culture of *C. acetobutylicum* allowed separation of acidogenic and solventogenic growth by adjusting the external pH and detailed description of this technology was in section 2.6. During acidogenic growth, the OD_{600} of the *fcd* mutant culture was ~3.6 which was slightly lower than that of the wild type. After ~14 h of the pH shift, the culture of the *fcd* mutant entered solventogenesis, and the final OD_{600} of the culture during the steady-state was ~3.2 which was also lower than the wild type. In terms of glucose consumption, the *fcd* mutant utilized more glucose during acidogenesis than during solventogenesis, which was similar to the wild type strain. However, the *fcd* mutant consumed less glucose than the wild type during both acidogenesis and solventogenesis, which led to slightly lower production of acetic acid (~39 mM) and decreased (~50%) concentrations of acetone and butanol, respectively. During acidogenesis, butyrate concentration was comparable to the wild type, while production of acetone and butanol was significantly reduced (at least 75%) although these were not predominant metabolites during this phase. Besides, ~54% more butyrate was accumulated during solventogenic growth as compared to acetic acid formed (~10 mM) which was comparable to the wild type. Moreover, ethanol formation was also disturbed during both acidogenic and solventogenic growth. The results indicated that *fcd* was positively related to the generation of acetone, butanol and ethanol during acidogenic and solventogenic growth, and butyrate metabolism was also influenced during solventogenic growth due to deletion of the *fcd* gene.

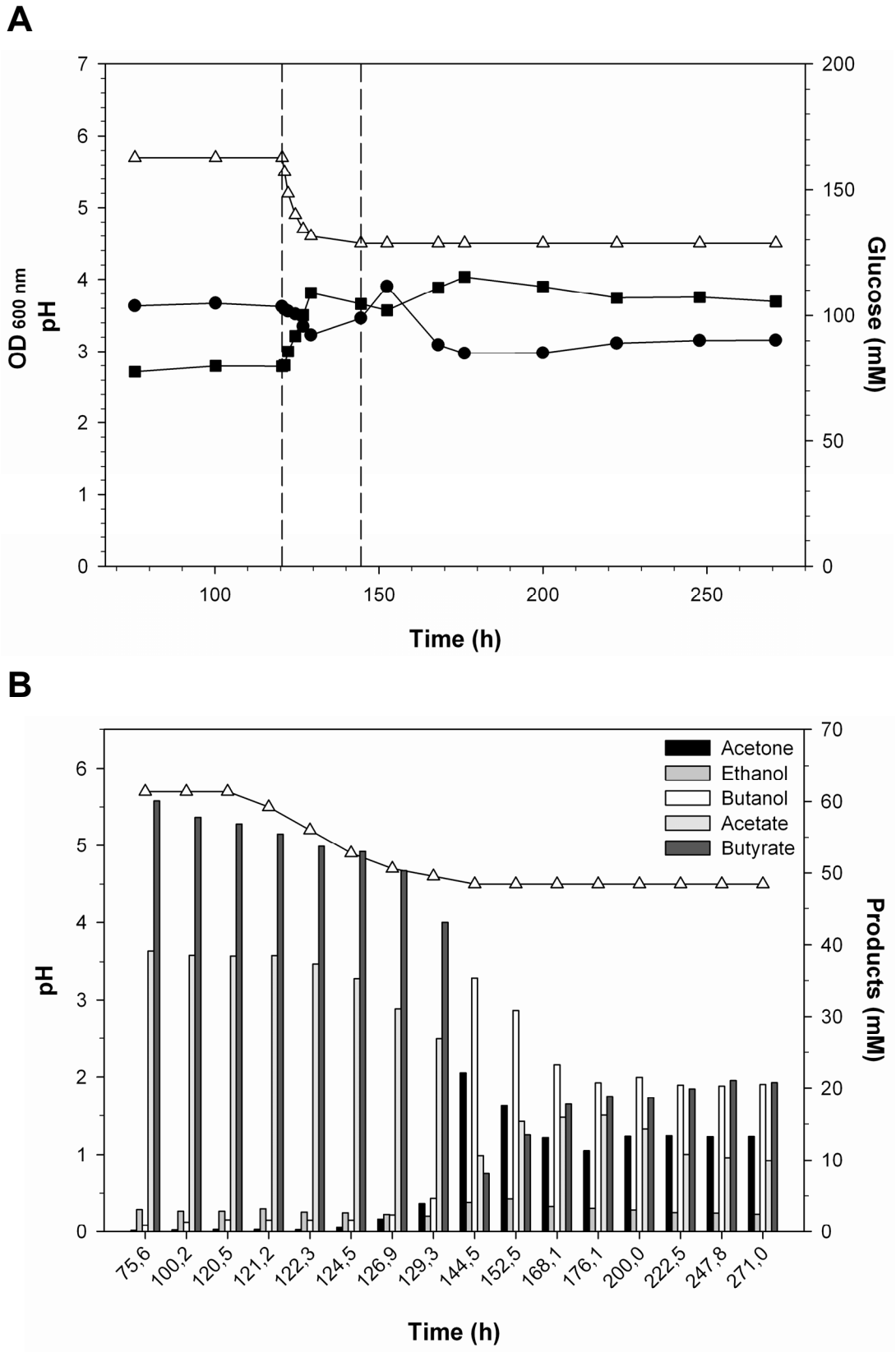

Fig. 7. Fermentation profile of the phosphate-limited continuous culture of the *fcd* mutant. (A) Growth, glucose consumption and pH in the course of fermentation. Dashed lines indicate the dynamic pH shift. (B) Fermentation products from the steady-state acidogenesis to solventogenesis. Each grouped bar set corresponds to each time-point. The fermentation profile of this mutant resembles that of the mutants of the other two genes of the *etfB-etfA-fcd* gene cluster (Fig. 10, 13). Quantification of metabolites was done with an internal standard of known concentration (section 2.11.2). Symbols: *triangles*, pH; *circles*, OD at 600 nm; *squares*, residual glucose concentration

3.2.1.3 Transcriptional analysis of the *fcd* mutant as compared to the wild type

After characterizing the *fcd* mutant in continuous fermentation, microarray experiments were carried out to detect transcriptome changes caused by the *fcd* mutation. Cells of steady-state acidogenic and solventogenic growth of the chemostat culture of the *fcd* mutant were used for RNA isolation and subsequent microarray experiments. RNA samples from the same growth phases of the wild type continuous culture were employed as the reference in transcriptional analyses. Detailed experimental processes of microarray experiments and methods for data analysis were described in section 2.10. Slides covalently coupled with oligonucleotide probes (2 identical spots for 1 gene) were hybridized with combined labelled cDNA containing 80 pmol of Cy3 and Cy5 (GE Healthcare Europe GmbH, Munich, Germany) from the *fcd* mutant and wild type, followed by scanning using a GenePix 4000B microarray scanner and GenePix Pro 4.0 software (Axon Instruments, Union City, USA). The ratio of medians, the ratio of means and the regression ratio were automatically calculated by GenePix Pro 6.0 software (Axon Instruments, Union City, USA) based on intensities of fluorescence signals the *fcd* mutant and wild type (reference) cDNA samples when analyzing scanned microarray images. Normalization was carried out by setting the arithmetic mean of the ratios equal to 1. Background correction was then conducted by subtracting the background value plus one standard deviation from the foreground value. The ratio of medians, the ratio of means and the regression ratio (they differed by less than 30%) were used to correct for spot morphology of features of one hybridization and the ratio of medians was used to calculated for the final ratio (average of the two ratios of medians from two identical spots) which was subsequently taken its logarithm (to the basis of 2). The results from microarray experiments were calculated by mean of one hybridization and its dye-flip hybridization.

As mentioned previously (section 2.10.6), a logarithmic ratio format was used in transcriptional analysis for convenience to tell induced and repressed genes. A positive logarithmic ratio indicated a gene up-regulated in the *fcd* mutant, whereas a negative logarithmic ratio represented a down-regulated gene of the *fcd* mutant as compared to the wild type. In addition, a logarithmic ratio larger than 1.60 was for significant induction in contrast to a ratio less than -1.60 which meant this gene was significantly repressed when the *fcd* gene was mutated. As a result, the higher a positive logarithmic ratio was, the more noticeable a gene was up-regulated in the *fcd* mutant, and a gene was down-regulated more significantly when its negative logarithmic ratio was lower.

Through microarray experiments of the *fcd* mutant, it was found that the expression profiles of most genes responsible for the central metabolic pathways (Fig. 2) were not significantly altered as compared to the wild type. Interestingly, a *pfor* (*CA_C2229*) was repressed by ~60% (did not reach the criterion referred to as "significant", see section 2.10.6) during solventogenic growth of the *fcd* mutant. Pfor functions at the node of pyruvate to acetyl-CoA (Fig. 2). Therefore, it suggested that the *fcd* gene affected carbon flux flowing through the C_4 route. This is in accordance with the decreased glucose consumption of solventogenic cells of the *fcd* mutant (Fig. 7). In addition, an antagonistic expression pattern was observed at pH 5.7 with the two paralogs of aldehyde/alcohol dehydrogenase genes, *adhE1* and *adhE2*. This was similar to what was found previously (Grimmler *et al*., 2011). Moreover, the hydrogenase gene (*CA_C0028*) was induced mildly during the steady-state solventogenic growth. The expression patterns of the central metabolic genes in the *fcd* mutant are listed in Table 8.

Table 8. Expression patterns of the central metabolic genes compared to wild type in the *fcd* mutant during acidogenic and solventogenic growth

ID	Protein function[a]	Ratio[b]	
		pH 5.7	pH 4.5
CA_P0035	AdhE2, aldehyde-alcohol dehydrogenase	1.32	0.52
CA_P0078	ThlB, acetyl coenzyme A acetyltransferase	0.41	0.27
CA_P0162	AdhE1, aldehyde dehydrogenase (NAD^+)	-1.64	1.00
CA_P0163	CtfA, butyrate-acetoacetate CoA-transferase subunit A	-1.45	1.35
CA_P0164	CtfB, butyrate-acetoacetate CoA-transferase subunit B	-1.56	0.96
CA_P0165	Adc, acetoacetate decarboxylase	0.12	0.42
CAC0028	HydA, hydrogene dehydrogenase	0.13	1.13
CAC0267	Ldh, lactate dehydrogenase	-0.49	-0.25
CAC1543	Ldh, lactate dehydrogenase	0.32	0.08
CAC1742	Pta, phosphate acetyltransferase	0.43	-0.16
CAC1743	Ack, acetate kinase	0.09	-0.14
CAC2229	Pfor, pyruvate ferredoxin oxidoreductase	0.12	-1.29
CAC2499	Pfor, pyruvate ferredoxin oxidoreductase	-1.35	—
CAC2708	Hbd, β-hydroxybutyryl-CoA dehydrogenase	0.36	-0.93
CAC2709	EtfA, electron transfer flavoprotein alpha-subunit	0.50	-0.82
CAC2710	EtfB, electron transfer flavoprotein beta-subunit	0.33	-0.68
CAC2711	Bcd, butyryl-CoA dehydrogenase	0.75	-0.31
CAC2712	Crt, crotonase	1.09	-0.32
CAC2873	ThlA, acetyl-CoA acetyltransferase	0.57	-0.95
CAC3075	Buk, butyrate kinase	0.22	-0.26
CAC3076	Ptb, phosphate acetyltransferase	0.52	-0.22
CAC3552	Ldh, lLactate dehydrogenase	0.01	0.01

Genes are listed in order of ORFs, and considered as significantly up-regulated when the logarithmic ratio was ≥1.60 and as significantly down-regulated when the logarithmic ratio was ≤ -1.60. The given values in the table are mean of results of two hybridizations with dye swaps

[a] Protein names based on Nölling *et al.* (2001)

[b] The expression ratio as the logarithm to the basis of 2

On the other hand, transcription of 31 genes in acidogenic cells and 66 genes in solventogenic cells was observed to be strongly induced in the *fcd* mutant, while 9 genes during acidogenesis and 6 genes during solventogenesis showed significant repression. Each was in comparison to the status at the same pH value of the wild type chemostat culture. Results are listed in Table 9-12, respectively.

Table 9. Significantly up-regulated genes compared to wild type in the *fcd* mutant during acidogenic growth

ID	Protein function[a]	Ratio[b]
CA_P0036	Uncharacterized, ortholog of YgaT of *B. subtillis*	1.77
CA_P0148	Phospholipase C	1.82
CAC0102	O-acetylhomoserine sulfhydrylase	2.31
CAC0103	Adenylylsulfate kinase	2.78
CAC0104	Adenylylsulfate reductase	2.58
CAC0105	Ferredoxin	2.37
CAC0106	ABC-type probable sulfate transporter, periplasmic binding protein	2.01

Table 9. (continued)

ID	Protein function[a]	Ratio[b]
CAC0107	ABC-type sulfate transporter, ATPase component	1.70
CAC0383	PTS cellobiose-specific component IIA	6.11
CAC0384	PTS system, cellobiose-specific component BII	5.74
CAC0385	Beta-glucosidase	6.37
CAC0386	PTS cellobiose-specific component IIC	5.64
CAC0387	Hypothetical protein	5.43
CAC0410	Uncharacterized small conserved protein	2.12
CAC0413	Uncharacterized small conserved protein	1.66
CAC0562	Predicted membrane protein	1.90
CAC0563	Predicted membrane protein	1.63
CAC0946	ComE-like protein	1.97
CAC1101	Hypothetical protein	2.27
CAC1360	Uncharacterized protein of BioY family	7.03
CAC1361	Dithiobiotin synthetase	7.42
CAC1362	Adenosylmethionine-8-amino-7-oxononanoate aminotranferase	6.54
CAC2203	Possible hook-associated protein, flagellin family	1.74
CAC2241	Cation transport P-type ATPase	2.16
CAC2242	Predicted transcriptional regulator	2.12
CAC2438	Predicted phosphatase	2.15
CAC2655	Uncharacterized membrane-associated protein	1.77
CAC2681	Hypothetical protein	1.62
CAC2702	Possible signal transduction protein	1.61
CAC2850	Proline/glycine betaine ABC-type transport system, ATPase component	1.80
CAC3379	Uncharacterized protein	1.97

Genes are listed in order of ORFs and considered as significantly up-regulated when the logarithmic ratio was ≥1.60. The given values in the table are mean of results of two hybridizations with dye swaps.

[a] Protein names based on Nölling *et al.* (2001)

[b] The expression ratio as the logarithm to the basis of 2

During the steady-state acidogenic growth of the *fcd* mutant, 31 genes were significantly up-regulated as compared to wild type (Table 9). Among these, 9 genes encoded membrane-associated proteins (*CA_P0148*, *CA_C0383*, *CA_C0384*, *CA_C0385*, *CA_C0386*, *CA_C0387*, *CA_C0562*, *CA_C0563*, *CA_C2655*), suggesting inactivation of *CA_C2542* affected the characteristics of the cell membrane. In addition, 6 genes (*CA_P0036*, *CA_C0410*, *CA_C0946*, *CA_C2438*, *CA_C2702*, *CA_C3379*) were shown to be strongly induced in this phase as compared to wild type where they expressed at highly levels (Janssen *et al.*, 2010), although 5 of them were classified as "uncharacterized, hypothetical or predicted" (Nölling *et al.*, 2001). Noticeably, a putative operon for cysteine synthesis (*CA_C0102-CA_C0110*, *CA_C0108-CA_C0110* did not pass the filter criterion, section 2.10.6) was significantly up-regulated, suggesting an induced sulfur metabolism at pH 5.7 in the *fcd* mutant culture. In addition, the gene for the carbohydrate (Beta-glucoside) metabolism (*CA_C0385*), cation transporter (*CA_C2241*) and the cluster for biotin synthesis (*CA_C1360-CA_C1362*) were also significantly up-regulated.

Table 10. Significantly down-regulated genes compared to wild type in the *fcd* mutant during acidogenic growth

ID	Protein function[a]	Ratio[b]
CA_P0162	AdhE1, Aldehyde dehydrogenase (NAD^+)	-1.64
CAC0570	PTS enzyme II, ABC component	-5.01
CAC2542	FAD/FMN-containing dehydrogenase	-3.28
CAC2772	Permease	-1.78
CAC2952	Tagatose 1,6-diphosphate aldolase	-5.08
CAC2953	Galactose-6-phosphate isomerase	-4.90
CAC2954	Galactose-6-phosphate isomerase	-4.97
CAC2956	PTS system enzyme IIC component (galactitol/fructose specific)	-5.72
CAC2957	PTS system IIB component (galactitol/fructose specific)	-6.97

Genes are listed in order of ORFs and considered as significantly down-regulated when the logarithmic ratio was ≤ -1.60. The given values in the table are mean of results of two hybridizations with dye swaps

[a] Protein name based on Nölling *et al.* (2001)

[b] The expression ratio as the logarithm to the basis of 2

During the steady-state acidogenic growth of the *fcd* mutant, 9 genes were significantly down-regulated as compared to wild type (Table 10). Among these, *CA_C0570* for PTS system enzyme II was strongly repressed, suggesting that carbohydrate transport was likely attenuated. In addition, expression of a cluster (*CAC2952-CAC2957*, *CAC2955* did not pass the filter criterion, section 2.10.6) was shown to be noticeably repressed, which suggested that the putative galactose metabolism and transport of the mutant strain was affected. Besides, a membrane-related protein-coding gene, *CA_C2772*, was also down-regulated.

CA_P0162 (*adhE1*) coding for a bifunctional aldehyde/alcohol dehydrogenase (AdhE1) was also included in this data set, which corresponded to the negligible production of butanol during acidogenesis where its concentration was significantly decreased to ~1 mM as compared to wild type (~4.6 mM).

In summary, the most remarkable down-regulated genes during the steady-state acidogenic growth of the *fcd* mutant chemostat culture were involved in carbohydrate metabolism and transport.

Table 11. Significantly up-regulated genes compared to wild type in the *fcd* mutant during solventogenic growth

ID	Protein function[a]	Ratio[b]
CA_P0004	Cysteine protease	1.63
CA_P0036	Uncharacterized, ortholog of YgaT of *B.subtillis*	3.88
CA_P0037	Uncharacterized, ortholog of YgaS of *B.subtillis*	3.70
CA_P0168	Alpha-amylase	1.65
CAC0014	Aminotransferase	6.12
CAC0015	D-3-phosphoglycerate dehydrogenase	6.12
CAC0016	Related to HTH domain of SpoOJ/ParA/ParB/RepB family, involved in chromosome partitioning	5.14
CAC0017	Seryl-tRNA synthetase	5.74

Table 11. (continued)

ID	Protein function[a]	Ratio[b]
CAC0102	O-acetylhomoserine sulfhydrylase	1.65
CAC0103	Adenylylsulfate kinase	1.90
CAC0104	Adenylylsulfate reductase	1.80
CAC0105	Ferredoxin	1.65
CAC0232	1-Phosphofructokinase (fructoso 1-phosphate kinase)	1.88
CAC0233	PTS system, IIA component	2.08
CAC0242	Predicted permease	3.42
CAC0383	PTS cellobiose-specific component IIA	1.90
CAC0561	Cellulase CelE ortholog, dockerin domain	2.13
CAC0562	Predicted membrane protein	3.21
CAC0563	Predicted membrane protein	3.20
CAC0574	Pectate lyase H	1.76
CAC0662	Sugar ABC transporter, periplasmic sugar-bindind protein	2.09
CAC0663	Hypothetical protein	2.38
CAC0664	Sugar-binding periplasmic protein	1.72
CAC0861	ABC-type multidrug transport system, ATPase component	1.63
CAC0862	Transmembrane protein	1.97
CAC0863	Sensory transduction histidine kinase	2.12
CAC0879	ABC-type polar amino acid transport system, ATPase component	1.69
CAC0892	3-Deoxy-7-phosphoheptulonate synthase	1.77
CAC0897	Fusion chorismate mutase and shikimate 5-dehydrogenase	1.70
CAC0910	Probably cellulosomal scaffolding protein precursor	2.03
CAC0911	Possible processive endoglucanase	1.98
CAC0912	Possible non-processive endoglucanase	2.30
CAC0913	Possible non-processive endoglucanase	1.99
CAC0914	Cellulosome integrating cohesin-containing protein	1.66
CAC0915	Endoglucanase A precursor (endo-1,4-beta-glucanase)	1.66
CAC0929	SAM-dependent methyltransferase	1.61
CAC0930	Cystathionine gamma-synthase	2.70
CAC0980	Pyruvate-formate lyase	2.11
CAC0981	Pyruvate-formate-lyase-activating enzyme	2.43
CAC0983	Hypothetical protein	1.88
CAC1314	Hypothetical protein	1.97
CAC1315	Peptodoglycan-binding domain containing protein	2.28
CAC1360	Uncharacterized protein of BioY family	6.84
CAC1361	Dithiobiotin synthetase	7.02
CAC1363	Superoxide dismutase, Cu-Zn family	2.50
CAC2405	Predicted glycosyltransferase	1.78
CAC2445	5-Aminoimidazole-4-carboxamide ribonucleotide transformylase	1.93
CAC2446	Hypothetical protein	2.48
CAC2517	Extracellular neutral metalloprotease	1.84
CAC2535	Predicted protein	2.65
CAC2536	Glycosyltransferase	3.05
CAC2537	Predicted phosphatase	2.94
CAC2543	Electron-transferring flavoprotein large subunit	2.66
CAC2544	Electron-transferring flavoprotein small subunit	2.69
CAC2545	Hypothetical protein	1.91
CAC2681	Hypothetical protein	2.05
CAC2695	Diverged metallo-dependent hydrolase	1.66
CAC3092	Germination specific amidase	1.80
CAC3157	Tryptophan synthase alpha chain	1.86

Table 11. (continued)

ID	Protein function[a]	Ratio[b]
CAC3158	Tryptophan synthase subunit beta	1.75
CAC3159	Phosphoribosylanthranilate isomerase	1.96
CAC3160	Indole-3-glycerol phosphate synthase	1.73
CAC3161	Anthranilate phosphoribosyltransferase	1.90
CAC3421	Acyl carrier protein phosphodiesterase	2.41
CAC3469	Endoglucanase family	2.49
CAC3470	Hypothetical protein	1.96

Genes are listed in order of ORFs and considered as significantly up-regulated when the logarithmic ratio was ≥1.60. The given values in the table are mean of results of two hybridizations with dye swaps

[a] Protein name based on Nölling *et al.* (2001)

[b] The expression ratio as the logarithm to the basis of 2

During the steady-state solventogenic growth of the *fcd* mutant, 66 genes were significantly up-regulated as compared to wild type (Table 11). Among these, 5 genes encoding membrane-associated proteins (*CA_C0383*, *CA_C0562*, *CA_C0563*, *CA_C0861*, *CA_C0862*) were repressed, suggesting that inactivation of *CA_C2542* affected characteristics of the cell membrane during solventogenesis. In addition, 15 genes (*CA_P0004*, *CA_P0168*, *CA_C0561*, *CA_C0574*, *CA_C0910-CA_C0915*, *CA_C1314-CA_C1315*, *CA_C2405*, *CA_C2517*, *CA_C3469*) were shown to be strongly induced in this phase as compared to wild type where they expressed at highly levels (Janssen *et al.*, 2010), although 6 of them were classified as "possible, hypothetical or predicted" (Nölling *et al.*, 2001). Noticeably, a putative operon for cysteine synthesis (*CA_C0102-CA_C0110*, *CA_C0106-CA_C0110* did not pass the filter criterion, section 2.10.6) and other related genes (*CA_C0929*, *CA_C0930*) for methionine synthesis pathway were significantly up-regulated, which resembled that during acidogenesis, suggesting an increased sulfur metabolism in both phases of the *fcd* mutant chemostat culture. In addition, genes related to carbohydrate metabolism and transport (*CA_C0232*, *CA_C0233*, *CA_C0662*, *CA_C0664*, *CA_C2536*) were also significantly up-regulated. Moreover, a possible transcription unit for serine biosynthesis, *CA_C0014-CA_C0017*, revealed the highest signal value among the regulated genes. This finding was in accordance with elevated expression of genes for cysteine synthesis in the mutant culture, because serine was the precursor for cysteine synthesis. Similarly, the requirement for tryptophan was also probably raised, because the transcription level of related genes was induced at pH 4.5 (*CA_C3157-CA_C3161*). Higher expression of *CA_C0892* and *CA_C0897* implied increased flux in the biosynthesis pathway of chorismate and was consistent with the enhanced tryptophan synthesis. Interestingly, the operon *CA_P0037-CA_P0036* (Janssen *et al.*, 2010) displayed enhanced expression level during solventogenesis, which was also observed during acidogenesis of the *fcd* mutant chemostat culture. Northern blot analysis and DNA microarray experiments had revealed that in wild type chemostat culture this operon was exclusively highly expressed during steady-state acidogenic growth (Janssen *et al.*, 2010). Results obtained in this study indicated the negative regulation of *CA_P0037-CA_P0036* operon by *fcd* gene and their unknown function during solventogenesis. Besides, *CA_C2544* (*etfB*) and *CA_C2543* (*etfA*) were adjacent to *fcd* (*CA_C2542*) gene in chromosome of *C. acetobutylicum* (Nölling *et al.*, 2001) and this cluster displayed comparable expression patterns (Grimmler *et al.*, 2011). Mutation in *fcd* gene, however, resulted in significant induction of upstream *etfB* (*CA_C2544*) and *etfA* (*CA_C2543*) during solventogenic growth, implying a unknown and potential regulation mechanism in between.

Table 12. Significantly down-regulated genes compared to wild type in the *fcd* mutant during solventogenic growth

ID	Protein function[a]	Ratio[b]
CAC0120	Membrane-associated methyl-accepting chemotaxis protein	-1.70
CAC0273	2-Isopropylmalate synthase	-1.68
CAC0975	Predicted P-loop kinase or ATPase distantly related to phosphoenolpyruvate carboxykinase	-1.67
CAC3526	FMN-binding protein	-2.03
CAC3527	Ferredoxin	-1.71
CAC3633	Hypothetical protein	-1.72

Genes are listed in order of ORFs and considered as significantly down-regulated when the logarithmic ratio was ≤ -1.60. The given values in the table are mean of results of two hybridizations with dye swaps

[a] Protein name based on Nölling *et al.* (2001)

[b] The expression ratio as the logarithm to the basis of 2

During the steady-state solventogenic growth of the *fcd* mutant, only 6 genes were significantly down-regulated as compared to the wild type (Table 12). Among these, the most remarkable were two oxidoreductase-coding genes (*CA_C3526* and *CA_C3527*). In the wild type chemostat culture, *CA_C3526* was shown to be highly induced at pH 4.5 (Janssen *et al.*, 2010). This indicated that *CA_C2542* exerted a positive regulation on *CA_C3526*. Other down-regulated genes were those relative to metabolism of amino acids (*CA_C0273*) or gluconeogenesis (*CA_C0975*), as well as chemotaxis (*CA_C0120*).

3.2.2 Characterization of the mutant of the *etfA* of the *etfB-etfA-fcd* cluster

3.2.2.1 Generation of the mutant of the *etfA* of the *etfB-etfA-fcd* cluster

Clustered genes *etfB-etfA-fcd* code for the second EtfA/B-dependent dehydrogenase complex. To further elucidate its roles, *etfA* and *etfB* genes of this cluster were subsequently mutated using the ClosTron system and the resultant mutant strains were characterized using continuous cultures and microarray experiments.

Strategies for generation of an *etfA* ClosTron mutant were identical to that for the *fcd* mutant strain, which were described in detail in Methods and Materials (section 2.7.3.1, 2.9). Target sites (where intron could insert) in *etfA* gene were predicted using a web-based intron targeting and design tool (www.clostron.com) and a target site with the highest score (7.129) was selected. Consequently, the target site in the *etfA* gene was determined at 1128/1129 bp (the length of the *etfA* gene is 1,182 bp) and the intron was predicted to insert into this site at an antisense direction according to information given. In addition, four primers for SOE (splicing by overlap extension) PCR (section 2.7.3.1) (Ho *et al.*, 1989) were simultaneously designed (*etfA*-IBS, *etfA*-EBS1d, *etfA*-EBS2 and EBS universal; Table 38, Appendix section). They were used for the mutation of recognition sites of the intron retargeting region in pMTL007C-E2 whose intron was able to insert into the predicted *etfA* target site by a specific recognition of *etfA* gene via its mutated retargeting region. SOE PCR produced the mutated intron retargeting region which was then ligated with pMTL007C-E2 backbone to generate retargeted intron expression vector specific for *etfA* (pMTL007C-E2::cac-*etfA*-1128a, Table 7,

section 2.4). This vector was subsequently transformed into *E. coli* containing pAN2 for *in vivo* methylation (section 2.9.1). Retargeted and methylated pMTL007C-E2::cac-*etfA*-1128a was electroporated into *C. acetobutylicum* (section 2.9.2), followed by screening of thiamphenicol- and erythromycin-resistant colonies (section 2.9.3).

After electroporation and screening steps, 5 clones of the putative *etfA* mutant were selected and the correct insertion of the intron was verified by PCR and subsequent Southern hybridization. Erythromycin-resistant clones (putative *etfA* mutant) were verified by standard PCR (section 2.7.2.1) using four different primers. *etfA* gene-specific primers (*etfA*-Forward and -Reverse primers, Table 39, Appendix section) were used first. The wild type genomic DNA gave a band at 1,153 bp, while correct mutants exhibited a product of 2,934 bp, ~1.8 kb larger than that of the wild type, which corresponded to the size of the intron inserting into the target gene (Fig. 8A). Another set of primers, an intron specific primer (EBS universal, Table 38, Appendix section) and an *etfA*-Reverse primer, were employed to verify an exon-intron junction part of the mutated gene, leading to a product of 303 bp, whereas the wild type was not supposed to result in a product (Fig. 8B). Besides, a primer pair specific for pMTL007C-E2 plasmid (pMTL007CE2check-Forward and -Reverse primers, Table 40, Appendix section) was used for confirmation of the loss of this shuttle vector from mutant cells and only pMTL007C-E2 plasmid control gave a band at 517 bp (Fig. 8C). Moreover, *CA_P0175* (*repA*) gene-specific primers (*repA*-Forward and -Reverse primers, Table 39, Appendix section) were used to verify the presence of pSOL1 megaplasmid which carried key genes for solventogenesis and products (1,003 bp) were visible in both the *etfA* mutant and the wild type (Fig. 8D). Confirmation of the presence of pSOL1 was necessary when conducting mutagenesis in *C. acetobutylicum*. In case of pSOL1 loss, the strain constructed would in fact be a double mutant with the *etfA* gene and the pSOL1 as a whole mutated.

To further confirm the correct insertion of the intron, i.e., that only one copy of the intron had inserted into the *etfA* gene, Southern hybridization was carried out with the intron-specific probe. Detailed methods of Southern hybridization were described in detail previously (section 2.7.5). 590 bp of the intron-specific probe was PCR amplified using intron specific primers (ISP-Forward and -Reverse primers, Table 40, Appendix section) and pMTL007 plasmid was used as the template. The intron-specific probe (fragment) was located at a intron-erythromycin gene junction section (339-928 bp) in the intron (1,781 bp in length) where a 774 bp of erythromycin gene resided (710-1,483 bp). Genomic DNA of the *etfA* mutant as well as that of the wild type were digested with *Eco*RV-HF at 37 °C for 16 hours before they were transferred from an agarose gel to a positively charged nylon membrane which was then hybridized overnight with the biotin-labeled intron-specific probe at 42 °C. Genomic DNA of the *etfA* mutant exhibited a single band at ~12 kb, demonstrating that the *etfA* mutant possessed only one copy of the intron on the chromosome and thus only the *etfA* gene was mutated. No hybridization signal was observed for wild type genomic DNA, as expected, because the intron-specific probe used did not hybridize to any original DNA sequence in *C. acetobutylicum*. Restricted pMTL007C-E2 with *Hin*dIII was used as a positive control, showing a signal at 8.9 kb which was equal to the size of linear pMTL007C-E2 plasmid (Fig. 9A). Consequently, after confirmation by PCR and Southern hybridization, it was proved that a single *etfA* mutant had been generated.

The presence of the pSOL1 megaplasmid was detected via the iodine-exposed starch plate test (section 2.5.1, 2.9.4), because pSOL1-containing cells degraded starch in solidified media and formed halos when exposed with iodine. To confirm the presence of the pSOL1 in the *etfA* mutant cells, about 45 colonies of the *etfA* mutant strain were re-streaked on a RCA

(reinforced clostridial agar) plate which contained 1% starch. After 24 h of incubation at 37 °C under anaerobic conditions, colonies still containing pSOL1 degraded the surrounding starch and formed halos when the starch-containing plate was stained with potassium iodine solution (Lugol) solution (Fig. 9B). Through this test, it was demonstrated that the *etfA* mutant strain generated by the ClosTron system still carried the pSOL1 megaplasmid.

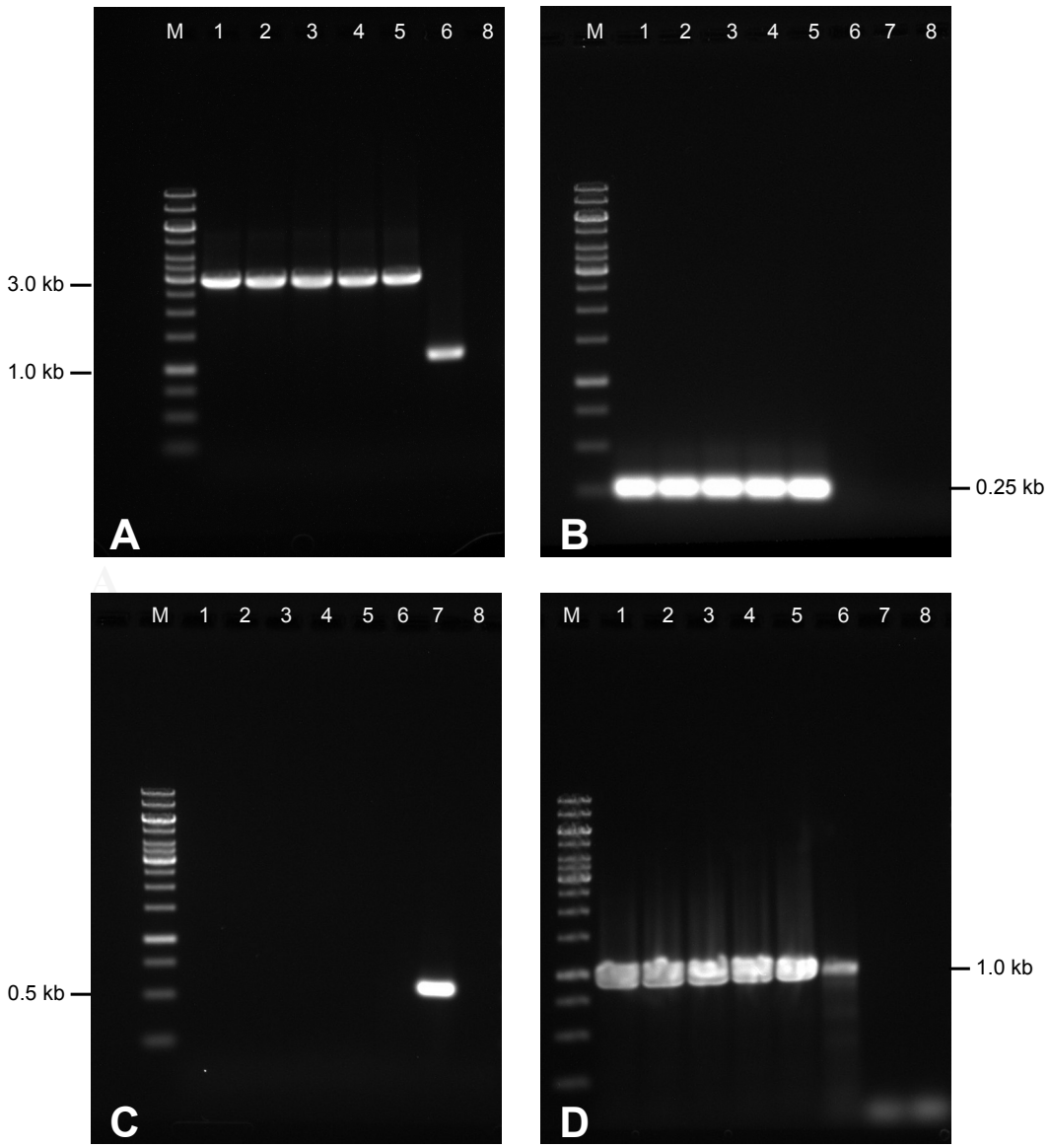

Fig. 8. PCR verification of the *etfA* mutant. (A) *etfA* gene-specific primers; (B) EBS universal primer and *etfA*-Reverse primer; (C) pMTL007C-E2 specific primers; (D) *CA_P0175* (*repA*) gene-specific primers. M, marker; lane 1-5, genomic DNA samples from different clones of the *etfA* mutant; lane 6, wild type genomic DNA; lane 7, pMTL007C-E2 plasmid; lane 8, deionized water as the negative control

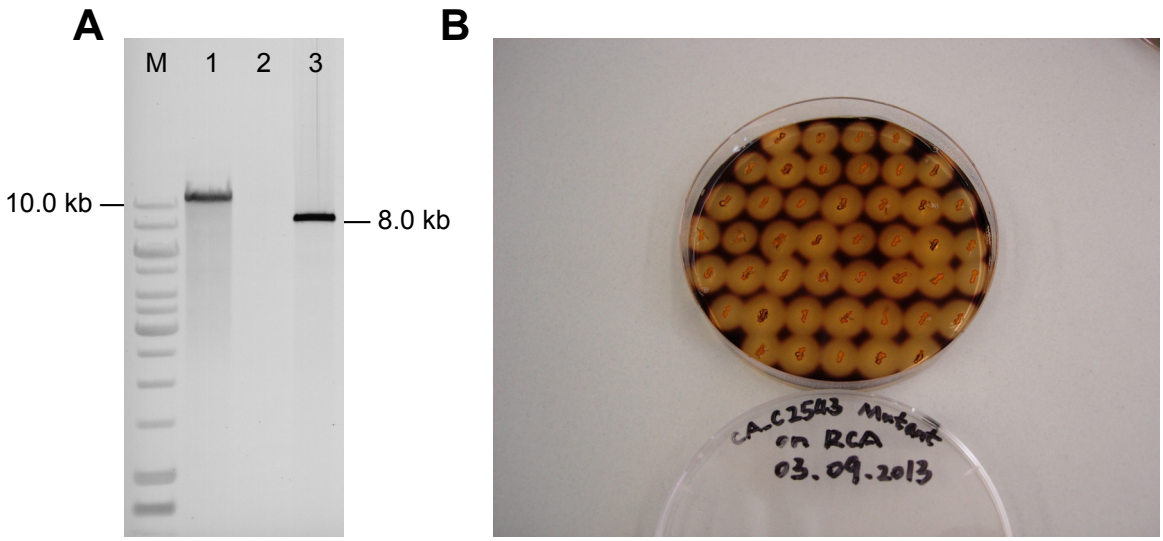

Fig. 9. Southern hybridization and starch plate test of the *etfA* mutant. *Eco*RV-digested genomic DNA samples were hybridized with biotin-labelled intron-specific DNA probe (A). M, marker; lane 1, genomic DNA of the *etfA* mutant; lane 2, wild type genomic DNA; lane 3, pMTL007C-E2 digested with *Hin*dIII as a positive control. (B) The *etfA* mutant colonies were re-streaked on an agar plate containing starch, colonies still carrying the pSOL1 megaplasmid formed halos when staining with potassium iodine solution

3.2.2.2 Continuous fermentation of the mutant of the *etfA* of the *etfB-etfA-fcd* cluster

After verifying the *etfA* mutant at molecular and phenotypical levels, continuous fermentation was performed to characterize this mutant strain (Fig. 10) and correct insertion of the intron in the *etfA* gene was monitored by PCR using *etfA* gene-specific primers (*etfA*-Forward and -Reverse primers, Table 39, Appendix section) which flanked the intron insertion site. Methods for chemostat culture of *C. acetobutylicum* were described in detail previously (section 2.6).

During acidogenic growth of the continuous culture of the *etfA* mutant, the OD_{600} was ~3.8 which was comparable to that of the wild type. After 22 h of the pH shift, the *etfA* mutant culture entered solventogenesis, and the final OD_{600} of the culture in the steady-state was ~3.3, which was lower than the wild type. In terms of glucose consumption, the *etfA* mutant utilized more glucose during acidogenesis than during solventogenesis, which was similar to the wild type strain. However, the *etfA* mutant consumed less glucose than the wild type during both acidogenic and solventogenic growth, which led to slightly lower production of acetic acid (~38 mM) and decreased (~33%) concentrations of acetone and butanol, respectively. During acidogenesis, butyrate concentration was comparable to the wild type, while production of acetone and butanol was reduced (at least 37%) although these were not predominant metabolites during this phase. Besides, a little more butyrate was accumulated during solventogenic growth, whereas acetic acid formed (~10 mM) was comparable to the wild type during this phase. Moreover, ethanol formation was also altered during both acidogenic and solventogenic growth. The results indicated that the *etfA* of the *etfB-etfA-fcd* cluster was positively related to the generation of all three solvents during acidogenic and solventogenic growth, and mutation of this gene also slightly affected butyrate metabolism during solventogenesis.

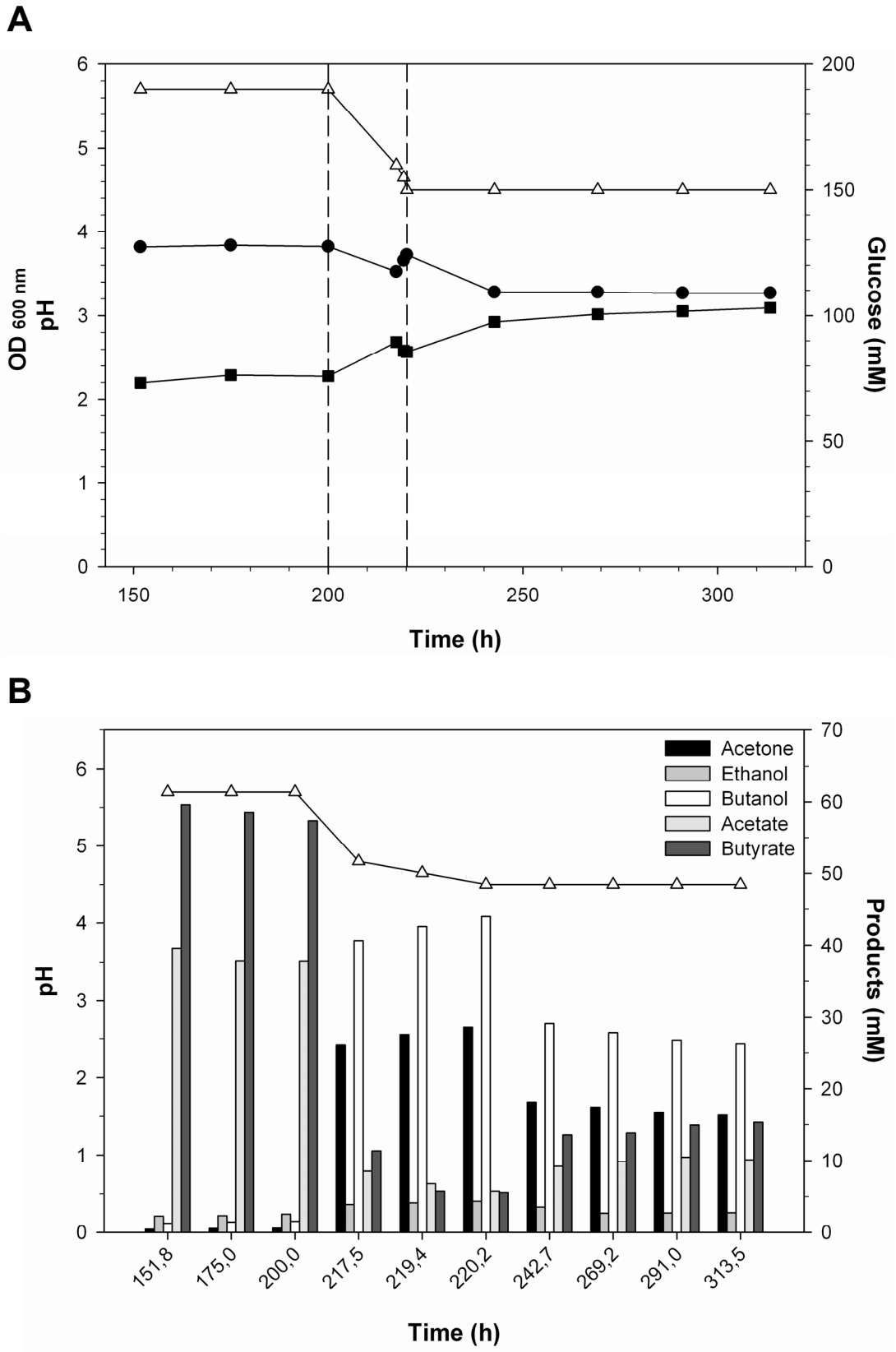

Fig. 10. Fermentation profile of the phosphate-limited continuous culture of the *etfA* mutant. (A) Growth, glucose consumption and pH in the course of fermentation. Dashed lines indicate the dynamic pH shift. (B) Fermentation products from the steady-state acidogenesis to solventogenesis. Each grouped bar set corresponds to each time-point. The fermentation profile of this mutant resembles that of the mutants of the other two genes of the *etfB-etfA-fcd* gene cluster (Fig. 7, 13). Quantification of metabolites was done with an internal standard of known concentration (section 2.11.2). Symbols: *triangles*, pH; *circles*, OD at 600 nm; *squares*, residual glucose concentration

3.2.2.3 Transcriptional analysis of the mutant of the *etfA* of the *etfB-etfA-fcd* cluster as compared to the wild type

After characterizing the *etfA* mutant in continuous fermentation, microarray experiments were conducted to detect transcriptome changes caused by inactivation of the *etfA* gene of the *etfB-etfA-fcd* cluster. Cells of steady-state acidogenic and solventogenic growth of the chemostat culture of the *etfA* mutant were used for RNA preparation and the following microarray experiments. cDNA samples from the same growth phases of the wild type continuous culture were utilized as the reference in transcriptional analyses. Detailed experimental processes concerning microarray experiments and methods for data analysis were described in Materials and Methods (section 2.10). Slides covalently coupled with oligonucleotide probes (2 identical spots for 1 gene) were hybridized with combined labelled cDNA containing 80 pmol of Cy3 and Cy5 (GE Healthcare Europe GmbH, Munich, Germany) from the *etfA* mutant and wild type, followed by scanning using a GenePix 4000B microarray scanner and GenePix Pro 4.0 software (Axon Instruments, Union City, USA). The ratio of medians, the ratio of means and the regression ratio were automatically calculated by GenePix Pro 6.0 software (Axon Instruments, Union City, USA) based on intensities of fluorescence signals the *etfA* mutant and wild type (reference) cDNA samples when analyzing scanned microarray images. Normalization was carried out by setting the arithmetic mean of the ratios equal to 1. Background correction was then conducted by subtracting the background value plus one standard deviation from the foreground value. The ratio of medians, the ratio of means and the regression ratio (they differed by less than 30%) were used to correct for spot morphology of features of one hybridization and the ratio of medians was used to calculated for the final expression ratio (average of the two ratios of medians from two identical spots) which was subsequently taken its logarithm (to the basis of 2). The results from microarray experiments were calculated by mean of one hybridization and its dye-flip hybridization.

As mentioned previously (section 2.10.6), a logarithmic ratio format was used in transcriptional analysis for convenience to discriminate up-regulated and down-regulated genes. A positive logarithmic ratio indicated a gene induced in the *etfA* mutant, whereas a negative logarithmic ratio represented a repressed gene of the *etfA* mutant as compared to the wild type. In addition, a logarithmic ratio larger than 1.60 was for significant induction in contrast to a ratio less than -1.60 which meant this gene was significantly repressed when the *etfA* of the *etfB-etfA-fcd* cluster was deleted. As a result, the higher a positive logarithmic ratio was, the more noticeable a gene was up-regulated in the *etfA* mutant, and a gene was down-regulated in a more significant level when its negative logarithmic ratio was lower.

Through microarray experiments of the mutant of the *etfA* gene of the *etfB-etfA-fcd* cluster, it was found that the expression profiles of most genes responsible for the central metabolic pathways (Fig. 2) were not significantly altered as compared to the wild type. Interestingly, a *pfor* (*CA_C2229*) was repressed by ~64% (did not reach the criterion referred to as "significant") during solventogenic growth, which was similar to what was observed in the *fcd* mutant (Table 8). Pfor functions at the node of pyruvate to acetyl-CoA (Fig. 2). Therefore, it suggested that the *etfA* gene of the *etfB-etfA-fcd* cluster affected carbon flux flowing through the C_4 route. This is in accordance with the decreased glucose consumption of solventogenic cells of the *etfA* mutant (Fig. 10). In addition, the expression of the *bcs* operon (*CA_C2708-CA_C2712*) and *thlA* (*CA_C2873*) was down-regulated during solventogenesis of the *etfA* mutant, suggesting that the *etfA* gene of the *etfB-etfA-fcd* cluster influenced the C_4 metabolism of *C. acetobutylicum* at pH 4.5 (Fig. 2). Moreover, an antagonistic expression

pattern was observed at pH 5.7 with the two paralogs of aldehyde/alcohol dehydrogenase genes, *adhE1* and *adhE2*. This is similar to what was reported previously (Grimmler *et al*., 2011). The expression patterns of central metabolic genes in the mutant of the *etfA* gene of the *etfB-etfA-fcd* cluster are listed in Table 13.

Table 13. Expression patterns of the central metabolic genes compared to wild type in the mutant of the *etfA* of the *etfB-etfA-fcd* cluster during acidogenic and solventogenic growth

ID	Protein function[a]	Ratio[b]	
		pH 5.7	pH 4.5
CA_P0035	AdhE2, aldehyde-alcohol dehydrogenase	-1.95	—
CA_P0078	ThlB, acetyl coenzyme A acetyltransferase	-0.43	0.22
CA_P0162	AdhE1, aldehyde dehydrogenase (NAD^+)	1.42	0.65
CA_P0163	CtfA, butyrate-acetoacetate CoA-transferase subunit A	1.41	1.06
CA_P0164	CtfB, butyrate-acetoacetate CoA-transferase subunit B	0.87	0.97
CA_P0165	Adc, acetoacetate decarboxylase	2.72	0.42
CAC0028	HydA, hydrogene dehydrogenase	-0.62	0.42
CAC0267	Ldh, lactate dehydrogenase	-2.77	-0.22
CAC1543	Ldh, lactate dehydrogenase	1.21	-0.64
CAC1742	Pta, phosphate acetyltransferase	-1.08	0.11
CAC1743	Ack, acetate kinase	-1.26	0.01
CAC2229	Pfor, pyruvate ferredoxin oxidoreductase	-0.33	-1.47
CAC2499	Pfor, pyruvate ferredoxin oxidoreductase	—	—
CAC2708	Hbd, β-hydroxybutyryl-CoA dehydrogenase	-0.80	-0.78
CAC2709	EtfA, electron transfer flavoprotein alpha-subunit	-0.51	-1.39
CAC2710	EtfB, electron transfer flavoprotein beta-subunit	-0.43	-1.58
CAC2711	Bcd, butyryl-CoA dehydrogenase	-0.57	-1.35
CAC2712	Crt, crotonase	-0.73	-1.45
CAC2873	ThlA, acetyl-CoA acetyltransferase	-0.15	-1.64
CAC3075	Buk, butyrate kinase	-0.97	-0.79
CAC3076	Ptb, phosphate acetyltransferase	-0.86	-1.29
CAC3552	Ldh, lLactate dehydrogenase	—	—

Genes are listed in order of ORFs, and considered as significantly up-regulated when the logarithmic ratio was ≥1.60 and as significantly down-regulated when the logarithmic ratio was ≤ -1.60. The given values in the table are mean of results of two hybridizations with dye swaps

[a] Protein names based on Nölling *et al.* (2001)

[b] The expression ratio as the logarithm to the basis of 2

On the other hand, transcription of 188 genes in acidogenic cells and 34 genes in solventogenic cells was observed to be strongly induced when inactivating the *etfA* gene of the *etfB-etfA-fcd* cluster, while 89 genes during acidogenesis and 41 genes during solventogenesis showed noticeable repression. Each was in comparison to the status at the same pH value of the wild type chemostat culture. Results were listed in Table 14-17, respectively.

Table 14. Significantly up-regulated genes compared to wild type in the mutant of the *etfA* gene of the *etfB-etfA-fcd* cluster during acidogenic growth

ID	Protein function[a]	Ratio[b]
CA_P0004	Cysteine protease	2.78
CA_P0053	Xylanase, glycosyl hydrolase family	1.84
CA_P0054	Xylanase/chitin deacetylase family enzyme	1.76
CA_P0058	Rare lipoprotein A	2.98
CA_P0065	Predicted secreted metalloprotease	1.62
CA_P0129	Glycogen-binding regulatory subunit of S/T protein phosphatase I	2.83
CA_P0133	Antibiotic-resistance protein, alpha/beta superfamily hydrolase	2.29
CA_P0134	Hypothetical protein	2.56
CA_P0135	Oxidoreductase	2.63
CA_P0136	AstB/ChuR/NirJ-related protein	2.69
CA_P0137	UDP-glucuronosyltransferases	2.77
CA_P0138	Hypothetical protein	2.64
CA_P0139	Possible D-alanyl carrier protein, acyl carrier protein family	2.85
CA_P0148	Phospholipase C	3.66
CA_P0160	Secreted protein containing cell-adhesion domains	1.91
CA_P0165	Adc Acetoacetate decarboxylase	2.72
CA_P0168	Alpha-amylase	2.94
CA_P0173	Archaeal-type Fe-S oxidoreductase	2.32
CA_P0174	Membrane protein	2.37
CAC0029	Distantly related to cell wall-associated hydrolase, similar to YycO of *B. subtilis*	2.82
CAC0030	Hypothetical protein	2.68
CAC0078	Putative accessory gene regulator protein	3.05
CAC0079	Hypothetical protein	3.24
CAC0082	Predicted membrane protein	3.33
CAC0140	Predicted permease	1.73
CAC0141	Membrane permease, predicted cation efflux pumps	1.73
CAC0175	Hypothetical protein	2.42
CAC0176	Oligopeptide-binding protein, periplasmic component	2.41
CAC0183	Transcriptional regulators, sugar kinase	1.95
CAC0184	Predicted acetyltransferase	1.89
CAC0253	NifH Nitrogenase iron protein (nitrogenase component II)	2.45
CAC0254	NifHD Nitrogen regulatory protein PII (nitrogen fixation NifHD)	2.97
CAC0255	NifHD Nitrogen regulatory protein PII (nitrogen fixation NifHD)	2.62
CAC0256	NifD Nitrogenase molybdenum-iron protein, alpha chain (nitrogenase component I)	2.92
CAC0259	Fusion NifN/K+NifB (NifN-nitrogenase iron molybdenum cofactor biosinthesis protein, NifK-nitrogenase molibdenum-iron protein beta chain	1.75
CAC0381	Methyl-accepting chemotaxis protein	2.18
CAC0383	PTS cellobiose-specific component IIA	3.66
CAC0384	PTS system, cellobiose-specific component BII	3.06
CAC0385	Beta-glucosidase	3.56
CAC0387	Hypothetical protein	3.34
CAC0488	Hypothetical protein	2.90

Table 14. (continued)

ID	Protein function[a]	Ratio[b]
CAC0489	4-Phosphopantetheinyl transferase	1.95
CAC0490	Predicted sugar kinase	1.99
CAC0491	Uncharacterized probably secreted protein	1.74
CAC0537	Acetylxylan esterase, acyl-CoA esterase, strong similarity to C-terminal region of endoglucanase E precursor	2.57
CAC0542	Methyl-accepting chemotaxis protein	3.18
CAC0555	Predicted membrane protein	2.24
CAC0658	Fe-S oxidoreductase	2.92
CAC0660	Hypothetical protein	2.94
CAC0663	Hypothetical protein	5.55
CAC0666	Sugar permease	3.92
CAC0667	Sugar-binding periplasmic protein	4.50
CAC0702	Predicted lipoprotein	1.99
CAC0703	Sugar ABC-transporter, ATPase component	2.19
CAC0704	Sugar ABC transporter, permease protein	2.19
CAC0705	Sugar ABC transporter, permease protein	2.09
CAC0746	Secreted protease metal-dependent protease	1.85
CAC0756	Multimeric flavodoxin WrbA	2.04
CAC0792	D-amino acid aminotransferase	2.80
CAC0814	3-Oxoacyl-[acyl-carrier-protein] synthase III	4.07
CAC0816	Lipase-esterase related protein	3.75
CAC0842	Hypothetical protein	2.46
CAC0910	Probably cellulosomal scaffolding protein precursor	1.78
CAC0911	Possible processive endoglucanase	2.25
CAC0912	Possible non-processive endoglucanase	2.63
CAC1010	Predicted phosphohydrolase	2.77
CAC1073	Hypothetical protein	3.53
CAC1074	Predicted permease	3.25
CAC1078	Predicted phosphohydrolase	3.55
CAC1079	Uncharacterized protein, related to enterotoxins of other clostridia	3.00
CAC1080	Uncharacterized protein, probably surface-located	3.64
CAC1081	Uncharacterized protein, probably surface-located	3.59
CAC1102	Predicted membrane protein	2.25
CAC1312	Hypothetical protein	1.82
CAC1336	Hypothetical protein	1.80
CAC1337	Spore coat protein	1.92
CAC1354	Phosphotransferase system IIA component	2.25
CAC1532	Protein containing CheW-repeats	2.98
CAC1533	Hypothetical protein	2.40
CAC1775	Predicted membrane protein	4.72
CAC1817	Stage V sporulation protein, SpoVS	2.54
CAC1868	Uncharacterized secreted protein	2.70
CAC1986	Hypothetical protein	1.90
CAC1988	Ferrichrome-binding periplasmic protein	3.47

Table 14. (continued)

ID	Protein function[a]	Ratio[b]
CAC1989	ABC-type iron (III) transport system, ATPase component	3.45
CAC1990	ABC-type iron (III) transport system, permease component	2.13
CAC1991	Uncharacterized protein	3.27
CAC1992	Molybdenum cofactor biosynthesis protein C	3.12
CAC1993	Molybdenum cofactor biosynthesis enzyme MoaA, Fe-S oxidoreductase	3.07
CAC1994	Molybdopterin biosynthesis enzyme, MoaB	2.43
CAC1995	Hypothetical protein	3.56
CAC1996	Hypothetical protein	3.57
CAC1997	Predicted glycosyltransferase	3.73
CAC1998	ABC-type transport system, ATPase component	3.73
CAC1999	Hypothetical protein	3.61
CAC2000	Indolepyruvate ferredoxin oxidoreductase	3.82
CAC2001	Indolepyruvate ferredoxin oxidoreductase, subunit alpha	3.88
CAC2002	Predicted iron-sulfur flavoprotein	3.74
CAC2003	Predicted permease	3.98
CAC2004	Siderophore/Surfactin synthetase related protein	2.04
CAC2005	Siderophore/Surfactin synthetase related protein	3.37
CAC2006	Enzyme of siderophore/surfactin biosynthesis	4.06
CAC2007	Predicted glycosyltransferase	4.04
CAC2008	3-Oxoacyl-(acyl-carrier-protein) synthase	3.96
CAC2009	3-Hydroxyacyl-CoA dehydrogenase	4.07
CAC2010	Predicted Fe-S oxidoreductase	4.24
CAC2011	Possible 3-oxoacyl-[acyl-carrier-protein] synthase III	4.35
CAC2012	Enoyl-CoA hydratase	4.31
CAC2013	Hypothetical protein	4.17
CAC2014	Predicted esterase	4.38
CAC2015	Hypothetical protein	4.23
CAC2016	Enoyl-CoA hydratase	4.24
CAC2017	Acyl carrier protein	4.42
CAC2018	Aldehyde ferredoxin oxidoreductase	3.94
CAC2019	Malonyl CoA-acyl carrier protein transacylase	3.91
CAC2020	Molybdopterin biosynthesis enzyme	2.68
CAC2021	Molybdopterin biosynthesis enzyme, MoeA (short form)	2.32
CAC2022	Molybdopterin biosynthesis enzyme, moaB	2.44
CAC2023	Membrane protein	2.62
CAC2024	Phosphatidylglycerophosphate synthase related protein (fragment)	2.60
CAC2026	Predicted flavodoxin	2.97
CAC2040	ATPase component	2.14
CAC2226	Branched-chain amino acid aminotransferase/4-amino-4-deoxychorismate lyase	2.28
CAC2227	Phosphoserine phosphatase family enzyme	1.98
CAC2252	Alpha-glucosidase fused to unknown alpha-amylase C-terminal	1.97
CAC2307	Anti-sigma F factor	2.14
CAC2308	SpoIIAA Anti-anti-sigma factor (antagonist of SpoIIAB)	2.17

Table 14. (continued)

ID	Protein function[a]	Ratio[b]
CAC2342	Predicted membrane protein	1.77
CAC2382	Single-strand DNA-binding protein	2.36
CAC2404	Glycosyltransferase	2.88
CAC2405	Predicted glycosyltransferase	3.04
CAC2517	Extracellular neutral metalloprotease	3.16
CAC2518	Extracellular neutral metalloprotease	2.59
CAC2544	Electron-transferring flavoprotein small subunit	1.63
CAC2577	Uncharacterized protein, (inactivated)	2.05
CAC2578	Glycosyltransferase	2.65
CAC2579	Hypothetical protein	2.79
CAC2580	Hypothetical protein	2.90
CAC2581	6-Pyruvoyl-tetrahydropterin synthase related domain, conserved membrane protein	2.95
CAC2584	Protein containing CheW-repeats	3.40
CAC2597	Hypothetical protein	1.85
CAC2663	Protein containing cell-wall hydrolase domain	3.35
CAC2678	Hypothetical protein	1.80
CAC2695	Diverged Metallo-dependent hydrolase	4.06
CAC2716	Predicted glycosyl transferase from UDP-glucuronosyltransferase family	3.33
CAC2722	Predicted protein (beta propeller fold)	2.37
CAC2806	Predicted phosphohydrolase	1.81
CAC2807	Endo-1,3(4)-beta-glucanase	3.23
CAC2808	Beta-lactamase	3.65
CAC2810	Possible glucoamylase (diverged)	2.83
CAC2938	Hypothetical protein	2.49
CAC2944	N-terminal domain intergin-like repeats and c-terminal-cell wall-associated hydrolase domain	4.01
CAC3034	MutS-like mismatch repair protein, ATPase	1.89
CAC3060	ATPase	2.03
CAC3061	Membrane protein	2.36
CAC3062	Hydrolase	2.12
CAC3063	Transcriptional regulator, LytR family	2.06
CAC3064	UDP-N-acetylglucosamine 2-epimerase	1.96
CAC3065	Possible O-antigen/teichoic acid transporter	1.96
CAC3067	Predicted membrane protein	2.33
CAC3068	Glycosyltransferase	2.32
CAC3069	Predicted glycosyltransferase	2.47
CAC3070	Glycosyltransferase	2.54
CAC3071	Glycosyltransferase	2.68
CAC3072	Mannose-1-phosphate guanylyltransferase	2.65
CAC3073	Sugar transferase involved in lipopolysaccharide synthesis	2.61
CAC3085	Protein containing cell adhesion domain	3.24
CAC3086	Protein containing cell adhesion domain	3.30
CAC3251	Sensory transduction protein	2.86

Table 14. (continued)

ID	Protein function[a]	Ratio[b]
CAC3298	BdhB NADH-dependent butanol dehydrogenase B (BDH II)	2.78
CAC3319	Signal transduction histidine kinase	2.81
CAC3355	Polyketide synthase	3.11
CAC3408	NADH oxidase (two distinct flavin oxidoreductase domains)	2.35
CAC3409	Transcriptional regulators, LysR family	2.08
CAC3412	Predicted protein-S-isoprenylcysteine methyltransferase	3.87
CAC3422	Sugar proton symporter (possible xylulose)	3.11
CAC3423	Acetyltransferase (ribosomal protein N-acetylase subfamily)	2.21
CAC3460	Hypothetical protein	2.55
CAC3558	Probable S-layer protein	3.70
CAC3565	Uncharacterized secreted protein, containing cell adhesion domain	2.66
CAC3581	Hydrolase	1.94
CAC3633	Hypothetical protein	2.11
CAC3635	Oligopeptide ABC transporter, ATPase component	2.62
CAC3636	Oligopeptide ABC transporter, ATPase component	2.63
CAC3637	Oligopeptide ABC transporter, permease component	2.75
CAC3638	Oligopeptide ABC transporter, permease component	2.45
CAC3639	DNA-binding protein	3.01
CAC3684	Polygalacturonase	2.01

Genes are listed in order of ORFs and considered as significantly up-regulated when the logarithmic ratio was ≥1.60. The given values in the table are mean of results of two hybridizations with dye swaps

[a] Protein name based on Nölling *et al.* (2001)

[b] The expression ratio as the logarithm to the basis of 2

During the steady-state acidogenic growth of the *etfA* (from the *etfB-etfA-fcd* cluster) mutant culture, 188 genes were significantly up-regulated as compared to the wild type (Table 14). This indicated that the *etfA* of the *etfB-etfA-fcd* cluster exerted profound effects on acidogenic metabolism and corresponded to the prolonged period of the mutant culture to enter the steady-state acidogenesis. Among these, 29 genes encoded membrane-associated proteins, suggesting inactivation of *etfA* affected the characteristics of the cell membrane. In addition, 6 genes (*CA_C0029*, *CA_C1081*, *CA_C2252*, *CA_C2342*, *CA_C2810*, *CA_C2938*) were shown to be strongly induced in this growth phase as compared to wild type where they expressed at high levels (Janssen *et al.*, 2010), although 4 of them were classified as "uncharacterized, hypothetical or predicted" proteins (Nölling *et al.*, 2001). Besides, expression of 5 genes (*CA_P0053*, *CA_P0054*, *CA_P0129*, *CA_C0385*, *CA_C2018*) was significantly up-regulated, displaying a modified carbohydrate metabolism. Moreover, two possible operon were transcribed at high levels (*CA_C0253-CA_C0259*, *CA_C1988-CA_C2026*) as compared to wild type, suggesting the nitrogen fixation and synthesis of fatty acids were interfered by mutation of *etfA*. Elevated transcript levels of five glycosyltransferase genes were also noticeable. This phenomenon indicated that metabolism of oligosaccharides had probably changed. Among the genes for oxidoreductase, *CA_P0173*, *CA_C2000-CA_C2002*, and *CA_C2010* were induced. Among induced genes in acidogenic cells, 15 had different expression profile as compared to that of the wild type. They

(*CA_P0004*, *CA_P0065*, *CA_P0129*, *CA_P0168*, *CA_C0254-CA_C0256*, *CA_C0746*, *CA_C0910-CA_C0912*, *CA_C2404-CA_C2405*, *CA_C2517* and *CA_C3684*) gave increased transcript levels during the steady-state acidogenesis of the *etfA* mutant chemostat culture, while the wild type culture highly expressed these genes during solventogenesis.

adc (*CA_P0165*) was transcribed at a higher level but the acetone production decreased. Similarly, *bdhB* (*CA_C3298*) was also highly expressed, but butanol formation decreased. Sporulation-related genes, e.g. *CA_C1337*, *CA_C1817*, *CA_C2307* and *CA_C2308* were also significantly up-regulated, but spores did not form in the steady-state of chemostat cultures.

Table 15. Significantly down-regulated genes compared to wild type in the mutant of the *etfA* gene of the *etfB-etfA-fcd* cluster during acidogenic growth

ID	Protein function[a]	Ratio[b]
CA_P0035	AdhE2 Aldehyde-alcohol dehydrogenase	-1.95
CA_P0116	Xylanase, glycosyl hydrolase	-2.74
CA_P0117	Possible beta-xylosidase diverged	-3.04
CA_P0118	Possible xylan degradation enzyme	-3.26
CA_P0119	Possible xylan degradation enzyme	-3.36
CA_P0120	Possible xylan degradation enzyme	-3.44
CAC0014	Aminotransferase	-4.50
CAC0015	D-3-phosphoglycerate dehydrogenase	-4.68
CAC0016	Related to HTH domain of SpoOJ/ParA/ParB/RepB family, involved in chromosome partitioning	-4.59
CAC0017	Seryl-tRNA synthetase	-4.81
CAC0018	Putative NADPH-quinone reductase	-2.93
CAC0117	Protein cheY homolog	-2.79
CAC0118	CheA Chemotaxis protein	-2.89
CAC0119	CheW Chemotaxis protein	-2.75
CAC0120	Membrane-associated methyl-accepting chemotaxis protein	-2.91
CAC0121	CheR Chemotaxis protein methyltransferase	-2.54
CAC0156	MltF PTS system, mannitol-specific IIA domain	-2.21
CAC0267	Ldh L-lactate dehydrogenase	-2.77
CAC0687	CysE Serine acetyltransferase	-1.95
CAC0882	Predicted membrane protein, hemolysin III homolog	-2.02
CAC0980	PflB Pyruvate-formate lyase	-3.47
CAC0981	PflA Pyruvate-formate-lyase-activating enzyme	-3.71
CAC0983	Hypothetical protein	-3.32
CAC1175	Hypothetical protein	-2.52
CAC1176	hypothetical protein	-1.87
CAC1181	Phage related protein, YorF of *B.subtilis* homolog	-2.12
CAC1219	Hypothetical protein	-1.89
CAC1225	Hypothetical protein	-1.88
CAC1227	Hypothetical protein	-2.12
CAC1319	GlpF Glycerol uptake facilitator protein	-3.98
CAC1320	GlpP Glycerol-3-phosphate responsive antiterminator (mRNA-binding)	-2.01

Table 15. (continued)

ID	Protein function[a]	Ratio[b]
CAC1321	GlpK glycerol kinase	-3.06
CAC1322	GlpA Glycerol-3-phosphate dehydrogenase	-1.78
CAC1390	PurE phosphoribosylaminoimidazole carboxylase catalytic subunit	-2.83
CAC1391	PurC phosphoribosylaminoimidazole-succinocarboxamide synthase	-2.96
CAC1392	PurF amidophosphoribosyltransferase	-2.87
CAC1393	PurM phosphoribosylaminoimidazole synthetase	-3.09
CAC1394	PurN phosphoribosylglycinamide formyltransferase	-3.10
CAC1395	PurH bifunctional phosphoribosylaminoimidazolecarboxamide formyltransferase/ cyclohydrolase	-3.08
CAC1396	PurD phosphoribosylamine-glycine ligase	-2.69
CAC1406	Transcriptional antiterminator	-2.72
CAC1465	Transcriptional regulator	-1.82
CAC1547	TrxA Thioredoxin	-2.03
CAC1620	Small acid-soluble spore protein	-2.09
CAC1655	PurQ/PurL bifunctional enzyme phosphoribosylformylglycinamidine synthase	-2.10
CAC1780	Nicotinate phosphoribosyltransferase	-1.61
CAC1846	MotA flagellar motor protein	-2.00
CAC1862	Hypothetical protein	-3.66
CAC1900	Phage regulatory protein, containing Zn-finger	-3.71
CAC1904	Hypothetical protein	-3.24
CAC1909	Ribonuclease D	-3.63
CAC1910	Predicted membrane protein	-2.77
CAC1912	Uncharacterized phage related protein	-6.60
CAC1930	Uncharacterized protein	-2.21
CAC1931	Hypothetical protein	-4.72
CAC1933	DnaL hypothetical protein	-3.98
CAC1936	Hypothetical protein	-3.41
CAC1938	Predicted hydrolase	-4.81
CAC1940	Hypothetical protein	-3.74
CAC1941	AbrB Transcription regulator	-4.35
CAC1942	Hypothetical protein	-2.81
CAC1944	Hypothetical protein	-2.18
CAC1949	Possible protein	-3.67
CAC2445	5-Aminoimidazole-4-carboxamide ribonucleotide transformylase	-2.61
CAC2446	Hypothetical protein	-2.85
CAC2587	Predicted protein	-4.58
CAC2592	6-Pyruvoyl-tetrahydropterin synthase related domain, conserved membrane protein	-3.62
CAC2772	Permease	-1.96
CAC2849	Proline/glycine betaine ABC-type transport system, permease component fused to periplasmic component	-1.85
CAC2850	Proline/glycine betaine ABC-type transport system, ATPase component	-1.94
CAC3045	Hydrolase	-2.99
CAC3046	Transcriptional regulator	-3.03

Table 15. (continued)

ID	Protein function[a]	Ratio[b]
CAC3047	Uncharacterized membrane protein	-2.66
CAC3049	Glycosyltransferase	-3.13
CAC3050	Exopolysaccharide biosynthesis protein	-3.99
CAC3051	Glycosyltransferase	-3.45
CAC3053	Histidinol phosphatase related enzyme	-3.74
CAC3054	Phosphoheptose isomerase	-3.90
CAC3055	Sugar kinase	-4.71
CAC3056	Nucleoside-diphosphate-sugar pyrophosphorylase	-4.71
CAC3057	Glycosyltransferase	-4.77
CAC3058	Mannose-1-phosphate guanylyltransferase	-5.30
CAC3059	Sugar transferase	-4.93
CAC3421	Acyl carrier protein phosphodiesterase	-2.56
CAC3458	Uncharacterized protein, homolog of *B. anthracis*	-1.91
CAC3592	Hypothetical protein	-2.09
CAC3641	Oligopeptide ABC transporter, ATPase component	-4.64
CAC3642	Oligopeptide ABC transporter, ATPase component	-4.79
CAC3647	AbrB Transition state regulatory protein	-3.16

Genes are listed in order of ORFs and considered as significantly down-regulated when the logarithmic ratio was ≤ -1.60. The given values in the table are mean of results of two hybridizations with dye swaps

[a] Protein name based on Nölling *et al.* (2001)

[b] The expression ratio as the logarithm to the basis of 2

During the steady-state acidogenic growth of the *etfA* (from the *etfB-etfA-fcd* cluster) mutant, 89 genes were significantly down-regulated as compared to wild type (Table 15). Among these, *CA_P0116-CA_P0120* for xylan degradation was strongly down-regulated. In addition, 8 membrane-associated genes (*CA_C0882*, *CA_C1319−CA_C1322*, *CA_C1910*, *CA_C2592* and *CA_C3047*) and a cluster (*CA_C0117-CA_C0121*) for chemotaxis were also significantly repressed, suggesting some changes had been occurred in the cell mebrane.

Besides, the expression of clusters (*CA_C0014-CA_C0017* and *CA_C1390-CA_C1396*) was shown to be noticeably repressed, which revealed the biosynthesis of serine and purines of the mutant strain was affected. Another down-regulated cluster (*CA_C3049-CA_C3059*) suggested a change of the sugar metabolism.

Interestingly, *adhE2* (*CA_P0035*) was significantly down-regulated at pH 5.7, while the expression of *adhE1* (*CAP0162*) was up-regulated (logarithmic ratio 1.4 to the basis of 2). This indicated a negative correlation between them and was in accordance with a previous study (Grimmler *et al.*, 2011).

Table 16. Significantly up-regulated genes compared to wild type in the mutant of the *etfA* gene of the *etfB-etfA-fcd* cluster during solventogenic growth

ID	Protein function[a]	Ratio[b]
CA_P0036	Uncharacterized, ortholog of YgaT of *B.subtillis*	5.31
CA_P0037	Uncharacterized, ortholog of YgaS of *B.subtillis*	5.03
CAC0014	Aminotransferase	6.07
CAC0015	SerA D-3-phosphoglycerate dehydrogenase	6.22
CAC0016	Related to HTH domain of SpoOJ/ParA/ParB/RepB family, involved in chromosome partitioning	6.07
CAC0017	SerS seryl-tRNA synthetase	6.94
CAC0018	Putative NADPH-quinone reductase	3.99
CAC0102	O-acetylhomoserine sulfhydrylase	1.84
CAC0103	CysC Adenylylsulfate kinase	2.04
CAC0104	Adenylylsulfate reductase	2.10
CAC0105	Ferredoxin	2.24
CAC0106	ABC-type probable sulfate transporter, periplasmic binding protein	1.67
CAC0107	ABC-type sulfate transporter, ATPase component	2.76
CAC0109	CysD sulfate adenylyltransferase subunit 2	2.10
CAC0110	CysN GTPase, sulfate adenylate transferase subunit 1	2.11
CAC0528	ABC transporter, ATPase component (two ATPase domains)	2.11
CAC0929	SAM-dependent methyltransferase	2.02
CAC0930	metB Cystathionine gamma-synthase	2.06
CAC0931	Cysteine synthase	2.64
CAC0980	PflB Pyruvate-formate lyase	3.09
CAC0981	PflA Pyruvate-formate-lyase-activating enzyme	3.05
CAC0983	Hypothetical protein	2.87
CAC1465	Transcriptional regulator	1.80
CAC1609	Zn-finger containing protein	1.81
CAC2241	Cation transport P-type ATPase	2.03
CAC2445	5-Aminoimidazole-4-carboxamide ribonucleotide transformylase	2.81
CAC2446	Hypothetical protein	3.09
CAC2544	EtfB Electron-transferring flavoprotein small subunit	2.84
CAC2545	Hypothetical protein	2.20
CAC2688	Alpha/beta superfamily hydrolase (possible chloroperoxidase)	2.09
CAC3088	NtrC family transcriptional regulator, ATPase domain	1.76
CAC3325	Periplasmic amino acid binding protein	1.64
CAC3421	Acyl carrier protein phosphodiesterase	2.93
CAC3515	Alpha/beta superfamily hydrolase (possible peptidase)	2.82

Genes are listed in order of ORFs and considered as significantly up-regulated when the logarithmic ratio was ≥1.60. The given values in the table are mean of results of two hybridizations with dye swaps

[a] Protein name based on Nölling *et al.* (2001)

[b] The expression ratio as the logarithm to the basis of 2

During the steady-state solventogenic growth of the *etfA* (from the *etfB-etfA-fcd* cluster) mutant, 34 genes were significantly up-regulated as compared to the wild type (Table 16). Among these, *CA_P0037-CA_P0036* operon showed the most remarkable transcript level, proposing its unknown roles during solventogenesis. Moreover, a possible transcription unit for serine biosynthesis (*CA_C0014-CA_C0017*) also displayed noticeable high signal level. In addition, two clusters for cysteine and methionine biosynthesis (*CA_C0102-CA_C0107*, *CA_C109-CA_C0110*, *CA_C0929-CA_C0931*) were significantly induced, indicating active formation of these two amino acids. Besides, a gene (*CA_C3421*) participating in the synthesis of pantothenate and CoA was induced. Interestingly, *pflA-pflB* cluster (*CA_C0980-CA_C0981*) was strongly up-regulated, revealing an opposite transcription profile to that during acidogenic growth, where its expression level was decreased by at least 90% as compared to wild type. Last but not the least, *etfB* (*CA_C2544*) of *etfB-etfA-fcd* cluster was transcribed in an induced manner.

Table 17. Significantly down-regulated genes compared to wild type in the mutant of the *etfA* gene of the *etfB-etfA-fcd* cluster during solventogenic growth

ID	Protein function[a]	Ratio[b]
CA_P0160	Secreted protein containing cell-adhesion domains	-2.28
CAC0232	FruB 1-phosphofructokinase (fructoso 1-phosphate kinase)	-2.26
CAC0233	PTS system, IIA component	-2.77
CAC0316	Ornithine carbomoyltransferase	-2.07
CAC0318	Membrane permease, predicted cation efflux pumps	-2.26
CAC0319	ABC transporter ATP-binding protein	-1.82
CAC0380	Periplasmic amino acid-binding protein	-2.24
CAC0383	PTS cellobiose-specific component IIA	-2.91
CAC0384	PTS system, cellobiose-specific component BII	-3.24
CAC0385	Beta-glucosidase	-3.27
CAC0387	Hypothetical protein	-3.04
CAC0570	PTS enzyme II, ABC component	-3.11
CAC0936	HisG ATP phosphoribosyltransferase	-1.97
CAC0937	HisD Histidinol dehydrogenase	-2.17
CAC0938	HisB Imidazoleglycerol-phosphate dehydratase	-2.40
CAC0939	HisH Glutamine amidotransferase	-2.24
CAC0940	HisA Phosphoribosylformimino-5-aminoimidazole carboxamide ribonucleotide isomerase	-2.55
CAC0941	HisF Imidazoleglycerol-phosphate synthase	-2.42
CAC0942	Phosphoribosyl-AMP cyclohydrolase	-2.52
CAC0943	Phosphoribosyl-ATP pyrophosphohydrolase	-2.31
CAC0973	ArgG argininosuccinate synthase	-3.43
CAC0974	ArgH Argininosuccinate lyase	-2.91
CAC0975	Predicted P-loop kinase or ATPase distantly related to phosphoenolpyruvate carboxykinase	-1.87
CAC1084	Beta-glucosidase family protein	-2.03
CAC1319	GlpF Glycerol uptake facilitator protein	-2.41
CAC1322	GlpA Glycerol-3-phosphate dehydrogenase	-2.05

Table 17. (continued)

ID	Protein function[a]	Ratio[b]
CAC2020	MoeA Molybdopterin biosynthesis enzyme	-1.94
CAC2227	Phosphoserine phosphatase family enzyme	-1.90
CAC2388	ArgD N-acetylornithine aminotransferase	-3.14
CAC2389	ArgB Acetylglutamate kinase	-2.00
CAC2391	ArgJ bifunctional ornithine acetyltransferase/N-acetylglutamate synthase protein	-3.07
CAC2613	GlcK Transcriptional regulator	-2.11
CAC2959	GalK galactokinase	-2.45
CAC2960	GalE UDP-galactose 4-epimerase	-2.52
CAC2961	GalT galactose-1-phosphate uridylyltransferase	-1.74
CAC3526	FMN-binding protein	-2.08
CAC3527	Ferredoxin	-2.21
CAC3619	Amino acid ABC transporter, permease component	-2.82
CAC3620	Amino acid (probably glutamine) ABC transporter, periplasmic binding protein component	-2.74
CAC3622	Possible subunit of benzoyl-CoA reductase/2-hydroxyglutaryl-CoA dehydratase	-2.00
CAC3625	Fe-S oxidoreductase	-1.74

Genes are listed in order of ORFs and considered as significantly down-regulated when the logarithmic ratio was ≤ -1.60. The given values in the table are mean of results of two hybridizations with dye swaps

[a] Protein name based on Nölling *et al.* (2001)

[b] The expression ratio as the logarithm to the basis of 2

During the steady-state solventogenic growth of the *etfA* (from the *etfB-etfA-fcd* cluster) mutant, 41 genes were significantly down-regulated as compared to the wild type (Table 17). Among these, two membrane-associated protein-coding genes (*CA_C0383* and *CA_C0384*) and two other genes (*CA_C0233* and *CA_C0570*) were for the PTS system. The decreased expression level of these genes indicated carbohydrate metabolism and transport were influenced due to inactivation of *etfA* at pH 4.5. Moreover, three additional genes for membrane-associated protein showed decreased signals (*CA_C0318*, *CA_C1319* and *CA_C1322*). In addition, a cluster for histidine biosynthesis (*CA_C0936-CA_C0943*), genes in synthesis pathways of arginine (*CA_C0316*, *CA_C0973-CA_C0974* and *CA_C2388-CA_C2391*, *CA_C2390* did not pass the applied filter criterion, section 2.10.6) and a gene probably for glycine, serine and threonine metabolism (*CA_C2227*) revealed noticeably repressed expression levels. Decreased transcripts of genes for these amino acids indicated that mutation in *etfA* affected metabolism of amino acids and the requirement of the *etfA* mutant culture for amino acids had probably been altered. This could be further supported by the down-regulated expression of genes for the transport of amino acids (*CA_C0380*, *CA_C3619* and *CA_C3620*). In addition, some genes for carbohydrate metabolism were found to be significantly down-regulated during solventogenesis, suggesting altered energy metabolism (*CA_C0232*, *CA_C0385*, *CA_C0975*, *CA_C1084* and *CA_C2959-CA_C2961*).

The number of genes that were regulated during acidogenesis of the *etfA* mutant was approximately 3 times more than that during solventogenesis, suggesting that the mutation in the *etfA* of the *etfB-etfA-fcd* cluster resulted in a more comprehensive influence on gene expression pattern in acidogenic cells.

3.2.3 Characterization of the mutant of the *etfB* of the *etfB-etfA-fcd* cluster

3.2.3.1 Generation of the mutant of the *etfB* of the *etfB-etfA-fcd* cluster

After generation and analyses of mutants of the *fcd* and *etfA* genes of the *etfB-etfA-fcd* cluster, the *etfB* gene was subsequently knocked out using the ClosTron system (Heap *et al.*, 2007, 2010a, 2010b), and the resultant mutant strain was characterized using continuous fermentation and microarray experiments.

Strategies for generation of an *etfB* ClosTron mutant were identical to that for the *fcd* and *etfA* mutant strains and they were described in detail in Methods and Materials (section 2.7.3.1, 2.9). Target sites (where intron could insert) in *etfB* gene were predicted using a web-based intron targeting and design tool (www.clostron.com) and a target site with the highest score (8.831) was selected. Consequently, the target site in the *etfB* gene was determined at 523/524 bp (the length of the *etfB* gene is 789 bp) and the intron was predicted to insert into this site at a sense direction according to information given. In addition, four primers for SOE (splicing by overlap extension) PCR (section 2.7.3.1) (Ho *et al.*, 1989) were simultaneously designed (*etfB*-IBS, *etfB*-EBS1d, *etfB*-EBS2 and EBS universal; Table 38, Appendix section). They were used for the mutation of recognition sites of the intron retargeting region in pMTL007C-E2 whose intron was able to insert into the predicted *etfB* target site by a specific recognition of *etfB* gene via its mutated retargeting region. SOE PCR produced the mutated intron retargeting region which was then ligated with pMTL007C-E2 backbone to generate retargeted intron expression vector specific for *etfB* (pMTL007C-E2::cac-*etfB*-523s, Table 7, section 2.4). This vector was subsequently transformed into *E. coli* containing pAN2 for *in vivo* methylation (section 2.9.1). Retargeted and methylated pMTL007C-E2::cac-*etfB*-523s was electroporated into *C. acetobutylicum* (section 2.9.2), followed by screening of thiamphenicol- and erythromycin-resistant colonies (section 2.9.3).

After electroporation and screening steps, 4 clones of the putative *etfB* mutant were selected and the correct insertion of the intron was verified by PCR and subsequent Southern hybridization. Erythromycin-resistant clones (putative *etfB* mutant) were verified by standard PCR (section 2.7.2.1) using four different primers. *etfB* gene-specific primers (*etfB*-Forward and -Reverse primers, Table 39, Appendix section) were used first. The wild type genomic DNA gave a band at 753 bp, while the correct mutants exhibited products at 2,534 bp, ~1.8 kb larger than that of the wild type, which corresponded to the size of the intron inserting into the target gene (Fig. 11A). Another set of primers, an intron specific primer (EBS universal, Table 38, Appendix section) and an *etfB*-Forward primer, were employed to verify an exon-intron junction part of the mutated gene, leading to a product of 737 bp, whereas the wild type was not supposed to result in a product (Fig. 11A). Besides, a primer pair specific for pMTL007C-E2 plasmid (pMTL007CE2check-Forward and -Reverse primers, Table 40, Appendix section) was used for confirmation of the loss of this shuttle vector from mutant cells and only pMTL007C-E2 plasmid control gave a band at 517 bp (Fig. 11B). Moreover, *CA_P0175* (*repA*) gene-specific primers (*repA*-Forward and -Reverse primers, Table 39, Appendix section) were used to verify the presence of pSOL1 megaplasmid which carried key genes for solventogenesis and products (1,003 bp) were visible in both the *etfB* mutant and the wild type (Fig. 11B). Confirmation of the presence of pSOL1 was necessary when conducting mutagenesis in *C. acetobutylicum*. In case of pSOL1 loss, the strain constructed would in fact be a double mutant with the *etfB* gene and the pSOL1 as a whole mutated.

To further confirm the correct insertion of the intron, i.e., that only one copy of the intron had inserted into the *etfB* gene, Southern hybridization was conducted with the intron-specific probe. Detailed methods of Southern hybridization were described previously (section 2.7.5). 590 bp of the intron-specific probe was PCR amplified using intron specific primers (ISP-Forward and -Reverse primers, Table 40, Appendix section) and pMTL007 plasmid was used as the template. The intron-specific probe (fragment) was located at an intron-erythromycin gene junction section (339-928 bp) in the intron (1,781 bp in length) where 774 bp of erythromycin gene resided (710-1,483 bp). Genomic DNA of the *etfB* mutant as well as that of the wild type were digested with *Eco*RV-HF at 37 °C for 16 hours before they were transferred from an agarose gel to a positively charged nylon membrane which was then hybridized overnight with the biotin-labeled intron-specific probe at 42 °C. Genomic DNA of the *etfB* mutant exhibited a single band at ~12 kb, demonstrating that the *etfB* mutant possessed only one copy of the intron on the chromosome and thus only the *etfB* gene was mutated. No hybridization signal was observed for wild type genomic DNA, as expected, because the intron-specific probe used did not hybridize to any original DNA sequence in *C. acetobutylicum*. Restricted pMTL007C-E2 with *Hin*dIII was used as a positive control, showing a signal at 8.9 kb which was equal to the size of linear pMTL007C-E2 plasmid (Fig. 12A). Consequently, after confirmation by PCR and Southern hybridization, it was proved that a single *etfB* mutant had been generated.

The presence of the pSOL1 megaplasmid was detected via the iodine-exposed starch plate test (section 2.5.1, 2.9.4), because pSOL1-containing cells was able to degrade starch in solidified media and form halos when exposed with iodine. To confirm the presence of the pSOL1 in the *etfB* mutant cells, about 40 colonies of the *etfB* mutant strain were re-streaked on a RCA (reinforced clostridial agar) plate which contained 1% starch. After 24 h of incubation at 37 °C under anaerobic conditions, colonies still containing pSOL1 degraded the surrounding starch and formed halos when the starch-containing plate was stained with potassium iodine solution (Lugol) solution (Fig. 12B). Through this test, it was demonstrated that the *etfB* mutant strain generated by the ClosTron system still carried the pSOL1 megaplasmid.

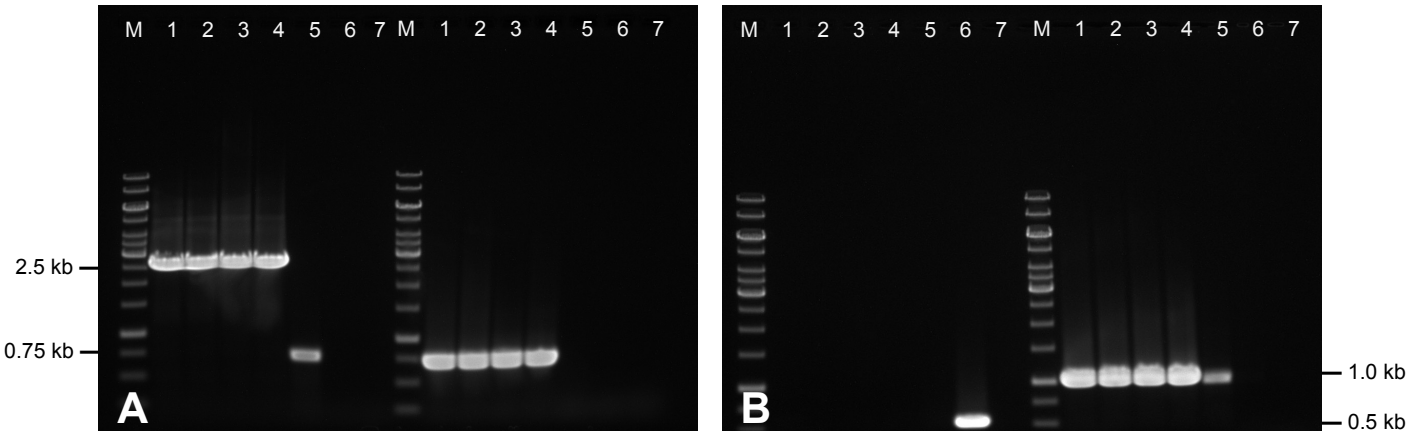

Fig. 11. PCR verification of the *etfB* mutant. (A) *etfB* gene-specific primers (left), and EBS universal primer and *etfB*-Forward primer (right); (B) pMTL007C-E2 specific primers (left), and *CA_P0175* (*repA*) gene-specific primers (right). M, marker; lane 1-4, genomic DNA samples from different clones of the *etfB* mutant; lane 5, wild type genomic DNA; lane 6, pMTL007C-E2 plasmid; lane 7, deionized water as the negative control

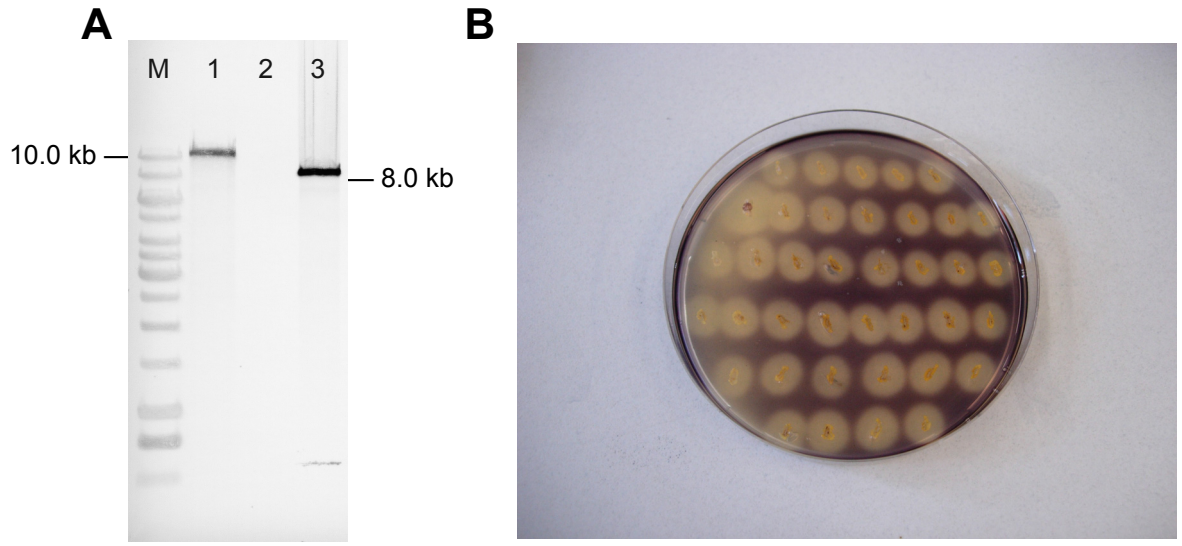

Fig. 12. Southern hybridization and starch plate test of the *etfB* mutant. *Eco*RV-digested genomic DNA samples of the *etfB* mutant and wild type were hybridized with biotin-labelled intron-specific DNA probe (A). M, marker; lane 1, genomic DNA of the *etfB* mutant; lane 2, wild type genomic DNA; lane 3, pMTL007C-E2 digested with *Hin*dIII as a positive control. (B) The *etfB* mutant colonies were re-streaked on an agar plate containing starch, colonies still carrying the pSOL1 megaplasmid formed halos when staining with potassium iodine solution

3.2.3.2 Continuous fermentation of the mutant of the *etfB* of the *etfB-etfA-fcd* cluster

After confirming the *etfB* mutant at molecular and phenotypical levels, continuous fermentation was carried out in order to characterize this mutant strain (Fig. 13) and correct insertion of the intron in the *etfB* gene was monitored by PCR using *etfB* gene-specific primers (*etfB*-Forward and -Reverse primers, Table 39, Appendix section) which flanked the intron insertion site. Methods for chemostat culture of *C. acetobutylicum* were described in detail previously (section 2.6).

During acidogenic growth of the continuous culture of the *etfB* mutant, the OD_{600} was ~3.8 which was comparable to that of the wild type and the *etfA* (*CA_C2543*) mutant. After 22 h of the pH shift, the culture of the *etfB* mutant entered solventogenesis, and the final OD_{600} of the culture during the steady-state was ~3.1 which was lower than the wild type and similar to that of the *fcd* and *etfA* mutant. In terms of glucose consumption, the *etfB* mutant utilized more glucose during acidogenesis than during solventogenesis, which was similar to the wild type strain. However, the *etfB* mutant consumed less glucose than the wild type during both acidogenic and solventogenic growth, which led to slightly lower production of acetic acid (~38 mM) and decreased (~37%) concentrations of acetone and butanol, respectively. During acidogenesis, butyrate concentration was comparable to the wild type, while production of acetone and butanol was reduced more than 50% although these were not predominant metabolites during this phase. Besides, more butyrate (~33%) was accumulated during solventogenic growth, whereas acetic acid formed (~10 mM) was comparable to the wild type during this phase. Moreover, ethanol formation was also disturbed during acidogenic and solventogenic growth of the *etfB* mutant. The results indicated that the *etfB* gene of the *etfB-etfA-fcd* cluster was positively related to the generation of all three solvents during acidogenic and solventogenic growth, and mutation of this gene also affected butyrate metabolism during solventogenesis.

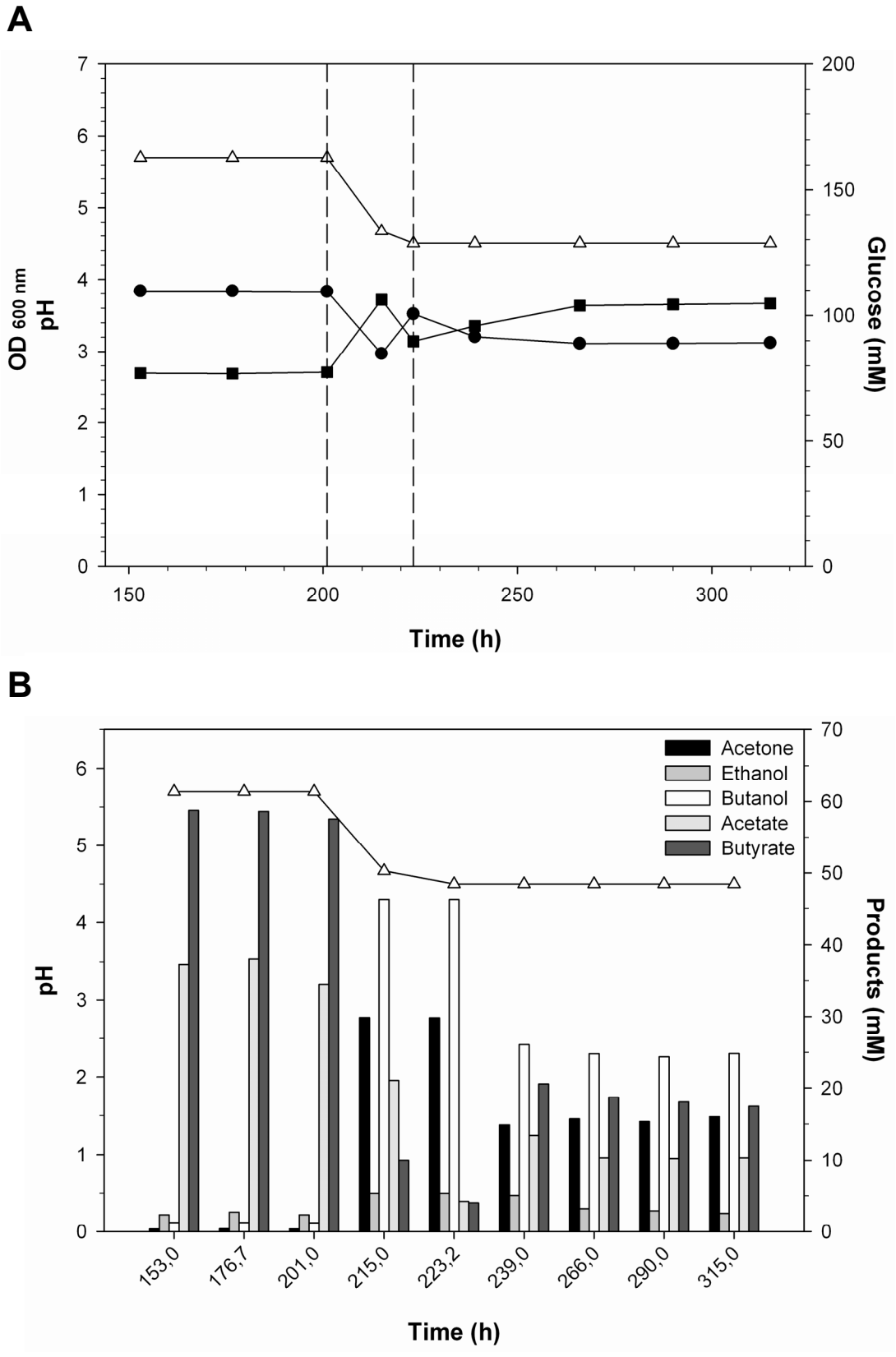

Fig. 13. Fermentation profile of the phosphate-limited continuous culture of the *etfB* mutant. (A) Growth, glucose consumption and pH in the course of fermentation. Dashed lines indicate the dynamic pH shift. (B) Fermentation products from the steady-state acidogenesis to solventogenesis. Each grouped bar set corresponds to each time-point. The fermentation profile of this mutant resembles that of the mutants of the other two genes of the *etfB-etfA-fcd* gene cluster (Fig. 7, 10). Quantification of metabolites was done with an internal standard of known concentration (section 2.11.2). Symbols: *triangles*, pH; *circles*, OD at 600 nm; *squares*, residual glucose concentration

3.2.3.3 Transcriptional analysis of the mutant of the *etfB* of the *etfB-etfA-fcd* cluster as compared to the wild type

After characterizing the *etfB* mutant in continuous fermentation, microarray experiments were performed to detect transcriptome changes caused by inactivation of the *etfB* gene. Cells of steady-state acidogenic and solventogenic growth of the chemostat culture of the *etfB* mutant were used for RNA preparation and the following microarray experiments. cDNA (complementary DNA) samples from the same growth phases of the wild type continuous culture were utilized as the reference in transcriptional analyses. Detailed experimental processes involved in microarray experiments and methods for data analysis were described in Materials and Methods (section 2.10). Slides covalently coupled with oligonucleotide probes (2 identical spots for 1 gene) were hybridized with combined labelled cDNA containing 80 pmol of Cy3 and Cy5 (GE Healthcare Europe GmbH, Munich, Germany) from the *etfB* mutant and wild type, followed by slides scanning using a GenePix 4000B microarray scanner and GenePix Pro 4.0 software (Axon Instruments, Union City, USA). The ratio of medians, the ratio of means and the regression ratio were automatically calculated by GenePix Pro 6.0 software (Axon Instruments, Union City, USA) based on intensities of fluorescence signals the *etfB* mutant and wild type (reference) cDNA samples when analyzing scanned microarray images. Normalization was carried out by setting the arithmetic mean of the ratios equal to 1. Background correction was then conducted by subtracting the background value plus one standard deviation from the foreground value. The ratio of medians, the ratio of means and the regression ratio (they differed by less than 30%) were used to correct for spot morphology of features of one hybridization and the ratio of medians was used to calculated for the final expression ratio (average of the two ratios of medians from two identical spots) which was subsequently taken its logarithm (to the basis of 2). The results from microarray experiments were calculated by mean of one hybridization and its dye-flip hybridization.

As mentioned previously (section 2.10.6), a logarithmic ratio format was used in transcriptional analysis for convenience to discriminate up-regulated and down-regulated genes. A positive logarithmic ratio indicated a gene induced in the *etfB* mutant, whereas a negative logarithmic ratio represented a repressed gene of the *etfB* mutant as compared to the wild type. In addition, a logarithmic ratio larger than 1.60 was for significant induction in contrast to a ratio less than -1.60 which meant this gene was significantly repressed when the *etfB* gene was deleted. As a result, the higher a positive logarithmic ratio was, the more noticeable a gene was up-regulated in the *etfB* mutant, and a gene was down-regulated in a more significant level when its negative logarithmic ratio was lower.

Through microarray experiments of the mutant of the *etfB* gene of the *etfB-etfA-fcd* cluster, it was found that the expression profiles of most genes responsible for the central metabolic pathways (Fig. 2) were not significantly altered as compared to the wild type. Interestingly, a *pfor* (*CA_C2229*) was repressed by ~75% during solventogenic growth of the *etfB* mutant, which was similar to what was found in the mutants of the *fcd* and *etfA* of the *etfB-etfA-fcd* cluster (Table 8, 13). Pfor functions at the node of pyruvate to acetyl-CoA (Fig. 2). Therefore, it suggested that the *etfB* gene of the *etfB-etfA-fcd* cluster affected carbon flux flowing through the C_4 route. This is in accordance with the decreased glucose consumption of solventogenic cells of the *etfB* mutant (Fig. 13). In addition, the expression of the *bcs* operon (*CA_C2708-CA_C2712*) was down-regulated during solventogenesis, suggesting that the *etfB* gene of the *etfB-etfA-fcd* cluster influenced the C_4 metabolism of *C. acetobutylicum* at pH 4.5 (Fig. 2). This phenomenon resembles what was found in the mutant of the *etfA* gene of the

etfB-etfA-fcd cluster (Table 13). Moreover, an antagonistic expression pattern was observed at pH 5.7 with the two paralogs of aldehyde/alcohol dehydrogenase genes, *adhE1* and *adhE2*. This is similar to what was reported previously (Grimmler *et al*., 2011). Besides, *adc* gene (*CA_P0165*) was strongly induced in acidogenic cells of the *etfB* mutant and a gene encoding a lactate dehydrogenase (CA_C0267) was significantly repressed at pH 5.7. Also, the transcript levels of acetate synthesis genes, *pta* and *ack*, were decreased (2-fold for *pta* and 4-fold for *ack*) during acidogenic growth of the *etfB* mutant. This was consistent with the slighty declined production of acetic acid during this phase (Fig. 13). The expression patterns of central metabolic genes in the mutant of the *etfB* gene of the *etfB-etfA-fcd* cluster are listed in Table 18.

Table 18. Expression patterns of the central metabolic genes compared to wild type in the mutant of the *etfB* of the *etfB-etfA-fcd* cluster during acidogenic and solventogenic growth

ID	Protein function[a]	Ratio[b]	
		pH 5.7	pH 4.5
CA_P0035	AdhE2, aldehyde-alcohol dehydrogenase	-1.02	—
CA_P0078	ThlB, acetyl coenzyme A acetyltransferase	-0.55	—
CA_P0162	AdhE1, aldehyde dehydrogenase (NAD^+)	1.53	0.22
CA_P0163	CtfA, butyrate-acetoacetate CoA-transferase subunit A	1.50	0.34
CA_P0164	CtfB, butyrate-acetoacetate CoA-transferase subunit B	1.18	0.06
CA_P0165	Adc, acetoacetate decarboxylase	3.20	0.67
CAC0028	HydA, hydrogene dehydrogenase	-0.13	0.14
CAC0267	Ldh, lactate dehydrogenase	-2.67	-0.38
CAC1543	Ldh, lactate dehydrogenase	1.38	-0.30
CAC1742	Pta, phosphate acetyltransferase	-1.00	-0.60
CAC1743	Ack, acetate kinase	-1.99	-0.77
CAC2229	Pfor, pyruvate ferredoxin oxidoreductase	-0.91	-2.03
CAC2499	Pfor, pyruvate ferredoxin oxidoreductase	—	—
CAC2708	Hbd, β-hydroxybutyryl-CoA dehydrogenase	-0.62	-0.97
CAC2709	EtfA, electron transfer flavoprotein alpha-subunit	-1.07	-1.10
CAC2710	EtfB, electron transfer flavoprotein beta-subunit	-0.13	-1.02
CAC2711	Bcd, butyryl-CoA dehydrogenase	-0.65	-1.03
CAC2712	Crt, crotonase	-0.45	-0.99
CAC2873	ThlA, acetyl-CoA acetyltransferase	-0.29	-0.43
CAC3075	Buk, butyrate kinase	-1.16	-0.75
CAC3076	Ptb, phosphate acetyltransferase	-0.34	-0.77
CAC3552	Ldh, lactate dehydrogenase	—	—

Genes are listed in order of ORFs, and considered as significantly up-regulated when the logarithmic ratio was ≥1.60 and as significantly down-regulated when the logarithmic ratio was ≤ -1.60. The given values in the table are mean of results of two hybridizations with dye swaps

[a] Protein names based on Nölling *et al.* (2001)

[b] The expression ratio as the logarithm to the basis of 2

On the other hand, transcription of 177 genes in acidogenic cells and 49 genes in solventogenic cells was observed to be strongly induced when inactivating the *etfB* gene of the *etfB-etfA-fcd* cluster, while 60 genes during acidogenesis and 14 genes during solventogenesis showed noticeable repression. Each was in comparison to the status at the same pH value of the wild type chemostat culture. Results were listed in Table 19-22, respectively.

Table 19. Significantly up-regulated genes compared to wild type in the mutant of the *etfB* gene of the *etfB-etfA-fcd* cluster during acidogenic growth

ID	Protein function[a]	Ratio[b]
CA_P0004	Cysteine protease	2.99
CA_P0057	Putative glycoportein or S-layer protein	2.66
CA_P0058	Rare lipoprotein	4.04
CA_P0112	Hypothetical protein	2.31
CA_P0129	Glycogen-binding regulatory subunit of S/T protein phosphatase I	3.72
CA_P0134	Hypothetical protein	3.16
CA_P0135	Oxidoreductase	2.73
CA_P0136	AstB/ChuR/NirJ-related protein	2.57
CA_P0137	UDP-glucuronosyltransferase, *B.subtilis* related YpfP	2.96
CA_P0138	Hypothetical protein	2.49
CA_P0139	Possible D-alanyl carrier protein, acyl carrier protein family	2.82
CA_P0148	Phospholipase C	4.30
CA_P0165	Adc Acetoacetate decarboxylase	3.20
CA_P0168	Alpha-amylase	2.96
CA_P0173	Archaeal-type Fe-S oxidoreductase	2.91
CA_P0174	Membrane protein	2.79
CAC0029	Distantly related to cell wall-associated hydrolase, similar to YycO *B subtilis*	3.42
CAC0030	Hypothetical protein	2.87
CAC0033	ABC family protein kinase	1.94
CAC0078	AgrB putative accessory gene regulator protein	2.65
CAC0079	Hypothetical protein	3.22
CAC0082	Predicted membrane protein	2.48
CAC0110	CysN GTPase, sulfate adenylate transferase subunit 1	1.93
CAC0139	Predicted permease	2.18
CAC0175	Hypothetical protein	2.33
CAC0176	Oligopeptide-binding protein, periplasmic component	2.58
CAC0183	Transcriptional regulator, sugar kinase	2.01
CAC0252	Molybdate-binding protein	1.69
CAC0254	NifHD Nitrogen regulatory protein PII (nitrogen fixation NifHD)	2.97
CAC0255	NifHD Nitrogen regulatory protein PII (nitrogen fixation NifHD)	2.32
CAC0256	NifD Nitrogenase molybdenum-iron protein, alpha chain (nitrogenase component I)	2.22
CAC0381	Methyl-accepting chemotaxis protein	2.09
CAC0383	PTS cellobiose-specific component IIA	3.25
CAC0384	PTS system, cellobiose-specific component BII	2.55
CAC0385	Beta-glucosidase	3.24
CAC0387	Hypothetical protein	1.68
CAC0488	Hypothetical protein	3.12
CAC0489	4-Phosphopantetheinyl transferase	1.97
CAC0490	Predicted sugar kinase	2.31
CAC0491	Uncharacterized probably secreted protein	1.74
CAC0537	Acetylxylan esterase, acyl-CoA esterase or lipase, strong similarity to C-terminal region of endoglucanase E precursor	2.64

Table 19. (continued)

ID	Protein function[a]	Ratio[b]
CAC0542	Methyl-accepting chemotaxis protein	2.50
CAC0555	Predicted membrane protein	2.25
CAC0660	Hypothetical protein	3.56
CAC0663	Hypothetical protein	5.74
CAC0664	Sugar-binding periplasmic protein	3.55
CAC0666	Sugar permease	4.52
CAC0702	Predicted lipoprotein	1.97
CAC0703	Sugar ABC-transporter, ATP-ase component	2.81
CAC0704	Sugar ABC transporter, permease protein	2.59
CAC0705	Sugar ABC transporter, permease protein	2.73
CAC0746	Secreted protease metal-dependent protease	1.98
CAC0792	D-amino acid aminotransferase	2.66
CAC0814	3-Oxoacyl-[acyl-carrier-protein] synthase III	4.06
CAC0815	Methyl-accepting chemotaxis protein	3.38
CAC0816	Lipase-esterase related protein	4.49
CAC0844	Barstar-like protein ribonuclease (barnase) inhibitor	1.98
CAC0912	Possible non-processive endoglucanase	1.92
CAC1010	Predicted phosphohydrolase	3.18
CAC1072	Fe-S oxidoreductase	4.15
CAC1076	Hypothetical protein	1.73
CAC1078	Predicted phosphohydrolase	3.88
CAC1079	Uncharacterized protein, related to enterotoxins of other clostridia	3.01
CAC1080	Uncharacterized protein, probably surface-located	3.91
CAC1081	Uncharacterized protein, probably surface-located	3.56
CAC1102	Predicted membrane protein	2.99
CAC1336	Hypothetical protein	1.88
CAC1337	Spore coat protein	2.72
CAC1354	Phosphotransferase system IIA component	2.56
CAC1532	Protein containing CheW-repeats	3.12
CAC1533	Hypothetical protein	2.84
CAC1669	Carbon starvation protein	1.74
CAC1775	Predicted membrane protein	5.50
CAC1817	Stage V sporulation protein, SpoVS	3.11
CAC1868	Uncharacterized secreted protein	2.64
CAC1986	Hypothetical protein	2.01
CAC1988	Ferrichrome-binding periplasmic protein	3.48
CAC1989	ABC-type iron (III) transport system, ATPase component	3.49
CAC1990	ABC-type iron (III) transport system, permease component	2.12
CAC1991	Uncharacterized protein	3.52
CAC1992	MoaC molybdenum cofactor biosynthesis protein C	2.89
CAC1993	MoaA Molybdenum cofactor biosynthesis enzyme, Fe-S oxidoreductase	2.88
CAC1994	MoaB Molybdopterin biosynthesis enzyme	2.70
CAC1996	Hypothetical protein	2.97

Table 19. (continued)

ID	Protein function[a]	Ratio[b]
CAC1997	Predicted glycosyltransferase	3.03
CAC1998	ABC-type transport system, ATPase component	3.17
CAC1999	Hypothetical protein	3.17
CAC2000	Indolepyruvate ferredoxin oxidoreductase	4.17
CAC2002	Predicted iron-sulfur flavoprotein	3.26
CAC2003	Predicted permease	3.54
CAC2005	Siderophore/surfactin synthetase related protein	3.04
CAC2006	Enzyme of siderophore/surfactin biosynthesis	4.34
CAC2007	Predicted glycosyltransferase	3.76
CAC2008	3-Oxoacyl-(acyl-carrier-protein) synthase	3.05
CAC2009	MmgB 3-Hydroxyacyl-CoA dehydrogenase	4.11
CAC2010	Predicted Fe-S oxidoreductase	3.05
CAC2011	FabH Possible 3-oxoacyl-[acyl-carrier-protein] synthase III	4.95
CAC2012	FadB Enoyl-CoA hydratase	4.21
CAC2013	Hypothetical protein	4.21
CAC2014	Predicted esterase	3.97
CAC2015	Hypothetical protein	4.33
CAC2016	FadB Enoyl-CoA hydratase	4.69
CAC2017	Acyl carrier protein	3.81
CAC2018	Aldehyde ferredoxin oxidoreductase	3.96
CAC2019	Malonyl CoA-acyl carrier protein transacylase	3.02
CAC2021	MoeA Molybdopterin biosynthesis enzyme	2.50
CAC2022	MoaB Molybdopterin biosynthesis enzyme	2.72
CAC2023	Membrane protein	2.88
CAC2024	Phosphatidylglycerophosphate synthase related protein (fragment)	2.44
CAC2025	Hypothetical protein	2.47
CAC2026	Predicted flavodoxin	3.18
CAC2040	ATPase component	2.49
CAC2107	Protein contains cell adhesion domain	3.27
CAC2226	Branched-chain amino acid aminotransferase/4-amino-4-deoxychorismate lyase	2.02
CAC2252	Alpha-glucosidase fused to unknown alpha-amylase C-terminal	1.82
CAC2308	SpoIIAA Anti-anti-sigma factor (antagonist of SpoIIAB)	2.65
CAC2342	Predicted membrane protein	1.95
CAC2375	Oligopeptide ABC-type transporter, permease	1.89
CAC2382	Single-strand DNA-binding protein	2.76
CAC2389	ArgB Acetylglutamate kinase	1.94
CAC2404	Glycosyltransferase	2.84
CAC2405	Predicted glycosyltransferase	2.62
CAC2517	NrpE Extracellular neutral metalloprotease	3.30
CAC2518	Extracellular neutral metalloprotease	2.02
CAC2541	Reductase/isomerase/elongation factor common domain	2.20
CAC2542	FAD/FMN-containing dehydrogenase	6.08
CAC2543	EtfA Electron-transferring flavoprotein large subunit	6.87

Table 19. (continued)

ID	Protein function[a]	Ratio[b]
CAC2544	EtfB Electron-transferring flavoprotein small subunit	5.67
CAC2574	Predicted S-adenosylmethionine-dependent methyltransferase	2.08
CAC2576	6-Pyruvoyl-tetrahydropterin synthase related protein	2.17
CAC2577	Uncharacterized protein	2.42
CAC2580	Hypothetical protein	2.80
CAC2581	6-pyruvoyl-tetrahydropterin synthase related domain, conserved membrane protein	3.51
CAC2584	Protein containing CheW-repeats	3.71
CAC2663	Protein containing cell-wall hydrolase domain	3.77
CAC2678	Hypothetical protein	1.77
CAC2695	Diverged Metallo-dependent hydrolase	4.82
CAC2716	Predicted glycosyl transferase from UDP-glucuronosyltransferase family	3.02
CAC2722	Predicted protein (beta propeller fold)	2.46
CAC2806	Predicted phosphohydrolase	2.21
CAC2807	Endo-1,3(4)-beta-glucanase	2.51
CAC2808	Beta-lactamase class C domain containing protein	3.93
CAC2810	Possible glucoamylase (diverged)	3.06
CAC2938	Hypothetical protein	2.74
CAC2944	N-terminal domain intergin-like repeats and c-terminal-cell wall-associated hydrolase domain	4.23
CAC3060	ATPase	2.49
CAC3061	Membrane protein	2.15
CAC3062	Hydrolase	1.91
CAC3064	UDP-N-acetylglucosamine 2-epimerase	2.02
CAC3065	Possible O-antigen/teichoic acid transporter	1.96
CAC3067	Predicted membrane protein	2.12
CAC3068	Glycosyltransferase	2.11
CAC3069	Predicted glycosyltransferase	2.06
CAC3070	Glycosyltransferase	2.17
CAC3071	Glycosyltransferase	2.96
CAC3072	Mannose-1-phosphate guanylyltransferase	2.56
CAC3073	Sugar transferase involved in lipopolysaccharide synthesis	2.43
CAC3085	Protein containing cell-adhesion domain	3.29
CAC3086	Protein containing cell adhesion domain	3.14
CAC3251	Sensory transduction protein	2.87
CAC3298	BdhB NADH-dependent butanol dehydrogenase B	2.82
CAC3355	Polyketide synthase	2.87
CAC3408	NADH oxidase (two distinct flavin oxidoreductase domains)	2.61
CAC3409	Transcriptional regulators	2.33
CAC3412	Predicted protein-S-isoprenylcysteine methyltransferase	4.41
CAC3422	Sugar proton symporter (possible xylulose)	2.75
CAC3423	Acetyltransferase (ribosomal protein N-acetylase subfamily)	2.19
CAC3460	Hypothetical protein	3.10
CAC3558	Probable S-layer protein	4.06

Table 19. (continued)

ID	Protein function[a]	Ratio[b]
CAC3565	Uncharacterized secreted protein, containing cell adhesion domain	2.95
CAC3633	Hypothetical protein	2.37
CAC3635	Oligopeptide ABC transporter, ATPase component	3.03
CAC3636	Oligopeptide ABC transporter, ATPase component	2.60
CAC3637	Oligopeptide ABC transporter, permease component	2.36
CAC3638	Oligopeptide ABC transporter, permease component	2.47
CAC3639	DNA-binding protein	3.41
CAC3684	Polygalacturonase	2.22

Genes are listed in order of ORFs and considered as significantly up-regulated when the logarithmic ratio was ≥1.60. The given values in the table are mean of results of two hybridizations with dye swaps

[a] Protein name based on Nölling *et al.* (2001)

[b] The expression ratio as the logarithm to the basis of 2

During the steady-state acidogenic growth of the *etfB* (from the *etfB-etfA-fcd* cluster) mutant, 177 genes were significantly up-regulated as compared to the wild type (Table 19). This indicated that mutation in the *etfB* of the *etfB-etfA-fcd* cluster exerted profound effects on acidogenic metabolism and corresponded to the prolonged period of the mutant culture to enter the steady-state acidogenesis. Among genes regulated in this data set, the overwhelming majority was included in that of the *etfA* (from the *etfB-etfA-fcd* cluster) mutant during the same growth phase (Table 14). This finding indicated that mutation in the *etfA* and *etfB* led to highly similar metabolic influences during acidogenic growth and they probably functioned similarly during this phase.

The most remarkable difference between gene expression profiles in these two mutants was that, *CA_C2544-CA_C2542* (*etfB-etfA-fcd*) cluster revealed significant induction in the *etfB* mutant transcriptome but not in the *etfA* mutant. This suggests a complex interplay between genes of this cluster.

Table 20. Significantly down-regulated genes compared to wild type in the mutant of the *etfB* gene of the *etfB-etfA-fcd* cluster during acidogenic growth

ID	Protein function[a]	Ratio[b]
CA_P0116	Xylanase, glycosyl hydrolase	-2.10
CA_P0118	Possible xylan degradation enzyme	-3.28
CA_P0119	Possible xylan degradation enzyme	-3.22
CA_P0120	Possible xylan degradation enzyme	-3.47
CAC0014	Aminotransferase	-3.51
CAC0015	SerA D-3-phosphoglycerate dehydrogenase	-3.40
CAC0016	Related to HTH domain of SpoOJ/ParA/ParB/RepB family, involved in chromosome partitioning	-4.32
CAC0017	SerS seryl-tRNA synthetase	-3.96
CAC0018	Putative NADPH-quinone reductase	-2.49

Table 20. (continued)

ID	Protein function[a]	Ratio[b]
CAC0156	PTS system, mannitol-specific IIA domain	-2.74
CAC0267	Ldh L-lactate dehydrogenase	-2.67
CAC0393	*kdgR* operon repressor	-1.94
CAC0572	Predicted membrane protein	-1.91
CAC0687	CysE Serine acetyltransferase	-2.01
CAC0882	Predicted membrane protein	-1.95
CAC0980	PflB Pyruvate-formate lyase	-4.07
CAC0981	PflA Pyruvate-formate-lyase-activating enzyme	-3.77
CAC0983	Hypothetical protein	-3.15
CAC1227	Hypothetical protein	-1.81
CAC1320	GlpP Glycerol-3-phosphate responsive antiterminator	-2.10
CAC1390	PurE phosphoribosylaminoimidazole carboxylase catalytic subunit	-2.57
CAC1391	PurC phosphoribosylaminoimidazole-succinocarboxamide synthase	-3.08
CAC1392	PurF amidophosphoribosyltransferase	-2.79
CAC1393	PurM phosphoribosylaminoimidazole synthetase	-3.19
CAC1394	PurN phosphoribosylglycinamide formyltransferase	-2.76
CAC1395	PurH bifunctional phosphoribosylaminoimidazolecarboxamide formyltransferase/cyclohydrolase	-3.05
CAC1396	PurD phosphoribosylamine-glycine ligase	-2.28
CAC1547	TrxA Thioredoxin	-2.49
CAC1655	PurQ/PurL bifunctional enzyme phosphoribosylformylglycinamidine synthase (synthetase domain/glutamine amidotransferase domain)	-3.01
CAC1743	Acetate kinase	-1.99
CAC1846	Flagellar motor protein	-1.95
CAC1900	Phage regulatory protein, containing Zn-finger	-3.31
CAC1904	Hypothetical protein	-3.44
CAC1909	Ribonuclease D	-3.01
CAC1910	Predicted membrane protein	-2.38
CAC1912	Uncharacterized phage related protein	-5.93
CAC1930	Uncharacterized protein	-2.50
CAC1933	Hypothetical protein	-4.05
CAC1936	Hypothetical protein	-3.47
CAC1942	Hypothetical protein	-3.11
CAC1949	Possible protein	-2.91
CAC2445	5-Aminoimidazole-4-carboxamide ribonucleotide transformylase	-2.80
CAC2446	Hypothetical protein	-2.94
CAC2592	6-Pyruvoyl-tetrahydropterin synthase related domain, membrane protein	-3.53
CAC2849	Proline/glycine betaine ABC-type transport system, permease component fused to periplasmic component	-2.13
CAC3045	Hydrolase	-2.86
CAC3049	Glycosyltransferase	-3.22
CAC3051	Glycosyltransferase	-2.88
CAC3054	Phosphoheptose isomerase	-4.54
CAC3055	Sugar kinase	-5.19

Table 20. (continued)

ID	Protein function[a]	Ratio[b]
CAC3058	Mannose-1-phosphate guanylyltransferase	-5.80
CAC3059	Sugar transferase	-5.13
CAC3224	PurR purine operon repressor	-1.72
CAC3288	Iron-regulated ABC transporter ATPase subunit	-2.08
CAC3421	Acyl carrier protein phosphodiesterase	-2.16
CAC3458	Uncharacterized protein, homolog of *B. anthracis*	-2.15
CAC3461	Hypothetical protein	-2.40
CAC3575	FabD acyl-carrier-protein S-malonyltransferase	-1.66
CAC3592	Hypothetical protein	-1.93
CAC3647	AbrB Transition state regulatory protein	-3.69

Genes are listed in order of ORFs and considered as significantly down-regulated when the logarithmic ratio was ≤ -1.60. The given values in the table are mean of results of two hybridizations with dye swaps

[a] Protein name based on Nölling *et al.* (2001)

[b] The expression ratio as the logarithm to the basis of 2

During the steady-state acidogenic growth of the *etfB* (from the *etfB-etfA-fcd* cluster) mutant, 60 genes were significantly down-regulated as compared to the wild type (Table 20). Similar to the gene expression pattern in the data set "up-regulated during acidogenesis" of the *etfB* mutant (Table 19), majority of genes in the *etfB* mutant "down-regulated during acidogenesis" set was also included in the corresponding *etfA* mutant data set (Table 15). This further indicated similar roles of these two genes for ETF subunits. Among the genes down-regulated, the expression of clusters (*CA_C0014-CA_C0017* and *CA_C1390-CA_C1396*) was shown to be noticeably repressed, which displayed the biosynthesis of serine and purines of the *etfB* mutant strain was interfered. Besides, the carbohydrate metabolism in this phase was also affected, which was observed from the decreased expression level of genes *CA_C3054-CA_C3055*, *CA_C3058-CA_C3059*, *CA_P0116* and *CA_P0118-CA_P0120*.

Table 21. Significantly up-regulated genes compared to wild type in the mutant of the *etfB* gene of the *etfB-etfA-fcd* cluster during solventogenic growth

ID	Protein function[a]	Ratio[b]
CA_P0036	Uncharacterized, ortholog of YgaT of *B.subtillis*	5.57
CA_P0037	Uncharacterized, ortholog of YgaS of *B.subtillis*	5.39
CA_P0144	Possible steroid binding protein	2.04
CA_P0145	Hypothetical protein	1.95
CA_P0153	Predicted transcriptional regulator	2.51
CA_P0154	Membrane protein	2.20
CA_P0168	Alpha-amylase	1.96
CAC0102	O-acetylhomoserine sulfhydrylase	6.28
CAC0103	CysC Adenylylsulfate kinase	6.84
CAC0104	Adenylylsulfate reductase	7.06
CAC0105	Ferredoxin	7.02

Table 21. (continued)

ID	Protein function[a]	Ratio[b]
CAC0106	ABC-type probable sulfate transporter, periplasmic binding protein	6.25
CAC0109	CysD sulfate adenylyltransferase subunit 2	7.08
CAC0110	CysN GTPase, sulfate adenylate transferase subunit 1	6.59
CAC0264	Predicted membrane protein	1.73
CAC0385	Beta-glucosidase	2.00
CAC0386	PTS cellobiose-specific component IIC	2.08
CAC0387	Hypothetical protein	2.03
CAC0562	Predicted membrane protein	1.63
CAC0580	Hypothetical protein	2.03
CAC0830	Response regulator	2.26
CAC0831	Sensory transduction histidine kinase	1.92
CAC0878	Amino acid ABC transporter permease component	2.13
CAC0879	ABC-type polar amino acid transport system, ATPase component	2.35
CAC0880	Periplasmic amino acid binding protein	2.46
CAC0929	SAM-dependent methyltransferase	3.37
CAC0930	MetB Cystathionine gamma-synthase	4.10
CAC0932	Hypothetical protein	3.98
CAC0984	ABC transporter, ATP-binding protein	2.46
CAC0985	ABC transporter, permease component	2.86
CAC0986	Lipoprotein, attached to the cytoplasmic membrane	3.56
CAC2086	Stage III sporulation protein AH, SpoIIIAH	2.23
CAC2089	Stage III sporulation protein AE, SpoIIIAE	1.68
CAC2092	stage III sporulation protein SpoAB	2.10
CAC2235	CysK Cysteine synthase/cystathionine beta-synthase	3.35
CAC2236	Uncharacterized conserved protein	1.93
CAC2383	Predicted xylanase/chitin deacetylase	2.22
CAC2517	NrpE Extracellular neutral metalloprotease	1.69
CAC2542	FAD/FMN-containing dehydrogenase	5.03
CAC2543	EtfA Electron-transferring flavoprotein large subunit	5.21
CAC2544	EtfB Electron-transferring flavoprotein small subunit	4.66
CAC2545	Hypothetical protein	2.26
CAC2681	Hypothetical protein	2.40
CAC2783	CysD O-acetylhomoserine sulfhydrylase	2.92
CAC2903	LysM domain containing membrane protein	2.00
CAC2906	Spore coat protein	2.35
CAC3325	Periplasmic amino acid binding protein	3.38
CAC3326	Amino acid ABC-type transporter, permease component	3.56
CAC3665	Alpha/beta superfamily hydrolase	2.98

Genes are listed in order of ORFs and considered as significantly up-regulated when the logarithmic ratio was ≥1.60. The given values in the table are mean of results of two hybridizations with dye swaps

[a] Protein name based on Nölling *et al.* (2001)

[b] The expression ratio as the logarithm to the basis of 2

Unlike the gene expression profile during acidogenesis, the transcript pattern during solventogenesis of the *etfB* mutant differed from that in the *etfA* mutant. During the steady-state solventogenic growth, 49 genes were significantly up-regulated in the *etfB* (from the *etfB-etfA-fcd* cluster) mutant as compared to the wild type (Table 21). Among these, 5 genes encoded membrane-associated proteins (*CA_P0154*, *CA_C0264*, *CA_C0386*, *CA_C0562* and *CA_C0986*), suggesting inactivation of *etfB* changed the characteristics of the cell membrane during solventogenesis. In addition, 2 genes (*CA_P0168* and *CA_C2517*) were shown to be strongly induced during this phase as compared to wild type where they highly expressed (Janssen *et al.*, 2010). Besides, the expression of genes for the transport of amino acids were induced (*CA_C0878-CA_C0880* and *CA_C3325-CA_C3326*), indicating increased demand for amino acids in the *etfB* mutant culture. Besides, sporulation-related genes were also up-regulated (*CA_C2086*, *CA_C2089*, *CA_C2092* and *CA_C2906*).

On the other hand, the most noticeable genes regulated in this set were *CA_C0102-CA_C0107*, *CA_C0109-CA_C0110*, *CA_C0929-CA_C0930*, *CA_C2235* and *CA_C2783*, as well as *CA_P0037-CA_P0036* operon (Janssen *et al.*, 2010), which were responsible for biosynthesis of cysteine and methionine, as well as unclear pathways, respectively. Their transcript abundance was elevated from 7.5-fold to 135-fold, which showed similar induction intensities as those in the corresponding data set of the *etfA* mutant.

Last but not least, the cluster *CA_C2544-CA_C2542* displayed strongly induced expression (25.2-fold~37-fold), which was similar to expression patterns of these genes during acidogenesis of the *etfB* mutant.

Table 22. Significantly down-regulated genes compared to wild type in the mutant of the *etfB* gene of the the *etfB-etfA-fcd* cluster during solventogenic growth

ID	Function[a]	Ratio[b]
CAC0316	Ornithine carbomoyltransferase	-2.04
CAC0318	Membrane permease, predicted cation efflux pumps	-1.92
CAC0319	ABC transporter ATP-binding protein	-1.83
CAC0380	Periplasmic amino acid-binding protein	-1.80
CAC0973	ArgG argininosuccinate synthase	-2.77
CAC0974	ArgH Argininosuccinate lyase	-2.69
CAC0975	Predicted P-loop kinase or ATPase distantly related to phosphoenolpyruvate carboxykinase	-2.08
CAC2229	Pyruvate ferredoxin oxidoreductase	-2.03
CAC2388	ArgD N-acetylornithine aminotransferase	-3.02
CAC2390	ArgC N-acetyl-gamma-glutamyl-phosphate reductase	-2.28
CAC2391	ArgJ bifunctional ornithine acetyltransferase/N-acetylglutamate synthase protein	-2.60
CAC3526	FMN-binding protein	-2.92
CAC3527	Ferredoxin	-2.84
CAC3619	Amino acid ABC transporter, permease component	-1.66

Genes are listed in order of ORFs and considered as significantly down-regulated when the logarithmic ratio was ≤ -1.60. The given values in the table are mean of results of two hybridizations with dye swaps

[a] Protein name based on Nölling *et al.* (2001)

[b] The expression ratio as the logarithm to the basis of 2

During the steady-state solventogenic growth of the *etfB* (from the *etfB-etfA-fcd* cluster) mutant, only 14 genes were significantly down-regulated as compared to the wild type (Table 22), and overwhelming majority of these genes was included in the data set of the *etfA* mutant at the same pH. Among these, 6 genes were responsible for biosynthesis of arginine (*CA_C0316*, *CA_C0973-CA_C0974*, *CA_C2388*, *CA_C2390* and *CA_C2391*) and 2 genes encoded transporters for amino acids (*CA_C0380* and *CA_C3619*). Besides, the expression of genes for electron transfer was also significantly decreased (*CA_C3526-CA_C3527*). In addition, the gene coding for pyruvate ferredoxin oxidoreductase (Pfor) was noticeably repressed, indicating the reaction of oxidative decarboxylation from pyruvate to acetyl-CoA and carbon dioxide in the central metabolism was interfered when the *etfB* was disrupted. This was also consistent with lower glucose consumption during solventogenic growth of the *etfB* mutant.

The number of genes that were significantly regulated during acidogenesis was approximately 3 times higher than that during solventogenesis of the *etfB* mutant, suggesting that mutation in the *etfB* resulted in more comprehensive influences on acidogenic cells. This is comparable to that observed in the *etfA* (from the *etfB-etfA-fcd* cluster) mutant.

3.2.4 Comparison of the mutant phenotype of each gene of the *etfB-etfA-fcd* cluster

The gene product of the *etfB-etfA-fcd* cluster is the second EtfA/B-dependent dehydrogenase complex whose roles remains unclear. Using the ClosTron system (Heap *et al.*, 2007, 2010a, 2010b), mutation in each gene of this cluster was achieved and characterization of these three mutants was conducted by continuous fermentation.

During the steady-states acidogenic growth of continuous cultures of these three mutants, butyrate production was not altered and the concentration of acetic acid was slightly decreased, which indicated that the *etfB-etfA-fcd* cluster did not exert significant influences on generation of acids in chemostat cultures at pH 5.7. Production of acetone and butanol during acidogenesis, however, was reduced by at least 37% in these mutants. This phenomenon suggested that the *etfB-etfA-fcd* cluster affected their formation at pH 5.7, although acetone and butanol were not main metabolites during this phase. Ethanol formation was also decreased (at least 25%) in these mutants during acidogenic growth.

During solventogenesis, the production of acetone and butanol was decreased by at least one third in the *fcd*, *etfA* and *etfB* mutants. This indicated that all genes from the *etfB-etfA-fcd* cluster were involved in the generation of acetone and butanol in chemostat cultures at pH 4.5. Ethanol production was also reduced during this phase. Acetate formation was not interfered during this phase and butyrate concentrations were increased by different extent (18-54%).

In summary, the *etfB-etfA-fcd* cluster was positively involved in the production of acetone, butanol and ethanol during acidogenic and solventogenic growth of continuous cultures. However, the mutant phenotype of each gene of the cluster differed in terms of butyrate concentration during solventogenesis. Approximately 54% more butyrate was left in supernatant of the *fcd* mutant as compared to that of the wild type, whereas in the *etfB* and *etfA* mutants butyric acid was accumulated at a lower level than in the *fcd* mutant (13%, 23%, respectively). Different butyrate accumulation in these three mutants during solventogenic growth suggested their distinct roles in butyrate metabolism.

3.2.5 Characterization of the *fcd/htpG* double mutant

Before the *fcd* mutant (section 3.2.1) was successfully generated, several attempts had been carried out for mutagenesis of this gene using the pMTL007 shuttle vector, the first generation plasmid of the ClosTron system (Heap *et al.*, 2007). During these attempts, a double mutant (mutation in the *fcd* and a previously unknown gene) was obtained although the original aim was to achieve a single mutagenesis of the *fcd* gene. This double mutant was verified by Southern blotting and presence of the pSOL1 megaplasmid was checked using starch plate test (section 2.5.1, 2.9.4). The second insertion site was subsequently determined to be in the *htpG* (*CA_C3315*) which was described in next section (see 3.2.6).

3.2.5.1 Generation of the *fcd/htpG* double mutant

Generation of the *fcd/htpG* ClosTron mutant was unexpected and the only difference between methods for acquisition of the *fcd* single mutant and the *fcd/htpG* double mutant was the shuttle vector used. The first generation plasmid of the ClosTron system, pMTL007 (instead of pMTL007C-E2 for successful acquisition of the *fcd* single mutant), led to generation of the *fcd/htpG* double mutant. Retargeted pMTL007::cac-*fcd*-1065a (Table 7, section 2.4) contained a *fac* promoter whose expression relied on an IPTG induction (section 2.5.2.2, 2.9.3) (Heap *et al.*, 2007).

Strategies for mutagenesis were described in detail in Methods and Materials (section 2.7.3.1, 2.9). Prediction of target sites (where intron could insert), design of primers for mutation of recognition sites of intron retargeting region on pMTL007, methods of plasmid construction, electroporation of *C. acetobutylicum*, screening of clones and PCR verification were all identical to that for generation of the *fcd* single mutant (see section 3.2.1).

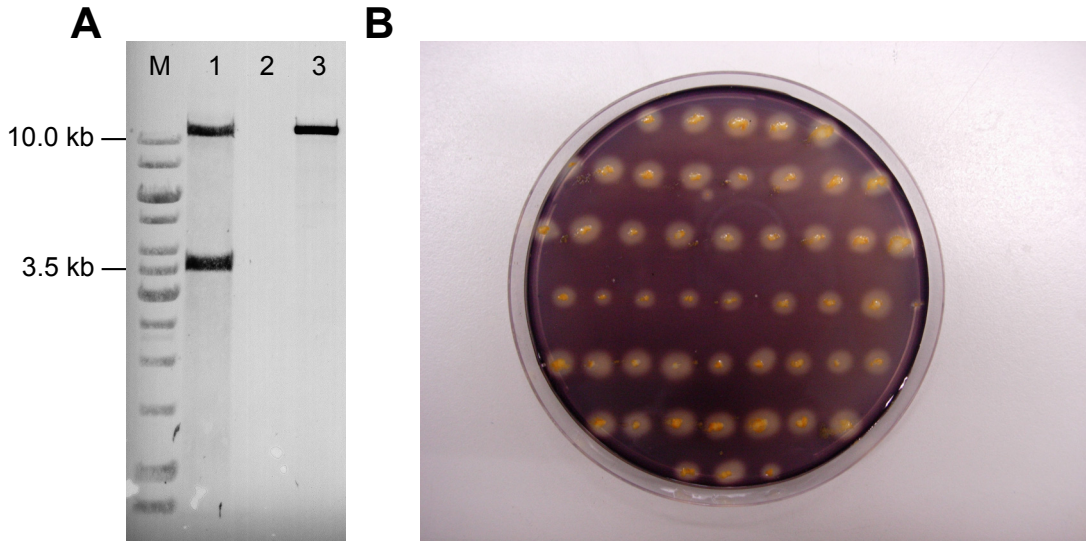

Fig. 14. Southern hybridization and starch plate test of the *fcd/htpG* double mutant. *Eco*RV-digested genomic DNA samples of the *fcd/htpG* double mutant and wild type were hybridized with biotin-labelled intron-specific DNA probe (A). M, marker; lane 1, genomic DNA of the *fcd/htpG* double mutant; lane 2, wild type genomic DNA; lane 3, pMTL007 digested with *Hin*dIII as a positive control. (B) The *fcd/htpG* mutant colonies were re-streaked on an agar plate containing starch, colonies still carrying the pSOL1 megaplasmid formed halos when staining with potassium iodine solution

As mentioned in the last paragraph, a PCR confirmation (section 2.7.2.1) was first carried out for this double mutant in the same way to that for the *fcd* single mutant, using *fcd* gene-specific primers (*fcd*-Forward and -Reverse primers, Table 39, Appendix section) for checking correct insertion of the intron, an intron specific primer (EBS universal, Table 38, Appendix section) and a *fcd*-Reverse primer for checking an intron-exon junction part, and a primer pair specific for pMTL007 plasmid (pMTL007check-Forward and -Reverse primers, Table 40, Appendix section) for confirming loss of this shuttle vector from mutant cells. Results were similar to that from the *fcd* single mutant (see section 3.2.1). As a result, the double mutant was not recognized by PCR and it seemed to be a *fcd* single mutant.

To further confirm insertion of the intron, i.e., that only one copy of the intron had inserted into *fcd* gene, Southern hybridization was performed with the intron-specific probe. Detailed methods of Southern hybridization were described previously (section 2.7.5). 590 bp of the intron-specific probe was PCR amplified using intron specific primers (ISP-Forward and -Reverse primers, Table 40, Appendix section) and pMTL007 plasmid was used as the template. The intron-specific probe (fragment) was located at an intron-erythromycin gene junction section (339-928 bp) in the intron (1,781 bp in length) where 774 bp of erythromycin gene resided (710-1,483 bp). Genomic DNA of the *fcd/htpG* double mutant as well as that of the wild type were digested with *Eco*RV-HF at 37 °C for 16 hours before they were transferred from an agarose gel to a positively charged nylon membrane which was then hybridized overnight with the biotin-labeled intron-specific probe at 42 °C. Instead of acquisition of a single product, two bands at ~12 kb and 3.6 kb were obtained for this mutant, demonstrating that it possessed two copies of the intron on the chromosome and it was a double mutant. The band of 3.6 kb was, as expected, to be for the *fcd* gene (Fig. 6A) and thus *fcd* gene and an additional gene (*htpG* gene, see section 3.2.6 for mining of this gene) were inserted with the intron. No hybridization signal was observed for wild type genomic DNA, as expected, because the intron-specific probe used did not hybridize to any original DNA sequence in *C. acetobutylicum*. Restricted pMTL007 with *Hin*dIII was used as a positive control, showing a signal at 11.8 kb which was equal to the size of linear pMTL007 plasmid (Fig. 14A). Consequently, after confirmation by Southern hybridization, it was proved that a double mutant had been generated.

The presence of the pSOL1 megaplasmid was detected via the iodine-exposed starch plate test (section 2.5.1, 2.9.4), because pSOL1-containing cells was able to degrade starch in solidified media and form halos when exposed with iodine. To confirm the presence of the pSOL1 in the *fcd/htpG* double mutant cells, about 50 colonies of this mutant strain were re-streaked on a RCA (reinforced clostridial agar) plate which contained 1% starch. After 24 h of incubation at 37 °C under anaerobic conditions, colonies still containing pSOL1 degraded the surrounding starch and formed halos when the starch-containing plate was stained with potassium iodine solution (Lugol) solution (Fig. 14B). Through this test, it was demonstrated that the *fcd/htpG* double mutant strain generated by the ClosTron system still carried the pSOL1 megaplasmid.

3.2.5.2 Continuous fermentation of the *fcd/htpG* double mutant

After confirming the *fcd/htpG* double mutant at molecular and phenotypical levels, continuous fermentation was performed to characterize this mutant (Fig. 15). Methods for chemostat culture of *C. acetobutylicum* were described in detail previously (section 2.6).

During acidogenic growth of the continuous culture of the *fcd/htpG* double mutant, the OD_{600} was ~3.4 which was lower than that of the wild type and all mutants of genes in the *etfB-etfA-fcd* cluster. After ~14 h of the pH shift, the culture of the *fcd/htpG* double mutant entered solventogenesis. During the pH shift, a "pocket" phenotype, at which the OD_{600} of the culture decreased continuously and then increased, was observed. This suggested that this double mutant underwent an extended period of adaptation for a more acidic environment (from pH 5.7 to pH 4.5). The final OD_{600} of the culture during the steady-state solventogenic growth was ~4.0, which was higher than the wild type and mutants of genes from the *etfB-etfA-fcd* cluster during this phase. In terms of glucose consumption, the *fcd/htpG* double mutant utilized more glucose during acidogenesis than during solventogenesis, which was similar to the wild type strain. However, the *fcd/htpG* double mutant consumed less glucose than the wild type during both acidogenesis and solventogenesis, which led to slightly lower production of acetic acid (~40 mM) and butyric acid (~53 mM) during acidogenesis and decreased (~40%) concentrations of acetone and butanol during solventogenic growth. During acidogenesis, production of acetone and butanol was also reduced more than 89% although these were not predominant metabolites during this phase. Besides, more butyrate (~54%) was formed during solventogenic growth, whereas acetic acid formed (~14 mM) was slightly higher than the wild type during the same growth phase. Moreover, ethanol formation was also disturbed during acidogenic and solventogenic growth of the *fcd/htpG* double mutant. The results indicated that double mutation in the *fcd* and *htpG* (see section 3.2.6) significantly interfered the generation of all three solvents and butyrate metabolism during solventogenic growth, and the mutation also affected production of acetate and butyrate during acidogenesis.

3.2.6 Characterization of the *htpG* mutant

3.2.6.1 Identification of the *htpG* from the *fcd/htpG* double mutant

As introduced in section 3.2.5, an unexpected *fcd/htpG* (*CA_C2542/CA_C3315*) double mutant was generated using the first generation plasmid of the ClosTron system (pMTL007 plasmid, Table 7, section 2.4), in spite of original goal of deleting a *fcd* gene in *C. acetobutylicum*. After verification of this double mutant by Southern blotting (standard PCR with one primer pair for the *fcd* gene was not able to detect this unexpected second mutation), a 3.6 kb band (for the *fcd* gene) and a ~12 kb band (for a unknown gene at the beginning) were visible. Therefore, it became an important question to identify what the second mutated gene was. To deal with this problem, an DNA ligase-mediated PCR was performed. This strategy was developed from a RNA ligase-mediated rapid amplification of 5' and 3' cDNA ends (RLM-RACE) (GeneRacer^{TM} kit, Invitrogen Life Technologies).

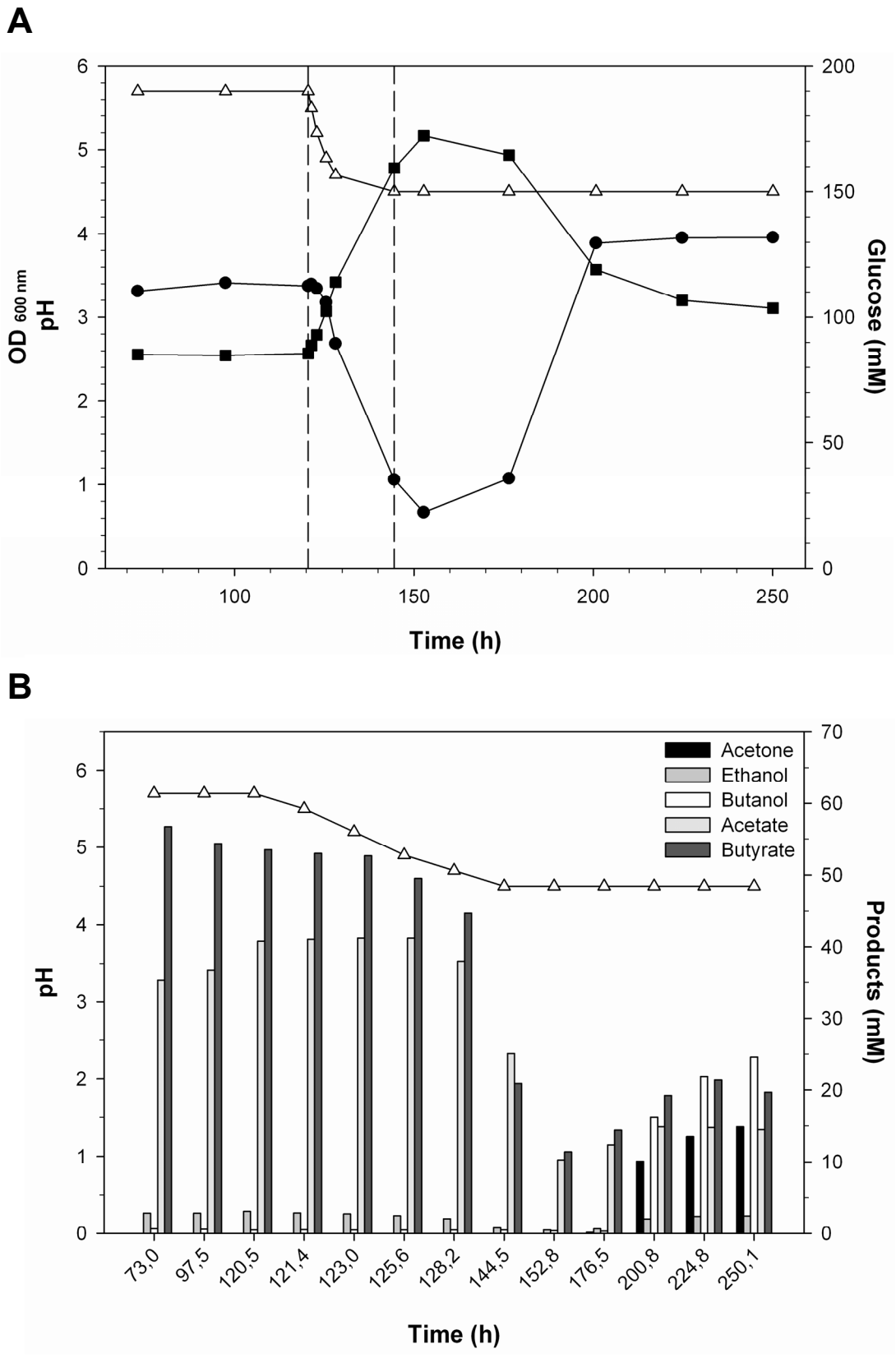

Fig. 15. Fermentation profile of the phosphate-limited continuous culture of the *fcd/htpG* double mutant. (A) Growth, glucose consumption and pH in the course of fermentation. Dashed lines indicate the dynamic pH shift. (B) Fermentation products from the steady-state acidogenesis to solventogenesis. Each grouped bar set corresponds to each time-point. The experiment was duplicated and the figure represents one exemplary fermentation. Quantification of metabolites was done with an internal standard of known concentration (section 2.11.2). Symbols: *triangles*, pH; *circles*, OD at 600 nm; *squares*, residual glucose concentration

To figure out the second mutated gene, a 2,687 bp of DNA fragment (adaptor) from pMTL007 plasmid was obtained by digestion of the plasmid with *Eco*RV-HF and *Hin*dIII (section 2.7.3.1) and subsequent purification (section 2.7.2.4). In addition, genomic DNA (10 µg) of the *fcd/htpG* double mutant was digested with *Eco*RV-HF for 16 h at 37 °C. Thereafter, 1 µL digested genomic DNA was ligated with the adapter (section 2.7.3.1) overnight at 14 °C. Only *Eco*RV-digested sticky ends of the adapter were able to be ligated with *Eco*RV-digested genomic DNA fragments. This ligation reaction resulted in production of a pool of relatively large DNA fragments, some of which carried the known DNA sequence flanking *Eco*RV recognition sites (the sequences of the adaptor and the intron contained in a certain fragment of digested genomic DNA). This allowed a PCR using this ligation reaction mixture as the template and primers specific for the adaptor (Adaptor-*Eco*RV-primer, Table 40, Appendix section) and the intron (Intron-Forward and -Reverse primers, Table 40, Appendix section), respectively, to acquire PCR products which might contain sequence information between the intron and the *Eco*RV recognition site. In this PCR, products could be only given where the ligated adapter with an intron-containing genomic DNA fragment was the reaction template. PCR products obtained were supposed to contain two fragments, one was the *fcd*-adapter section and the other covered part of the second mutated gene (*htpG*). Bands obtained from this DNA ligase-mediated PCR were then excised and purified (section 2.7.2.4), followed by sequencing (Eurofins Genomics, Ebersberg, Germany).

Sequences of the PCR products were subsequently aligned using NCBI BLAST (http://blast.ncbi.nlm.nih.gov/Blast.cgi?PAGE_TYPE=BlastSearch&BLAST_SPEC=MicrobialGenomes) and megablast program (highly similar sequences) was selected.

At the beginning it was not possible to identify the direction of the intron inserted into the second gene. Therefore, two primers specific for the intron were designed for the amplification reaction. They were Intron-Forward primer and Intron-Reverse primer (Table 40, Appendix section) which were located at both ends of the intron with opposite extension directions. As a result, two independent standard PCRs were conducted using different primer pairs (Intron-Forward and Adaptor-*Eco*RV-primer, Intron-Reverse and Adaptor-*Eco*RV-primer) and the genomic DNA fragments ligated with the adaptor were employed as the template. The composition and program of the PCR was described previously (section 2.7.2.1).

Intron-Reverse primer and Adaptor-*Eco*RV-primer gave several bands (Fig. 16, lane 1), so did Intron-Forward primer and Adaptor-*Eco*RV-primer (Fig. 16, lane 2). A ~1.4 kb band in lane 1 was first excised and purified (section 2.7.2.4). The purified PCR product was then sent for sequencing and the resultant sequence information was aligned using BLAST. The PCR product of ~1.4 kb (in lane 1) turned out to be part of the *htpG* gene (*CA_C3315*) which codes for a molecular chaperon (Nölling *et al.*, 2001) (Fig. 16). Consequently, the second mutated gene on the chromosome of the *fcd/htpG* double mutant was determined to be *htpG* gene which was subjected to further confirmation afterwards.

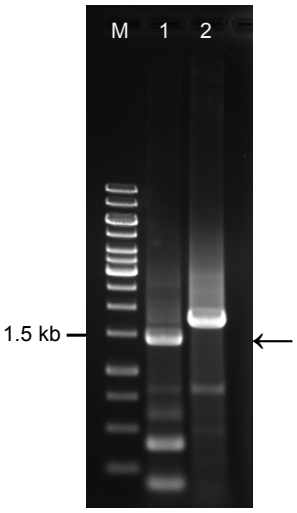

Fig. 16. Determination of the second mutated gene from the genomic DNA of the *fcd/htpG* double mutant. M, marker; Lane 1, intron-Reverse primer and Adaptor-*Eco*RV-primer; Lane 2, intron-Forward primer and Adaptor-*Eco*RV-primer. The ~1.4 kb PCR product in lane 1 was determined as the second target gene of the intron

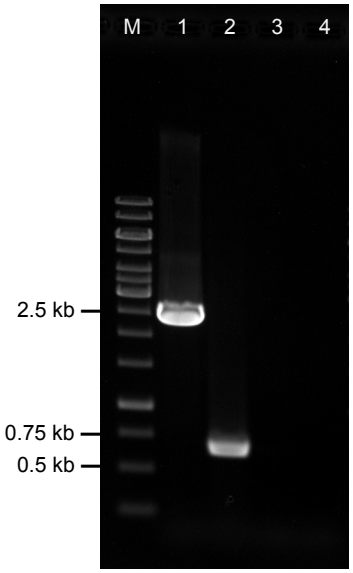

Fig. 17. Confirmation of insertion of the intron into the *htpG* gene of the *fcd/htpG* double mutant. *htpG* gene-specific primers were used to this end. Lane 1, genomic DNA of the *fcd/htpG* double mutant; lane 2, wild type genomic DNA; lane 3, pMTL007 plasmid; lane 4, deionized water as the negative control

3.2.6.2 Confirmation of intron insertion into the *htpG* in the *fcd/htpG* double mutant

An *htpG* gene-specific primer pair was designed (*htpG*2-Forward and Reverse primers, Table 39, Appendix section) to verify that the intron definitely inserted into this gene apart from *fcd* in the *fcd/htpG* double mutant. For this, a standard PCR was performed (section 2.7.2.1) using this primer pair and genomic DNA of the *fcd/htpG* double mutant was used as the template. Wild type genomic DNA gave a band at 663 bp and the *fcd/htpG* mutant

exhibited a product of 2,444 bp, ~1.8 kb larger than that of the wild type, which corresponded to the size of the intron inserting into the *htpG* gene (Fig. 17). As a result, it was proved that in the *fcd/htpG* double mutant *htpG* was the second target gene where the intron had inserted.

3.2.6.3 Generation of the *htpG* mutant

After determining the second mutated gene apart from the *fcd* in the *fcd/htpG* double mutant, the *htpG* gene was then knocked out to elucidate its potential roles. The resultant mutant strain was characterized using continuous fermentation and microarray experiments.

Strategies for generation of a *htpG* ClosTron mutant were identical to that for the *fcd*, *etfA* and *etfB* mutant strains and they were described in detail in Methods and Materials (section 2.7.3.1, 2.9). Target sites (where intron could insert) in *htpG* gene were predicted using a web-based intron targeting and design tool (www.clostron.com) and a target site with the highest score (8.406) was selected. Consequently, the target site in the *htpG* gene was determined at 266/267 bp (the length of the *htpG* gene is 1,875 bp) and the intron was predicted to insert into this site at an antisense direction according to information given. In addition, four primers for SOE (splicing by overlap extension) PCR (section 2.7.3.1) (Ho *et al.*, 1989) were simultaneously designed (*htpG*-IBS, *htpG*-EBS1d, *htpG*-EBS2 and EBS universal; Table 38, Appendix section). They were used for the mutation of recognition sites of the intron retargeting region on pMTL007C-E2 whose intron was able to insert into the predicted *htpG* target site by a specific recognition of the *htpG* gene via its mutated retargeting region. SOE PCR produced the mutated intron retargeting region which was then ligated with pMTL007C-E2 backbone to generate retargeted intron expression vector specific for *htpG* (pMTL007C-E2::cac-*htpG*-266a, Table 7, section 2.4). This vector was subsequently transformed into *E. coli* containing pAN2 for *in vivo* methylation (section 2.9.1). Retargeted and methylated pMTL007C-E2::cac-*htpG*-266a was electroporated into *C. acetobutylicum* (section 2.9.2), followed by screening of thiamphenicol- and erythromycin-resistant colonies (section 2.9.3).

After electroporation and screening, 8 clones of the putative *htpG* mutant were selected and the correct insertion of the intron was verified by PCR and subsequent Southern hybridization. Erythromycin-resistant clones (putative *htpG* mutant) were verified by standard PCR (section 2.7.2.1) using four different primers. *htpG* gene-specific primers (*htpG*-Forward and -Reverse primers, Table 39, Appendix section) were used first. The wild type genomic DNA gave a band of 284 bp, while the correct mutants exhibited products of 2,065 bp, ~1.8 kb larger than that of the wild type, which corresponded to the size of the intron inserting into the target gene (Fig. 18A). Another set of primers, an intron specific primer (EBS universal, Table 38, Appendix section) and an *htpG*-Reverse primer, were also employed to verify an exon-intron junction part of mutated gene, leading to a product of 389 bp, whereas the wild type was not supposed to result in a product (Fig. 18B). Besides, a primer pair specific for pMTL007C-E2 plasmid (pMTL007CE2check-Forward and -Reverse primers, Table 40, Appendix section) was used for confirmation of the loss of this shuttle vector from mutant cells and only pMTL007C-E2 plasmid control gave a band at 517 bp (Fig. 18C). Moreover, *CA_P0175* (*repA*) gene-specific primers (*repA*-Forward and -Reverse primers, Table 39, Appendix section) were used to verify the presence of pSOL1 megaplasmid which carried key genes for solventogenesis and products (1,003 bp) were visible both in the *htpG* mutant and the wild type (Fig. 18D). Confirmation of the presence of pSOL1 was necessary when conducting

mutagenesis in *C. acetobutylicum*. In case of pSOL1 loss, the strain constructed would in fact be a double mutant with the *htpG* gene and the pSOL1 as a whole mutated.

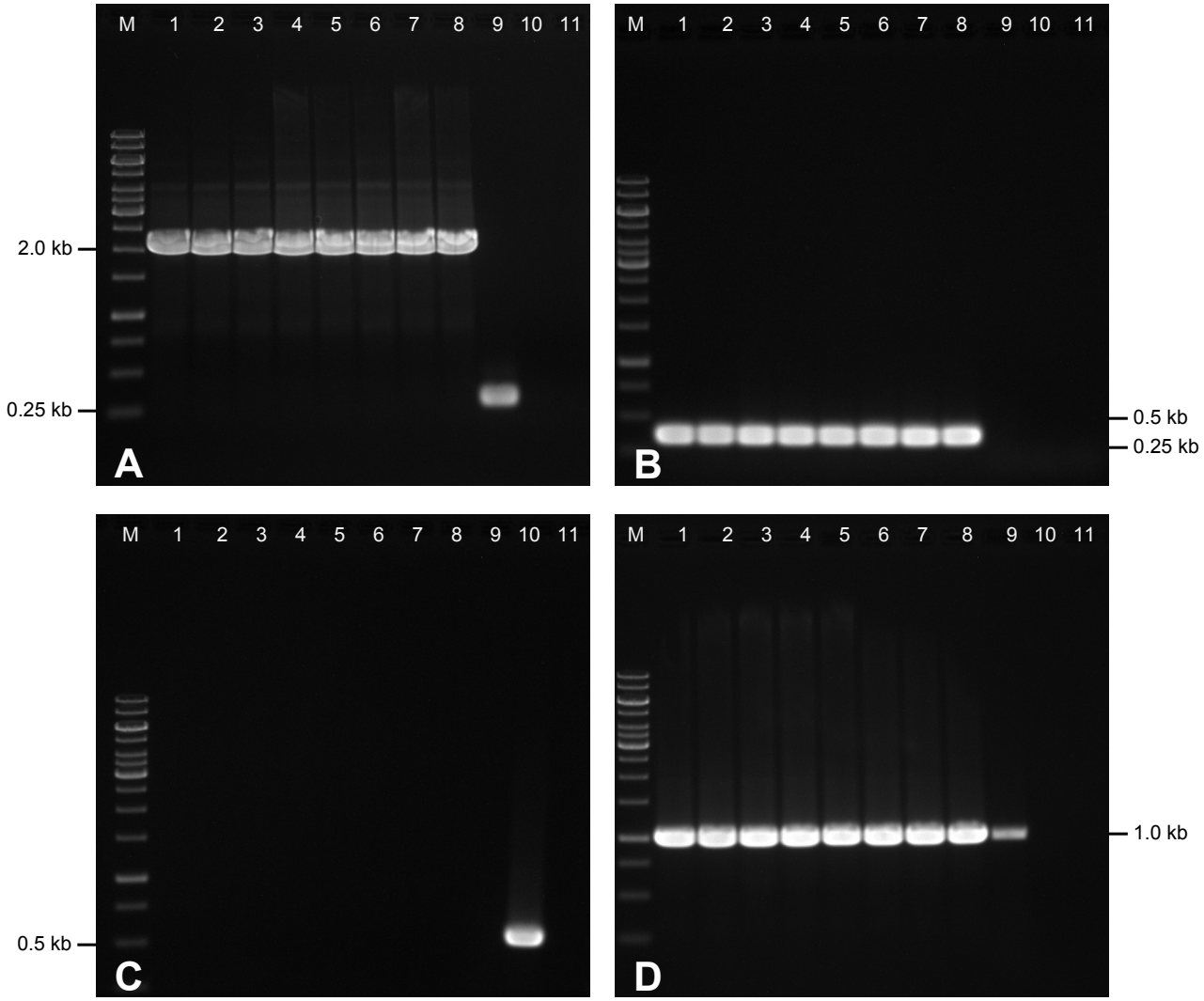

Fig. 18. PCR verification of the *htpG* mutant. (A) *htpG* gene-specific primers; (B) EBS universal primer and *htpG*-Reverse primer; (C) pMTL007C-E2 specific primers; (D) *CA_P0175* (*repA*) gene-specific primers. M, marker; lane 1-8, genomic DNA from different clones of the *htpG* mutant; lane 9, wild type genomic DNA; lane 10, pMTL007C-E2; lane 11, deionized water as the negative control

To further confirm the correct insertion of the intron, i.e., that only one copy of the intron had inserted into the *htpG* gene, Southern hybridization was conducted with the intron-specific probe. Detailed methods of Southern hybridization were described in detail previously (section 2.7.5). 590 bp of the intron-specific probe was PCR amplified using intron specific primers (ISP-Forward and -Reverse primers, Table 40, Appendix section) and pMTL007 plasmid was used as the template. The intron-specific probe (fragment) was located at an intron-erythromycin gene junction section (339-928 bp) in the intron (1,781 bp in length) where 774 bp of erythromycin gene resided (710-1,483 bp). Genomic DNA of the *htpG* mutant as well as that of the wild type were digested with *Hin*dIII or *Eco*RV-HF at 37 °C for 16 hours before they were transferred from an agarose gel to a positively charged nylon

membrane which was then hybridized overnight with the biotin-labeled intron-specific probe at 42 °C. *Hin*dIII-digested genomic DNA of the *htpG* mutant exhibited a single band at ~7 kb, demonstrating that the *htpG* mutant possessed only one copy of the intron on the chromosome and thus only the *htpG* gene was mutated. No hybridization signal was observed for wild type genomic DNA digested with *Hin*dIII, as expected, because the intron-specific probe used did not hybridize to any original DNA sequence in *C. acetobutylicum*. *Eco*RV-digested genomic DNA of the *htpG* mutant exhibited a single band at ~12 kb, further demonstrating that the *htpG* mutant possessed only one copy of the intron on the chromosome and the size of this band was identical to that of the upper band observed in the *fcd/htpG* double mutant genomic DNA which was also digested with *Eco*RV (Fig. 14A). No hybridization signal was detected for wild type genomic DNA digested with *Eco*RV, as expected. Restricted pMTL007C-E2 with *Hin*dIII was used as a positive control, showing a signal at 8.9 kb which was equal to the size of linear pMTL007C-E2 (Fig. 19A). Consequently, after confirmation by PCR and Southern hybridization, it was proved that a single *htpG* mutant had been generated.

The presence of the pSOL1 megaplasmid could be detected via the iodine-exposed starch plate test (section 2.5.1, 2.9.4), because pSOL1-containing cells were able to degrade starch in solidified media and form halos when exposed with iodine. To confirm the presence of the pSOL1 in the *htpG* mutant cells, about 30 colonies of the *htpG* mutant strain were re-streaked on a RCA (reinforced clostridial agar) plate which contained 1% starch. After 24 h of incubation at 37 °C under anaerobic conditions, colonies still containing pSOL1 degraded the surrounding starch and formed halos when the starch-containing plate was stained with potassium iodine solution (Lugol) solution (Fig. 19B). Through this test, it was demonstrated that the *htpG* mutant strain generated by the ClosTron system still carried the pSOL1 megaplasmid.

3.2.6.4 Continuous fermentation of the *htpG* mutant

After confirming the *htpG* mutant at molecular and phenotypical levels, continuous fermentation was carried out to characterize this mutant strain (Fig. 20) and correct insertion of the intron in the *htpG* gene was monitored by PCR using *htpG* gene-specific primers (*htpG*-Forward and -Reverse primers, Table 39, Appendix section) which flanked the intron insertion site. Methods for chemostat cultures of *C. acetobutylicum* were described in detail previously (section 2.6). During acidogenic growth of the continuous culture of the *htpG* mutant, the OD_{600} was ~4.2 which was higher than the wild type and the mutants of each gene from the *etfB-etfB-fcd* cluster, as well as the *fcd/htpG* double mutant. After 14 h of the pH shift, the culture of the *htpG* mutant entered solventogenesis, and the final OD_{600} of the culture during the steady-state was ~3.2 which was lower than the wild type and the *fcd/htpG* double mutant, and similar to that of the *fcd*, *etfA* and *etfB* mutant. In terms of glucose consumption, the *htpG* mutant utilized more glucose during acidogenesis than during solventogenesis, which was similar to the wild type strain. However, the *htpG* mutant consumed less glucose than the wild type during acidogenesis. Glucose consumption during solventogenic growth of the *htpG* mutant culture was similar to the wild type.

During acidogenesis of the *htpG* mutant culture, butyrate concentration was comparable to the wild type and concentration of acetic acid was slightly lower. Besides, the production of solvents was identical to the wild type during this phase, although these were not the main metabolites. On the other hand, butyrate and acetate were formed at the wild type level

during solventogenic growth in the *htpG* mutant, so was the generation of solvents during this phase. To sum up, results revealed that mutation in the *htpG* gene did not exert significant effects on the production of metabolites during both acidogenic and solventogenic growth.

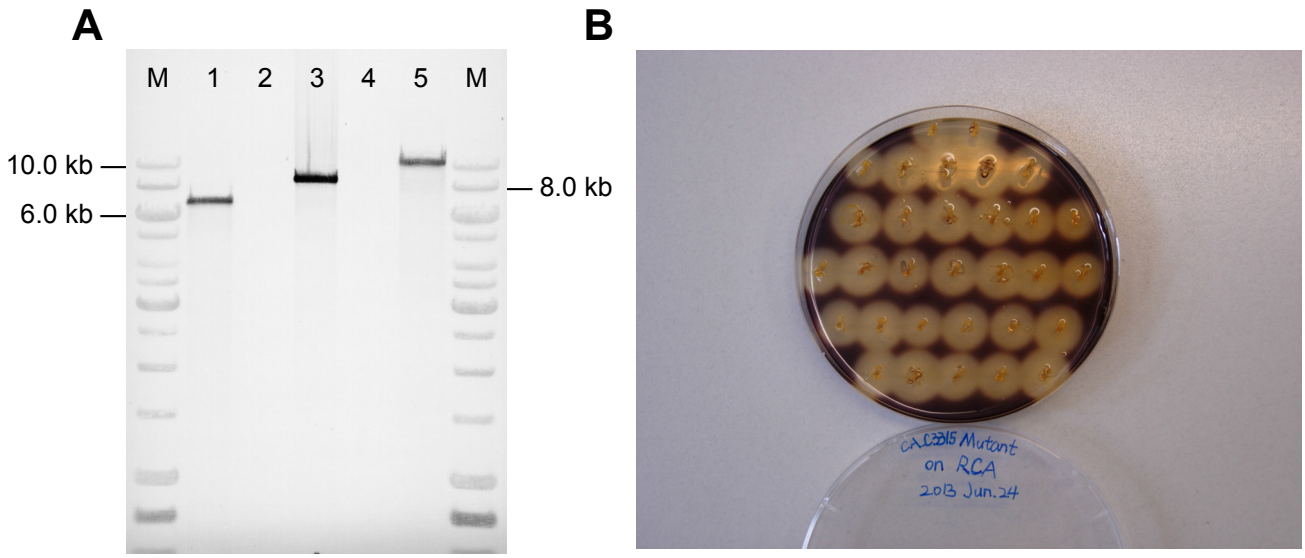

Fig. 19. Southern hybridization and starch plate test of the *htpG* mutant. Digested genomic DNA samples of the *htpG* mutant and wild type were hybridized with biotin-labelled intron-specific DNA probe (A). M, marker; lane 1, genomic DNA of the *htpG* mutant digested with *Hin*dIII; lane 2, wild type genomic DNA (*Hin*dIII); lane 3, pMTL007C-E2 digested with *Hin*dIII as a positive control; lane 4, wild type genomic DNA digested with *Eco*RV; lane 5, genomic DNA of the *htpG* mutant (*Eco*RV). (B) The *htpG* mutant colonies were re-streaked on an agar plate containing starch, colonies still carrying the pSOL1 megaplasmid formed halos when staining with potassium iodine solution

3.2.7 Comparison of phenotypes of the *fcd*, *htpG* and *fcd/htpG* mutant

Characterization of the *fcd*, *htpG* and *fcd/htpG* mutant was successfully conducted. During acidogenesis where solvents were not main metabolites, production of acetone, butanol and ethanol was decreased in the *fcd* single mutant and the *fcd/htpG* double mutant, whereas in the *htpG* mutant their concentrations were not affected. Besides, concentrations of these three solvents were significantly reduced during solventogenic growth of the *fcd* single mutant and the *fcd/htpG* double mutant and no changes were observed in the *htpG* mutant. On the other hand, butyrate concentration was increased during solventogenesis only in the *fcd* single mutant and the *fcd/htpG* double mutant. As a result, it was further demonstrated that the *fcd* gene was positively related to the generation of acetone, butanol and ethanol, and suggested that metabolism of butyric acid was influenced by *fcd* gene during solventogenic growth.

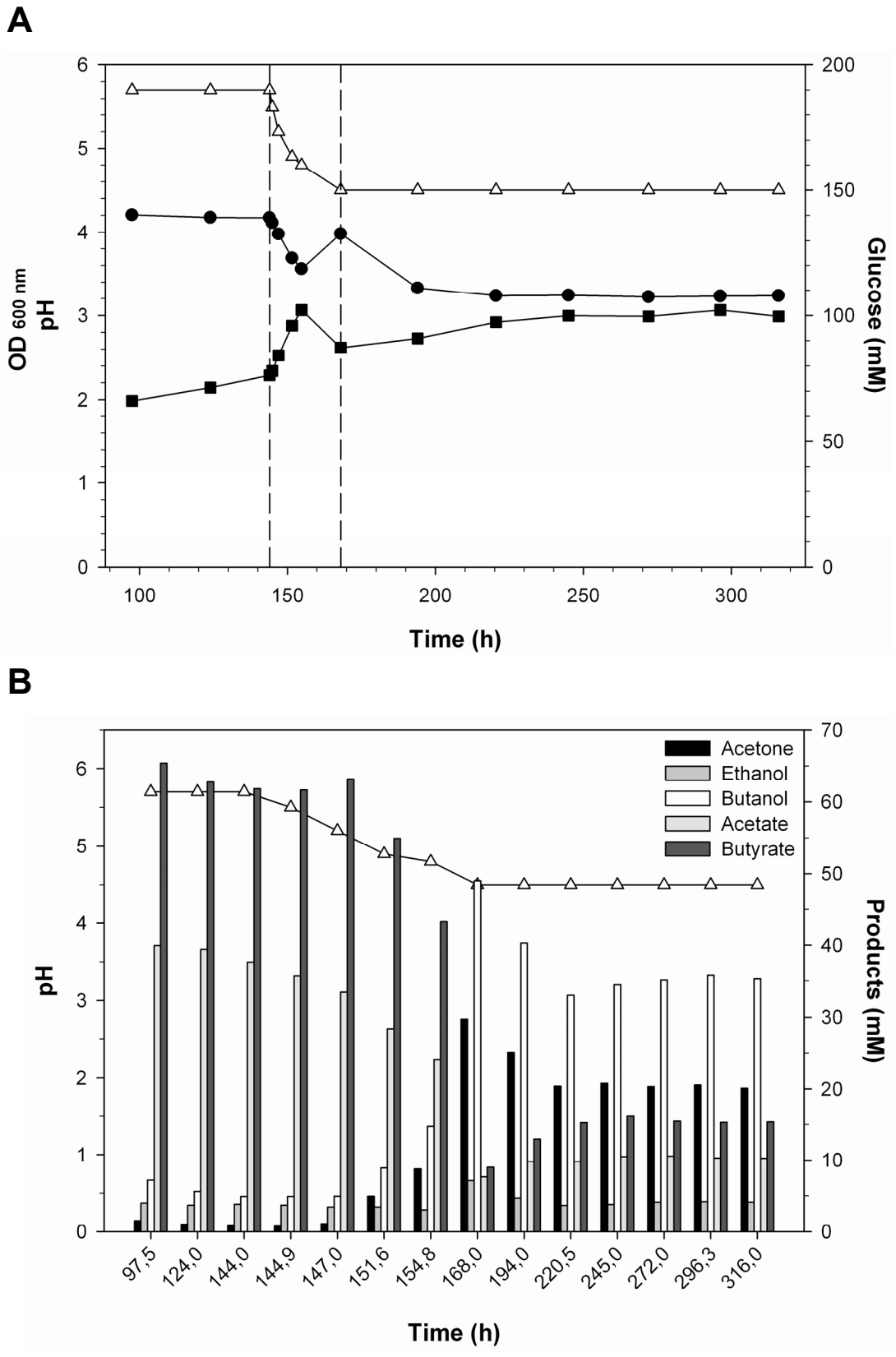

Fig. 20. Fermentation profile of the phosphate-limited continuous culture of the *htpG* mutant. (A) Growth, glucose consumption and pH in the course of fermentation. Dashed lines indicate the dynamic pH shift. (B) Fermentation products from the steady-state acidogenesis to solventogenesis. Each grouped bar set corresponds to each time-point. Quantification of metabolites was done with an internal standard of known concentration (section 2.11.2). Symbols: *triangles*, pH; *circles*, OD at 600 nm; *squares*, residual glucose concentration

3.3 Functional analyses of pSOL1 and the genes located on this megaplasmid

The genome of *C. acetobutylicum* consists of a chromosome and the pSOL1 megaplasmid, the latter contains 178 genes coding for different enzymes (Nölling *et al.*, 2001). The pSOL1 megaplasmid possesses a *sol* operon (*CA_P0162*-*CA_P0164*) containing *adhE1* and *ctfA/B* which were regarded as the genes for key enzymes responsible for the production of solvents (Cooksley *et al.*, 2012; Lehmann *et al.*, 2012a). However, many aspects remained unclear about the function of genes located on pSOL1 and this megaplasmid as a whole.

In this study, two gene candidates (*CA_P0175* and *CA_P0177*) were verified to be indispensable for the stable presence of the pSOL1 in *C. acetobutylicum*. Besides, one of two resultant pSOL1-free mutant strains (generated by respective inactivation of these two genes) was characterized using continuous fermentation and microarray experiments. In addition, several genes located on pSOL1, *CA_P0162* (*adhE1*), *CA_P0059* (Cooksley *et al.*, 2012) and *CA_P0129*, were characterized using identical strategies. Results obtained supplied a concrete view on roles of this pSOL1 megaplasmid and the genes located on it.

3.3.1 Characterization of a pSOL1-free mutant strain

3.3.1.1 Generation of a pSOL1-free mutant strain (the *repA* mutant)

repA (*CA_P0175*) encodes the replication protein of pSOL1, which is of importance for transfer of the pSOL1 from parental cells to the offspring (Nölling *et al.*, 2001). As a result, it was hypothesized that inactivation of *repA* gene might lead to loss of pSOL1 from the cell. To test this assumption, the ClosTron technology was employed to knock out the *repA* gene.

Strategies for generation of a *repA* ClosTron mutant were identical to that for mutants described in the last section (section 3.2) and they were introduced in detail in Methods and Materials (section 2.7.3.1, 2.9). Target sites (where the intron could insert) in *repA* gene were predicted using a web-based intron targeting and design tool (www.clostron.com) and a target site with the highest score (9.356) was selected. Consequently, the target site in the *repA* gene was determined at 273/274 bp (the length of the *repA* gene is 1,011 bp) and the intron was predicted to insert into this site at an antisense direction according to information given. In addition, four primers for SOE (splicing by overlap extension) PCR (section 2.7.3.1) (Ho *et al.*, 1989) were simultaneously designed (*repA*-IBS, *repA*-EBS1d, *repA*-EBS2 and EBS universal; Table 38, Appendix section). They were used for the mutation of recognition sites of the intron retargeting region on pMTL007C-E2 whose intron was able to insert into the predicted *repA* target site by a specific recognition of *repA* gene via its mutated retargeting region. SOE PCR produced the mutated intron retargeting region which was then ligated with pMTL007C-E2 backbone to generate retargeted intron expression vector specific for *repA* (pMTL007C-E2::cap-*repA*-273a, Table 7, section 2.4). This vector was subsequently transformed into *E. coli* containing pAN2 for *in vivo* methylation (section 2.9.1). Retargeted and methylated pMTL007C-E2::cap-*repA*-273a was electroporated into *C. acetobutylicum* (section 2.9.2), followed by screening of thiamphenicol-resistant colonies (section 2.9.3).

Screening of erythromycin-resistant colonies was infeasible in this case, because it was assumed that inactivation of the *repA* gene resulted in loss of the pSOL1 megaplasmid and thus the erythromycin-resistant gene located within the intron was also lost along with the

pSOL1 carrying *repA* gene where the intron inserted. Consequently, transformants grew on a solidified CGM (clostridia growth medium) plate (15 µg/mL thiamphenicol) were transferred to a new CGM agar plate (15 µg/mL thiamphenicol) using toothpicks to ensure the presence of pMTL007C-E2::cap-*repA*-273a (Table 7, section 2.4) in transformant cells, instead of transferring to a CGM agar plate supplemented with erythromycin. This transfer step was then repeated once for the same purpose. Presence of pMTL007C-E2::cap-*repA*-273a in transformants allowed constitutive expression of the intron which could insert into the target site of *repA* gene and led to removal of the pSOL1 from cells if the hypothesis became true. Afterwards, 10 colonies were picked and inoculated in CGM liquid media (15 µg/mL thiamphenicol), followed by isolation of genomic DNA and subsequent verification by PCR (section 2.7.2.1) and Southern blotting (section 2.7.5).

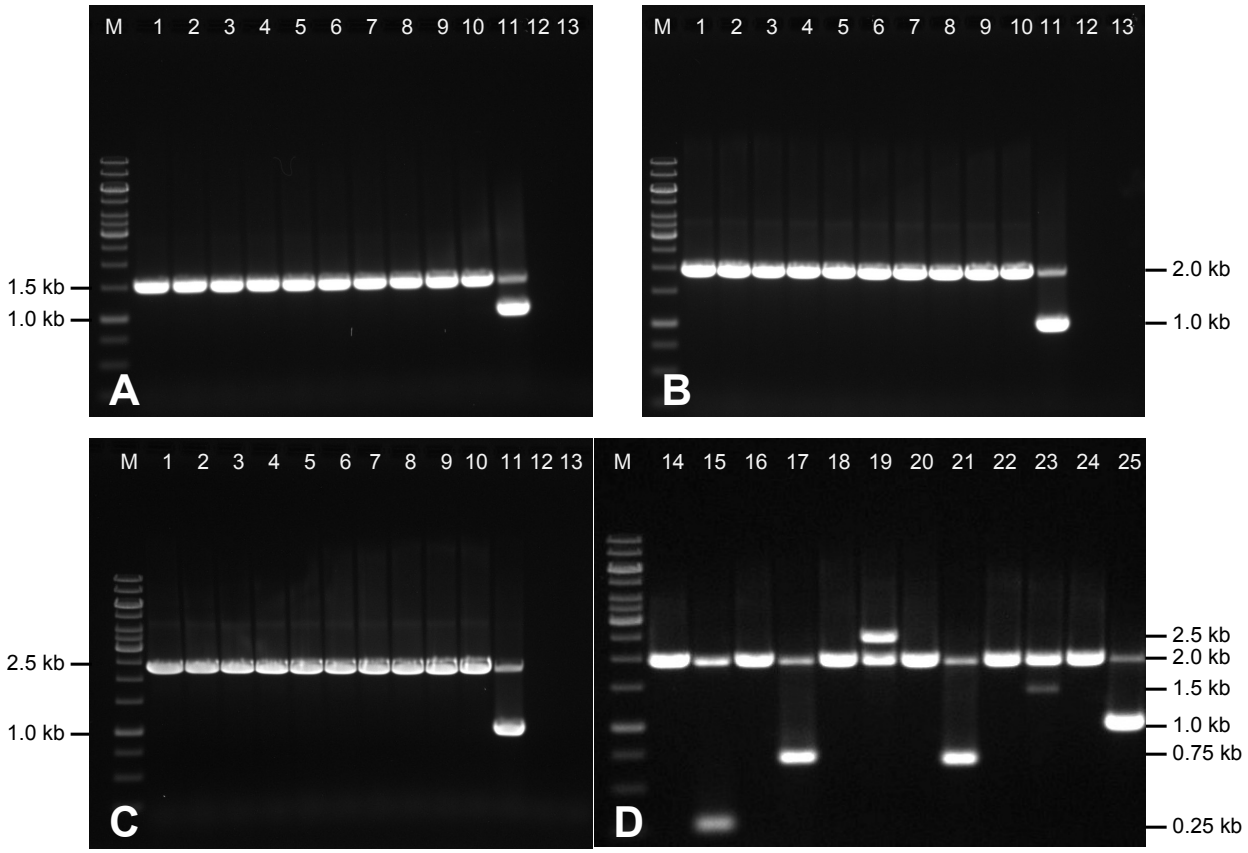

Fig. 21. PCR verification of the *repA* (pSOL1-free) mutant strain. (A) *CA_C2306-2308* and *repA* gene-specific primers; (B) *CA_C0570* and *repA* gene-specific primers; (C) *CA_C1692-CA_C1693* and *repA* gene-specific primers; (D) *CA_C0570* gene-specific primers and gene-specific primers for *CA_P0059* (lane 14-15), *CA_P0129* (lane 16-17), *CA_P0162* (lane 18-19), *CA_P0165* (lane 20-21), *CA_P0168* (lane 22-23) and *CA_P0175* (lane 24-25). M, marker; lane 1-10, genomic DNA from different clones of the *repA* mutant; lane 11, wild type genomic DNA; lane 12, pMTL007C-E2 plasmid; lane 13, deionized water as the negative control; lane 14, 16, 18, 20, 22 and 24, genomic DNA from the *repA* mutant; lane 15, 17, 19, 21, 23 and 25, wild type genomic DNA

To verify putative *repA* mutant clones, two primer pairs were used in a PCR reaction to check a chromosomal fragment and a pSOL1 gene simultaneously. Gene-specific primers for three chromosomal sections, *CA_C0570* (*0570*-Forward and -Reverse primers, Table 39, Appendix

section) (1,969 bp), *CA_C2306-2308* (*sigF* operon-Forward and -Reverse primers, Table 39, Appendix section) (1,543 bp) and *CA_C1692-1693* (*ftsAZ*-Forward and -Reverse primers, Table 39, Appendix section) (2,342 bp), were respectively utilized along with *repA* (*CA_P0175*) gene-specific primer (*repA*-Forward and -Reverse primers, Table 39, Appendix section) (1,003 bp) to detect whether the pSOL1 had been lost. The *repA* mutant clones produced only one band for the chromosomal fragment, while two products (a chromosomal fragment and a *repA* fragment) were given from the wild type (Fig. 21A-C). On the other hand, *CA_C0570* gene-specific primers were used along with primer pairs for six different pSOL1-borne genes (Table 39, Appendix section), *CA_P0059* (270 bp), *CA_P0129* (714 bp), *CA_P0162* (2,498 bp), *CA_P0165* (687 bp), *CA_P0168* (1,448 bp) and *CA_P0175* (1,003 bp), to test loss of the pSOL1. The *repA* mutant clones still gave only one band for *CA_C0570* fragment as compared to the wild type genomic DNA which produced two products (Fig. 21D). From these amplification steps, it was demonstrated that a *repA* mutant was generated using the ClosTron system. The *repA* mutant was free of the pSOL1 megaplasmid and inactivation of the *repA* gene led to loss of the pSOL1.

To further confirm that the pSOL1 megaplasmid had been removed from the *repA* mutant, Southern hybridization was conducted with the intron-specific or *repA*-specific probe. Detailed methods of Southern hybridization were described previously (section 2.7.5). *repA*-specific probe was 1,003 bp in length (1,011 bp for *repA* gene) and it was PCR amplified using *repA* gene-specific primers (*repA*-Forward and -Reverse primers, Table 39, Appendix section) and wild type genomic DNA was used as the template. The probe was then biotin-labelled according to the official manual (section 2.7.5.2). 590 bp of the intron-specific probe was also PCR amplified using intron-specific primers (ISP-Forward and -Reverse primers, Table 40, Appendix section) and pMTL007 plasmid was used as the template. The intron-specific probe (fragment) was located at a intron-erythromycin gene junction section (339-928 bp) in the intron (1,781 bp in length) where 774 bp of erythromycin gene resided (710-1,483 bp). Genomic DNA of the *repA* mutant (pSOL1-free) as well as that of the wild type were digested with *Eco*RV-HF at 37 °C for 16 hours before they were transferred from an agarose gel to a positively charged nylon membrane which was then hybridized overnight with the biotin-labeled intron-specific or *repA*-specific probe at 42 °C. When the intron-specific probe was employed, genomic DNA of this pSOL1-free mutant did not exhibit a band, demonstrating that there was not a copy of the intron on the mutant chromosome and the pSOL1 had been removed which carried *repA* gene where the intron inserted. No hybridization signal was observed for wild type genomic DNA, as expected, because the intron-specific probe used did not hybridize to any original DNA sequence in *C. acetobutylicum*. Restricted pMTL007C-E2 with *Hin*dIII was used as a positive control, showing a signal at 8.9 kb which was equal to the size of linear pMTL007C-E2 (Fig. 22A). When the *repA*-specific probe was used, the pSOL1-free strain genomic DNA still did not display a band, which proved that *repA* gene was not present and thus the pSOL1 where *repA* resides was absent. Wild type genomic DNA, as a positive control, gave a band at ~7.8 kb and *Hin*dIII-restricted pMTL007C-E2 did not show a signal (Fig. 22B). Consequently, it was demonstrated that a pSOL1-free mutant, caused by inactivation of the *repA* gene, had been generated.

The presence of the pSOL1 megaplasmid was detected via the iodine-exposed starch plate test (section 2.5.1, 2.9.4), because pSOL1-containing cells were able to degrade starch in solidified media and form halos when exposed with iodine. To confirm the absence of the pSOL1 in the pSOL1-free (*repA*) mutant, about 50 colonies of this strain were re-streaked on a RCA (reinforced clostridial agar) plate which contained 1% starch. After 24 h of incubation

at 37 °C under anaerobic conditions, none of colonies degraded the surrounding starch and formed halos when the starch-containing plate was stained with potassium iodine solution (Lugol) solution (Fig. 22C). Through this test, it was further demonstrated that this pSOL1-free mutant strain generated by the ClosTron system retargeting pSOL1-borne *repA* gene did not carry the pSOL1 megaplasmid.

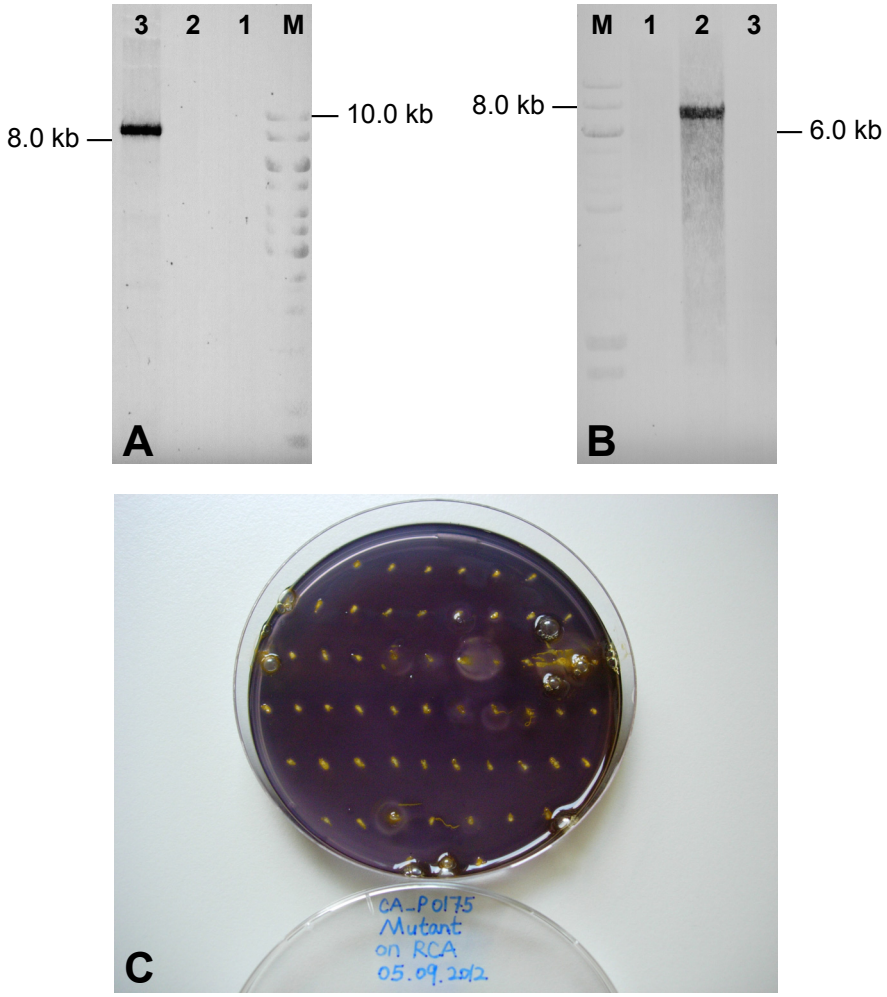

Fig. 22. Southern hybridization and starch plate test of the *repA* (pSOL1-free) mutant strain. *Eco*RV-digested genomic DNA samples of the *repA* mutant and wild type were hybridized with biotin-labelled intron- (A) or *repA*-specific (B) DNA probe. M, marker; lane 1, genomic DNA of the *repA* mutant; lane 2, wild type genomic DNA; lane 3, pMTL007C-E2 plasmid digested with *Hin*dIII. (C) The *repA* mutant colonies were re-streaked on an agar plate containing starch, no colonies formed halos when staining with potassium iodine solution

3.3.1.2 Continuous fermentation of the *repA* (pSOL1-free) mutant

After confirming the *repA* mutant at molecular and phenotypical levels, continuous fermentation was carried out to characterize this mutant strain (Fig. 23). Loss of the pSOL1 megaplasmid was monitored by PCR using three primer pairs for chromosomal fragments *CA_C0570*, *CA_C2306-2308* and *CA_C1692-1693* plus primers for pSOL1-borne *repA* (*0570*-Forward and -Reverse primers, *sigF* operon-Forward and -Reverse primers, *ftsAZ*-Forward and -Reverse primers and *repA*-Forward and -Reverse primers, Table 39, Appendix section). Methods for chemostat cultures of *C. acetobutylicum* were described in detail previously (section 2.6).

During acidogenic growth of the continuous culture of this pSOL1-free strain, the OD_{600} was ~3.6 which was slightly lower than that of the wild type. After ~16 h of the pH shift, the culture of the pSOL1-free strain reached pH 4.5, and the final OD_{600} of the culture during the steady-state of this phase was ~2.5 which was also lower than the wild type (~3.8). During the pH shift, a "pocket" phenotype was observed, which was similar to that of the *fcd/htpG* double mutant culture. This suggested that the pSOL1-free mutant cells required extended time for adaptation of a more acidic environment (pH 5.7-pH 4.5). In terms of glucose consumption, this pSOL1-free strain utilized more glucose during acidogenesis than that at pH 4.5, which was identical to the wild type strain. However, the pSOL1-free strain consumed less glucose than the wild type during acidogenic growth and especially during growth at pH 4.5, which led to lower production of acetic acid (~34 mM) during acidogenesis and abolished (0 mM) concentrations of acetone and butanol during both growth phases. During acidogenesis, butyrate concentration was comparable to the wild type. However, more butyrate (~153.8%) and acetate (~81.8%) were detected at pH 4.5 and their concentrations would be even higher, if the OD_{600} of the mutant culture at pH 4.5 was normalized to the wild type level (from ~2.5 to ~3.8). Moreover, ethanol formation was also lowered during acidogenic growth and growth at pH 4.5 of the pSOL1-free mutant. These results demonstrated that loss of the pSOL1 megaplasmid resulted in complete inability to produce acetone and butanol during acidogenic growth and growth at pH 4.5, and the pSOL1 affected metabolism of butyric acid at pH 4.5. Acetate metabolism was also influenced by the megaplasmid during both growth phases.

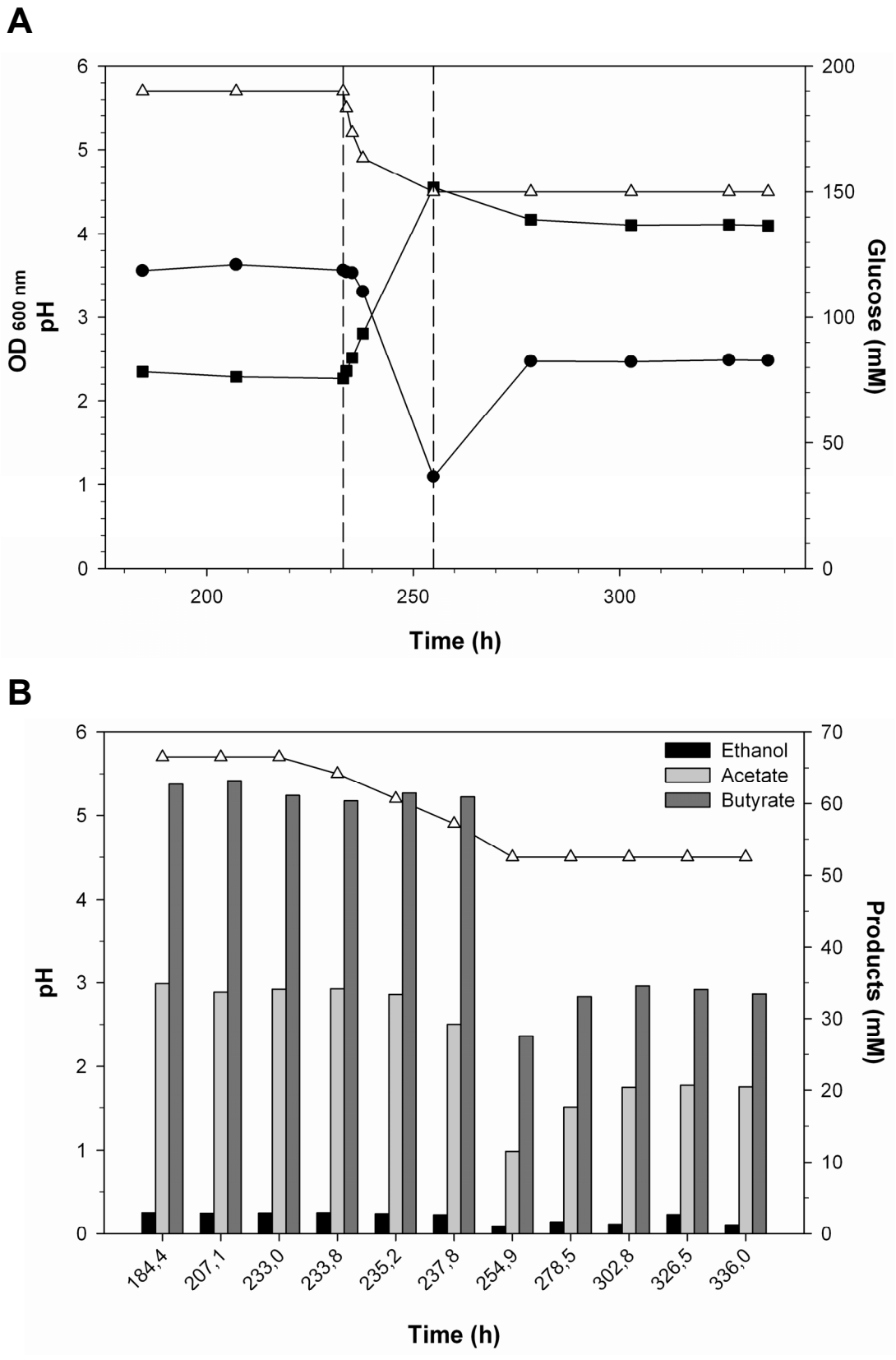

Fig. 23. Fermentation profile of the phosphate-limited continuous culture of the *repA* (pSOL1-free) mutant strain. (A) Growth, glucose consumption and pH in the course of fermentation. Dashed lines indicate the dynamic pH shift. (B) Fermentation products from the steady-state acidogenesis to solventogenesis. Each grouped bar set corresponds to each time-point. The experiment was triplicated and the figure represents one exemplary fermentation. Quantification of metabolites was done with an internal standard of known concentration (section 2.11.2). Symbols: *triangles*, pH; *circles*, OD at 600 nm; *squares*, residual glucose concentration

3.3.1.3 Transcriptional analysis of the *repA* (pSOL1-free) mutant as compared to the wild type

After characterizing the *repA* (pSOL1-free) mutant in continuous fermentation, microarray experiments were carried out to detect transcriptome changes caused by loss of the pSOL1 megaplasmid. Cells of steady-state acidogenic growth and growth at pH 4.5 of the chemostat culture of the pSOL1-free strain were used for RNA isolation and subsequent microarray experiments. Complementary DNA (cDNA) samples from the same growth phases of the wild type continuous culture were employed as the reference in transcriptional analyses. Detailed experimental processes concerning microarray experiments and methods for data analysis were described in Materials and Methods section (section 2.10). Slides covalently coupled with oligonucleotide probes (2 identical spots for 1 gene) were hybridized with combined labelled cDNA containing 80 pmol of Cy3 and Cy5 (GE Healthcare Europe GmbH, Munich, Germany) from the pSOL1-free mutant and wild type, followed by scanning using a GenePix 4000B microarray scanner and GenePix Pro 4.0 software (Axon Instruments, Union City, USA). The ratio of medians, the ratio of means and the regression ratio were automatically calculated by GenePix Pro 6.0 software (Axon Instruments, Union City, USA) based on intensities of fluorescence signals the pSOL1-free mutant and wild type (reference) cDNA samples when analyzing scanned microarray images. Normalization was carried out by setting the arithmetic mean of the ratios equal to 1. Background correction was then conducted by subtracting the background value plus one standard deviation from the foreground value. The ratio of medians, the ratio of means and the regression ratio (they differed by less than 30%) were used to correct for spot morphology of features of one hybridization and the ratio of medians was used to calculated for the final ratio (average of the two ratios of medians from two identical spots) which was subsequently taken its logarithm (to the basis of 2). The results from microarray experiments were calculated by mean of one hybridization and its dye-flip hybridization.

As mentioned previously (section 2.10.6), a logarithmic ratio format was used in transcriptional analysis for convenience to discriminate induced and repressed genes. A positive logarithmic ratio indicated a gene up-regulated in the pSOL1-free mutant, whereas a negative logarithmic ratio represented a down-regulated gene of the pSOL1-free mutant as compared to the wild type. In addition, a logarithmic ratio larger than 1.60 was for significant induction in contrast to a ratio less than -1.60 which meant this gene was significantly repressed when the pSOL1 was removed. As a result, the higher a positive logarithmic ratio was, the more noticeable a gene was up-regulated in the pSOL1-free mutant, and a gene was down-regulated more significantly when its negative logarithmic ratio was lower.

Through microarray experiments of the *repA* (pSOL1-free) mutant, it was found that the expression profiles of all genes responsible for the central metabolic pathways (Fig. 2) were not significantly altered as compared to the wild type. Those genes located on the pSOL1 megaplasmd did not give expression ratios, which corresponded to the fact that the pSOL1 was absent in this mutant. The expression patterns of central metabolic genes in the *repA* (pSOL1-free) mutant are listed in Table 23.

Table 23. Expression patterns of the central metabolic genes compared to wild type in the *repA* (pSOL1-free) mutant during acidogenic growth and growth at pH 4.5

ID	Protein function[a]	Ratio[b]	
		pH 5.7	pH 4.5
CA_P0035	AdhE2, aldehyde-alcohol dehydrogenase	—	—
CA_P0078	ThlB, acetyl coenzyme A acetyltransferase	—	—
CA_P0162	AdhE1, aldehyde dehydrogenase (NAD^+)	—	—
CA_P0163	CtfA, butyrate-acetoacetate CoA-transferase subunit A	—	—
CA_P0164	CtfB, butyrate-acetoacetate CoA-transferase subunit B	—	—
CA_P0165	Adc, acetoacetate decarboxylase	—	—
CAC0028	HydA, hydrogene dehydrogenase	-0.48	-0.01
CAC0267	Ldh, lactate dehydrogenase	0.05	—
CAC1543	Ldh, lactate dehydrogenase	0.60	-0.22
CAC1742	Pta, phosphate acetyltransferase	-0.13	0.12
CAC1743	Ack, acetate kinase	0.02	-0.09
CAC2229	Pfor, pyruvate ferredoxin oxidoreductase	0.02	-0.27
CAC2499	Pfor, pyruvate ferredoxin oxidoreductase	—	—
CAC2708	Hbd, β-hydroxybutyryl-CoA dehydrogenase	0.33	-0.40
CAC2709	EtfA, electron transfer flavoprotein alpha-subunit	0.51	-0.18
CAC2710	EtfB, electron transfer flavoprotein beta-subunit	1.26	-0.35
CAC2711	Bcd, butyryl-CoA dehydrogenase	0.95	-0.29
CAC2712	Crt, crotonase	1.22	-0.41
CAC2873	ThlA, acetyl-CoA acetyltransferase	0.81	0.30
CAC3075	Buk, butyrate kinase	1.01	-0.23
CAC3076	Ptb, phosphate acetyltransferase	0.84	0.21
CAC3552	Ldh, lactate dehydrogenase	-0.95	—

Genes are listed in order of ORFs, and considered as significantly up-regulated when the logarithmic ratio was ≥1.60 and as significantly down-regulated when the logarithmic ratio was ≤ -1.60. The given values in the table are mean of results of two hybridizations with dye swaps

[a] Protein names based on Nölling *et al.* (2001)

[b] The expression ratio as the logarithm to the basis of 2

On the other hand, transcription of 43 genes in acidogenic cells and 80 genes during growth at pH 4.5 was observed to be strongly induced in the *repA* (pSOL1-free) mutant strain, while 70 genes during acidogenesis and 37 genes at pH 4.5 showed noticeable repression. Each was in comparison to the status at the same pH value of the wild type chemostat culture. Results were listed in Table 24-27, respectively.

Table 24. Significantly up-regulated genes compared to wild type in the *repA* (pSOL1-free) mutant during acidogenic growth

ID	Protein function[a]	Ratio[b]
CAC0102	O-acetylhomoserine sulfhydrylase	6.94
CAC0103	CysC Adenylylsulfate kinase	7.44
CAC0105	Ferredoxin	7.37
CAC0106	ABC-type probable sulfate transporter, periplasmic binding protein	7.56
CAC0107	ABC-type sulfate transporter, ATPase component	6.83

Table 24. (continued)

ID	Protein function[a]	Ratio[b]
CAC0109	CysD sulfate adenylyltransferase subunit 2	7.61
CAC0111	Glutamine-binding periplasmic protein fused to glutamine permease	1.76
CAC0390	Cystathionine gamma-synthase	2.65
CAC0542	Methyl-accepting chemotaxis protein	1.98
CAC0571	Predicted transcriptional regulator	2.79
CAC0573	Uncharacterized protein	2.49
CAC0878	Amino acid ABC transporter permease component	3.39
CAC0879	ABC-type polar amino acid transport system, ATPase component	3.74
CAC0880	Periplasmic amino acid binding protein	3.68
CAC0909	Methyl-accepting chemotaxis protein	2.05
CAC0910	Probably cellulosomal scaffolding protein precursor	2.03
CAC0912	Possible non-processive endoglucanase	2.12
CAC0929	SAM-dependent methyltransferase	3.38
CAC0930	metB Cystathionine gamma-synthase	4.45
CAC0984	ABC transporter, ATP-binding protein	2.57
CAC0985	ABC transporter, permease component	3.13
CAC0986	Lipoprotein, attached to the cytoplasmic membrane	2.96
CAC1411	Similar to toxic anion resistance protein TerA	1.93
CAC1412	Methyl methane sulfonate/mytomycin resistance protein, *B.subtilis* ortholog, TerE family protein	1.85
CAC1413	Similar to toxic anion resistance protein TerA	1.87
CAC2235	CysK Cysteine synthase/cystathionine beta-synthase	3.65
CAC2236	Uncharacterized conserved protein	2.26
CAC2438	Predicted phosphatase	1.72
CAC2681	Hypothetical protein	1.82
CAC2783	CysD O-acetylhomoserine sulfhydrylase	2.79
CAC2917	Acetyl esterase family enzyme	2.56
CAC2918	Mannose-6 phospate isomelase	2.90
CAC3059	Sugar transferase	2.03
CAC3325	Periplasmic amino acid binding protein	3.43
CAC3326	Amino acid ABC-type transporter, permease component	3.53
CAC3327	Amino acid ABC-type transporter, ATPase component	3.93
CAC3379	Uncharacterized protein	1.93
CAC3461	Hypothetical protein	2.79
CAC3583	Predicted permease	1.71
CAC3584	Predicted permease	1.86
CAC3585	ABC-type transporter, ATPase component	1.94
CAC3664	Predicted flavodoxin	3.25
CAC3665	Alpha/beta superfamily hydrolase	3.60

Genes are listed in order of ORFs and considered as significantly up-regulated when the logarithmic ratio was ≥1.60. The given values in the table are mean of results of two hybridizations with dye swaps

[a] Protein name based on Nölling *et al.* (2001)

[b] The expression ratio as the logarithm to the basis of 2

During the steady-state acidogenic growth of the *repA* (pSOL1-free) mutant, 43 genes were significantly up-regulated as compared to wild type (Table 24). Among these, the expression of genes responsible for cysteine and methionine biosynthesis showed the most noticeable pattern (*CA_C0102*-*CA_C0103*, *CA_C0105*-*CA_C0107*, *CA_C0109*, *CA_C0390*, *CA_C0929*-*CA_C0930*, *CA_C2235* and *CA_C2783*). In addition, genes encoding transporters of amino acids were also induced significantly (*CA_C0111*, *CA_C0878*-*CA_C0880* and *CA_C3325*-*CA_C3327*). These findings suggested that removal of pSOL1 megaplasmid led to altered levels of intracellular amino acids. Besides, the transcript levels of genes for carbohydrate metabolism were significantly increased (*CA_C0910*, *CA_C0912*, *CA_C2918* and *CA_C3059*). Moreover, genes involved in signal transduction (*CA_C0542* and *CA_C0909*) and stress response (*CA_C1411*-*CA_C1413*) displayed enhanced expression. Last but not least, genes for enzymes involved in central metabolism were not significantly affected in this growth phase.

Table 25. Significantly down-regulated genes compared to wild type in the *repA* (pSOL1-free) mutant during acidogenic growth

ID	Protein function[a]	Ratio[b]
CAC0014	Aminotransferase	-3.22
CAC0015	SerA D-3-phosphoglycerate dehydrogenase	-2.93
CAC0016	Related to HTH domain of SpoOJ/ParA/ParB/RepB family, involved in chromosome partitioning	-3.81
CAC0017	SerS seryl-tRNA synthetase	-3.12
CAC0175	Hypothetical protein	-2.37
CAC0176	Oligopeptide-binding protein, periplasmic component	-2.69
CAC0177	Oligopeptide transport permease protein	-2.26
CAC0178	Oligopeptide transport permease protein	-2.05
CAC0180	Oligopeptide ABC transporter, ATP-binding protein	-1.96
CAC0181	Similar to beta-lactamase	-1.98
CAC0182	Beta-glucosidase homolog	-2.06
CAC0191	Transcriptional regulator	-1.95
CAC0192	Similar to chloromuconate cycloisomerase	-2.18
CAC0253	NifH Nitrogenase iron protein (nitrogenase component II)	-2.03
CAC0254	NifHD Nitrogen regulatory protein PII	-2.06
CAC0256	NifD Nitrogenase molybdenum-iron protein, alpha chain (nitrogenase component I)	-2.56
CAC0457	Transcriptional regulator	-1.67
CAC0579	Serine protein kinase (PrkA protein), P-loop containing	-3.55
CAC0580	Hypothetical protein	-5.10
CAC0658	Fe-S oxidoreductase	-3.28
CAC0659	Predicted Zn-dependent peptidase	-4.08
CAC0660	Hypothetical protein	-3.83
CAC0662	Sugar ABC transporter, periplasmic sugar-bindind protein	-6.17
CAC0663	Hypothetical protein	-5.59
CAC0664	Sugar-binding periplasmic protein	-5.48
CAC0666	Sugar permease	-5.16
CAC0667	Sugar-binding periplasmic protein	-5.55
CAC1043	Xre family DNA-binding domain and TPR-repeat containing protein	-3.89

Table 25. (continued)

ID	Protein function[a]	Ratio[b]
CAC1072	Fe-S oxidoreductase	-3.14
CAC1073	Hypothetical protein	-3.30
CAC1074	Predicted permease	-3.65
CAC1315	Peptodoglycan-binding domain containing protein	-2.26
CAC1337	Spore coat protein	-5.21
CAC1347	Transaldolase	-2.54
CAC1348	Transketolase	-3.11
CAC1349	GalM Aldose-1-epimerase	-3.10
CAC1694	Sigma factor E processing enzyme, SpoIIGA	-1.96
CAC1775	Predicted membrane protein	-3.06
CAC1841	Uncharacterized protein, related to Spore coat protein CotS	-1.87
CAC1866	Putative 4-Cys ferredoxin	-3.02
CAC2135	ATP-dependent serine protease	-2.30
CAC2137	Cation transport P-type ATPase	-3.31
CAC2306	Sporulation sigma factor SigF	-1.99
CAC2308	SpoIIAA Anti-anti-sigma factor (antagonist of SpoIIAB)	-2.05
CAC2343	O-acetyl transferase	-2.15
CAC2354	Aminotransferase	-3.02
CAC2382	Single-strand DNA-binding protein	-2.56
CAC2406	Predicted permease, possible O-antigen transporter	-2.12
CAC2407	Response regulator	-1.88
CAC2408	Glycosyltransferase	-2.36
CAC2544	EtfB Electron-transferring flavoprotein small subunit	-1.91
CAC2556	Endoglucanase	-2.80
CAC2575	Rubrerythrin	-2.29
CAC2578	Glycosyltransferase	-2.07
CAC2579	Hypothetical protein	-2.31
CAC2580	Hypothetical protein	-2.19
CAC2581	6-Pyruvoyl-tetrahydropterin synthase related domain, conserved membrane protein	-2.04
CAC2611	Hypothetical protein	-1.93
CAC2663	Protein containing cell-wall hydrolase domain	-2.72
CAC2678	Hypothetical protein	-2.03
CAC2685	Trehalose/maltose hydrolase (phosphorylase)	-1.89
CAC2772	Permease	-2.05
CAC2791	Fe-S oxidoreductase	-3.51
CAC2796	Fe-S oxidoreductase	-2.19
CAC2863	Predicted membrane protein	-2.36
CAC2944	N-terminal domain intergin-like repeats and C-terminal-cell wall-associated hydrolase domain	-3.42
CAC3036	Superfamily I DNA helicase	-3.06
CAC3205	SpoIIE Stage II sporulation protein E	-2.18
CAC3421	Acyl carrier protein phosphodiesterase	-2.92
CAC3612	Hypothetical protein	-3.89

Genes are listed in order of ORFs and considered as significantly down-regulated when the logarithmic ratio was ≤ -1.60. The given values in the table are mean of results of two hybridizations with dye swaps

[a] Protein name based on Nölling *et al.* (2001)

[b] The expression ratio as the logarithm to the basis of 2

During the steady-state acidogenic growth of the *repA* (pSOL1-free) mutant culture, 70 genes were significantly down-regulated as compared to the wild type (Table 25). Among these, 8 genes coding for enzymes involved in carbohydrate metabolism (*CA_C0662-CA_C0664*, *CA_C0666-CA_C0667*, *CA_C1347-CA_C1349*, *CA_C2556* and *CA_C2685*) were strongly repressed. Besides, serine biosynthesis was interfered according to decreased expression of related genes (*CA_C0014-CA_C0017*, *CA_C0579* and *CA_C2135*). Other genes (*CA_C0176-CA_C0178* and *CA_C0180*, *CA_C0253-CA_C0254* and *CA_C0256*, *CA_C2354*) showed much lower transcript levels than the wild type, indicating effects of oligopeptide transport and nitrogen fixation had been exerted due to absence of pSOL1 megaplasmid. Moreover, the expression of sporulation-related genes were noticeably decreased (*CA_C1337*, *CA_C1694*, *CA_C1841*, *CA_C2306*, *CA_C2308* and *CA_C3205*), but spores were not formed in continuous cultivation. This implied unknown functions of these genes during acidogenesis. Last but not the least, 4 genes encoding membrane-associated proteins (*CA_C1775*, *CA_C2343*, *CA_C2581* and *CA_C2863*) were strongly down-regulated, suggesting that loss of the megaplasmid affected the characteristics of the cell membrane.

Table 26. Significantly up-regulated genes compared to wild type in the *repA* (pSOL1-free) mutant during growth at pH 4.5

ID	Protein function[a]	Ratio[b]
CAC0106	ABC-type probable sulfate transporter, periplasmic binding protein	6.82
CAC0109	CysD sulfate adenylyltransferase subunit 2	7.59
CAC0110	CysN GTPase, sulfate adenylate transferase subunit 1	6.80
CAC0316	ArgF/I Ornithine carbomoyltransferase	5.01
CAC0380	Periplasmic amino acid-binding protein	3.63
CAC0561	Cellulase	4.31
CAC0574	Pectate lyase	4.69
CAC0608	Diaminopimelate decarboxilase	1.96
CAC0746	Secreted protease metal-dependent protease	2.05
CAC0878	Amino acid ABC transporter permease component	3.68
CAC0879	ABC-type polar amino acid transport system, ATPase component	3.63
CAC0880	Periplasmic amino acid binding protein	3.49
CAC0895	AroA 3-phosphoshikimate 1-carboxyvinyltransferase	2.09
CAC0896	AroC chorismate synthase	2.09
CAC0897	Fusion chorismate mutase and shikimate 5-dehydrogenase	1.87
CAC0910	Probably cellulosomal scaffolding protein precursor	4.42
CAC0911	Possible processive endoglucanase	3.81
CAC0912	Possible non-processive endoglucanase family 5, secreted, CelA homolog secreted, dockerin domain	3.94
CAC0913	Possible non-processive endoglucanase	3.73
CAC0914	Cellulosome integrating cohesin-containing protein	3.83
CAC0915	Endoglucanase A precursor	3.99
CAC0916	Possible non-processive endoglucanase	3.68

Table 26. (continued)

ID	Protein function[a]	Ratio[b]
CAC0917	Cellulose-binding endoglucanase	3.86
CAC0918	Possible non-processive endoglucanase	3.90
CAC0919	Probably secreted sialidase	3.22
CAC0929	SAM-dependent methyltransferase	3.96
CAC0930	MetB Cystathionine gamma-synthase	4.94
CAC0973	ArgG argininosuccinate synthase	4.73
CAC0974	ArgH Argininosuccinate lyase	4.49
CAC0975	Predicted P-loop kinase or ATPase distantly related to phosphoenolpyruvate carboxykinase	2.93
CAC0984	ABC transporter, ATP-binding protein	2.35
CAC0985	ABC transporter, permease component	2.53
CAC0986	Lipoprotein, attached to the cytoplasmic membrane	2.82
CAC1023	NadC Nicotinate-nucleotide pyrophosphorylase	2.07
CAC1041	ArgS arginyl-tRNA synthetase	1.94
CAC1214	Xre family DNA-binding domain and TPR-repeat containing protein	1.89
CAC1280	Heat-inducible transcription repressor	1.68
CAC1315	Peptodoglycan-binding domain containing protein	2.44
CAC1390	PurE phosphoribosylaminoimidazole carboxylase catalytic subunit	1.95
CAC1392	PurF amidophosphoribosyltransferase	1.82
CAC1655	PurQ/PurL bifunctional enzyme phosphoribosylformylglycinamidine synthase (synthetase domain/glutamine amidotransferase domain)	2.58
CAC2235	CysK Cysteine synthase/cystathionine beta-synthase	2.98
CAC2236	Uncharacterized conserved protein	2.26
CAC2287	Acyl-CoA reductase, LuxC	3.10
CAC2288	Acyl-protein synthetase, LuxE	3.31
CAC2388	ArgD N-acetylornithine aminotransferase	5.76
CAC2389	ArgB Acetylglutamate kinase	5.73
CAC2390	ArgC N-acetyl-gamma-glutamyl-phosphate reductase	4.85
CAC2391	ArgJ bifunctional ornithine acetyltransferase/N-acetylglutamate synthase protein	4.82
CAC2403	Predicted membrane protein	1.74
CAC2406	Predicted permease, possible O-antigen transporter	1.74
CAC2407	CheY-like receiver domain of response regulator	1.69
CAC2644	CarB Carbamoylphosphate synthase large subunit	4.15
CAC2645	CarA carbamoyl-phosphate synthase small subunit	4.23
CAC2783	CysD O-acetylhomoserine sulfhydrylase	2.73
CAC2917	Acetyl esterase family enzyme	3.41
CAC2918	Mannose-6 phospate isomelase	3.39
CAC3019	Sensory transduction protein	3.72
CAC3038	Isoleucyl-tRNA synthetase	1.69
CAC3093	Phosphate permease	2.47
CAC3157	TrpA Tryptophan synthase alpha chain	2.03
CAC3158	TrpB tryptophan synthase subunit beta	2.31
CAC3159	TrpF Phosphoribosylanthranilate isomerase	2.63
CAC3160	TrpC Indole-3-glycerol phosphate synthase	2.34
CAC3161	TrpD Anthranilate phosphoribosyltransferase	2.18

Table 26. (continued)

ID	Protein function[a]	Ratio[b]
CAC3162	PabA Para-aminobenzoate synthase component II	2.64
CAC3163	ParB anthranilate synthase component I	2.37
CAC3325	Periplasmic amino acid binding protein	3.05
CAC3326	Amino acid ABC-type transporter, permease component	3.01
CAC3387	Pectate lyase	3.59
CAC3469	Endoglucanase	3.58
CAC3470	Hypothetical protein	2.36
CAC3589	Uncharacterized conserved membrane protein	1.84
CAC3619	Amino acid ABC transporter, permease component	2.07
CAC3620	Amino acid (probably glutamine) ABC transporter, periplasmic binding protein component	2.00
CAC3622	Possible subunit of benzoyl-CoA reductase/2-hydroxyglutaryl-CoA dehydratase	2.81
CAC3629	Oligopeptide ABC transporter, ATPase component	1.67
CAC3661	Glycosyltransferase	4.45
CAC3665	Alpha/beta superfamily hydrolase	3.61
CAC3694	TPR-repeat-containing protein	2.02

Genes are listed in order of ORFs and considered as significantly up-regulated when the logarithmic ratio was ≥1.60. The given values in the table are mean of results of two hybridizations with dye swaps

[a] Protein name based on Nölling *et al.* (2001)

[b] The expression ratio as the logarithm to the basis of 2

During the steady-state growth at pH 4.5 of the *repA* (pSOL1-free) mutant, 80 genes were significantly up-regulated as compared to the wild type (Table 26). Among these, several clustered genes involved in biosynthesis of amino acids or the intermediate were strongly induced (*CA_C0106*, *CA_C0109-CA_C0110*, *CA_C0929-CA_C0930*, *CA_C2235* and *CA_C2783* for cysteine and methionine; *CA_C0316*, *CA_C0973-CA_C0974*, *CA_C1041*, *CA_C2388-CA_C2391* and *CA_C2644-CA_C2645* for arginine; *CA_C0608* for lysine; *CA_C0895-CA_C0897* for chorismate; *CA_C3157-CA_C3163* for tryptophan). Moreover, the expression levels of 8 genes responsible for transport of amino acids were also significantly elevated (*CA_C0380*, *CA_C0878-CA_C0880*, *CA_C3325-CA_C3326*, *CA_C3619-CA_C3620*). These results revealed enhanced metabolism of amino acids due to loss of pSOL1 megaplasmid. In addition, carbohydrate metabolism seemed to became more active according to noticeably increased transcript levels of related genes (*CA_C0561*, *CA_C0910-CA_C0919*, *CA_C0975*, *CA_C2918* and *CA_C3469*). Besides, genes for biosynthesis of purines (*CA_C1390*, *CA_C1392* and *CA_C1655*) and pyrimidines (*CA_C2644-CA_C2645*) displayed significant up-regulation.

Table 27. Significantly down-regulated genes compared to wild type in the *repA* (pSOL1-free) mutant during growth at pH 4.5

ID	Protein function[a]	Ratio[b]
CAC0029	Distantly related to cell wall-associated hydrolase, similar to YycO of *B. subtilis*	-1.89
CAC0056	Hypothetical protein	-2.48
CAC0057	Hypothetical protein	-2.28
CAC0058	Hypothetical protein	-1.73
CAC0059	Hypothetical protein	-1.95
CAC0060	Predicted membrane protein	-2.08
CAC0061	Phage-related protein	-1.92
CAC0062	Hypothetical protein	-1.97
CAC0064	Hypothetical protein	-1.80
CAC0205	Predicted phosphohydrolase	-3.36
CAC0353	2,3-Cyclic-nucleotide 2'phosphodiesterase	-3.44
CAC0427	Glycerol-3-phosphate ABC-transporter, permease component	-3.24
CAC0428	Sugar permease	-3.57
CAC0429	Glicerol-3-phosphate ABC-transporter, periplasmic component	-3.40
CAC0430	Glycerophosphoryl diester phosphodiesterase	-3.78
CAC0552	Protein containing cell-adhesion domain	-2.28
CAC0553	Hypothetical protein	-2.29
CAC0554	Autolytic lysozime (1,4-beta-N-acetylmuramidase)	-2.21
CAC0562	Predicted membrane protein	-2.41
CAC0563	Predicted membrane protein	-2.25
CAC0742	Uncharacterized protein, containing predicted phosphatase domain	-2.82
CAC0946	Metallo beta-lactamase superfamily hydrolase	-3.01
CAC1337	Spore coat protein	-3.50
CAC1702	Hypothetical protein	-3.02
CAC1703	Methyl-accepting chemotaxis protein (fragment)	-3.39
CAC1704	Hypothetical protein	-3.19
CAC1775	Predicted membrane protein	-1.81
CAC2241	Cation transport P-type ATPase	-2.42
CAC2242	Predicted transcriptional regulator	-1.98
CAC2342	Predicted membrane protein	-3.15
CAC2392	Uncharacterized ABC transporter, ATPase component	-1.70
CAC2743	Predicted permease	-3.27
CAC2938	Hypothetical protein	-2.26
CAC3236	Possible transcriptional regulator	-3.80
CAC3237	MsmX Multiple sugar-binding ABC-transporter, ATP-binding protein	-3.26
CAC3379	Uncharacterized protein	-3.61
CAC3526	FMN-binding protein	-1.93

Genes are listed in order of ORFs and considered as significantly down-regulated when the logarithmic ratio was ≤ -1.60. The given values in the table are mean of results of two hybridizations with dye swaps

[a] Protein name based on Nölling *et al.* (2001)

[b] The expression ratio as the logarithm to the basis of 2

During the steady-state growth at pH 4.5 of the *repA* (pSOL1-free) mutant, 37 genes were significantly down-regulated as compared to wild type (Table 27). Among these, 12 genes (*CA_C0060*, *CA_C0427*-*CA_C0430*, *CA_C0562*-*CA_C0563*, *CA_C1775*, *CA_C2342*, *CA_C2743*, *CA_C2938* and *CA_C3237*) coded for membrane-associated proteins, which suggested absence of the megaplasmid resulted in altered characteristics of cell membrane. In addition, four genes for hydrolases (*CA_C0029*, *CA_C0205*, *CA_C0742* and *CA_C3379*) displayed decreased transcript levels. Moreover, the expression of *CA_C0946* and *CA_C2242* which were both related to the defense metabolism was noticeably decreased. Besides, two genes involved in sporulation, *CA_C1337* and *CA_C2089*, revealed remarkable down-regulation by at least 80%. Last but not least, genes for the critical enzymes in the central metabolic pathway did not show significant changes in their expression pattern, indicating the genes located on pSOL1 megaplasmid did not exert obvious regulatory effects on them.

3.3.2 Generation of the second pSOL1-free mutant (the *CA_P0177* mutant)

In addition to inactivation of the *repA* gene, *CA_P0177* coding for a SpoOJ regulator was also knocked out using the ClosTron technology (Heap *et al.*, 2007, 2010a, 2010b). This gene was annotated as a protein related to DNA partitioning (Nölling *et al.*, 2001) and it had been proposed that it was involved in sporulation processes (Tomas *et al.*, 2003). Besides, *spo0J* (*CA_C3729*, the gene for Stage 0 sporulation J DNA-binding protein) resides on the chromosome of *C. acetobutylicum*. It had been reported that *spo0J* was required for chromosome partitioning during sporulation and during vegetative growth mutation of *spo0J* led to generation of anucleate cells (Sonenshein *et al.*, 2002). As a result, it was hypothesized that inactivation of *CA_P0177*, like that of *repA*, might also result in loss of the pSOL1 megaplasmid owing to functional loss of segregation.

Strategies for generation of a *CA_P0177* ClosTron mutant were identical to that for the *repA* mutant and other mutant strains of genes from the *etfB*-*etfA*-*fcd* cluster (section 3.2), and they were described in detail in Methods and Materials (section 2.7.3.1, 2.9). Target sites (where the intron could insert) in the *CA_P0177* gene were predicted using a web-based intron targeting and design tool (www.clostron.com) and a target site with the highest score (9.348) was selected. Consequently, the target site in the *CA_P0177* gene was determined at 257/258 bp (the length of the *CA_P0177* gene is 750 bp) and the intron was predicted to insert into this site at a sense direction according to information given. In addition, four primers for SOE (splicing by overlap extension) PCR (section 2.7.3.1) (Ho *et al.*, 1989) were simultaneously designed (*spoOJ*-IBS, *spoOJ*-EBS1d, *spoOJ*-EBS2 and EBS universal; Table 38, Appendix section). They were used for the mutation of recognition sites of the intron retargeting region on pMTL007C-E2 whose intron was able to insert into the predicted *CA_P0177* target site by a specific recognition of *CA_P0177* gene via its mutated retargeting region. SOE PCR produced the mutated intron retargeting region which was then ligated with pMTL007C-E2 backbone to generate retargeted intron expression vector specific for *CA_P0177* (pMTL007C-E2::cap-*spoOJ*-257s, Table 7, section 2.4). This vector was subsequently transformed into *E. coli* containing pAN2 for *in vivo* methylation (section 2.9.1). Retargeted and methylated pMTL007C-E2::cap-*spoOJ*-257s was electroporated into *C. acetobutylicum* (section 2.9.2), followed by screening of thiamphenicol-resistant colonies (section 2.9.3).

Screening of erythromycin-resistant colonies was infeasible in this case (like for the *repA* mutation), because it was assumed that inactivation of *CA_P0177* gene resulted in loss of the pSOL1 megaplasmid and thus erythromycin-resistant gene located in the intron was also lost

along with the pSOL1 carrying *CA_P0177* gene where the intron inserted. Consequently, transformants grew on a solidified CGM (clostridia growth medium) plate (15 μg/mL thiamphenicol) were transferred to a new CGM agar plate (15 μg/mL thiamphenicol) using toothpicks to ensure the presence of pMTL007C-E2::cap-*spoOJ*-257s (Table 7, section 2.4) in transformant cells, instead of transferring to a CGM agar plate supplemented with erythromycin. This transfer step was then repeated once for the same purpose. Presence of pMTL007C-E2::cap-*spoOJ*-257s in transformants allowed constitutive expression of the intron which inserted into the target site of *CA_P0177* gene and led to removal of the pSOL1 from cells if the hypothesis became true. Afterwards, colonies were picked and inoculated in CGM liquid media, followed by isolation of genomic DNA and subsequent verification by PCR (section 2.7.2.1) and Southern blotting (section 2.7.5).

To verify putative *CA_P0177* mutant clones, two primer pairs were used simultaneously in a PCR reaction. *CA_C0570* gene-specific primers (*0570*-Forward and -Reverse primers, Table 39, Appendix section) were respectively used along with gene-specific primers for seven different pSOL1-borne genes (Table 39, Appendix section), *CA_P0059* (270 bp), *CA_P0129* (714 bp), *CA_P0162* (2,498 bp), *CA_P0165* (687 bp), *CA_P0168* (1,448 bp), *CA_P0175* (1,003 bp) and *CA_P0177* (707 bp), to test loss of the pSOL1. Like the *repA* mutant, the *CA_P0177* mutant clone gave only one band for *CA_C0570* as compared to the wild type genomic DNA which produced two products (Fig. 24). From these amplification reactions, it was demonstrated that the *CA_P0177* mutant was also free of the pSOL1 megaplasmid and inactivation of the *CA_P0177* gene led to loss of the pSOL1.

To further confirm that the pSOL1 megaplasmid had been removed from *CA_P0177* mutant cells, Southern hybridization was conducted with the intron-specific or *CA_P0177*-specific probe. Detailed methods of Southern hybridization were described previously (section 2.7.5). *CA_P0177*-specific probe was 707 bp in length (750 bp for *CA_P0177* gene) and it was PCR amplified using *CA_P0177* gene-specific primers (*spoOJ*-Forward and -Reverse primers, Table 39, Appendix section) and wild type genomic DNA was used as the template. *CA_P0177*-specific probe was then biotin-labelled according to the official manual (section 2.7.5.2). 590 bp of the intron-specific probe was PCR amplified using intron specific primers (ISP-Forward and -Reverse primers, Table 40, Appendix section) and pMTL007 plasmid was used as the template. The intron-specific probe (fragment) was located at an intron-erythromycin gene junction section (339-928 bp) in the intron (1,781 bp in length) where 774 bp of erythromycin gene resided (710-1,483 bp). Genomic DNA of the *CA_P0177* mutant as well as that of the wild type were digested with *Eco*RV-HF at 37 °C for 16 hours before they were transferred from an agarose gel to a positively charged nylon membrane which was then hybridized overnight with the biotin-labeled intron-specific or *CA_P0177*-specific probe at 42 °C. When the intron-specific probe was employed, genomic DNA of the *CA_P0177* mutant did not exhibit a band, demonstrating that there was not a copy of the intron in the mutant genome and the pSOL1 had been removed which carried *CA_P0177* gene where the intron inserted. No hybridization signal was observed for wild type genomic DNA, as expected, because the intron-specific probe used did not hybridize to any original DNA sequence in *C. acetobutylicum*. Restricted pMTL007C-E2 with *Hin*dIII was used as a positive control, showing a signal at 8.9 kb which was equal to the size of linear pMTL007C-E2 (Fig. 25A). When the *CA_P0177*-specific probe was used, the *CA_P0177* mutant strain genomic DNA still did not display a product, which indicated that *CA_P0177* gene was not present and thus the pSOL1 where *CA_P0177* resides was absent. Wild type genomic DNA, as a positive control, gave a band at ~7.8 kb and *Hin*dIII-restricted pMTL007C-E2 did not

show a signal (Fig. 25B). Consequently, it was proved that another pSOL1-free mutant strain had been generated by deleting the *CA_P0177* gene.

The presence of the pSOL1 megaplasmid was detected via the iodine-exposed starch plate test (section 2.5.1, 2.9.4), because pSOL1-containing cells were able to degrade starch in solidified media and form halos when exposed with iodine. To confirm the absence of the pSOL1 in the *CA_P0177* mutant, more than 30 colonies of this strain were re-streaked on a RCA (reinforced clostridial agar) plate which contained 1% starch. After 24 h of incubation at 37 °C under anaerobic conditions, none of colonies degraded the surrounding starch and formed halos when the starch-containing plate was stained with potassium iodine solution (Lugol) solution (Fig. 25C). Through this test, it was further demonstrated that the pSOL1-free mutant strain generated by the ClosTron system retargeting *CA_P0177* gene did not carry the pSOL1 megaplasmid.

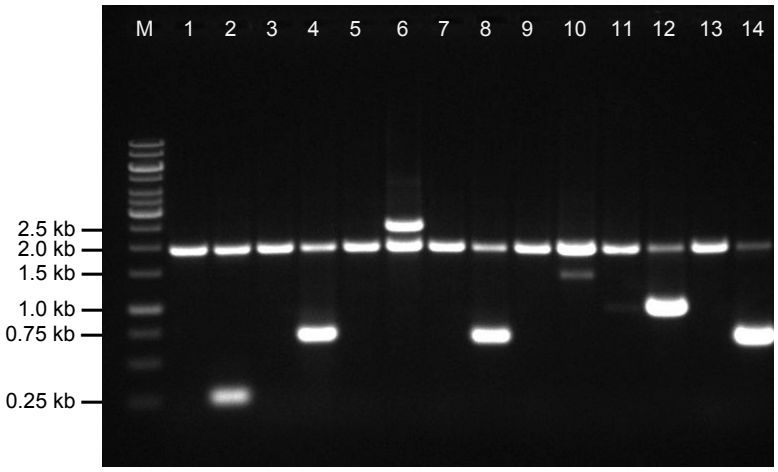

Fig. 24. PCR verification of the *CA_P0177* (the second pSOL1-free) mutant strain. *CA_C0570* gene-specific primers and specific primer pairs for *CA_P0059* (lane 1-2), *CA_P0129* (lane 3-4), *CA_P0162* (lane 5-6), *CA_P0165* (lane 7-8), *CA_P0168* (lane 9-10), *CA_P0175* (lane 11-12), *CA_P0177* (lane 13-14) were used to this end. M, marker. Lane 1, 3, 5, 7, 9, 11 and 13, genomic DNA of the *CA_P0177* mutant; lane 2, 4, 6, 8, 10, 12 and 14, wild type genomic DNA

Due to the same influence of the *CA_P0177* inactivation on the stable presence of the pSOL1 megaplasmid to the *repA* mutation, further characterization for this (the second) pSOL1-free (*CA_P0177*) mutant strain, i.e., continuous fermentation and transcriptional analysis, was not carried out. Identical researches had been performed for the *repA* (the first pSOL1-free) mutant strain (section 3.3.1).

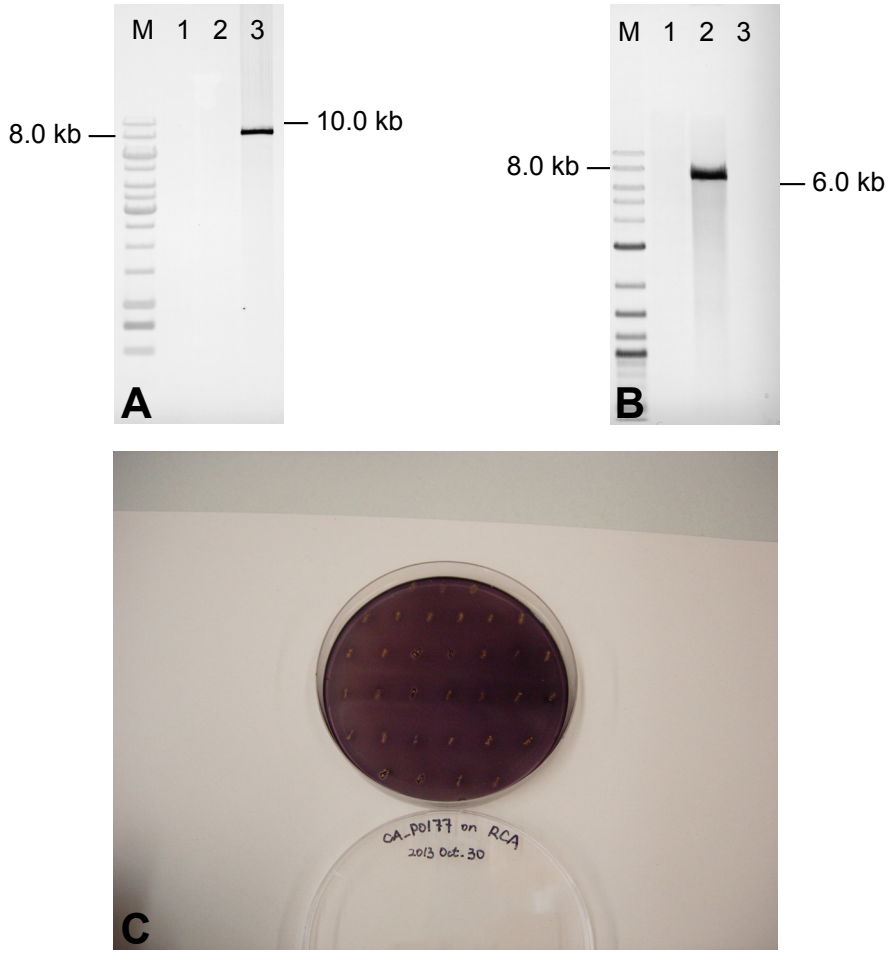

Fig. 25. Southern hybridization and starch plate test of the *CA_P0177* (the second pSOL1-free) mutant strain. *Eco*RV-digested genomic DNA of the *CA_P0177* mutant and wild type were hybridized with biotin-labelled intron- (A) or *CA_P0177*-specific (B) DNA probe. M, marker; lane 1, genomic DNA of the *CA_P0177* mutant; lane 2, wild type genomic DNA; lane 3, pMTL007C-E2 plasmid digested with *Hin*dIII. (C) The *CA_P0177* mutant colonies were re-streaked on an agar plate containing starch, no colonies formed halos when staining with potassium iodine solution

3.3.3 Characterization of the *CA_P0129* (*GbRs*) mutant

3.3.3.1 Generation of the *GbRs* mutant

To further investigate the function of genes located on the pSOL1 megaplasmid, the *CA_P0129* (*GbRs*) gene was selected as the next candidate for analysis.

GbRs encodes a glycogen-binding regulatory subunit of serine/threonine protein phosphatase I (GbRs) and is located in reverse direction on pSOL1 megaplasmid (Nölling *et al.*, 2001). According to the analyses of a protein-protein BLAST and a megablast (http://blast.ncbi.nlm.nih.gov/Blast.cgi), no counterparts of this gene were observed with identities of above 41% in other microorganisms, except for other industrial clostridial strains, i.e., *C. acetobutylicum* DSM 1731 (Bao *et al.*, 2011) and *C. acetobutylicum* EA 2018 (Hu *et al.*, 2011). A transcription analysis of a continuous culture of *C. acetobutylicum* showed that expression of *GbRs* was significantly induced during solventogenic growth (pH 4.5) (Janssen *et al.*, 2010; Grimmler *et al.*, 2011). Similar patterns were also observed in a batch culture

where *GbRs* transcript level was strongly elevated during solventogenesis (Alsaker and Papoutsakis., 2005). These results suggested significance of *GbRs* during solventogenesis. Unfortunately, its roles remained less understood. As a result, a *GbRs* mutant was constructed in this study using the ClosTron system, followed by mutant characterization by continuous fermentation and microarray experiments.

Strategies for generation of a *GbRs* ClosTron mutant were identical to that for all other mutant strains constructed in this study and they were described in detail in Methods and Materials (section 2.7.3.1, 2.9). Target sites (where the intron could insert) in *GbRs* gene were predicted using a web-based intron targeting and design tool (www.clostron.com) and a target site with the highest score (9.905) was selected. Consequently, the target site in the *GbRs* gene was determined at 303/304 bp (the length of the *GbRs* gene is 744 bp) and the intron was predicted to insert into this site at an antisense direction according to information given. In addition, four primers for SOE (splicing by overlap extension) PCR (section 2.7.3.1) (Ho *et al.*, 1989) were simultaneously designed (*GbRs*-IBS, *GbRs*-EBS1d, *GbRs*-EBS2 and EBS universal, Table 38, Appendix section). They were used for the mutation of recognition sites of the intron retargeting region on pMTL007C-E2 whose intron was able to insert into the predicted *GbRs* target site by a specific recognition of *GbRs* gene via its mutated retargeting region. SOE PCR produced the mutated intron retargeting region which was then ligated with pMTL007C-E2 backbone to generate retargeted intron expression vector specific for *GbRs* (pMTL007C-E2::cac-*GbRs*-303a, Table 7, section 2.4). This vector was subsequently transformed into *E. coli* containing pAN2 for *in vivo* methylation (section 2.9.1). Retargeted and methylated pMTL007C-E2::cac-*GbRs*-303a was electroporated into *C. acetobutylicum* (section 2.9.2), followed by screening of thiamphenicol- and erythromycin-resistant colonies (section 2.9.3).

After electroporation and screening, 10 erythromycin-resistant clones of the putative *GbRs* mutant were selected and the correct insertion of the intron was verified by PCR and subsequent Southern hybridization. Because *GbRs* resided on the pSOL1, *GbRs* gene-specific primers (*GbRs*-Forward and -Reverse primers, Table 39, Appendix section) were used to check correction insertion of the intron and pSOL1 presence. *repA* gene-specific primers (Table 39, Appendix section) were not used. Consequently, erythromycin-resistant clones (putative *GbRs* mutant) were verified by standard PCR (section 2.7.2.1) using three different primers. *GbRs* gene-specific primers were used first. The wild type genomic DNA gave a band at 714 bp, while the correct mutants exhibited products of 2,495 bp, ~1.8 kb larger than that of the wild type, which corresponded to the size of the intron inserting into the target gene (Fig. 26A). In addition to verification of correct insertion of the intron, this PCR also confirmed the presence of the pSOL1 in *GbRs* mutant cells. Another set of primers, an intron specific primer (EBS universal, Table 38, Appendix section) and a *GbRs*-Reverse primer, were employed to verify an exon-intron junction part of the mutated gene, leading to a product of 676 bp, whereas the wild type was not supposed to result in a product (Fig. 26B). Besides, a primer pair specific for pMTL007C-E2 plasmid (pMTL007CE2check-Forward and -Reverse primers, Table 40, Appendix section) was used for confirmation of the loss of this shuttle vector from mutant cells and only pMTL007C-E2 plasmid control gave a band at 517 bp (Fig. 26C). To sum up, it proved that a *GbRs* mutant had been generated.

To further confirm the correct insertion of the intron, i.e., that only one copy of the intron had inserted into *GbRs* gene, Southern hybridization was conducted with the intron-specific probe. Detailed methods of Southern hybridization were described previously (section 2.7.5). 590 bp of the intron-specific probe was PCR amplified using intron-specific primers (ISP-Forward

and -Reverse primers, Table 40, Appendix section) and pMTL007 plasmid was used as the template. The intron-specific probe (fragment) was located at a intron-erythromycin gene junction section (339-928 bp) in the intron (1,781 bp in length) where 774 bp of erythromycin gene resided (710-1,483 bp). Genomic DNA of the *GbRs* mutant as well as that of the wild type were digested with *Eco*RV-HF or *Hin*dIII at 37 °C for 16 hours before they were transferred from an agarose gel to a positively charged nylon membrane which was then hybridized overnight with the biotin-labeled intron-specific probe at 42 °C. *Eco*RV-digested genomic DNA of the *GbRs* mutant exhibited a single band at ~12 kb, demonstrating that the *GbRs* mutant possessed only one copy of the intron on the chromosome and thus only the *GbRs* gene was mutated. No hybridization signal was observed for wild type genomic DNA, as expected, because the intron-specific probe used did not hybridize to any original DNA sequence in *C. acetobutylicum*. Restricted pMTL007C-E2 with *Hin*dIII was used as a positive control, showing a signal at 8.9 kb which was equal to the size of linear pMTL007C-E2 (Fig. 26D). On the other hand, *Hin*dIII-digested genomic DNA of the *GbRs* mutant was hybridized with the intron-specific probe. A single band at ~5 kb was displayed in the *GbRs* mutant, whereas wild type genomic DNA digested with the same enzyme did not produce a band. Restricted pMTL007C-E2 with *Hin*dIII was used as a positive control which produced a band at ~8.9 kb (Fig. 26E). Consequently, after confirmation by PCR and Southern hybridization, it was proved that a single *GbRs* mutant had been generated.

The presence of the pSOL1 megaplasmid was detected via the iodine-exposed starch plate test (section 2.5.1, 2.9.4), because pSOL1-containing cells were able to degrade starch in solidified media and form halos when exposed with iodine. To confirm the presence of the pSOL1 in the *GbRs* mutant, about 50 colonies of the *GbRs* mutant strain were re-streaked on a RCA (reinforced clostridial agar) plate which contained 1% starch. After 24 h of incubation at 37 °C under anaerobic conditions, colonies still containing pSOL1 degraded the surrounding starch and formed halos when the starch-containing plate was stained with potassium iodine solution (Lugol) solution (Fig. 27A). Through this test, it was demonstrated that the *GbRs* mutant strain generated by the ClosTron system still carried the pSOL1 megaplasmid.

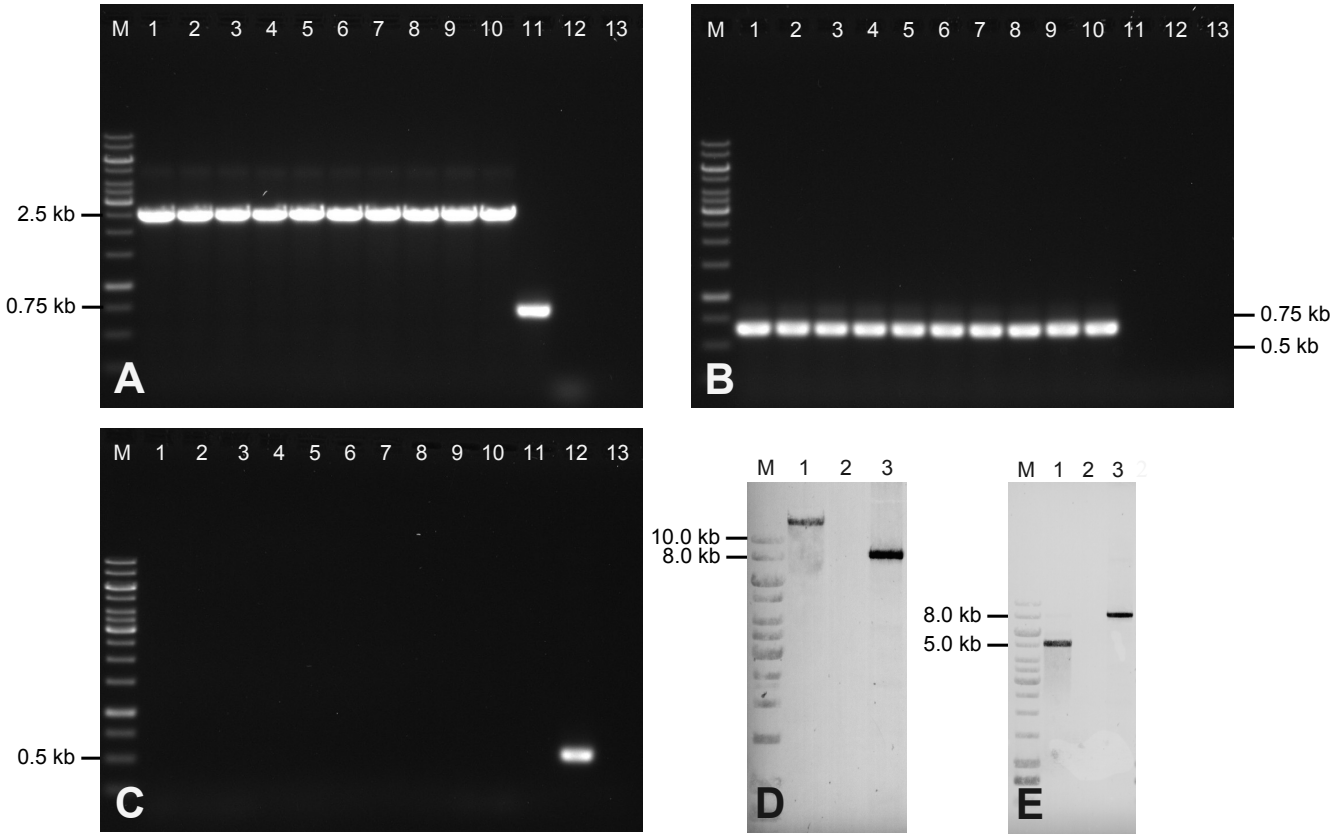

Fig. 26. PCR verification and Southern hybridization of the *CA_P0129* (*GbRs*) mutant. (A) *GbRs* gene-specific primes; (B) EBS universal primer and *GbRs*-Reverse primer; (C) pMTL007C-E2 specific primers. M, marker; lane 1-10, genomic DNA samples from different clones of the *GbRs* mutant; lane 11, wild type genomic DNA; lane 12, pMTL007C-E2 plasmid; lane 13, deionized water as the negative control. *Eco*RV- (D) or *Hin*dIII-digested (E) genomic DNA samples of the *GbRs* mutant and wild type were hybridized with biotin-labelled intron-specific DNA probe. M, marker; lane 1, genomic DNA of the *GbRs* mutant; lane 2, wild type genomic DNA; lane 3, pMTL007C-E2 digested with *Hin*dIII

3.3.3.2 Inability of the *GbRs* mutant to produce granulose

Granulose, an amylopectin-like α-polyglucan (Gavard and Milhaud, 1952; Whyte and Strasdine, 1972; Robson *et al.*, 1974), is a storage substance accumulated in clostridial cells which are in early sporulation processes (Dürre, 2005). Because granulose is a ploymer of glucose, knock out of the gene for a glycogen-binding regulatory subunit (GbRs) might affect synthesis of granulose. To test this assumption the *GbRs* mutant culture (OD_{600}≈1.0) was spread on a semicircle section of a CBM (clostridium basal medium, section 2.5.1) agar plate along with the wild type culture (OD_{600}≈1.0) which was plated on the other half. For this experiment three plates were spread with identical cultures (the *GbRs* mutant and wild type cultures) for different test time-point. After cultivation under anaerobic conditions for 24, 48 and 90 h, CBM plates were treated with iodine vapor in a ventilation hood to detect granulose formation. Colonies producing granulose became dark blue when staining with iodine, whereas the original color (yellow) remained unchanged for non-granulose-forming colonies (section 2.9.4). Wild type colonies started to produce granulose after 48 h of cultivation. However, the *GbRs* mutant did not synthesize granulose during this experimental process. Consequently, it was proved that mutation in *GbRs* led to inability to produce granulose and *GbRs* was a indispensable gene for granulose formation in *C. acetobutylicum* (Fig. 27B-D).

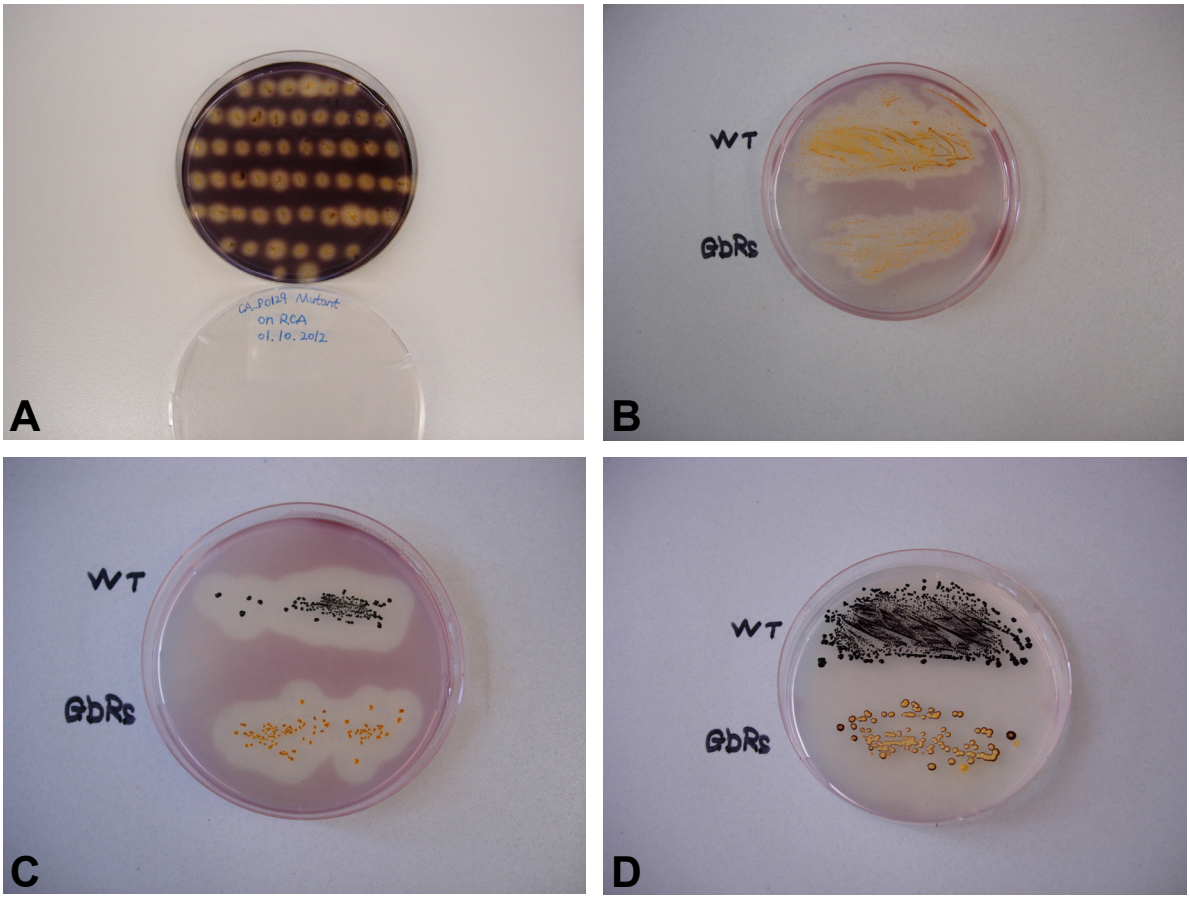

Fig. 27. Starch plate and granulose-production test of the *CA_P0129* mutant strain. (A) The *CA_P0129* mutant colonies were re-streaked on an agar plate containing starch, colonies still carrying the pSOL1 megaplasmid formed halos when staining with potassium iodine solution. (B-D) The *CA_P0129* mutant culture and the wild type culture were spread on CBM agar plates, followed by iodine vapor treatment when cultivated for 24 h (B), 48 h (C) and 90 h (D).

3.3.3.3 Continuous fermentation of the *GbRs* mutant

After confirming the *GbRs* mutant at molecular and phenotypical levels, continuous fermentation was carried out to characterize this mutant strain (Fig. 28) and correct insertion of the intron in the *GbRs* gene was monitored by PCR using *GbRs* gene-specific primers (*GbRs*-Forward and -Reverse primers, Table 39, Appendix section) which flanked the intron insertion site. Methods for chemostat cultures of *C. acetobutylicum* were described in detail previously (section 2.6).

During acidogenic growth of the continuous culture of the *GbRs* mutant, the OD_{600} was ~3.8, which was comparable to that of the wild type. After ~14 h of the pH shift, the culture of the *GbRs* mutant entered solventogenesis, and the final OD_{600} of the culture during the steady-state was ~3.3 which was lower than the wild type. In terms of glucose consumption, the *GbRs* mutant utilized more glucose during acidogenesis than during solventogenesis, which was similar to the wild type strain. However, the *GbRs* mutant consumed less glucose than the wild type during both acidogenesis and solventogenesis, which led to slightly lower production of acetic acid (~37 mM) (acidogenesis) and significantly decreased production of acetone and butanol (solventogenesis), respectively. During acidogenesis, concentrations of

butyrate and acetone were not altered as comparable to the wild type, whereas formation of butanol was decreased although this was not a main product during this phase. Besides, a little more butyrate (~23.8%) was detected during solventogenic growth, whereas acetic acid formed (~10 mM) was comparable to the wild type. Moreover, ethanol formation was also slightly reduced during acidogenic and solventogenic growth of the *GbRs* chemostat culture. These results indicated that *GbRs* was positively related to the generation of acetone and butanol during solventogenesis, and mutation of this gene also affected butyrate metabolism during the same phase.

3.3.3.4 Transcriptional analysis of the *GbRs* mutant as compared to the wild type

After characterizing the *GbRs* mutant in continuous fermentation, microarray experiments were performed to detect transcriptome changes caused by the inactivation of the *GbRs* gene. Cells of the steady-state acidogenic and solventogenic growth of the chemostat culture of the *GbRs* mutant were used for RNA preparation and the following microarray experiments. cDNA (complementary DNA) samples from the same growth phases of the wild type continuous culture were utilized as the reference in transcriptional analysis. Detailed experimental processes involved in microarray experiments and methods for data analysis were described in Materials and Methods (section 2.10). Slides covalently coupled with oligonucleotide probes (2 identical spots for 1 gene) were hybridized with combined labelled cDNA containing 80 pmol of Cy3 and Cy5 (GE Healthcare Europe GmbH, Munich, Germany) from the *GbRs* mutant and wild type, followed by slides scanning using a GenePix 4000B microarray scanner and GenePix Pro 4.0 software (Axon Instruments, Union City, USA). The ratio of medians, the ratio of means and the regression ratio were automatically calculated by GenePix Pro 6.0 software (Axon Instruments, Union City, USA) based on intensities of fluorescence signals the *GbRs* mutant and wild type (reference) cDNA samples when analyzing scanned microarray images. Normalization was carried out by setting the arithmetic mean of the ratios equal to 1. Background correction was then conducted by subtracting the background value plus one standard deviation from the foreground value. The ratio of medians, the ratio of means and the regression ratio (they differed by less than 30%) were used to correct for spot morphology of features of one hybridization and the ratio of medians was used to calculated for the final expression ratio (average of the two ratios of medians from two identical spots) which was subsequently taken its logarithm (to the basis of 2). The results from microarray experiments were calculated by mean of one hybridization and its dye-flip hybridization.

As mentioned previously (section 2.10.6), a logarithmic ratio format was used in transcriptional analysis for convenience to discriminate up-regulated and down-regulated genes. A positive logarithmic ratio indicated a gene induced in the *GbRs* mutant, whereas a negative logarithmic ratio represented a repressed gene of the *GbRs* mutant as compared to wild type. In addition, a logarithmic ratio larger than 1.60 was for significant induction in contrast to a ratio less than -1.60 which meant this gene was significantly repressed when *GbRs* gene was deleted. As a result, using wild type as a reference, the higher a positive logarithmic ratio was, the more noticeable a gene was up-regulated in the *GbRs* mutant, and a gene was down-regulated in a more significant level when its negative logarithmic ratio was lower.

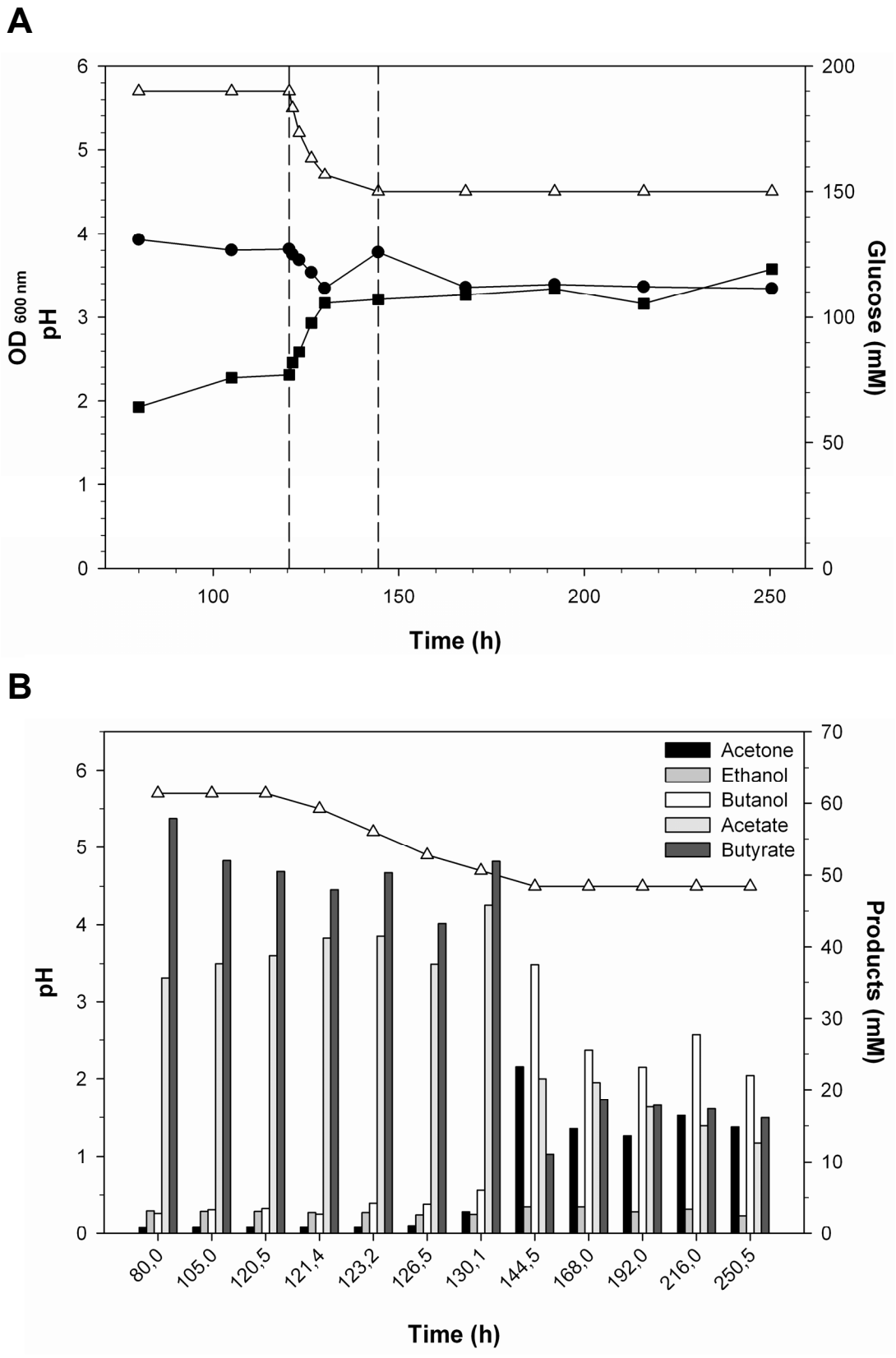

Fig. 28. Fermentation profile of the phosphate-limited continuous culture of the *CA_P0129* (*GbRs*) mutant. (A) Growth, glucose consumption and pH in the course of fermentation. Dashed lines indicate the dynamic pH shift. (B) Fermentation products from the steady-state acidogenesis to solventogenesis. Each grouped bar set corresponds to each time-point. The experiment was duplicated and the figure represents one exemplary fermentation. Quantification of metabolites was done with an internal standard of known concentration (section 2.11.2). Symbols: *triangles*, pH; *circles*, OD at 600 nm; *squares*, residual glucose concentration

Through microarray experiments of the *GbRs* mutant, it was found that the expression profiles of most genes responsible for the central metabolic pathways (Fig. 2) were not significantly altered as compared to the wild type. The expression of a *pfor* (*CA_C2229*), *thlA* (*CA_C2873*) and the *bcs* operon (*CA_C2708-CA_C2712*) was slightly up-regulated during acidogenesis of a chemostat culture of the *GbRs* mutant (Fig. 2, Table 28). However, the production of metabolites by this mutant during this phase was not significantly changed (section 3.3.3.3). In addition, an antagonistic expression pattern was observed at pH 5.7 with the two paralogs of aldehyde/alcohol dehydrogenase genes, *adhE1* and *adhE2*. This is similar to what was reported previously (Grimmler *et al*., 2011). The expression patterns of central metabolic genes in the *GbRs* mutant are listed in Table 28.

Table 28. Expression patterns of the central metabolic genes compared to wild type in the *GbRs* mutant during acidogenic and solventogenic growth

ID	Protein function[a]	Ratio[b]	
		pH 5.7	pH 4.5
CA_P0035	AdhE2, aldehyde-alcohol dehydrogenase	1.77	—
CA_P0078	ThlB, acetyl coenzyme A acetyltransferase	—	0.21
CA_P0162	AdhE1, aldehyde dehydrogenase (NAD^+)	-1.71	-0.76
CA_P0163	CtfA, butyrate-acetoacetate CoA-transferase subunit A	—	-0.49
CA_P0164	CtfB, butyrate-acetoacetate CoA-transferase subunit B	—	0.10
CA_P0165	Adc, acetoacetate decarboxylase	-0.70	0.18
CAC0028	HydA, hydrogene dehydrogenase	0.12	0.87
CAC0267	Ldh, lactate dehydrogenase	—	-0.28
CAC1543	Ldh, lactate dehydrogenase	0.10	-0.67
CAC1742	Pta, phosphate acetyltransferase	0.57	-0.40
CAC1743	Ack, acetate kinase	0.66	-0.36
CAC2229	Pfor, pyruvate ferredoxin oxidoreductase	0.95	-0.07
CAC2499	Pfor, pyruvate ferredoxin oxidoreductase	—	—
CAC2708	Hbd, β-hydroxybutyryl-CoA dehydrogenase	1.03	0.54
CAC2709	EtfA, electron transfer flavoprotein alpha-subunit	1.15	0.43
CAC2710	EtfB, electron transfer flavoprotein beta-subunit	0.60	-0.26
CAC2711	Bcd, butyryl-CoA dehydrogenase	0.89	0.06
CAC2712	Crt, crotonase	0.70	0.09
CAC2873	ThlA, acetyl-CoA acetyltransferase	0.83	-0.23
CAC3075	Buk, butyrate kinase	0.31	0.19
CAC3076	Ptb, phosphate acetyltransferase	0.10	-0.08
CAC3552	Ldh, lactate dehydrogenase	—	0.28

Genes are listed in order of ORFs, and considered as significantly up-regulated when the logarithmic ratio was ≥1.60 and as significantly down-regulated when the logarithmic ratio was ≤ -1.60. The given values in the table are mean of results of two hybridizations with dye swaps

[a] Protein names based on Nölling *et al.* (2001)

[b] The expression ratio as the logarithm to the basis of 2

On the other hand, transcription of 17 genes in acidogenic cells and 23 genes in solventogenic cells was observed to be strongly induced in the *GbRs* (*CA_P0129*) mutant, while 46 genes during acidogenesis and 24 genes during solventogenesis showed noticeable repression. Each

was in comparison to the status at the same pH value of the wild type chemostat culture. Results were listed in Table 29-32, respectively.

Table 29. Significantly up-regulated genes compared to wild type in the *GbRs* mutant during acidogenic growth

ID	Protein function[a]	Ratio[b]
CA_P0035	AdhE2 Aldehyde-alcohol dehydrogenase	1.77
CA_P0083	SAM-dependent methyltransferase	1.83
CAC0105	Ferredoxin	3.66
CAC0106	ABC-type probable sulfate transporter, periplasmic binding protein	3.50
CAC0107	ABC-type sulfate transporter, ATPase component	4.08
CAC0109	CysD sulfate adenylyltransferase subunit 2	4.21
CAC0430	Glycerophosphoryl diester phosphodiesterase	1.79
CAC0562	Predicted membrane protein	1.94
CAC0563	Predicted membrane protein	1.99
CAC0946	Metallo beta-lactamase superfamily hydrolase	1.82
CAC1547	TrxA Thioredoxin	2.40
CAC1548	TrxB Thioredoxin reductase	2.19
CAC1571	Glutathione peroxidase	2.17
CAC2849	Proline/glycine betaine ABC-type transport system, permease component fused to periplasmic component	2.88
CAC2850	Proline/glycine betaine ABC-type transport system, ATPase component	2.49
CAC3325	Periplasmic amino acid binding protein	1.96
CAC3326	Amino acid ABC-type transporter, permease component	2.05

Genes are listed in order of ORFs and considered as significantly up-regulated when the logarithmic ratio was ≥1.60. The given values in the table are mean of results of two hybridizations with dye swaps

[a] Protein name based on Nölling *et al.* (2001)

[b] The expression ratio as the logarithm to the basis of 2

During the steady-state acidogenic growth of the *GbRs* mutant, 17 genes were significantly up-regulated as compared to the wild type (Table 29). Among these, 3 genes encoded membrane-associated proteins (*CA_C0430*, *CA_C0562* and *CA_C0563*), which suggested that inactivation of *GbRs* affected the characteristics of the cell membrane. Remarkably, the expression of genes responsible for cysteine biosynthesis (*CA_C0105*-*CA_C0107* and *CA_C0109*) was induced. Moreover, the transcript levels of 4 genes involved in transport of amino acids (proline/glycine and cysteine) were also significantly elevated (*CA_C2849*-*CA_C2850*, *CA_C3325*-*CA_C3326*). In addition, genes related to defense metabolism (*CA_C0946*, *CA_C1547*-*CA_C1548* and *CA_C1571*) displayed increased expression abundance. Besides, two genes located on the pSOL1 megaplasmid, *CA_P0083* and *CA_P0035* (*adhE2*), were highly expressed. The latter was an alcohol dehydrogenase gene which was only expressed during alcohologenic growth (Fontaine *et al.*, 2002) and not during acidogenesis and solventogenesis. Microarray experiments for the *GbRs* mutant indicated that the expression of *adhE2* was negatively influenced by *GbRs* during acidogenesis.

Table 30. Significantly down-regulated genes compared to wild type in the *GbRs* mutant during acidogenic growth

ID	Protein function[a]	Ratio[b]
CA_P0112	Hypothetical protein	-1.84
CA_P0129	Glycogen-binding regulatory subunit of S/T protein phosphatase I	-2.44
CA_P0141	Periplasmic hydrogenase small subunit, dehydrogenase	-1.86
CA_P0142	Periplasmic hydrogenase large subunit, dehydrogenase	-1.94
CA_P0143	Hydrogenase maturation protease delta subunit	-2.30
CA_P0144	Possible steroid binding protein	-2.25
CA_P0145	Hypothetical protein	-2.53
CA_P0162	AdhE1 Aldehyde dehydrogenase (NAD^+)	-1.71
CAC0253	NifH Nitrogenase iron protein (nitrogenase component II)	-1.65
CAC0255	NifHD Nitrogen regulatory protein PII	-1.68
CAC0580	Hypothetical protein	-2.31
CAC0658	Fe-S oxidoreductase	-1.99
CAC0660	Hypothetical protein	-2.45
CAC0661	ABC transporter ATP-binding protein (multidrug resistance protein)	-2.30
CAC0662	Sugar ABC transporter, periplasmic sugar-bindind protein	-5.53
CAC0663	Hypothetical protein	-5.43
CAC0664	Sugar-binding periplasmic protein	-5.00
CAC0665	ABC-type sugar transport system, permease component	-4.87
CAC0666	Sugar permease	-4.04
CAC0667	Sugar-binding periplasmic protein	-5.09
CAC1072	Fe-S oxidoreductase	-1.88
CAC1336	Hypothetical protein	-1.82
CAC1337	Spore coat protein	-1.74
CAC1347	Transaldolase	-2.09
CAC1349	GalM Aldose-1-epimerase	-2.42
CAC1363	Superoxide dismutase, Cu-Zn family	-1.63
CAC2086	Stage III sporulation protein AH, SpoIIIAH	-2.45
CAC2087	Stage III sporulation protein AG, SpoIIIAG	-1.68
CAC2091	Stage III sporulation protein AC, SpoIIIAC	-1.76
CAC2092	Stage III sporulation protein SpoAB	-2.00
CAC2137	Cation transport P-type ATPase	-1.65
CAC2342	Predicted membrane protein	-1.88
CAC2365	Small acid-soluble spore protein	-2.39
CAC2382	Single-strand DNA-binding protein	-1.70
CAC2383	Predicted xylanase/chitin deacetylase	-2.81
CAC2460	Hypothetical protein	-2.53
CAC2610	L-Frucose isomerase related protein	-2.00
CAC2611	Hypothetical protein	-1.82
CAC2695	Diverged Metallo-dependent hydrolase(Zn), peptodoglycan-binding domain	-2.11
CAC2722	Predicted protein (beta propeller fold)	-1.61
CAC2791	Fe-S oxidoreductase	-1.71
CAC2903	LysM domain containing membrane protein	-2.22
CAC2906	Spore coat protein, CotS-related	-2.04
CAC3244	Spore cortex-lytic enzyme, pre-pro-form (diverged form of N-acetylmuramyl-L-alanine amidase), peptidoglycan-binding domain	-1.89

Table 30. (continued)

ID	Protein function[a]	Ratio[b]
CAC3318	Hypothetical protein	-2.42
CAC3612	Hypothetical protein	-2.65

Genes are listed in order of ORFs and considered as significantly down-regulated when the logarithmic ratio was ≤ -1.60. The given values in the table are mean of results of two hybridizations with dye swaps

[a] Protein name based on Nölling *et al.* (2001)

[b] The expression ratio as the logarithm to the basis of 2

During the steady-state acidogenic growth of the *GbRs* mutant culture, 46 genes were significantly down-regulated as compared to the wild type (Table 30). Among these, a putative operon *CA_C0661-CA_C0667*, a cluster related to carbohydrate transport (Nölling *et al.*, 2001), showed the most remarkable repression. Moreover, 3 genes (*CA_C1349*, *CA_C2383*, *CA_C2610*) in this data set were involved in carbohydrate metabolism. Besides, part of a possible operon (*CA_C0253*, *CA_C0255*) for nitrogen fixation was strongly repressed. A similar phenomenon was found for a cluster *CA_C2086-CA_C2087* and *CA_C2091-CA_C2092*, which was associated with sporulation. *CA_C1337*, *CA_C2365*, *CA_C2906* and *CA_C3244* involved in spore formation were also significantly down-regulated. In addition, the expression of hydrogenase-coding genes (*CA_P0141-CA_P0143*) and genes for membrane proteins (*CA_C2342* and *CA_C2903*) were significantly down-regulated. Interestingly, the transcript level of *adhE1* (*CA_P0162*) was noticeably decreased, indicating it suffered from a positive regulation of *GbRs* during acidogenesis. And an antagonistic expression pattern was observed between *adhE1* and *adhE2* (*CA_P0035*) in this growth phase, the latter was significantly induced during acidogenesis of the *GbRs* mutant culture. This antagonistic expression between *adhE1* and *adhE2* was consistent with what was observed in a wild type chemostat culture (Grimmler *et al.*, 2011).

Table 31. Significantly up-regulated genes compared to wild type in the *GbRs* mutant during solventogenic growth

ID	Protein function[a]	Ratio[b]
CA_P0004	Cysteine protease	2.26
CA_P0036	Uncharacterized, ortholog of YgaT of *B.subtillis*	4.54
CA_P0037	Uncharacterized, ortholog of YgaS of *B.subtillis*	4.48
CA_P0130	Hypothetical protein	3.18
CAC0104	Adenylylsulfate reductase	1.67
CAC0105	Ferredoxin	1.79
CAC0107	ABC-type sulfate transporter, ATPase component	2.44
CAC0109	CysD sulfate adenylyltransferase subunit 2	2.15
CAC0110	CysN GTPase, sulfate adenylate transferase subunit 1	1.64
CAC0264	Predicted membrane protein	2.01
CAC1314	Hypothetical protein	1.74
CAC1390	PurE phosphoribosylaminoimidazole carboxylase catalytic subunit	1.82
CAC1392	PurF amidophosphoribosyltransferase	1.89
CAC1393	PurM phosphoribosylaminoimidazole synthetase	1.66

Table 31. (continued)

ID	Protein function[a]	Ratio[b]
CAC1472	Amino acid permease	1.66
CAC1655	PurQ/PurL bifunctional enzyme phosphoribosylformylglycinamidine synthase (synthetase domain/glutamine amidotransferase domain)	2.21
CAC2388	ArgD N-acetylornithine aminotransferase	1.99
CAC2391	ArgJ bifunctional ornithine acetyltransferase/N-acetylglutamate synthase protein	1.82
CAC2517	NrpE Extracellular neutral metalloprotease	2.35
CAC2621	Cell wall hydrolase (autolysin), glycosyl hydrolase, peptodoglycan-binding domain	1.80
CAC2772	Permease	2.31
CAC2914	PanB Ketopantoate hydroxymethyltransferase	1.84
CAC3285	Predicted amino acid transporter	1.91

Genes are listed in order of ORFs and considered as significantly up-regulated when the logarithmic ratio was ≥1.60. The given values in the table are mean of results of two hybridizations with dye swaps

[a] Protein name based on Nölling *et al.* (2001)

[b] The expression ratio as the logarithm to the basis of 2

During the steady-state solventogenic growth of the *GbRs* mutant culture, 23 genes were significantly up-regulated as compared to the wild type (Table 31). Among these, an operon with unknown functions (*CA_P0037*-*CA_P0036*) showed the most remarkable induction. This operon was strongly up-regulated during acidogenesis of a wild type chemostat culture (Janssen *et al.*, 2010). Besides, 5 genes (*CA_C0104*, *CA_C0105*, *CA_C0107*, *CA_C0109* and *CA_C0110*) in a cluster involved in cysteine biosynthesis displayed dramatic induction. Moreover, the expression level of *CA_C2388* and *CA_C2391* for synthesis of arginine was significantly elevated. A similar phenomenon was found for genes *CA_C1390*, *CA_C1392*, *CA_C1393* and *CAC1655*, which were associated with formation of purines. In addition, the transcript levels of genes for the transport of amino acids (*CA_C1472* and *CA_C3285*) and genes for proteolysis (*CA_P0004* and *CA_C2517*) were significantly enhanced.

Table 32. Significantly down-regualted genes compared to wild type in the *GbRs* mutant during solventogenic growth

ID	Protein function[a]	Ratio[b]
CAC0014	Aminotransferase	-5.33
CAC0015	SerA D-3-phosphoglycerate dehydrogenase	-5.64
CAC0016	Related to HTH domain of SpoOJ/ParA/ParB/RepB family, involved in chromosome partitioning	-5.93
CAC0017	SerS seryl-tRNA synthetase	-6.05
CAC0018	Putative NADPH-quinone reductase	-3.05
CAC0056	Hypothetical protein	-2.23
CAC0057	Hypothetical protein	-1.92
CAC0058	Hypothetical protein	-2.07
CAC0059	Hypothetical protein	-1.82
CAC0061	Phage-related protein	-1.91

Table 32. (continued)

ID	Protein function[a]	Ratio[b]
CAC0062	Hypothetical protein	-1.66
CAC0063	Hypothetical protein	-1.72
CAC0064	Hypothetical protein	-1.97
CAC0065	Hypothetical protein	-1.98
CAC0550	Possible sigma factor	-1.72
CAC0552	Protein containing cell-adhesion domain	-2.03
CAC0553	Hypothetical protein	-1.89
CAC0554	Autolytic lysozime (1,4-beta-N-acetylmuramidase), glycosyl hydrolase , peptodoglycan-binding domain	-1.82
CAC0893	Prephenate dehydrogenase	-2.01
CAC1322	GlpA Glycerol-3-phosphate dehydrogenase	-2.14
CAC2241	Cation transport P-type ATPase	-2.19
CAC2242	Predicted transcriptional regulator	-2.37
CAC2433	HtrA-like serine protease	-1.74
CAC3421	Acyl carrier protein phosphodiesterase	-2.46

Genes are listed in order of ORFs and considered as significantly down-regulated when the logarithmic ratio was ≤ -1.60. The given values in the table are mean of results of two hybridizations with dye swaps

[a] Protein name based on Nölling *et al.* (2001)

[b] The expression ratio as the logarithm to the basis of 2

During the steady-state solventogenic growth of the *GbRs* mutant culture, 24 genes were significantly down-regulated as compared to the wild type (Table 32). Among these, a possible operon (*CA_C0014-CA_C0017*) for biosynthesis of serine displayed the most remarkable repression. Moreover, the expression of two genes coded for proteins for biosynthesis of other amino acids and vitamins was also strongly repressed (*CA_C0893*, *CA_C3421*). In addition, part of a putative operon consisting of genes for hypothetical proteins (*CA_C0056-CA_C0065*, *CA_C0060* did not pass the filter criterion, section 2.10.6) showed noticeable low transcript levels. Besides, *CA_C0552*, *CA_C2242* and *CA_C2433* encoding regulation-related proteins revealed significantly decreased expression. Last but not the least, the transcript level of *CA_C0554*, a gene involved in autolysis of the cell, were also significantly down-regulated.

3.3.4 Characterization of the *CA_P0162* (*adhE1*) mutant

3.3.4.1 Continuous fermentation of the *adhE1* mutant

The *sol* operon consists of *adhE1* (*CA_P0162*) and *ctfA/B* (*CA_P0163* and *CA_P0164*) genes which are responsible for solvent production under batch conditions (Cookley *et al.*, 2012). AdhE1 is one of the two bifunctional aldehyde/alcohol dehydrogenases (AADHs) in *C. acetobutylicum*, the only bacterial example with two AADHs (AdhE1 and AdhE2) (Fontaine *et al.*, 2002). Although AdhE1 is the principle dehydrogenase for production of solvents in batch cultures (Cookley *et al.*, 2012), gene regulatory networks behind its expression remained less understood. As a result, a *adhE1* mutant obtained from Prof. Nigel

P. Minton (University of Nottingham) (Cookley *et al.*, 2012) was characterized in this study using continuous fermentation and transcriptional analysis to understand its fermentation profiles and regulatory mechanisms.

Continuous fermentation was first conducted for the *adhE1* mutant (Fig. 29) and correct insertion of the intron in the *adhE1* gene was monitored by PCR using *adhE1* gene-specific primers (*adhE1*-Forward and -Reverse primers, Table 39, Appendix section) which flanked the intron insertion site. Methods for chemostat culture of *C. acetobutylicum* were described in detail previously (section 2.6). During acidogenic growth of the continuous culture of the *adhE1* mutant, the OD_{600} was ~3.6 which was slightly lower than that of the wild type and was comparable to the pSOL1-free (*CA_P0175*) mutant. Two days after the *adhE1* mutant culture reached the steady-state acidogenic growth, a pH shift was initiated and the pH value of the culture started to decrease, which was accompanied with continuous decrease of the OD_{600} of the mutant culture. After ~16 h of the pH shift, the culture of the *adhE1* mutant entered solventogenesis. And the decrease of the OD_{600} of the culture did not stop until ~9 h later, after which the culture started to grow again (the OD_{600} increased). This suggested that the *adhE1* mutant culture required extended time for adaptation to a more acidic environment (pH 5.7-pH 4.5), which also had been observed in the fermentation processes of the *fcd/htpG* double mutant and a pSOL1-free (*CA_P0175*) mutant strain. The final OD_{600} of the *adhE1* mutant during the steady-state solventogenic growth was ~1.7 which was ~55.7% lower than the wild type (~3.8) and 33.2% lower than the pSOL1-free (*CA_P0175*) mutant (~2.5). In terms of glucose consumption, the *adhE1* mutant utilized more glucose during acidogenesis than during solventogenesis, which was similar to the wild type strain. However, the *adhE1* mutant consumed less glucose than the wild type during acidogenesis and especially during solventogenesis, which led to slightly lower production of acetic acid (~37 mM) at pH 5.7, and negligible concentrations of all three solvents at pH 4.5. During acidogenesis, the butyrate concentration was comparable to the wild type, while production of acetone and butanol was reduced by more than 65% although these were not predominant metabolites during this phase. More butyrate (~51%) was formed during solventogenic growth, whereas acetic acid formed (~10 mM) was comparable to the wild type. Concentrations of both acids would be much higher during solventogenesis if normalizing the OD_{600} of the *adhE1* mutant culture to wild type level. Ethanol formation was slightly affected during acidogenic growth of the *adhE1* mutant. These results indicated that during solventogenic growth inactivation of *adhE1* nearly abolished production of acetone, butanol and ethanol, suggesting that *adhE1* was an indispensable gene for the solvent formation. In addition, metabolism of butyrate and acetate during solventogenesis was significantly influenced by the mutation in *adhE1*.

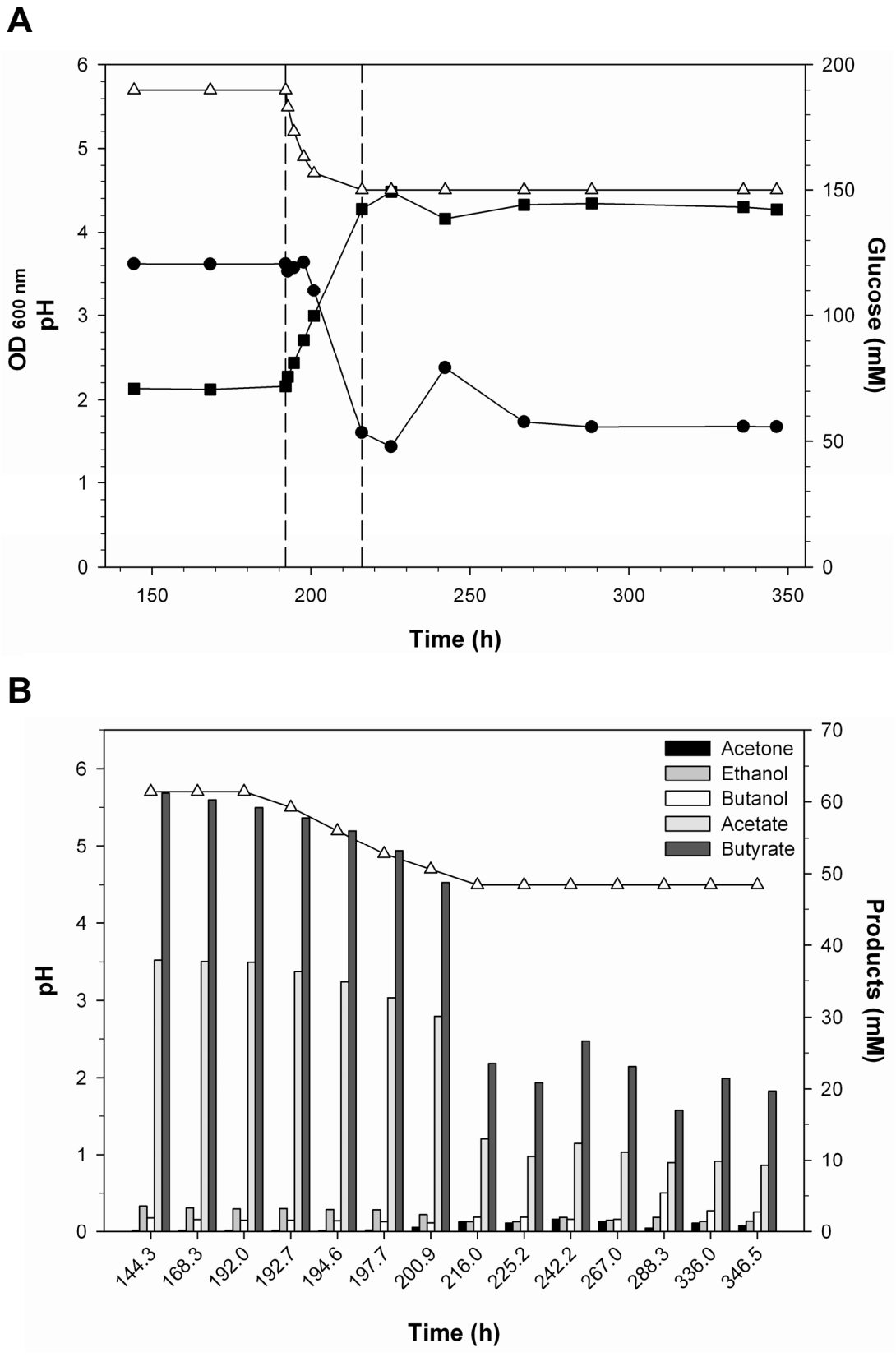

Fig. 29. Fermentation profile of the phosphate-limited continuous culture of the *CA_P0162* (*adhE1*) mutant. (A) Growth, glucose consumption and pH in the course of fermentation. Dashed lines indicate the dynamic pH shift. (B) Fermentation products from the steady-state acidogenesis to solventogenesis. Each grouped bar set corresponds to each time-point. Quantification of metabolites was done with an internal standard of known concentration (section 2.11.2). Symbols: *triangles*, pH; *circles*, OD at 600 nm; *squares*, residual glucose concentration

3.3.4.2 Transcriptional analysis of the *adhE1* mutant as compared to the wild type

After characterizing the *adhE1* mutant in continuous fermentation, microarray experiments were performed to detect transcriptome changes caused by inactivation of the *adhE1* gene. Cells of the steady-state acidogenic and solventogenic growth of the chemostat culture of the *adhE1* mutant were used for RNA preparation and the following microarray experiments. cDNA (complementary DNA) samples from the same growth phases of the wild type continuous culture were utilized as the reference in transcriptional analyses. Detailed experimental processes involved in microarray experiments and methods for data analysis were described in Materials and Methods (section 2.10). Slides covalently coupled with oligonucleotide probes (2 identical spots for 1 gene) were hybridized with combined labelled cDNA containing 80 pmol of Cy3 and Cy5 (GE Healthcare Europe GmbH, Munich, Germany) from the *adhE1* mutant and wild type, followed by slides scanning using a GenePix 4000B microarray scanner and GenePix Pro 4.0 software (Axon Instruments, Union City, USA). The ratio of medians, the ratio of means and the regression ratio were automatically calculated by GenePix Pro 6.0 software (Axon Instruments, Union City, USA) based on intensities of fluorescence signals the *adhE1* mutant and wild type (reference) cDNA samples when analyzing scanned microarray images. Normalization was carried out by setting the arithmetic mean of the ratios equal to 1. Background correction was then conducted by subtracting the background value plus one standard deviation from the foreground value. The ratio of medians, the ratio of means and the regression ratio (they differed by less than 30%) were used to correct for spot morphology of features of one hybridization and the ratio of medians was used to calculate the final expression ratio (average of the two ratios of medians from two identical spots) which was subsequently taken its logarithm (to the basis of 2). The results from microarray experiments were calculated by mean of one hybridization and its dye-flip hybridization.

As mentioned previously (section 2.10.6), a logarithmic ratio format was used in transcriptional analysis for convenience to discriminate up-regulated and down-regulated genes. A positive logarithmic ratio indicated a gene induced in the *adhE1* mutant, whereas a negative logarithmic ratio represented a repressed gene of the *adhE1* mutant as compared to the wild type. In addition, a logarithmic ratio larger than 1.60 was for significant induction in contrast to a ratio less than -1.60 which meant this gene was significantly repressed when the *adhE1* gene was deleted. As a result, the higher a positive logarithmic ratio was, the more noticeable a gene was up-regulated in the *adhE1* mutant, and a gene was down-regulated in a more significant level when its negative logarithmic ratio was lower.

Through microarray experiments of the *adhE1* mutant, it was found that the expression profiles of most genes responsible for the central metabolic pathways (Fig. 2) were not significantly altered as compared to the wild type. Interestingly, a *pfor* (*CA_C2229*) was repressed by ~51% (did not reach the criterion referred to as “significant”) during solventogenic growth of the *adhE1* mutant. Pfor functions at the node of pyruvate to acetyl-CoA (Fig. 2). Therefore, it suggested that the *adhE1* gene affected carbon flux flowing through the C_4 route. This is in accordance with the decreased glucose consumption of solventogenic cells of the *adhE1* mutant (Fig. 29). In addition, the transcript level of *adc* was elevated at pH 5.7, whereas a *ldh* (*CA_C0267*) was repressed during acidogenesis. The expression patterns of central metabolic genes in the *adhE1* mutant are listed in Table 33.

Table 33. Expression patterns of the central metabolic genes compared to wild type in the *adhE1* mutant during acidogenic and solventogenic growth

ID	Protein function[a]	Ratio[b]	
		pH 5.7	pH 4.5
CA_P0035	AdhE2, aldehyde-alcohol dehydrogenase	-1.29	3.20
CA_P0078	ThlB, acetyl coenzyme A acetyltransferase	—	—
CA_P0162	AdhE1, aldehyde dehydrogenase (NAD^+)	-1.42	-3.83
CA_P0163	CtfA, butyrate-acetoacetate CoA-transferase subunit A	—	-4.16
CA_P0164	CtfB, butyrate-acetoacetate CoA-transferase subunit B	—	-4.19
CA_P0165	Adc, acetoacetate decarboxylase	2.82	0.46
CAC0028	HydA, hydrogene dehydrogenase	0.32	0.40
CAC0267	Ldh, lactate dehydrogenase	-2.87	-0.10
CAC1543	Ldh, lactate dehydrogenase	0.57	-0.16
CAC1742	Pta, phosphate acetyltransferase	-0.59	-0.19
CAC1743	Ack, acetate kinase	-0.74	0.14
CAC2229	Pfor, pyruvate ferredoxin oxidoreductase	0.37	-1.04
CAC2499	Pfor, pyruvate ferredoxin oxidoreductase	—	—
CAC2708	Hbd, β-hydroxybutyryl-CoA dehydrogenase	0.02	-0.64
CAC2709	EtfA, electron transfer flavoprotein alpha-subunit	-0.47	-0.26
CAC2710	EtfB, electron transfer flavoprotein beta-subunit	-0.70	-0.24
CAC2711	Bcd, butyryl-CoA dehydrogenase	-0.67	-0.45
CAC2712	Crt, crotonase	-0.77	-1.02
CAC2873	ThlA, acetyl-CoA acetyltransferase	-0.58	0.39
CAC3075	Buk, butyrate kinase	-1.01	-0.67
CAC3076	Ptb, phosphate acetyltransferase	-0.93	-0.52
CAC3552	Ldh, lactate dehydrogenase	—	1.37

Genes are listed in order of ORFs, and considered as significantly up-regulated when the logarithmic ratio was ≥1.60 and as significantly down-regulated when the logarithmic ratio was ≤ -1.60. The given values in the table are mean of results of two hybridizations with dye swaps

[a] Protein names based on Nölling *et al.* (2001)

[b] The expression ratio as the logarithm to the basis of 2

On the other hand, transcription of 159 genes in acidogenic cells and 127 genes in solventogenic cells was observed to be strongly induced in the *adhE1* mutant strain, while 63 genes during acidogenesis and 73 genes during solventogenesis showed noticeable repression. Each was in comparison to the status at the same pH value of the wild type chemostat culture. Results were listed in Table 34-37, respectively.

Table 34. Significantly up-regulated genes compared to wild type in the *adhE1* mutant during acidogenic growth

ID	Protein function[a]	Ratio[b]
CA_P0004	Cysteine protease	3.02
CA_P0053	Xynb Xylanase, glycosyl hydrolase	1.84
CA_P0057	Putative glycoportein or S-layer protein	2.55
CA_P0058	Rare lipoprotein	3.66

Table 34. (continued)

ID	Protein function[a]	Ratio[b]
CA_P0065	Predicted secreted metalloprotease	1.88
CA_P0085	Hypothetical secreted protein (fragment)	1.74
CA_P0086	Permease, probably tetracycline resistance protein	1.94
CA_P0129	Glycogen-binding regulatory subunit of S/T protein phosphatase I	2.78
CA_P0133	Antibiotic-resistance protein, alpha/beta superfamily hydrolase	2.04
CA_P0134	Hypothetical protein	2.13
CA_P0135	Oxidoreductase	2.16
CA_P0136	AstB/chuR/NirJ-related protein	2.15
CA_P0137	Similar to UDP-glucuronosyltransferases, *B.subtilis* YpfP related	2.08
CA_P0138	Hypothetical protein	2.36
CA_P0139	Possible D-alanyl carrier protein, acyl carrier protein family	2.23
CA_P0148	Phospholipase C	3.58
CA_P0149	Xre family DNA-binding domain and TRP-repeats containing protein	1.92
CA_P0165	Adc Acetoacetate decarboxylase	2.82
CA_P0168	Alpha-amylase	2.62
CA_P0173	Archaeal-type Fe-S oxidoreductase	2.95
CA_P0174	Membrane protein	3.41
CAC0029	Distantly related to cell wall-associated hydrolase, similar to YycO of *B. subtilis*	2.53
CAC0030	Hypothetical protein	3.05
CAC0078	AgrB putative accessory gene regulator protein	2.88
CAC0079	Hypothetical protein	3.11
CAC0080	AgrC Histidine kinase-like ATPase	1.97
CAC0082	Predicted membrane protein	2.63
CAC0138	ABC transporter, ATP-binding component	1.83
CAC0193	Uncharacterized conserved membrane protein	2.32
CAC0252	Molybdate-binding protein	1.71
CAC0256	NifD Nitrogenase molybdenum-iron protein, alpha chain	2.18
CAC0333	Hypothetical protein, CF-7 family	1.94
CAC0381	Methyl-accepting chemotaxis protein	2.25
CAC0385	Beta-glucosidase	1.63
CAC0386	PTS cellobiose-specific component IIC	2.89
CAC0387	Hypothetical protein	2.04
CAC0488	Hypothetical protein	2.23
CAC0489	4-Phosphopantetheinyl transferase	2.01
CAC0490	Predicted sugar kinase, N-terminal region-uncharacterized conserved protein	1.83
CAC0491	Uncharacterized probably secreted protein	2.08
CAC0492	Alanine racemase	1.92
CAC0537	Acetylxylan esterase, acyl-CoA esterase or lipase, strong similarity to C-terminal region of endoglucanase E precursor	3.04
CAC0542	Methyl-accepting chemotaxis protein	2.41
CAC0658	Fe-S oxidoreductase	1.93
CAC0660	Hypothetical protein	3.09
CAC0663	Hypothetical protein	3.78
CAC0666	Sugar permease	3.04

Table 34. (continued)

ID	Protein function[a]	Ratio[b]
CAC0702	Predicted lipoprotein	1.86
CAC0746	Secreted protease metal-dependent protease	2.65
CAC0756	Multimeric flavodoxin	2.34
CAC0792	D-amino acid aminotransferase	2.72
CAC0814	3-oxoacyl-[acyl-carrier-protein] synthase III	4.09
CAC0816	Lipase-esterase related protein	3.13
CAC0842	Hypothetical protein	1.93
CAC0898	AroK Shikimate kinase	1.77
CAC1010	Predicted phosphohydrolase	3.47
CAC1022	Thioesterase II of alpha/beta hydrolase superfamily	1.84
CAC1072	Fe-S oxidoreductase	3.44
CAC1078	Predicted phosphohydrolase	3.79
CAC1079	Uncharacterized protein, related to enterotoxins of other clostridia	2.66
CAC1080	Uncharacterized protein, probably surface-located	2.92
CAC1081	Uncharacterized protein, probably surface-located	2.73
CAC1102	Predicted membrane protein	2.57
CAC1312	Hypothetical protein	2.26
CAC1354	Phosphotransferase system IIA component	1.79
CAC1529	Beta-xylosidase, family 43 glycosyl hydrolase	1.69
CAC1532	Protein containing CheW-repeats	3.46
CAC1533	Hypothetical protein	1.86
CAC1669	CstA Carbon starvation protein	2.57
CAC1775	Predicted membrane protein	4.62
CAC1817	Stage V sporulation protein, SpoVS	2.00
CAC1868	Uncharacterized secreted protein, homolog YxkC of *B. subtilis*	1.93
CAC1988	Ferrichrome-binding periplasmic protein	3.00
CAC1989	ABC-type iron (III) transport system, ATPase component	2.77
CAC1990	ABC-type iron (III) transport system, permease component	2.05
CAC1991	Uncharacterized protein	2.85
CAC1992	MoaC molybdenum cofactor biosynthesis protein C	2.46
CAC1994	MoaB Molybdopterin biosynthesis enzyme	1.87
CAC1996	Hypothetical protein	3.06
CAC1997	Predicted glycosyltransferase	3.34
CAC1998	ABC-type transport system, ATPase component	3.20
CAC1999	Hypothetical protein	3.16
CAC2000	Indolepyruvate ferredoxin oxidoreductase	3.28
CAC2002	Predicted iron-sulfur flavoprotein	3.18
CAC2003	Predicted permease	3.39
CAC2004	Siderophore/Surfactin synthetase related protein	1.71
CAC2005	Siderophore/Surfactin synthetase related protein	3.09
CAC2006	Enzyme of siderophore/surfactin biosynthesis	3.28
CAC2007	Predicted glycosyltransferase	3.50
CAC2008	PksF 3-oxoacyl-(acyl-carrier-protein) synthase	3.38

Table 34. (continued)

ID	Protein function[a]	Ratio[b]
CAC2009	MmgB 3-Hydroxyacyl-CoA dehydrogenase	3.74
CAC2010	Predicted Fe-S oxidoreductase	3.53
CAC2011	FabH Possible 3-oxoacyl-[acyl-carrier-protein] synthase III	3.46
CAC2012	FadB Enoyl-CoA hydratase	3.50
CAC2013	Hypothetical protein	3.66
CAC2014	Predicted esterase	3.50
CAC2015	Hypothetical protein	3.54
CAC2016	FadB Enoyl-CoA hydratase	3.80
CAC2017	Acyl carrier protein	3.55
CAC2018	Aldehyde ferredoxin oxidoreductase	3.73
CAC2019	Malonyl CoA-acyl carrier protein transacylase	3.10
CAC2022	MoaB Molybdopterin biosynthesis enzyme	1.92
CAC2023	Membrane protein, related to copy number protein from *C. perfringens* plasmid pIP404	2.51
CAC2024	Phosphatidylglycerophosphate synthase related protein (fragment)	2.64
CAC2025	Hypothetical protein	2.38
CAC2026	Predicted flavodoxin	2.58
CAC2040	ABC transporter, ATPase component	2.20
CAC2071	Spo0A protein, CheY-like receiver domain and HTH-type DNA binding domain	1.90
CAC2182	Hypothetical protein	1.97
CAC2382	Single-strand DNA-binding protein	2.54
CAC2404	Glycosyltransferase	2.54
CAC2405	Predicted glycosyltransferase	2.72
CAC2407	CheY-like receiver domain of response regulator	2.86
CAC2458	ferrodoxin oxidoreductase beta subunit	1.82
CAC2517	NrpE Extracellular neutral metalloprotease	3.56
CAC2518	Extracellular neutral metalloprotease	2.81
CAC2580	Hypothetical protein	3.28
CAC2581	6-Pyruvoyl-tetrahydropterin synthase related domain, conserved membrane protein	3.33
CAC2584	Protein containing CheW-repeats	2.53
CAC2597	Hypothetical protein	2.30
CAC2663	Protein containing cell-wall hydrolase domain	3.71
CAC2688	Alpha/beta superfamily hydrolase (possible chloroperoxidase)	2.03
CAC2695	Diverged Metallo-dependent hydrolase(Zn), peptodoglycan-binding domain	3.05
CAC2716	Predicted glycosyl transferase from UDP-glucuronosyltransferase family	2.79
CAC2807	Endo-1,3(4)-beta-glucanase	3.08
CAC2808	Beta-lactamase class C domain containing protein	3.09
CAC2810	Possible glucoamylase (diverged)	1.82
CAC2938	Hypothetical protein	2.53
CAC2944	N-terminal domain intergin-like repeats and C-terminal-cell wall-associated hydrolase domain	4.60
CAC3060	ATPase	1.99
CAC3063	Transcriptional regulator	2.07

Table 34. (continued)

ID	Protein function[a]	Ratio[b]
CAC3064	UDP-N-acetylglucosamine 2-epimerase	2.19
CAC3065	Possible O-antigen/teichoic acid transporter	2.38
CAC3067	Predicted membrane protein	2.29
CAC3069	Predicted glycosyltransferase	2.39
CAC3070	Glycosyltransferase	2.77
CAC3071	Glycosyltransferase	2.56
CAC3072	Mannose-1-phosphate guanylyltransferase	2.58
CAC3073	Sugar transferase involved in lipopolysaccharide synthesis	2.80
CAC3085	TPR-repeat-containing protein, Cell-adhesion domain	3.64
CAC3086	Protein containing cell adhesion domain	3.33
CAC3165	Hypothetical protein	1.94
CAC3251	Sensory transduction protein	2.92
CAC3298	BdhB NADH-dependent butanol dehydrogenase B	2.49
CAC3355	Polyketide synthase PksE	3.45
CAC3408	NADH oxidase (two distinct flavin oxidoreductase domains)	2.23
CAC3409	Transcriptional regulator	2.10
CAC3412	Predicted protein-S-isoprenylcysteine methyltransferase	2.90
CAC3422	Sugar proton symporter (possible xylulose)	3.47
CAC3558	Probable S-layer protein	3.21
CAC3565	Uncharacterized secreted protein, containing cell adhesion domain	3.29
CAC3581	Hydrolase	2.21
CAC3635	Oligopeptide ABC transporter, ATPase component	1.92
CAC3636	Oligopeptide ABC transporter, ATPase component	2.43
CAC3637	Oligopeptide ABC transporter, permease component	2.37
CAC3638	Oligopeptide ABC transporter, permease component	2.63
CAC3639	DNA-binding protein	1.73
CAC3657	NADP-dependent glyceraldehyde-3-phosphate dehydrogenase	1.73
CAC3694	TPR-repeat-containing protein	1.83

Genes are listed in order of ORFs and considered as significantly up-regulated when the logarithmic ratio was ≥1.60. The given values in the table are mean of results of two hybridizations with dye swaps

[a] Protein name based on Nölling *et al.* (2001)

[b] The expression ratio as the logarithm to the basis of 2

During the steady-state acidogenic growth of the *adhE1* mutant, 159 genes were significantly up-regulated as compared to the wild type (Table 34). Among these, 28 genes encoded membrane-associated proteins (*CA_P0057*, *CA_P0058*, *CA_P0148*, *CA_P0174*, *CA_C0082*, *CA_C0193*, *CA_C0386*, *CA_C0814*, *CA_C1102*, *CA_C1775*, *CA_C1988-CA_C1990*, *CA_C1998*, *CA_C2003*, *CA_C2006*, *CA_C2008-CA_C2009*, *CA_C2011-CA_C2012*, *CA_C2014*, *CA_C2016-CA_C2017*, *CA_C2019*, *CA_C2023*, *CA_C2581*, *CA_C2938* and *CA_C3067*), which suggested that inactivation of *adhE1* affected the characteristics of the cell membrane. In addition, 5 out of 159 genes (*CA_P0149*, *CA_C0029*, *CA_C1081*, *CA_C2810* and *CA_C2938*), were shown to be strongly induced during this growth phase

where they were highly expressed in a wild type chemostat culture (Janssen *et al.*, 2010). Noticeably, the expression of 14 genes involved in carbohydrate metabolism was increased (*CA_P0053*, *CA_P0129*, *CA_C0385*, *CA_C0490*, *CA_C0537*, *CA_C0666*, *CA_C1529*, *CA_C2018*, *CA_C2807*, *CA_C2810*, *CA_C3064*, *CA_C3072*, *CA_C3073*, *CA_C3422*). Moreover, the transcript levels of 8 genes coding for glycosyltransferases were significantly rised (*CA_P0137*, *CA_C1997*, *CA_C2404-CA_C2405*, *CA_C2716* and *CA_C3069-CA_C3071*). Besides, genes for cofactor synthesis showed elevated transcript levels (*CA_C0252*, *CA_C1991-CA_C1994*, *CA_C2022* and *CA_C2581*). Moreover, genes for antibiotic-resistance proteins (*CA_P0086*, *CA_P0133* and *CA_C2808*) and metabolism of amino acids (*CA_P0004*, *CA_C0078*, *CA_C0080*, *CA_C0492*, *CA_C0792*, *CA_C0898*, *CA_C2000*) revealed increased expression. Interestingly, Spo0A-coding gene (*CA_C2071*) was significantly induced by 3.7-fold and this gene had not been reported to suffer from regulation by other genes. Similarly, expression of *bdhB* (*CA_C3298*) was also rised by 5.6-fold, which indicated a negative regulation of *adhE1* to this butanol dehydrogenase-coding gene.

Table 35. Significantly down-regulated genes compared to wild type in the *adhE1* mutant during acidogenic growth

ID	Protein function[a]	Ratio[b]
CA_P0048	Related to methyl-accepting chemotaxis protein	-1.94
CA_P0116	Xylanase, glycosyl hydrolase	-2.28
CA_P0118	Possible xylan degradation enzyme	-2.79
CA_P0120	Possible xylan degradation enzyme	-3.25
CAC0117	Protein CheY homolog	-3.01
CAC0118	CheA Chemotaxis protein	-3.26
CAC0233	PTS system, IIA component	-2.10
CAC0267	Ldh L-lactate dehydrogenase	-2.87
CAC0395	KdgK 2-keto-3-deoxygluconate kinase	-1.78
CAC0495	Thiamine monophosphate syntase	-4.02
CAC0573	Uncharacterized protein	-1.67
CAC0980	PflB Pyruvate-formate lyase	-2.59
CAC0981	PflA Pyruvate-formate-lyase-activating enzyme	-2.96
CAC0983	Hypothetical protein	-1.96
CAC1029	FeoA-like protein, involved in iron transport	-1.81
CAC1031	FeoB FeoB-like GTPase, responsible for iron uptake	-1.70
CAC1175	Hypothetical protein, CF-35 family	-2.61
CAC1176	Hypothetical protein	-1.71
CAC1181	Phage related protein	-2.12
CAC1227	Hypothetical protein	-1.81
CAC1319	GlpF Glycerol uptake facilitator protein	-3.44
CAC1320	GlpP Glycerol-3-phosphate responsive antiterminator (mRNA-binding)	-2.04
CAC1321	GlpK glycerol kinase	-3.31
CAC1322	GlpA Glycerol-3-phosphate dehydrogenase	-1.79
CAC1357	Uncharacterized predicted metal-binding protein	-3.18
CAC1390	PurE phosphoribosylaminoimidazole carboxylase catalytic subunit	-2.30

Table 35. (continued)

ID	Protein function[a]	Ratio[b]
CAC1391	PurC phosphoribosylaminoimidazole-succinocarboxamide synthase	-2.18
CAC1392	PurF amidophosphoribosyltransferase	-1.88
CAC1393	PurM phosphoribosylaminoimidazole synthetase	-2.53
CAC1394	PurN phosphoribosylglycinamide formyltransferase	-2.68
CAC1395	PurH bifunctional phosphoribosylaminoimidazolecarboxamide formyltransferase/cyclohydrolase	-2.77
CAC1846	MotA flagellar motor protein	-2.14
CAC1862	Hypothetical protein	-4.00
CAC1888	Uncharacterized phage related protein	-7.40
CAC1900	Phage regulatory protein, containing Zn-finger	-4.01
CAC1904	Hypothetical protein	-3.72
CAC1909	Ribonuclease	-3.57
CAC1912	Uncharacterized phage related protein	-6.31
CAC1924	Hypothetical protein	-3.65
CAC1930	Uncharacterized protein	-2.45
CAC1933	Hypothetical protein	-4.50
CAC1936	Hypothetical protein	-3.96
CAC1940	Hypothetical protein	-3.78
CAC1941	AbrB Transcription regulator	-4.25
CAC1942	Hypothetical protein	-2.58
CAC1944	Hypothetical protein	-1.89
CAC1947	Phage related transcriptional regulator	-1.65
CAC1949	Possible protein	-4.13
CAC2592	6-Pyruvoyl-tetrahydropterin synthase related domain, conserved membrane protein	-3.76
CAC2649	Hypothetical protein	-1.65
CAC3044	Membrane protein	-1.77
CAC3045	Hydrolase	-3.03
CAC3047	Uncharacterized membrane protein	-2.13
CAC3049	Glycosyltransferase	-3.33
CAC3050	Protein possibly involved in exopolysaccharide biosynthesis	-4.20
CAC3054	Phosphoheptose isomerase	-4.89
CAC3058	Mannose-1-phosphate guanylyltransferase	-5.70
CAC3059	Sugar transferase	-5.70
CAC3461	Hypothetical protein	-2.88
CAC3592	Hypothetical protein	-1.85
CAC3608	ABC-type transport system, ATPase component	-2.06
CAC3642	Oligopeptide ABC transporter, ATPase component	-4.54
CAC3647	AbrB Transition state regulatory protein	-3.31

Genes are listed in order of ORFs and considered as significantly down-regulated when the logarithmic ratio was ≤ -1.60. The given values in the table are mean of results of two hybridizations with dye swaps

[a] Protein name based on Nölling *et al.* (2001)

[b] The expression ratio as the logarithm to the basis of 2

During the steady-state acidogenic growth of the *adhE1* mutant, 63 genes were significantly down-regulated as compared to the wild type (Table 35). Among these, 10 genes encoded membrane-associated proteins, suggesting inactivation of *adhE1* affected the characteristics of the cell membrane in this phase. In addition, three clusters involved in nucleotide biosynthesis (*CA_C1390-CA_C1395*) and carbohydrate metabolism (part of *CA_C3049-CA_C3059*, and *CA_P0116-CA_P0118*, *CA_P0120*), respectively, displayed strongly repression. Besides, expression of genes related to phage protein (*CA_C1181*, *CA_C1888*, *CA_C1900*, *CA_C1912* and *CA_C1947*) was noticeably decreased. Remarkably, the transcript levels of two genes (*CA_C1941* and *CA_C3647*) responsible for transition state were dropped to 10%. Moreover, three genes (*CA_C0267*, *CA_C0980* and *CA_C0981*) related to pyruvate metabolism were expressed in lower abundance.

Table 36. Significantly up-regulated genes compared to wild type in the *adhE1* mutant during solventogenic growth

ID	Protein function[a]	Ratio[b]
CA_P0004	Cysteine protease	1.80
CA_P0035	AdhE2 Aldehyde-alcohol dehydrogenase	3.20
CA_P0044	Hypothetical protein	2.05
CA_P0045	Glycosyl transferase	2.25
CA_P0098	Alpha-amylase	2.92
CA_P0143	Hydrogenase maturation protease delta subunit	1.91
CA_P0144	Possible steroid binding protein	1.90
CA_P0145	Hypothetical protein	1.75
CA_P0168	Alpha-amylase	2.52
CAC0102	O-acetylhomoserine sulfhydrylase	5.72
CAC0103	CysC Adenylylsulfate kinase	5.79
CAC0104	Adenylylsulfate reductase	5.86
CAC0105	Ferredoxin	5.63
CAC0106	ABC-type probable sulfate transporter, periplasmic binding protein	4.63
CAC0107	ABC-type sulfate transporter, ATPase component	5.68
CAC0108	ABC-type probable sulfate transporter, permease protein	5.19
CAC0109	CysD sulfate adenylyltransferase subunit 2	6.07
CAC0110	CysN GTPase, sulfate adenylate transferase subunit 1	5.21
CAC0111	Glutamine-binding periplasmic protein fused to glutamine permease	1.97
CAC0112	GlnQ glutamine ABC transporter (ATP-binding protein)	1.87
CAC0149	Hypothetical protein	1.87
CAC0155	Putative regulator of the PTS system for mannitol	2.40
CAC0156	PTS system, mannitol-specific IIA domain	2.23
CAC0233	PTS system, IIA component	2.62
CAC0253	NifH Nitrogenase iron protein (nitrogenase component II)	5.80
CAC0254	NifHD Nitrogen regulatory protein PII	6.34
CAC0255	NifHD Nitrogen regulatory protein PII	6.20
CAC0256	NifD Nitrogenase molybdenum-iron protein, alpha chain	6.33
CAC0257	NifK Nitrogenase molibdenum-iron protein, beta chain	4.81
CAC0258	NifE Nitrogenase iron-molibdenum cofactor biosinthesis protein	5.85

Table 36. (continued)

ID	Protein function[a]	Ratio[b]
CAC0259	Fusion NifN/K+NifB (NifN-nitrogenase iron molybdenum cofactor biosinthesis protein, NifK-nitrogenase molibdenum-iron protein beta chain)	6.29
CAC0260	NifV Homocitrate syntase, omega subunit	5.97
CAC0261	NifV Homocitrate synthase,alpha subunit	4.78
CAC0263	Phosphoserine phosphatase related protein	2.24
CAC0280	Molybdate transport system, permease component	2.86
CAC0281	Molybdate-binding periplasmic protein	3.21
CAC0282	Cytosine/guanine deaminase related protein	3.93
CAC0365	Phosphoglycerate dehydrogenase	2.26
CAC0366	Predicted permease	2.71
CAC0367	Arginine degradation protein	3.30
CAC0376	N-dimethylarginine dimethylaminohydrolase (similar to YkgA of *B.subtilis*)	1.64
CAC0378	Glutamine ABC transporter, ATP-binding protein	3.67
CAC0383	PTS cellobiose-specific component IIA	2.58
CAC0384	PTS system, cellobiose-specific component BII	3.43
CAC0385	Beta-glucosidase	3.28
CAC0386	PTS cellobiose-specific component IIC	2.83
CAC0387	Hypothetical protein	2.88
CAC0580	Hypothetical protein	2.15
CAC0608	Diaminopimelate decarboxilase	2.12
CAC0620	ABC transporter, periplasmic-binding	1.94
CAC0625	Possible periplasmic aspartyl protease	3.44
CAC0681	Nitrogen regulatory protein PII	1.82
CAC0682	Ammonium transporter (membrane protein)	3.95
CAC0750	Hypothetical protein	2.19
CAC0882	Predicted membrane protein, hemolysin III homolog	2.08
CAC0887	Adenine deaminase	1.91
CAC0893	Prephenate dehydrogenase	1.91
CAC0930	MetB Cystathionine gamma-synthase	2.40
CAC0931	Cysteine synthase	1.99
CAC0984	ABC transporter, ATP-binding protein	2.18
CAC0985	ABC transporter, permease component	2.42
CAC1267	D-alanyl-D-alanine carboxypeptidase	1.93
CAC1336	Hypothetical protein	3.82
CAC1337	Spore coat protein	3.47
CAC1338	Spore coat protein	2.79
CAC1348	Transketolase	1.90
CAC1363	Superoxide dismutase, Cu-Zn family	2.58
CAC1406	Transcriptional antiterminator	2.71
CAC1427	4-aminobutyrate aminotransferase	2.20
CAC1664	Glycogen phosphorylase	1.79
CAC1689	SigK sporulation sigma factor	2.27
CAC1695	SigE sporulation sigma factor	2.83
CAC1866	Putative 4-Cys ferredoxin	2.32

Table 36. (continued)

ID	Protein function[a]	Ratio[b]
CAC2020	MoeA Molybdopterin biosynthesis enzyme, fused to molibdopterin-binding domain	1.77
CAC2251	Uncharacterized conserved membrane protein	4.72
CAC2252	Alpha-glucosidase fused to unknown alpha-amylase C-terminal. domain	2.70
CAC2342	Predicted membrane protein	2.53
CAC2343	O-acetyl transferase	2.04
CAC2344	LPS biosynthesis protein	2.30
CAC2345	Glycosyltransferase	2.09
CAC2346	Glycosyltransferase	2.33
CAC2348	Glycosyltransferase	2.26
CAC2349	Hypothetical protein	3.10
CAC2350	Sugar transaminase, involved in dTDP-4-amino-4,6-dideoxyglucose biosynthesis	3.05
CAC2352	Hypothetical protein	2.16
CAC2383	Predicted xylanase/chitin deacetylase	1.98
CAC2459	2-Oxoacid ferredoxin oxidoreductase, alpha subunit	2.09
CAC2542	FAD/FMN-containing dehydrogenase	2.58
CAC2543	EtfA Electron-transferring flavoprotein large subunit	2.67
CAC2544	EtfB Electron-transferring flavoprotein small subunit	2.55
CAC2545	Hypothetical protein	2.02
CAC2611	Hypothetical protein	3.33
CAC2612	XylB Xylulose kinase	2.30
CAC2621	Cell wall hydrolase (autolysin), glycosyl hydrolase, peptodoglycan-binding domain	4.35
CAC2658	GlnA Glutamine synthetase type III	2.12
CAC2720	Sensory protein containing histidine kinase	3.57
CAC2721	Response regulator (CheY-like reciever domain and HTH-type DNA-binding domain)	3.88
CAC2728	Hypothetical protein	2.14
CAC2744	Predicted membrane protein	2.02
CAC2747	Protein containing LysM repeats and domain related to chitinase	2.15
CAC2776	Hypothetical protein	3.83
CAC2783	CysD O-acetylhomoserine sulfhydrylase	2.01
CAC2809	Predicted HD superfamily hydrolase	2.49
CAC2847	Ribosome-associated protein	1.85
CAC2862	UDP-N-acetylglucosamine 1-carboxyvinyltransferase	2.68
CAC2863	Predicted membrane protein	2.59
CAC2903	LysM domain containing membrane protein	1.72
CAC2905	Uncharacterized protein	2.22
CAC2906	Spore coat protein CotS related	2.16
CAC3008	Preicted protein	2.22
CAC3019	Sensory transduction protein	1.84
CAC3092	Amidase, germination specific	2.61
CAC3093	Phosphate permease	2.47

Table 36. (continued)

ID	Protein function[a]	Ratio[b]
CAC3265	Predicted membrane protein	1.91
CAC3266	Hypothetical protein	1.92
CAC3267	Specialized sigma subunit of RNA polymerase	2.15
CAC3285	Predicted amino acid transporter	2.21
CAC3325	Periplasmic amino acid binding protein	1.80
CAC3326	Amino acid ABC-type transporter, permease component	1.75
CAC3378	AldO/KetO reductase family enzyme	1.94
CAC3395	Predicted membrane protein	1.90
CAC3629	Oligopeptide ABC transporter, ATPase component	1.76
CAC3632	Oligopeptide ABC transporter, periplasmic substrate-binding component	1.95
CAC3660	Uncharacterized protein	1.87
CAC3661	Glycosyltransferase	4.38
CAC3662	Membrane associated sensory histidine kinase	3.09
CAC3663	Response regulator (CheY-like receiver domain and HTH-type DNA-binding domain)	3.31

Genes are listed in order of ORFs and considered as significantly up-regulated when the logarithmic ratio was ≥1.60. The given values in the table are mean of results of two hybridizations with dye swaps

[a] Protein name based on Nölling *et al.* (2001)

[b] The expression ratio as the logarithm to the basis of 2

During the steady-state solventogenic growth of the *adhE1* mutant, 127 genes were significantly up-regulated as compared to the wild type (Table 36). Among these, 14 genes encoded membrane-associated proteins (*CA_C0111*, *CA_C0112*, *CA_C0383*, *CA_C0384*, *CA_C0386*, *CA_C882*, *CA_C2251*, *CA_C2342*, *CA_C2744*, *CA_C2863*, *CA_C3093*, *CA_C3265*, *CA_C3395* and *CA_C3662*), which suggested inactivation of *adhE1* affected the characteristics of the cell membrane during solventogenesis. In addition, 7 genes (*CA_P0004*, *CA_P0044-CA_P0045*, *CA_P0168*, *CA_C254-CA_C0256*) were shown to be strongly induced in this growth phase as compared to wild type where they were highly expressed (Janssen *et al.*, 2010). Remarkably, a gene cluster (*CA_C0102-CA_C0110*) and genes (*CA_C0263*, *CA_C0930-CA_C0931* and *CA_C2783*) responsible for biosynthesis of cysteine and methionine showed elevated expression levels, indicating these pathways were negatively influenced by *adhE1*. Besides, the transcript levels of genes for nitrogen fixation were up-regulated (*CA_C0253-CA_C0261*). Interestingly, genes involved in sporulation (*CA_C1337-CA_C1338*, *CA_C1689*, *CA_C1695* and *CA_C2906*) expressed at least 3.5-fold higher than the wild type level during solventogenesis where spores had been already washed out. Last but not the least, *adhE2* (*CA_P0035*) encoding a bifunctional aldehyde/alcohol dehydrogenase was transcribed 9-fold higher, indicating *adhE1* inhibited the expression of *adhE2* during solventogenesis and the antagonistic expression patterns between *adhE1* and *adhE2* were caused by the negative regulation of *adhE1* to *adhE2*.

Table 37. Significantly down-regulated genes compared to wild type in the *adhE1* mutant during solventogenic growth

ID	Protein function[a]	Ratio[b]
CA_P0148	Phospholipase C	-4.54
CA_P0162	AdhE1 Aldehyde dehydrogenase (NAD^+)	-3.83
CA_P0163	Ctfa Butyrate-acetoacetate CoA-transferase subunit A	-4.16
CA_P0164	Ctfb Butyrate-acetoacetate CoA-transferase subunit B	-4.19
CAC0029	Distantly related to cell wall-associated hydrolase, similar to YycO of *B. subtilis*	-2.43
CAC0030	Hypothetical protein	-2.70
CAC0056	Hypothetical protein	-4.39
CAC0057	Hypothetical protein	-4.33
CAC0058	Hypothetical protein	-4.13
CAC0059	Hypothetical protein	-4.18
CAC0060	Predicted membrane protein	-2.72
CAC0061	Phage-related protein	-4.23
CAC0062	Hypothetical protein	-4.28
CAC0063	Hypothetical protein	-4.10
CAC0064	Hypothetical protein	-4.11
CAC0065	Hypothetical protein	-4.16
CAC0205	Predicted phosphohydrolase	-7.08
CAC0206	Hypothetical protein	-4.41
CAC0208	Predicted membrane protein	-1.88
CAC0316	ArgF/I Ornithine carbomoyltransferase	-2.11
CAC0353	2,3-Cyclic-nucleotide 2'phosphodiesterase	-4.81
CAC0380	Periplasmic amino acid-binding protein	-2.17
CAC0428	Sugar permease	-8.91
CAC0429	Glicerol-3-phosphate ABC-transporter, periplasmic component	-7.98
CAC0439	Hypothetical protein	-2.37
CAC0458	Permease	-2.38
CAC0495	Thiamine monophosphate syntase	-2.47
CAC0496	Uncharacterized conserved protein	-2.92
CAC0522	Predicted hydrolase	-1.88
CAC0542	Methyl-accepting chemotaxis protein	-2.00
CAC0549	Predicted transcriptional regulator	-1.79
CAC0552	Protein containing cell-adhesion domain	-4.66
CAC0554	Autolytic lysozime (1,4-beta-N-acetylmuramidase), glycosyl hydrolase , peptodoglycan-binding domain	-5.07
CAC0742	Uncharacterized protein, containing predicted phosphatase domain	-6.16
CAC0843	Ribonuclease precursor (barnase)	-4.08
CAC0844	Barstar-like protein ribonuclease (barnase) inhibitor	-4.12
CAC0935	HisZ ATP phosphoribosyltransferase regulatory subunit	-2.47
CAC0936	HisG ATP phosphoribosyltransferase	-2.17
CAC0938	HisB Imidazoleglycerol-phosphate dehydratase	-1.93
CAC0939	HisH Glutamine amidotransferase	-2.09
CAC0940	HisA Phosphoribosylformimino-5-aminoimidazole carboxamide ribonucleotide (ProFAR) isomerase	-1.89

Table 37. (continued)

ID	Protein function[a]	Ratio[b]
CAC0942	Phosphoribosyl-AMP cyclohydrolase	-2.18
CAC0943	Phosphoribosyl-ATP pyrophosphohydrolase	-2.20
CAC0946	ComE-like protein, Metallo beta-lactamase superfamily hydrolase	-4.62
CAC0974	ArgH Argininosuccinate lyase	-2.47
CAC0975	Predicted P-loop kinase or ATPase distantly related to phosphoenolpyruvate carboxykinase	-2.43
CAC1322	GlpA Glycerol-3-phosphate dehydrogenase	-4.15
CAC1323	NAD (FAD)-dependent dehydrogenase	-2.59
CAC1482	Uncharacterized membrane protein	-2.17
CAC1529	Beta-xylosidase, glycosyl hydrolase	-3.36
CAC1542	Predicted membrane protein	-1.92
CAC1702	Hypothetical protein	-5.97
CAC1703	Methyl-accepting chemotaxis protein (fragment)	-6.29
CAC1704	Hypothetical protein	-6.53
CAC1705	Periplasmic phosphate-binding protein	-5.63
CAC1706	Phosphate permease	-5.25
CAC1707	Permease component of ATP-dependent phosphate uptake system	-4.96
CAC1709	PhoU Phosphate uptake regulator	-4.99
CAC2366	Predicted membrane protein	-1.77
CAC2367	Uncharacterized protein containing predicted cell adhesion domain	-1.86
CAC2388	ArgD N-acetylornithine aminotransferase	-2.33
CAC2438	Predicted phosphatase	-5.86
CAC2743	Predicted permease	-6.72
CAC2938	Hypothetical protein	-3.44
CAC3017	Predicted xylanase/chitin deacetylase	-1.91
CAC3018	Rubrerythrin	-2.24
CAC3235	Uncharacterized conserved protein	-1.91
CAC3236	Possible transcriptional regulator	-4.44
CAC3237	MsmX Multiple sugar-binding ABC-transporter, ATP-binding protein	-4.33
CAC3343	Biotin synthase related domain containing protein	-1.75
CAC3379	Uncharacterized protein	-5.80
CAC3617	Uncharacterized membrane protein	-1.81
CAC3686	Metallo-beta-lactamase superfamily hydrolase	-3.84

Genes are listed in order of ORFs and considered as significantly down-regulated when the logarithmic ratio was ≤ -1.60. The given values in the table are mean of results of two hybridizations with dye swaps

[a] Protein name based on Nölling *et al.* (2001)

[b] The expression ratio as the logarithm to the basis of 2

During the steady-state solventogenic growth of the *adhE1* mutant, 73 genes were significantly down-regulated as compared to wild type (Table 37). Among these, 15 genes encoded membrane-associated proteins (*CA_P0148*, *CA_C0206*, *CA_C0208*, *CA_C0428*, *CA_C0429*, *CA_C1322*, *CA_C1323*, *CA_C1482*, *CA_C1542*, *CA_C2366*, *CA_C2438*, *CA_C2743*, *CA_C2938*, *CA_C3237*, *CA_C3617*), which suggested inactivation of *adhE1*

affected the characteristics of the cell membrane during solventogenesis. In addition, genes for biosynthesis of amino acids (*CA_C0935*-*CA_C0936*, *CA_C0938*-*CA_C0940*, *CA_C0942*-*CA_C0943* and *CA_C0316*, *CA_C0974*, *CA_C2388*) were transcribed at least 73% lower than the wild type levels. Interestingly, the expression of the *pst* operon (*CA_C1705*-*CA_C1709*, *CA_C1708* did not pass the filter criterion, section 2.6.10) for phosphate transport was strongly decreased. Moreover, genes related to chemotaxis (*CA_C0542* and *CA_C1703*) or resistance (*CA_C0946* and *CA_C3686*) were also significantly down-regulated. Noticeably, a putative operon (*CA_C0056*-*CA_C0065*) displayed repressed transcript levels and 9 out of 10 genes in this cluster encoded hypothetical proteins.

To sum up, inactivation of *adhE1* led to 222 and 200 genes significantly regulated during acidogenesis and solventogenesis, respectively. This suggested that *adhE1*, as an alcohol dehydrogenase gene, influenced the expression of a host of genes not only during solventogenic growth where ethanol and butanol were produced, but also during acidogenesis where acetic acid and butyric acid were main products, although the production of acids was not significantly affected at pH 5.7 (Fig. 29).

3.3.5 Continuous fermentation of the *CA_P0059* mutant

CA_P0059 is located on pSOL1 megaplasmid and annotated as the gene for a putative alcohol dehydrogenase (Nölling *et al.*, 2001). It was proposed that this gene was a promising candidate for elucidation of gene regulatory networks concerning solventogenesis because inactivation of this gene, unexpectedly, resulted in enhanced production of acetone, butanol and ethanol under batch conditions (Cooksley *et al.*, 2012). In addition, it was reported that the transcript level of *CA_P0059* was not significantly changed during the fermentation course of the wild type (Grimmler *et al.*, 2011). Consequently, it was necessary to characterize the *CA_P0059* mutant (from Prof. Nigel P. Minton, University of Nottingham; Cooksley *et al.*, 2012) using continuous fermentation to provide a new insight into roles of this gene.

Continuous fermentation was carried out to characterize the *CA_P0059* mutant strain (Fig. 30) and correct insertion of the intron in the *CA_P0059* gene was monitored by PCR using *CA_P0059* gene-specific primers (*p0059*-Forward and -Reverse primers, Table 39, Appendix section) which flanked the intron insertion site. Methods for chemostat cultures of *C. acetobutylicum* were described in detail previously (section 2.6). During acidogenic growth of the continuous culture of the *CA_P0059* mutant, the OD_{600} was ~3.5 which was lower than that of the wild type culture and comparable to the *adhE1* and pSOL1-free (*CA_P0175*) mutant strains. After ~14 h of the pH shift, the culture of the *CA_P0059* mutant entered solventogenesis, and the final OD_{600} of the mutant during the steady-state was ~3.1, which was lower than the wild type and higher than that of the *adhE1* and pSOL1-free (*CA_P0175*) mutant strains. In terms of glucose consumption, the *CA_P0059* mutant utilized more glucose during acidogenesis than during solventogenesis, which was similar to the wild type strain. However, the *CA_P0059* mutant consumed less glucose than the wild type during both acidogenesis and solventogenesis, which led to a slightly decreased (~16.7-20%) production of acetate and buryrate during acidogenesis, and decreased (~40%) concentrations of acetone and butanol during solventogenesis, respectively. During acidogenesis, production of acetone and butanol was reduced by at least 50% although these were not predominant metabolites during this phase. Besides, more butyrate (~30.8%) was accumulated during solventogenic growth, whereas acetic acid formed (~10 mM) was comparable to the wild

type. Moreover, ethanol formation was also disturbed during acidogenic and solventogenic growth of the *CA_P0059* mutant. These results indicated that *CA_P0059* was positively related to the generation of all three solvents during solventogenesis, which was opposite to that observed under batch culture conditions (Cooksley *et al.*, 2012). This suggested that fermentation ways affected fermentation profiles of this mutant. In addition, the results indicated that the mutation of *CA_P0059* influenced butyrate metabolism during solventogenic growth.

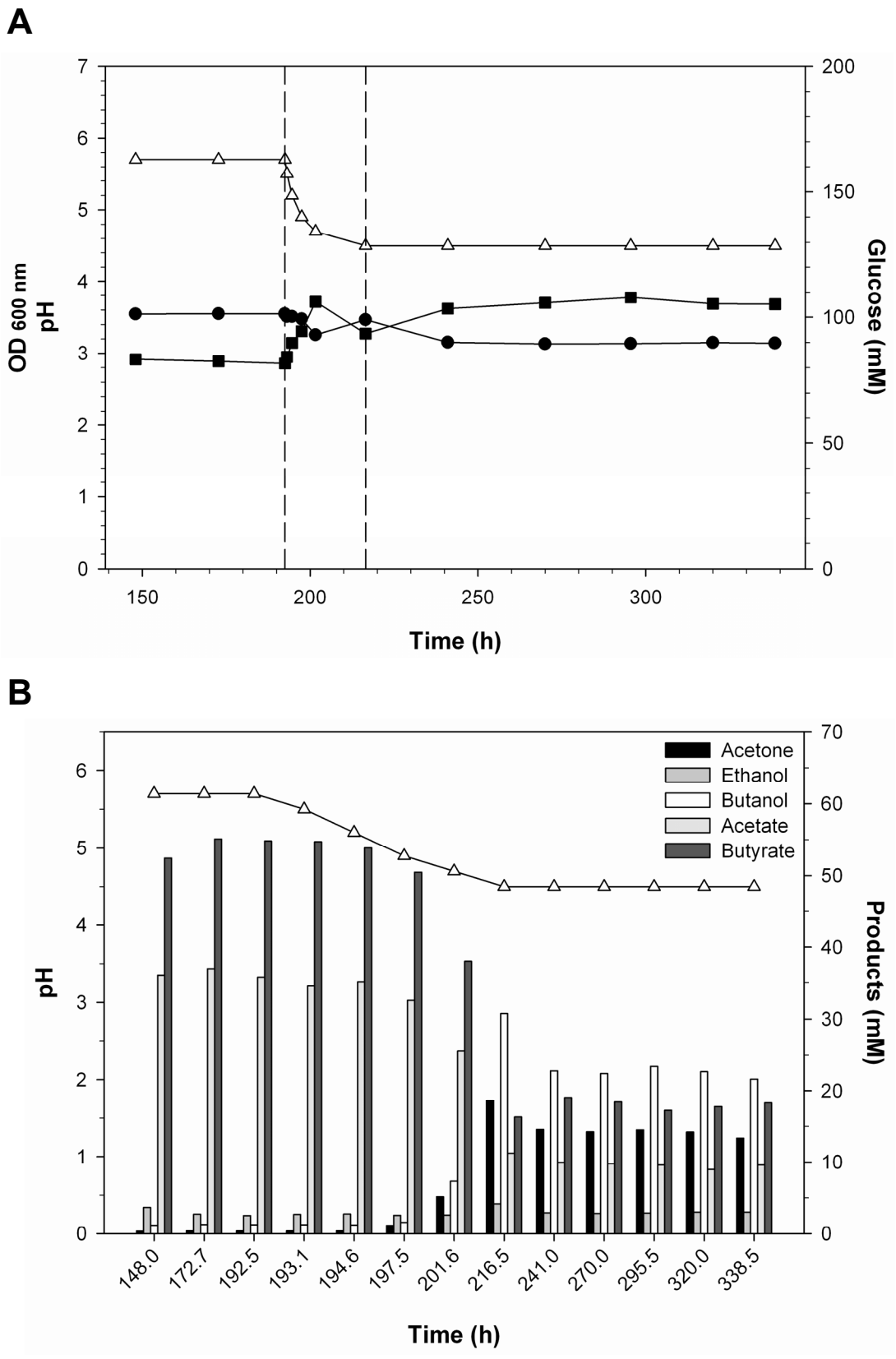

Fig. 30. Fermentation profile of the phosphate-limited continuous culture of the *CA_P0059* mutant. (A) Growth, glucose consumption and pH in the course of fermentation. Dashed lines indicate the dynamic pH shift. (B) Fermentation products from the steady-state acidogenesis to solventogenesis. Each grouped bar set corresponds to each time-point. Quantification of metabolites was done with an internal standard of known concentration (section 2.11.2). Symbols: *triangles*, pH; *circles*, OD at 600 nm; *squares*, residual glucose concentration

4 Discussion

4.1 Continuous fermentation

4.1.1 Advantages of continuous fermentation

Research on *C. acetobutylicum* has recently regained interest due to its biofuel production potential. Characterization of *C. acetobutylicum* strains was accomplished by two methods: batch fermentation or continuous fermentation, and utilization of different fermentation methods might result in observation of different phenotypes (Janssen *et al.*, 2010; Grimmler *et al.*, 2011; Cooksley *et al.*, 2012; Jang *et al.*, 2012; Lehmann *et al.*, 2012a, 2012b; Kuit *et al.*, 2012; Vasileva *et al.*, 2012). Batch fermentation is a traditional method for studies of microorganisms because it is close to natural conditions of growth. In batch cultures, however, the cultivation environment keeps changing, including changes of the concentrations of nutrients, pH, and the energy source, etc.. As a result, the cell status of the batch culture also continues to change during the whole growth. Furthermore, acid crash (Maddox *et al.*, 2000; Schuster *et al.*, 2001) frequently happens in batch cultures of *C. acetobutylicum*, which results in unsuccessful transition from acidogenesis to solventogenesis and therefore the events in the later growth phase (i.e. acid re-assimilation, solvent production, pH increase and sporulation) can not be observed.

To get an insight into the physiological function of a certain gene, a steady cell status is the prerequisite, because under this condition the gene-expression profile and the metabolic events are constant (Bahl *et al.*, 1986). Accordingly, continuous fermentation was the optimal choice to fulfill this requirement. In continuous cultures, fresh nutrients are continuously supplied and cell behavior is uniform in the steady-state. For *C. acetobutylicum*, two different physiological growth phases could be separated simply by adjusting the external pH. At pH 5.7, cells were acidogenic with acetic acid and butyric acid formed as the predominant products. Solvents acetone, butanol and ethanol were only very slightly produced during this phase. After the steady-state acidogenic growth, pH regulation was set to 4.5 and the pH of the culture decreased due to the production of acids by the culture. Subsequently, the culture entered solventogenic growth at pH 4.5 where the solvents acetone, butanol and ethanol were the main products, while the acids acetate and butyrate remained detectable. Afterwards, the culture reached the steady-state solventogenic growth. Consequently, the continuous culture is an effective methodology to get steady-state samples of both acidogenic and solventogenic growth for elucidation of the effects caused by a gene mutation on the physiology and the transcriptome.

Two examples from this study make the disadvantages of batch fermentation in terms of metabolic events during solventogenesis, precisely, from transition phase to solventogenesis clearer: a pSOL1-free strain (the *repA* (*CA_P0175*) mutant) and the *GbRs* (*CA_P0129*) mutant. For these two mutants, the batch cultures seemed to be inactive after the end of acidogenesis. This meant that, as compared to the wild type, the OD_{600} of these two mutant cultures started to decline immediately, acids were accumulated increasingly and the pH did not rise from the lowest value. In contrast, these two mutants revealed different growth and metabolite production during growth at low pH (pH 4.5) in chemostat cultures (Fig. 23 and Fig. 28). The above mentioned findings suggested that the batch culture possessed certain factors which disturbed transition from acidogenesis to growth at low pH and that continuous

fermentation was a reliable way to characterize *C. acetobutylicum* strains during both conditions.

Acid crash has been proposed to be the reason for the unsuccessful transition, which was attributed to vigorous growth, high metabolic efficiency and fast accumulation of acids during exponential growth (Maddox *et al.*, 2000; Schuster *et al.*, 2001). However, other aspects might also lead to transition failure, e.g. an uncontrolled pH, and the instability of the cell status during the course of batch fermentation, which were well handled in chemostat cultures. The importance of pH was further supported by research results concerning a *ptb* mutant (Lehmann *et al.*, 2012b). A *C. acetobutylicum ptb* mutant strain produced approximately 6 mM ethanol and 50 mM butanol under pH-uncontrolled batch conditions while ~270 mM ethanol and ~110 mM butanol were generated by this mutant when cultivating in a pH-regulated (≥5.0) batch culture. Nevertheless, formation of ethanol and butanol by *C. acetobutylicum* wild type was comparable under both conditions.

4.1.2 Continuous fermentation of the wild type strain of *C. acetobutylicum*

In this study, a continuous culture of *C. acetobutylicum* wild type strain was carried out first to understand its fermentation profiles under experimental conditions in our laboratory (section 2.6). The whole fermentation process was separated into two growth phases, acidogenic growth and solventogenic growth. This was achieved by adjusting the pH of the culture (pH 5.7 for acidogenesis and pH 4.5 for solventogenesis) using external KOH solution (2 M). During the steady-state acidogenic growth, concentrations of predominant products acetate and butyrate were ~45 mM and ~60 mM, respectively. In addition, small amounts of solvents acetone (~0.8 mM), butanol (~4.6 mM) and ethanol (~4 mM) were also produced by acidogenic cells. Slight production of solvents during acidogenic growth could be explained by the hot channel theory which suggested butanol was synthesized directly through the C_4 route instead of butyrate uptake (cold channel) (Jang *et al.*, 2012). On the other hand, acetone and butanol were the main metabolites during the steady-state solventogenic growth and their concentrations were ~24 mM and ~39 mM, respectively. About 3.8 mM of ethanol was also formed. Moreover, acetic acid (~11 mM) and butyric acid (~13 mM) were detected during this phase (Fig. 4).

Recently, there were two reports concerning continuous cultures of *C. acetobutylicum* wild type (Janssen *et al.*, 2010; Grimmler *et al.*, 2011). Generally, results obtained in this study were similar to those described in the above mentioned two publications, e.g., the slight production of solvents during acidogenesis and the concentration of butanol and butyrate during solventogenesis.

C. acetobutylicum re-assimilated acids from the transition from acidogenesis to stationary phase under batch culture conditions (Jones and Woods, 1986). A obvious decrease of the concentration of butyrate which was produced during exponential growth could be detected in batch cultures. In continuous cultures, however, it was not applicable to observe this decline trend of butyrate concentration. Because fresh media were continuously supplemented to the fermenter, accompanied by washing out of the culture to keep the culture volume constant (section 2.6). And concentrations of metabolites were real-time. As a result, it was not possible to determine whether butyrate uptake was present during solventogenesis of a continuous culture of a *C. acetobutylicum* strain. A further study, e.g., a ^{13}C-labelled butyrate feeding experiment, would facilitate to elucidate this unknown phenomenon (Dr. A.

Ehrenreich, personal communication). In this study, ~13 mM butyric acid was detected during the steady-state solventogenic growth of the wild type chemostat culture. It was speculated that either the wild type only generated this amount of butyrate during growth at pH 4.5, or ~13 mM was the residual butyrate concentration and a certain amount of butyrate had been utilized.

In terms of the re-assimilation of acetic acid, it could also not be determined whether it was present or not in a continuous culture of *C. acetobutylicum*. Therefore, according to what was discussed in the last paragraph, either the wild type strain only produced ~11 mM acetate during solventogenesis of a chemostat culture, or this value was for the residual acetate amount.

4.2 Use of DNA Microarrays

Among numerous studies on *C. acetobutylicum*, different experimental methods were employed. Due to limited information about the regulatory mechanisms of physiological events of this species, large scale gene expression studies were necessary to reveal the metabolic networks. DNA microarrays and 2D gel electrophoresis were two options for this purpose (Janssen *et al.*, 2010; Mao *et al.*, 2010, 2011; Grimmer *et al.*, 2011). Compared to the 2D gel electrophoresis where some protein spots could not be detected due to the intrinsic properties of the technology, our microarray technology platform showed an obvious advantage in employing oligonucleotide fragments for nearly all the open reading frames (ORFs) of the genome (99.8%) as probes. As a result, transcriptional profiles altered by a mutated gene were available, and the research of the effects of a certain gene mutation on the metabolism became feasible and convenient. Microarray results provided important information for the understanding of the regulatory networks of the metabolism of *C. acetobutylicum* (Hillmann *et al.*, 2009; Vasileva *et al.*, 2012).

4.3 Mutagenesis using the ClosTron technology

Using the ClosTron technology (Heap *et al.*, 2007, 2010a, 2010b), a set of 8 mutants had been generated in the present study, which demonstrated that this system was very valuable for disrupting genes of interest in *C. acetobutylicum*. All the mutants had been verified by PCR using two primer pairs flanking the intron insertion site and an exon-intron junction site, respectively (Heap *et al.*, 2007). Afterwards, Southern hybridization was employed, as proposed, for detection of the number of introns inserted in the chromosome (Cooksley *et al.*, 2012). Physiological changes of the mutants were then characterized by continuous cultures (section 2.6). From the whole fermentation processes of the chemostat cultures, it was clear that the gene mutation caused by the ClosTron intron insertion was stable. Because a continuous culture lasted at least 10 days to about 14 days, and the correct insertion of the intron was confirmed by PCR during the whole fermentation using primers flanking the intron insertion site of the mutated gene (Table 39, Appendix section).

However, two sets of attempts had been carried out to knock out the *fcd* (*CA_C2542*) gene of the *etfB-etfA-fcd* cluster, which resulted in a double mutant in the first try and a correct single mutant in the second (section 3.2.1, 3.2.5). The only difference between these two attempts was the shuttle vector used for retargeting the target gene *fcd*. In the first try, the 1st

generation of the ClosTron plasmid, pMTL007, was used and a subsequent induction step was required for the expression of the IPTG-induced *fac* promoter on this plasmid, which afterwards initiated the intron retro-homing (replication an insertion). This led to a double mutation with two insertion sites of the intron. One was in the target *fcd* gene and the other in *htpG* gene (section 3.2.6.1). The latter gene (*htpG*) was figured out by a DNA ligase-mediated PCR (section 2.7.2.3). A DNA fragment of known sequence was used as an adaptor which was ligated with *Eco*RV-digested genomic DNA fragments, and a PCR was subsequently performed using a primer pair for the junction of the DNA adaptor and the DNA fragment containing the intron (section 3.2.6.1; Table 40, Appendix section). It was reported that 4 double mutation examples out of approximately 150 mutants of different *Clostridium* species had been obtained using the ClosTron technology (Cooksley *et al.*, 2012). One possible explanation for this low frequency event in the present study was that in the 1st generation ClosTron system, the IPTG induction might be too strong to control the insertion fidelity. This was further supported by the correct single *fcd* mutant obtained in the second try, where 2nd generation ClosTron plasmid, pMTL007C-E2, was used (Table 7, section 2.4). The IPTG induction step was no longer needed for this system because a constitutive promoter (*fdx*) from a ferredoxin gene was employed for initiation of the intron expression. The intron, however, indeed inserted into *htpG* gene in the first try. One reason for this was that the *L. lactis* Ll.LtrB Group II intron could "retrotranspose" to other positions similar to the expected home at rates of 10^{-4} to 10^{-6} (Lambowitz and Zimmerly, 2011). Another explanation might be that the intron insertion site in a target gene was determined by an algorithm based on informatics, statistics and structural analysis (Dong *et al.*, 2010). And the intron insertion site was searched only within the target gene sequence instead of the whole genome in which another similar intron insertion site might exist, making an erroneous insertion of the intron into the second site (gene) possible (section 2.7.3.1).

HydA (hydrogenase) is responsible for the production of molecular hydrogen and ThlA (thiolase) converts acetyl-CoA to acetoacetyl-CoA, the first step in the C_4 pathways (Fig. 2). It had been proposed that the inactivation of *hydA* and *thlA* are lethal (Cooksley *et al.*, 2012). A similar phenomenon was also found during the mutagenesis of *bcd* (*CA_C2711* for a EtfA/B-dependent butyryl-CoA dehydrogenase, Bcd) in this study, although I had picked over 500 positive (erythromycin-resistant) clones with 3 different ClosTron retargeting plasmids (for different insertion sites of the intron) and verified these clones by PCR using primers flanking the predicted intron insertion sites (Table 39, Appendix section; section 2.9.3, 2.9.4). The butyrate/butanol metabolic pathway had been demonstrated not to be essential in the *hbd* (*CA_C2708* for a β-hydroxybutyryl-CoA dehydrogenase, Fig. 2) mutant, where the activity of thiolase and crotonase (Crt) was significantly reduced (~98.4% and ~99.7%, respectively) (Lehmann and Lütke-Eversloh, 2011). *crt*, *bcd*, *etfA, etfB* and *hbd* were part of the *bcs* operon (*CA_C2712-CA_C2708*; Boynton *et al.*, 1996), thus it was conceivable that Bcd activity might also be deleted by the knock-out of the *hbd* gene. 8 mutants were generated in this work, which indicated that the technology to construct the mutants could be carried out successfully. Based on the arguments above, a mutation of *bcd* gene was theoretically feasible. A possible explanation for the failure to construct such a mutant was that Bcd-EtfA/B complex might be involved in a certain redox reaction that affected viability, e.g., H_2 formation by hydrogenase (HydA) where excess reducing power was required to be converted into H_2 gas to maintain a redox balance in the cell (Cooksley *et al.*, 2012). In *Clostridium kluyveri*, a coupled ferredoxin and crotonyl-CoA reduction with NADH was proposed to be catalyzed by the Bcd/Etf complex (Li *et al.*, 2008). Reduced ferredoxin (Fd_{red}^{2-}) provided 2 electrons to 2 H^+ in the hydrogenase-catalyzing reaction to generate molecular hydrogen (Jones and Woods, 1986).

4.4 The physiological effects of the mutated genes

4.4.1 Physiological effects of the *etfB-etfA-fcd* cluster

The central metabolism of *C. acetobutylicum* consists of several steps from pyruvate to butyryl-CoA (Fig. 2). Many efforts had been conducted to elucidate the function of individual genes for each reaction in this C_4 route (Jiang *et al.*, 2009; Lehmann and Lütke-Eversloh, 2011; Lehmann *et al.*, 2012a, 2012b; Kuit *et al.*, 2012; Cooksley *et al.*, 2012). However, the enzymes for the pathway from β-hydroxybutyryl-CoA to butyryl-CoA, i.e., Crt and Bcd, were not characterized. It was mentioned previously (section 3.2, 4.3) that the inactivation of *bcd* gene might be lethal, and similarly it could be impossible to disrupt the ThlA-coding gene which is responsible for the conversion of acetyl-CoA to acetoacetyl-CoA in the central metabolism (Cooksley *et al.*, 2012). Therefore, investigation of roles of other genes which might be related to the regulation of C_4 products was of great interest. In addition to *bcd*, the gene encoding another EtfA/B-dependent dehydrogenase, FAD/FMN-containing dehydrogenase (Fcd, CA_C2542), resides on the chromosome of *C. acetobutylicum* (Nölling *et al.*, 2001), but its function remains unknown. An *etfB* (*CA_C2544*) and an *etfA* (*CA_C2543*) are located next to this *fcd* gene. In this study, the knock-out mutant of each gene of the *etfB-etfA-fcd* cluster was generated and characterized by chemostat cultures and DNA microarray experiments.

4.4.1.1 Transcriptional characteristics of the mutants of genes of the *etfB-etfA-fcd* cluster as compared to the wild type

Among the genes regulated during acidogenic or solventogenic growth of mutant cultures of each gene of the *etfB-etfA-fcd* cluster, significant induction of the mutated genes themselves was noticeable (Table 11, 14, 15, 19, 21). Specifically, in the *etfB* mutant, the whole *etfB-etfA-fcd* transcript was up-regulated by at least 25.3-fold, and *etfB* gene itself was induced by 3.1-fold in the *etfA* mutant where the expression of *etfA* and *fcd* was not significantly altered, and in the *fcd* mutant culture only *etfB* was significantly induced during solventogenesis. Based on all microarray data published or unpublished to date, the transcript level of the mutated gene was supposed to become strongly repressed or undetectable, which seemed to fulfill the general logic. For example, during acidogenesis the transcript level of *fcd* gene was down-regulated by 90% when *fcd* had been inactivated. It had been proposed that SigF drove its own expression in *C. acetobutylicum* (Bi *et al.*, 2011). Expression of *sigF* was under control of Spo0A~P and after a series of sequester-release mechanism the active SigF induced the *sigF* operon. For the *etfB-etfA-fcd* cluster, there might be a similar mechanism like SigF self-regulation based on the expression patterns of the clustered genes. The transcript levels of genes of the *etfB-etfA-fcd* cluster were relatively low, which was observed from the transcriptome information sets available from this study, although during solventogenesis they were elevated as compared to that during acidogenesis (Grimmler *et al.*, 2011). Therefore, it is hypothesized that after the transcription of this cluster a repression protein interacted with the Fcd-EtfA/B complex and then bound to the promoter region of this cluster which was upstream of *etfB* to prohibit their further expression, maintaining a stable amount of this electron-transfer system. When a gene of this cluster was disrupted, the functionality of this complex system was lost, with the result that the interaction with the repression protein stopped. As a consequence, the transcription of the *etfB-etfA-fcd* cluster kept working. Admittedly, more experimental verification is required for systematically

elucidating the concrete regulation mechanism of this gene cluster. *etfB*, *etfA* and *fcd* of the *etfB-etfA-fcd* cluster were disrupted by the ClosTron technology (Heap *et al.*, 2007, 2010a, 2010b) and verified by PCR and Southern hybridization (Fig. 5, 6A, 8, 9A, 11, 12A). Therefore, the corresponding protein did not function and the phenotype of each mutant in this study definitely resulted from the mutation in the corresponding gene. The high similarity of results of each gene mutant for *etfB-etfA-fcd* cluster demonstrated the correlation of functions of the genes in this cluster.

4.4.1.2 Physiological effects of the *etfB-etfA-fcd* cluster during acidogenic growth

etfB, *etfA* and *fcd* gene of the *etfB-etfA-fcd* cluster were inactivated, respectively, and characterized by continuous cultures. All three mutants showed comparable profiles of acidic metabolites during acidogenic growth. Butyric acid (~60 mM) and acetic acid (~40 mM) were generated as the main products and their concentrations were similar to the wild type. On the other hand, solvents were also slightly produced by these mutants during acidogenic growth although they were not predominant, which resembled the wild type. Moreover, concentrations of acetone, butanol and ethanol generated by these three mutants at pH 5.7 were at least 37%, 67% and 25% lower than that in the wild type culture, respectively (Fig. 4, 7, 10, 13). The results suggested that the *etfB-etfA-fcd* cluster influenced the production of the minute amount of solvents under acidogenic conditions.

4.4.1.3 Transcriptional characteristics of all three mutants of genes of the *etfB-etfA-fcd* cluster as compared to the wild type during the steady-state acidogenic growth

Although mutation in each gene of the *etfB-etfA-fcd* cluster led to extraordinarily similar phenotypes during acidogenic growth, the corresponding gene expression profiles were not completely identical between these three mutants. This suggested that Fcd and Etf to some extent played different roles during acidogenic growth in a continuous culture. Nevertheless, common observations were made for these strains.

A transcriptional analysis had been reported that a putative operon containing *CA_C0383*, *CA_C0384*, *CA_C0385* and *CA_C0386* was responsible for cellobiose transport and metabolism, because its expression was significantly induced when *C. acetobutylicum* cells were cultivated using cellobiose as the carbon source (Servinsky *et al.*, 2010). The microarray information of the *etfB*, *etfA* and *fcd* mutants for the *etfB-etfA-fcd* cluster suggested that, in addition to these four genes, *CA_C0387* might also be a member of this putative operon due to the fact that its transcript level was similar to the others, although it was annotated as a gene encoding a hypothetical protein (Nölling *et al.*, 2001). However, the high expression of this putative cellobiose operon in cells using glucose as the single carbohydrate source seemed to contradict this, whereas cellobiose, due to its structure, was catabolized by a similar pathway as glucose (Servinsky *et al.*, 2010). A similar phenomenon had been described in early publications where *CA_C0910-CA_C0919* encoding a putative cellulosome involved in the cellulose degradation (Nölling *et al.*, 2001; Lopez-Contreras *et al.*, 2003; Janssen *et al.*, 2010) had an increased expression level during solventogenesis in a chemostat culture where glucose was used as the single carbon source (Janssen *et al.*, 2010; Grimmler *et al.*, 2011). In spite of the obscure role of these non-glucose-associated catabolism genes

expressed in cells growing in medium where only glucose was used, it can be speculated that the high expression of *CA_C0383-CA_C0387* putative cellobiose operon might be to promote the usage of glucose, because it was observed that, as compared to the wild type, the glucose consumption was decreased during acidogenic growth of these mutants.

4.4.1.4 Transcriptional characteristics of the *fcd* mutant as compared to the wild type during the steady-state acidogenic growth

During acidogenic growth of the *fcd* mutant culture, the transcript levels of genes for cysteine biosynthesis, *CA_C0102-CA_C0107*, were significantly increased. In contrast, the expression of these genes during the same phase was not significantly up-regulated in both *etfB* and *etfA* mutants for the *etfB-etfA-fcd* cluster despite of a noticeably induced status of *CA_C0110* in the *etfB* mutant. This suggested that each individual gene in the *etfB-etfA-fcd* cluster possessed different capacity of regulation of cysteine synthesis. It was reported that the cysteine synthesis genes were strongly induced following acetate stress (Alsaker *et al.*, 2010), suggesting that the *fcd* mutant might suffer from a acetate stress under acidogenic conditions. The concentration of acetic acid during acidogenesis of the *fcd* mutant was not obviously changed as compared to the wild type (Fig. 4, 7). Therefore, the potential acetate stress was probably attributed to the cell membrane characteristics which were influenced by the mutation of the *fcd* gene. This assumption could be supported by the significant induction of membrane-associated genes during acidogenic growth of the *fcd* mutant (9 membrane-associated genes out of 31 induced genes during acidogenesis, Table 9).

adhE1 (*CA_P0162*) which codes for a bifunctional alcohol/aldehyde dehydrogenase was repressed by 68% during acidogenesis of a chemostat culture of the *fcd* mutant (Table 8, 10). It had been demonstrated that *adhE1* gene was responsible for the last two steps of butanol production in solventogenic cultures (Dürre *et al.*, 1995) and that it was highly expressed during solventogenesis in the wild type chemostat cultures (Janssen *et al.*, 2010; Grimmler *et al.*, 2011). During acidogenesis, the solvents acetone, butanol and ethanol were slightly generated in chemostat cultures, although they were only minute products during this phase (Janssen *et al.*, 2010; Grimmler *et al.*, 2011; Fig. 4, 7). Therefore, the down-regulation of *adhE1* appeared to make only little sense for butanol production during acidogenesis of the *fcd* mutant culture, although butanol concentration was indeed decreased by ~78% (~1 mM left). On the other hand, it was found that the repression of *adhE1* was coupled with the induction of *adhE2* (*CA_P0035*) by 2.5-fold, confirming the observation that *adhE1* was negatively related to the expression of *adhE2*, or vice versa. This phenomenon was in accordance with a previous finding (Grimmler *et al.*, 2011), whereas their regulation intensities were more pronounced in the data presented here, which indicated the influence of the *fcd* gene. *adhE2* was exclusively expressed during alcohologenic growth of a chemostat culture and the expression of the plasmid-borne *adhE2* was able to restore butanol production in a *C. acetobutylicum* degenerate DG1 strain which had lost the pSOL1 megaplasmid containing both *adhE1* and *adhE2* (Fontaine *et al.*, 2002). This revealed that *adhE2* was also responsible for butanol formation. As a result, the induction of *adhE2* during acidogenic growth of the *fcd* mutant culture explained the residual butanol formation during this phase where *adhE1* was significantly down-regulated. The complex relationship between *adhE1* and *adhE2* will be further discussed in the section for the *adhE1* mutant (section 4.4.3.3).

A gene that encoded part of a putative galactose PTS (phosphate transferase system), *CA_C2957* (for PTS IIB), and a monocistronic operon (*CA_C2956*) for PTS IIC, as well as a

polycistronic operon (*CA_C2954-CA_C2952*) for the tagatose-6-P pathway (Reid, 2005; Servinsky *et al.*, 2010) were all strongly repressed in a continuous culture of the *fcd* mutant during acidogenic growth (Table 10). This suggests that the *fcd* influenced the expression of these genes under acidogenic conditions. It had been reported that the putative CRE (catabolite-responsive element) sequences were identified in the promoter region of the starting gene of these operons, suggesting that they were likely under control of CcpA, a protein involved in CCR (carbon catabolite repression) (Mitchell, 1998; Rodionov *et al.*, 2001; Servinsky *et al.*, 2010; Ren, 2010). Therefore, the significant down-regulation of these genes for galactose transport and metabolism suggested that *fcd* was probably involved in an potential mechanism for the galactose CCR. Fcd might serve as a protein counteracting the repression caused by glucose utilization. When Fcd was present, galactose transport and metabolism functioned and CCR was stopped. In contrast, CCR was initiated when *fcd* was inactivated, thus transport and metabolism of galactose were inhibited and related genes were down-regulated. This hypothesis could be further supported by the transcript level of another gene during acidogenesis of the *fcd* mutant culture. It was found that *ccpA* was expressed slightly higher (~1.8-fold) when *fcd* gene was knocked out, suggesting that the amount of CcpA was likely increased accordingly. CCR was proposed to function at the protein level (Brückner and Titgemeyer, 2002) and enhanced amount of CcpA might facilitate its functionality in repression processes.

Two glucose transporters had been proposed, one was a *CA_C0570*-coding PTS II system which could be induced by glucose, maltose and starch, and the other was a constitutively expressed complex (CA_C1353 and CA_C1354) (Xiao *et al.*, 2011; Servinsky *et al.*, 2010). The expression of *CA_C0570* was significantly repressed in a continuous culture of the *fcd* mutant during acidogenesis (Table 10). This suggested that *fcd* was positively associated with glucose transport in acidogenic cells. To maintain the growth and metabolism of the mutant cells, the second glucose transporter, *CA_C1353*- and *CA_C1354*-coding system, had to be more operational, which their increased transcription levels confirmed. The transcript levels of *CA_C1353* and *CA_C1354* were mildly elevated by ~2.5-fold and ~1.5-fold, respectively. However, it was worth noting that their expression intensities in the *fcd* mutant remained relatively low. *CA_C1354* expression level resembled that of *CA_C0570* which had been repressed and the transcription of *CA_C1353* also remained low level, which was only one twentieth that of down-regulated *CA_C0570*. In a word, significant repression of *CA_C0570* was coupled with increased but still low transcript levels of *CA_C1353* and *CA_C1354*. There were three possible explanations for this correlation. The first was that CA_C0570 remained operational despite of the down-regulation of its mRNA abundance, and the second transport system consisting of CA_C1353 and CA_C1354 became slightly more active as a compensation to the reduced functionality of *CA_C0570*-coding PTS II system. The second possibility was that the repression of *CA_C0570* made it unable to transport enough glucose and the mildly elevated transcription of both *CA_C1353* and *CA_C1354* might be sufficient for the glucose transport due to the high efficiency of translation, and/or high stability and activity of the proteins. There were some protein examples with these properties, e.g., glyceraldehyde 3-phosphate dehydrogenase, a response regulator (CA_C3220), a flagellin, a Zn-dependent peptidase (CA_C3006) and seryl-tRNA synthetase (Schaffer *et al.*, 2002; Janssen *et al.*, 2010). The last explanation was that there might be a third glucose transport system in addition to the proposed two (CA_C0570, CA_C1353 and CA_C1354). A candidate might be the product of the operon for cellobiose transport and metabolism (*CA_C0383-CA_C0387*) which was highly expressed in the *fcd* mutant culture during acidogenesis. It was known that cellobiose was composed of glucose and it was metabolized via a similar pathway to glucose (Servinsky *et al.*, 2010).

4.4.1.5 Transcriptional characteristics of the mutants of *etfA/B* of the *etfB-etfA-fcd* cluster as compared to the wild type during the steady-state acidogenic growth

The knock-out mutation of *adc* (*CA_P0165*, encoding acetoacetate decarboxylase, Fig. 2) in either *C. acetobutylicum* ATCC 824 or EA 2018 strain resulted in noticeably decreased production of acetone and accumulation of acetic acid, which demonstrated its significance in acetate utilization and acetone formation under batch conditions (Jiang *et al.*, 2009; Lehmann *et al.*, 2012a). Nevertheless, the literature did not describe the transcription of this gene. The *adc* gene was up-regulated at least 6.5-fold exclusively in acidogenic cells of the mutants of *etfB* and *etfA* of the *etfB-etfA-fcd* cluster, suggesting *etfB* and *etfA* of the *etfB-etfA-fcd* cluster affected the transcript level of *adc* under acidogenic conditions (Table 14, 19). As mentioned previously (section 4.1.2), acetone could be generated during acidogenesis of a chemostat culture, but its concentration was low (<1 mM). And the production of acetone in the *etfA* and *etfB* mutant (*etfB-etfA-fcd* cluster) cultures was further decreased by at least 37% (Fig. 10 and Fig. 13). Consequently, highly expressed *adc* in acidogenic cells of the mutants of *etfA* and *etfB* of *etfB-etfA-fcd* cluster seemed not to be involved in the negligible acetone formation, which suggested that it might function in other unknown pathways.

In terms of the expression of genes for fatty acid synthesis (Alsaker and Papoutsakis, 2005), a remarkable difference was observed, as compared to wild type, during acidogenic growth of the mutant cultures of *etfB* and *etfA* of the *etfB-etfA-fcd* cluster. A huge gene cluster, *CA_C1988-CA_C2026*, showed significant up-regulation during acidogenesis of the mutant cultures of *etfB* and *etfA* of the *etfB-etfA-fcd* cluster (Table 14, 19). This result suggested that *etfA/B* of the *etfB-etfA-fcd* cluster affected the fatty acid synthesis during acidogenic growth. It was shown that part of these genes (*CA_C1988-CA_C2019*) were induced in the stationary phase of the wild type strain under batch culture conditions (Alsaker and Papoutsakis, 2005), and during the dynamic pH shift from acidogenesis to solventogenesis and solventogenic growth of a wild type continuous culture (Grimmler *et al.*, 2011). Grimmler *et al.* proposed that butanol stress did not trigger the expression of genes for fatty acid synthesis in a direct way (Grimmler *et al.*, 2011), because during the dynamic pH shift butanol remained low level as during acidogenesis and was not yet accumulated (section 4.1.2; Janssen *et al.*, 2010; Grimmler *et al.*, 2011). In this study, fatty acid synthesis genes were significantly up-regulated during the steady-state acidogenic growth of the *etfA/B* mutant cultures (the *etfB-etfA-fcd* cluster) in which butanol concentration was ~70% lower than the wild type (section 4.1.2; Fig. 10, 13). This finding further supported the suggestion that butanol stress was not a direct factor stimulating expression of genes for fatty acid synthesis. In addition, the higher expression of genes for fatty acid synthesis suggested that membrane characteristics might be altered during acidogenesis of the mutant cultures of *etfB* and *etfA* of the *etfB-etfA-fcd* cluster.

In *C. acetobutylicum*, the conversion from acetoacetyl-CoA to crotonyl-CoA (Fig. 2) was involved in two sets of homologous genes (Nölling *et al.*, 2001) which code for a β-hydroxybutyryl-CoA dehydrogenase and a enoyl-CoA hydratase (crotonase). *hbd* (*CA_C2708*) and *mmgB* (*CA_C2009*) code for β-hydroxybutyryl-CoA dehydrogenase, and *crt* (*CA_C2712*) and *fadB* (*CA_C2012* and *CA_C2016*) encode enoyl-CoA hydratase. *hbd*, part of the *bcs* operon (Boynton *et al*., 1996) along with *crt*, had been investigated (Lehmann and Lütke-Eversloh, 2011). And *mmgB* and *fadB* were located in a gene cluster for fatty acid synthesis (*CA_C1988-CA_C2026*). It had been proposed that *C. acetobutylicum* used *hbd* and *crt* for the conversion from acetoacetyl-CoA to crotonyl-CoA via β-hydroxybutyryl-CoA during acidogenic growth and *mmgB* and *fadB* were utilized for the same purpose during solventogenesis (Grimmler *et al.*, 2011). Because *hbd* and *crt* were strongly up-regulated

during acidogenic growth and repressed from the dynamic pH shift of a continuous culture of the wild type strain, whereas *mmgB* and *fadB* started to become induced at pH 5.5 during the pH shift and strongly expressed throughout solventogenesis (Grimmler *et al.*, 2011). In this study, the transcriptome data of mutants of *etfA/B* of the *etfB-etfA-fcd* cluster showed a remarkable induction (at least 16.8-fold) of *mmgB* and *fadB* during acidogenesis (Table 14, 19), while *hbd* and *crt* were mildly down-regulated (42% and 40% in the *etfA* mutant and 35% and 27% in the *etfB* mutant, respectively) during the same phase. Therefore, *etfA/B* of the *etfB-etfA-fcd* cluster appeared to simultaneously influence the expression of these two sets of homologous genes under acidogenic conditions. Moreover, it seemed that the up-regulation of *mmgB* and *fadB* in acidogenic cells was to compensate *hbd* and *crt* which were repressed during acidogenesis. In addition, it was noticeable that the strong up-regulation of *mmgB* and *fadB* during acidogenesis of the *etfA/B* mutants (the *etfB-etfA-fcd* cluster) was based on their low expression levels in the wild type (the reference). The enhanced intensities of transcription of *mmgB* and *fadB* remained relatively low, which were similar to that of *crt* that had been repressed. The low expression levels of *mmgB* and *fadB* support their biosynthetic roles.

4.4.1.6 Physiological effects of the *etfB-etfA-fcd* cluster during the steady-state solventogenic growth

It has been described that genes of the *etfB-etfA-fcd* cluster became induced from pH 4.9 during the dynamic pH shift and remained highly expressed throughout the solventogenic growth (Grimmler *et al.*, 2011). This suggested the potential role of this cluster during solventogenesis. Compared with the phenotype of the wild type strain (Fig. 4), concentrations of acetone, butanol and ethanol during solventogenesis of these three mutant cultures were decreased by at least 33.3%, 33.3% and 28.9%, respectively (Fig. 7, 10, 13). This suggested that the *etfB-etfA-fcd* cluster influenced the production of solvents at pH 4.5 in chemostat cultures. In addition to the commonly declined production of all three solvents in the *etfB*, *etfA* and *fcd* (the *etfB-etfA-fcd* cluster) mutant cultures, the acid-related events were also changed during solventogenic growth. Compared with the wild type culture where ~11 mM acetate and ~13 mM butyrate were detected under solventogenic conditions (Fig. 4), the *fcd* mutant culture showed the most obvious increase for butyrate (53.8%) and 17.7-33.8% more butyrate was detected in the mutants of *etfA/B* of the *etfB-etfA-fcd* cluster. These findings suggested that in addition to the effects on the production of solvents, the *etfB-etfA-fcd* cluster also influenced the butyrate metabolism during solventogenic growth.

4.4.1.7 Transcriptional characteristics of all three mutants of genes of the *etfB-etfA-fcd* cluster as compared to the wild type during the steady-state solventogenic growth

The transcriptome information of all three mutants of genes of the *etfB-etfA-fcd* cluster revealed a trait in common. That was, a *pfor* (*CA_C2229*, for pyruvate-ferredoxin oxidoreductase, Pfor) was down-regulated, although its expression level, except for in the *etfB* mutant (for the *etfB-etfA-fcd* cluster), did not reach the criterion referred to as "significant" (logarithmic ratio less than -1.60, section 2.10.6). Compared with the wild type, the transcript level of this *pfor* was repressed by 59% in the *fcd* mutant and 64% in the *etfA* mutant (for the *etfB-etfA-fcd* cluster), and its expression was reduced by 75% when *etfB* of

the *etfB-etfA-fcd* cluster was disrupted (Table 8, 13, 18). It is well known that the expression ratio is underestimated in cDNA microarrays when compared to other methods. For example, it was described that the *spo0A* was down-regulated 38-fold based on Northern blots whereas a 3.5-fold repression was observed in microarrays of the *spo0A* mutant (Harris *et al.*, 2002; Tomas *et al.*, 2003). As a result, it is possible that the transcript level of this *pfor* was even reduced more significantly than what observed in microarrays in these three mutants. The iron-sulfur-containing Pfor is the enzyme that catalyzed the irreversible oxidative decarboxylation of pyruvate to generate acetyl-CoA and CO_2 (Amador-Noguez *et al.*, 2010), the first reaction in the central metabolism after glycolysis. Therefore, the finding that production of all three solvents was obviously reduced during solventogenic growth in continuous cultures of the *etfB*, *etfA* and *fcd* mutants for the *etfB-etfA-fcd* cluster could be, to some extent, due to the repression of a *pfor* by disruption of these genes. For this reason, less carbon flowed through pyruvate to synthesize acetyl-CoA. In addition, it was found that genes coding for key enzymes of the C_4 pathway from acetyl-CoA to butyryl-CoA were somewhat down-regulated in these three mutants, although in the *etfA* mutant *thlA* was repressed by 68% (Table 8, 13, 18). It is proposed that the *etfB-etfA-fcd* cluster influenced the production of three solvents mainly by controlling the carbon flux through the central metabolic pathway, especially by a positive effect on the pyruvate/acetyl-CoA node. On the other hand, *CA_C2499* codes for the second Pfor paralog in *C. acetobutylicum*. This gene, unlike the main *pfor* (*CA_C2229*), is hardly ever expressed in both wild type and these three mutants (Table 8, 13, 18). This suggested that the *etfB-etfA-fcd* cluster did not exert influences on the expression of this gene. Consequently, the *etfB-etfA-fcd* cluster affected *CA_C2229*, the gene encoding the main Pfor in *C. acetobutylicum*.

CA_C0980 (*pflA*) and *CA_C0981* (*pflB*) were both strongly up-regulated in the *fcd* and *etfA* mutants, but not in the *etfB* mutant (Table 11, 16). These two genes encode a pyruvate-formate lyase and its activation enzyme, respectively. And they catalyzed the conversion of pyruvate and CoA to acetyl-CoA and formate. Inactivation of these two genes resulted in auxotrophy for formate or purins by *C. acetobutylicum* under batch culture conditions (Hönicke, 2014). This suggested that *pflAB* was associated with a biosynthetic process in *C. acetobutylicum*. Because of the attenuation at the node of pyruvate to acetyl-CoA (caused by the repression of a *pfor*), the induction of these two genes might function to supply additional acetyl-CoA to the bifurcated TCA cycle from which several amino acids could be synthesized (e.g., aspartate, methionine, glutamine) (Amador-Noguez *et al.*, 2010). Besides, the formate and acetyl-CoA generated might also facilitate the synthesis of NAD along with aspartate. It was described that aspartate, formate and acetyl-CoA are precursors for NAD biosynthesis in *Clostridium butylicum* (Foster and Moat, 1980).

Another gene which was noticeably regulated in all three mutant cultures was a gene coding for a ferredoxin (CA_C3527). It was strongly repressed when an individual gene of the *etfB-etfA-fcd* cluster was disrupted (Table 12, 17, 22). It had been reported that in *Clostridium kluyveri* the reduction of the ferredoxin with NADH was catalyzed by the butyryl-CoA dehydrogenase (Bcd)/Etf complex, so that the exergonic reduction reaction of crotonyl-CoA to butyryl-CoA promoted the endergonic reduction of ferredoxin (Li *et al.*, 2008; Herrmann *et al.*, 2008). In *C. acetobutylicum*, a similar mechanism had not yet been reported. In this study, the *etfB-etfA-fcd* cluster codes for a second EtfA/B-dependent dehydrogenase system in addition to the Bcd-EtfA/B complex but the reaction mechanisms of both of them in *C. acetobutylicum* remained unknown. Based on the significant down-regulation of *CA_C3527* in the *etfB*, *etfA* and *fcd* mutant (for the *etfB-etfA-fcd* cluster), it was speculated that this gene could be functionally associated with the *etfB-etfA-fcd* cluster, and CA_C3527 might also be

reduced with NADH via a Bcd/Etf complex-like Fcd-EtfA/B system. Unfortunately, it was not possible to determine the substrate of the Fcd-EtfA/B complex so far, but it might be an intermediate in the central pathways. The reason for this assumption was that the product of the *etfB-etfA-fcd* cluster influenced the production of solvents and butyric acid during solventogenic growth.

4.4.1.8 Physiological effects of the *fcd* mutant during the steady-state solventogenic growth

More butyrate (~20 mM) was detected during the steady-state solventogenic growth of a continuous culture of the *fcd* mutant as compared to the wild type (~13 mM), suggesting that the butyrate metabolism was affected by the *fcd* gene (Fig. 7). It was discussed that in the *fcd* mutant the carbon flux in the C_4 pathways might be decreased due to the down-regulation of a *pfor* (section 4.4.1.6) and that the presence of butyrate uptake in continuous cultures could not be identified so far (section 4.1.2). If butyrate re-assimilation was absent during solventogenesis of a continuous culture, deletion of the *fcd* gene seemed to promote the production of butyric acid because butyrate concentration was increased. The expression of key genes for butyrate synthesis, *ptb* and *buk*, was hardly altered during solventogenesis of the *fcd* mutant. Therefore, it was not reasonable that the concentration of butyric acid produced was elevated. Butyrate concentration was supposed to be decreased due to the repression of a *pfor* and the normal level of butyrate synthesis route. This suggested that butyrate uptake might exist during solventogenic growth of the *fcd* mutant culture. Butyrate utilization could be attenuated by the inactivation of the *fcd* gene if it was present during solventogenic growth of a chemostat culture. The amount of butyric acid synthesized by the *fcd* mutant was probably reduced due to the repression of a *pfor*, and residual butyrate concentration was higher.

Butyrate metabolism was also affected during solventogenesis of chemostat cultures of the mutants of *etfB* and *etfA* genes of the *etfB-etfA-fcd* cluster, although in these mutants this effect was not as significant as that in the *fcd* mutant. During solventogenic growth of the *etfB* and *etfA* mutant (for the *etfB-etfA-fcd* cluster) cultures butyrate concentrations were ~33.8% and ~17.7% higher than that in the wild type strain, and in the *fcd* mutant 53.8% more butyric acid was detected (Fig. 7, 10, 13). The repression of a *pfor* was also observed in these *etfB* and *etfA* mutants. As a result, this suggested that the *etfB* and *etfA* of the *etfB-etfA-fcd* cluster have a similar effect as the *fcd* gene in terms of the butyrate metabolism during solventogenesis, as discussed in the last paragraph. However, their impacts on butyrate concentration definitely appeared to be less pronounced as compared to *fcd* based on the butyrate concentrations detected. One possible reason might be that the functionality of *etfA/B* of the *etfB-etfA-fcd* cluster was slightly compensated. There were two sets of homologous genes coding for EtfA/B in *C. acetobutylicum* (Nölling *et al.*, 2001). One set was the *etfB-etfA-fcd* cluster, and the other set was the *bcs* operon which consisted of *crt*, *etfA*, *etfB*, *bcd* and *hbd* (Boynton *et al.*, 1996). When the *etfB* or *etfA* of *etfB-etfA-fcd* cluster was knocked out, corresponding genes from the *bcs* operon might to some extent be used to compensate the lost functionality. On the other hand, it was found that the expression of the *etfA* and *etfB* of the *bcs* operon was down-regulated by at least 2-fold when the *etfB* or *etfA* from the *etfB-etfA-fcd* cluster had been deleted.

It was reported that the acetone synthesis pathway was important for the acid uptake in *C. acetobutylicum* (Andersch *et al.*, 1983; Hartmanis *et al.*, 1984b). Other researchers, however, held the view that acetone synthesis pathway was unnecessary for butyrate uptake

(Meyer *et al.*, 1986; Desai *et al.*, 1999). Mutations in genes in the acetone synthesis route (*adc* and *ctfA*) revealed that butyrate re-assimilation was not related to this pathway (Lehmann *et al.*, 2012a) and the inactivation of *ptb* showed that other pathways for the uptake of this acid exist (Lehmann *et al.*, 2012b). The latter study, however, did not support the assumption that the production and the re-assimilation of butyric acid rely on the Ptb and Buk route (Desai *et al.*, 1999), because in the *ptb* mutant this route was blocked while butyrate utilization remained operational. In addition, a dual re-assimilation model of butyric acid had been proposed. In this model, CtfAB and Adc function when Ptb-Buk route was inactive, and vice versa (Lehmann *et al.*, 2012b). In continuous cultures of the mutants of *etfB*, *etfA* and *fcd* of the *etfB-etfA-fcd* cluster, both pathways for synthesis of acetone and butyrate were present, but the butyrate concentration was increased during solventogenic growth of these three mutants. As discussed in the last two paragraphs, butyrate uptake might be present in the chemostat cultures of these three mutants and the mutants of each gene of *etfB-etfA-fcd* cluster exerted influences on the re-assimilation of butyric acid. Therefore, it could be suggested that the *etfB-etfA-fcd* cluster was involved in butyrate utilization in continuous cultures. This suggestion provided a novel direction for understanding the mechanisms of the re-assimilation of butyric acid.

The expression of *pta* and *ack* for acetate synthesis was hardly altered during solventogenesis of the *fcd* mutant (Table 8). One of the *pfor* (*CA_C2229*) was found to be repressed under these conditions (section 4.4.1.6). Therefore, the acetate concentration was supposed to be decreased if the acetate uptake was absent in a continuous culture. But this was not the case. As compared to the wild type, the acetate concentration detected was not changed during solventogenesis of the *fcd* mutant (~10 mM, Fig. 7). Consequently, it could be suggested that the mutation of the *fcd* might hamper the utilization of acetate, if there would be continuous acetate uptake in the wild type. Because in solventogenic cells of the *fcd* mutant, the amount of acetate produced was probably declined according to the repression of the *pfor* (*CA_C2229*) and the residual acetate concentration was unchanged, the assimilated acetate amount was exclusively supposed to be decreased. In a word, the *fcd* might facilitate the re-assimilation of acetic acid in a continuous culture, if the acetate uptake was present.

4.4.2 Physiological effects of pSOL1 and genes located on it

In this study, the pSOL1 megaplasmid was cured, as well as mutants of two dehydrogenase-coding genes and a glycogen regulator gene located on pSOL1 were generated by the ClosTron technology (Heap *et al.*, 2007, 2010a, 2010b). The resulting strains were characterized by continuous fermentation, followed by microarray analyses.

Removal of the pSOL1 megaplasmid resulted in the inability to produce butanol and acetone throughout the fermentation process and ethanol formation was reduced by 68% (~1.2 mM) at lower pH (pH 4.5) that corresponded to solventogenic growth in the wild type strain (Fig. 23). Inactivation of *adhE1* (*CA_P0162*) led to the production of negligible amounts of butanol and acetone during solventogenic growth, and a 60% lower concentration of ethanol (~1.5 mM) was detected during this phase (Fig. 29). In addition, the *CA_P0059* mutant (Cooksley *et al.*, 2012) showed decreased generation of all three solvents under solventogenic conditions (Fig. 30). *CA_P0059* codes for a putative alcohol dehydrogenase (Nölling *et al.*, 2001), which was proposed to be involved in the production of butanol and ethanol (Papoutsakis, 2008). A *CA_P0059* mutant showed an enhanced formation of acetone, butanol and ethanol under batch culture conditions (Cooksley *et al.*, 2012). Moreover, the *CA_P0129*

mutant had a comparable phenotype to the *CA_P0059* mutant (Fig. 28). *CA_P0129* encodes a glycogen-binding regulatory subunit of S/T protein phosphatase I (Nölling *et al.*, 2001). And its high expression during solventogenesis of continuous cultures of the wild type strain was observed in microarray experiments (Janssen *et al.*, 2010; Grimmler *et al.*, 2011).

In terms of the production of acids, the phenotype of each mutant (for the pSOL1 and genes located on it) differed. The pSOL1-free strain produced a comparable amount of butyrate as the wild type during acidogenic growth, whereas its acetate production was decreased by 24.4% during this phase (Fig. 23). Acidogenic cells of the *CA_P0129* mutant generated similar concentration of butyrate and slightly declined amount of acetate as compared to the wild type (Fig. 28). The *adhE1* mutant had comparable acid phenotypes to the *CA_P0129* mutant at pH 5.7 (Fig. 29). The production of acetate and butyrate was both mildly decreased in the *CA_P0059* mutant culture during acidogenic growth (Fig. 30). During solventogenic growth, butyrate and acetate were still slightly formed in *C. acetobutylicum* wild type (Fig. 4). The production of acetic acid was comparable to the wild type in cultures of the *CA_P0059*, *CA_P0129* and *adhE1* mutants during the steady-state solventogenic growth (Fig. 28, 29, 30), while the pSOL1-free mutant strain formed 81.8% more acetic acid during this phase (Fig. 23). In these mutant cultures, the butyrate concentration was higher than the wild type at pH 4.5, especially in the pSOL1-free mutant culture where butyrate was accumulated ~153.9% higher.

4.4.2.1 Physiological effects of the pSOL1 megaplasmid as a whole

pSOL1 contains the *sol* operon consisting of *adhE1* and *ctfAB*, which is indispensable for solventogenesis, because AdhE1 was reported to be responsible for the last steps in the butanol/ethanol synthesis pathway (Dürre *et al.*, 1995).

Two pSOL1-free strains, M5 and DG1, have been reported before (Clark *et al.*, 1989; Nair and Papoutsakis, 1994). It was shown that the M5 mutant did not produce the solvents butanol and acetone, as well as spores (Clark *et al.*, 1989). Transcription analysis of the M5 strain was performed on the basis of batch cultures using a microarray containing probes for a part of (about one fourth) the genes (Tomas *et al.*, 2003). In addition, the strains M5 and DG1 were used as hosts for selective production of biofuels by expression of genes for acid re-assimilation *ctfAB*, and/or key genes for solventogenesis, i.e. *adhE1* and *adhE2* (Nair and Papoutsakis, 1994; Fontaine *et al.*, 2002; Sillers *et al.*, 2008; Lee *et al.*, 2009).

Although the above mentioned studies had been carried out, molecular networks regulated by pSOL1 megaplasmid and the genes on it were still unclear. The overwhelming majority of microarray results available to date are based on batch fermentations where the status of cells differed in each experiment, which brought an interfering factor for the accuracy of the results. Moreover, because the M5 strain was generated by chemical mutagenesis and was not checked by re-sequencing, there remained possibilities of mutations in other chromosomal sites. A good example was *C. acetobutylicum* EA 2018 strain (Zhang *et al.*, 1996), which produced a higher ratio (~70%) of butanol in solvents. This strain was generated by EMS (ethyl methanesulfonate) and NMNG (*N*-methyl-*N'*-nitro-*N*-nitrosoguanidine) mutagenesis in 1990s and the complete genome sequencing was published in 2011. Results showed that 26 insertion sites and 46 deletion sites existed in the genome of this strain when compared to the type strain *C. acetobutylicum* ATCC 824 (Hu *et al.*, 2011).

Due to the hazard that chemical mutagenesis might cause unknown mutation sites, a direct strategy for removal of the pSOL1 megaplasmid was required to maintain an intact wild-type pSOL1-free chromosome in *C. acetobutylicum* cells. A direct way to delete the pSOL1 megaplasmid was attempted and succeeded using the ClosTron technology in this study, and *CA_P0175* (*repA*) and *CA_P0177* (*spoOJ*) genes were chosen as the targets. *CA_P0175* coded for the replication protein of the pSOL1 megaplasmid (Nölling *et al.*, 2001), it was conceivable that inactivation of this gene would lead to inability of the megaplasmid to replicate so that no copies existed in the cells after cell division. *CA_P0177* encoded a protein involved in the chromosome segregation, a SpoOJ regulator of Soj/ParA family (Nölling *et al.*, 2001). This gene had been proposed to be related to the sporulation process, because the M5 mutant in which pSOL1 was lost did not form spores (Tomas *et al.*, 2003). A *spo0J* gene resides on the chromosome of *C. acetobutylicum*, and it has been reported that *spo0J* was required for chromosome partitioning during sporulation and during vegetative growth the mutation of *spo0J* led to generation of anucleate cells (Sonenshein *et al.*, 2002). In *Bacillus subtilis*, proteins of Soj/ParA family had been studied. It was reported that they played roles in chromosome replication, cell division and sporulation (Ireton *et al.*, 1994; Lin and Grossman, 1998; Murray and Errington, 2008). Besides, the roles of *par* genes (*parA* and *parB*) in chromosome replication were also demonstrated in *Vibrio cholerae* (Kadoya *et al.*, 2011). The results shown in this study provided a method to get immediately rid of the pSOL1 megaplasmid without chemical mutagenesis, leaving a single chromosome in the cell. Using the chemostat cultures and microarray technology, a reliable genome-wide transcription analysis was presented for elucidation of the effects of the absence of the pSOL1 megaplasmid on the chromosome.

In the continuous culture of the pSOL1-free (*CA_P0175*) mutant, the production of butanol and acetone was completely abolished during both acidogenesis and growth at pH 4.5 that triggered solventogenesis in the wild type (Fig. 23), which was consistent with the product profile of the M5 mutant in a pH-uncontrolled batch culture (Tomas *et al.*, 2003). This confirmed that the genes responsible for the generation of butanol and acetone were located on the megaplasmid. It had been reported that inactivation of acetoacetate decarboxylase (Adc)-coding gene nearly abolished the acetone formation in batch cultures (Jiang *et al.*, 2009; Lehmann *et al.*, 2012a; Cooksley *et al.*, 2012), and *ctfA* and *ctfB* were absolutely necessary for the production of acetone under the same conditions (Lehmann *et al.*, 2012a; Cooksley *et al.*, 2012). Moreover, a batch culture of an *adhE1*-defective strain produced a very small amount of all three solvents (Cooksley *et al.*, 2012). These findings indicated that *adc* and *adhE1-ctfA-ctfB* (*sol* operon) were indispensable for the production of acetone and butanol. The pSOL1 megaplasmid carried the *sol* locus and *adc* (Nölling *et al.*, 2001). Therefore, the non-production of acetone and butanol in the pSOL1-free mutant culture largely resulted from the loss of the *sol* locus and *adc*. In addition, the second alcohol dehydrogenase on the pSOL1, *adhE2*, had been studied under batch fermentations. However, functional loss of *adhE2* did not lead to changes in alcohol production (Cooksley *et al.*, 2012), which further indicated the significance of *adhE1* for butanol formation.

The central metabolic pathways of *C. acetobutylicum* have been displayed in numerous publications (Lehmann and Lütke-Eversloh, 2011; Lehmann *et al.*, 2012a, 2012b; Cooksley *et al.*, 2012); it was proposed that the biosynthesis of ethanol also required pSOL1-borne AdhE1 and AdhE2, two bifunctional aldehyde/alcohol dehydrogenases. However, ethanol was still formed by a pSOL1-free (*CA_P0175*) mutant culture throughout the whole fermentation process although at reduced concentrations (~27.5% during acidogenesis and ~68.4% during solventogenesis). This observation suggested that *adhE1* and/or *adhE2* were

involved in ethanol formation especially at pH 4.5, but one or more of the chromosomal genes for alcohol dehydrogenases might also be involved. In the M5 mutant cultures, the final ethanol concentration was only reduced by 30% (Tomas *et al.*, 2003). But this experiment was carried out in static flasks where pH was not regulated and the ethanol concentration was accumulative. On the chromosome of *C. acetobutylicum* are several annotated candidates for an alcohol dehydrogenase, i.e., *CA_C0462*, *CA_C1423*, *CA_C3298*, *CA_C3299*, *CA_C3335*, *CA_C3355*, *CA_C3375*, *CA_C3392* and *CA_C3484* (Nölling *et al.*, 2001). Unfortunately little is known about them yet. Only two proposed examples among these were *bdhA* (*CA_C3298*) and *bdhB* (*CA_C3299*) which code for two proposed butanol dehydrogenases, and they had been studied in batch fermentations. However, the functional loss of either of them did not result in changes in alcohol production (Cooksley *et al.*, 2012). All in all, the key enzyme for ethanol formation remained unclear and further studies are necessary.

During both acidogenesis and growth at pH 4.5 that triggered solventogenesis in the wild type, the pSOL1-borne 178 genes were not detectable in the pSOL1-free mutant culture. This was in agreement with the absence of their DNA templates. For chromosomal genes in the pSOL1-free mutant, 115 genes were significantly regulated during the steady-state acidogenic growth and 126 genes were strongly induced or repressed during growth at pH 4.5. This suggested that the loss of the pSOL1 megaplasmid resulted in profound alteration of the expression of the chromosomal genes during these two growth phases.

4.4.2.2 Transcriptional characteristics of a pSOL1-free (*CA_P0175*) mutant as compared to the wild type during the steady-state acidogenic growth

During acidogenesis of a pSOL1-free (*CA_P0175*) mutant strain, the production of butyrate and acetate was not significantly altered (Fig. 23). This was in accordance with the transcript levels of genes related to acid synthesis, i.e. *pta*, *ack*, *ptb* and *buk*. The expression of *pta* and *ack* was hardly changed, whereas *ptb* and *buk* were slightly but not significantly induced (Table 23). The up-regulation of *ptb* and *buk* corresponded to the phenomenon that lower OD_{600} of the pSOL1-free mutant culture (~3.6) as compared to the wild type culture (~3.9) led to a nearly identical butyrate concentration (~60 mM). The acidogenic phenotype of the pSOL1-free mutant suggested that genes located on the pSOL1 megaplasmid were not obviously involved in the generation of acids during this phase. In the M5 mutant, acid synthesis genes showed reduced transcript levels during the exponential and transition phases (Tomas *et al.*, 2003). Similar differences were also observed for genes of central metabolism. *hbd*, *crt*, *bcd* as well as accompanied *etfA/B* of the *bcs* operon (Boynton *et al.*, 1996) showed somewhat elevated expression levels during acidogenesis of a pSOL1-free mutant, while in M5 they were repressed during the exponential growth (Tomas *et al.*, 2003). In a pH-uncontrolled batch fermentation, the boundary of acidogenesis and solventogenesis is not clearly separated, although acids were the main products during the exponential growth and solvents became predominant during stationary phase. Accordingly, it was difficult to discriminate expression patterns of genes involved in the metabolism during the two physiological phases, i.e. acid and solvent production. Moreover, due to the accumulation of products during the whole course of batch fermentation, it was also hard to establish a correlation between specific gene expression and typical metabolite production.

Among other genes regulated during acidogenic growth of the pSOL1-free mutant culture, significant induction of genes associated with uptake and conversion of sulfate to cysteine, and methionine synthesis and transport, was observed (Table 24). It had been reported that

the expression of genes involved in cysteine and methionine biosynthesis were elevated following 45 mM acetate stress (Alsaker *et al.*, 2010) and this was in agreement with the expression patterns of the same set of genes during acidogenic growth of the pSOL1-free strain. Consequently, the increased transcription levels of these genes were probably a response to an acetate stress caused by the loss of the pSOL1 megaplasmid. The concentrations of acetic acid produced in the wild type and the pSOL1-free mutant culture were similar, so the similar acetate concentration led to a potential stress to the pSOL1-free mutant cells. In the transcriptome of acidogenesis of the pSOL1-free strain culture, six sporulation-associated genes were strongly repressed, including genes of the *sigE* operon and the *sigF* operon, as well as *spoIIE* (Table 25). SigE, SigF and SpoIIE are involved in sporulation but do not affect solventogenesis (Jones *et al.*, 2011; Tracy *et al.*, 2011; Bi *et al.*, 2011). *C. acetobutylicum* cells, however, did not produce spores during the steady-state acidogenic growth in chemostat cultures. As a result, the significant down-regulation of these sporulation genes might be involved in other physiological behaviors apart from sporulation. It is known that stresses might threaten growth and viability of cells and sporulation was regarded as a stress response (Paredes *et al.*, 2005). Therefore, the fact that sporulation-associated genes were repressed when pSOL1 was removed probably resulted in attenuation of cellular tolerances to environmental stimuli. In summary, the absence of the pSOL1 megaplasmid led to repression of sporulation genes which seemed to be related to cell viability, so that the mutant cells could not tolerate normal concentration of acetic acid. The resultant acetate stress caused induction of genes for metabolism and transport of cysteine and methionine as a response.

In addition, genes involved in serine synthesis were noticeably down-regulated during acidogenic growth of the pSOL1-free mutant strain (Table 25). This finding was opposite to results where cells were exposed to external acetate stress (Alsaker *et al.*, 2010; serine synthesis genes were induced following acetate stress), suggesting that their repression might not be involved in an acetate stress caused by loss of the pSOL1 megaplasmid. Moreover, biosynthesis of cysteine requires serine and cysteine synthesis genes were significantly up-regulated during acidogenesis, thus repression of serine formation genes suggested that the serine could be formed from another source, e.g., glycine. It had been demonstrated that glycine was synthesized primarily from threonine in *C. acetobutylicum* (Amador-Noguez *et al.*, 2010).

4.4.2.3 Physiological effects of a pSOL1-free (*CA_P0175*) mutant during growth at pH 4.5

At pH 4.5, the production of acetone and butanol remained completely abolished whereas some ethanol was formed in the pSOL1-free mutant culture. In terms of generation of acids, the pSOL1-free mutant produced more acetate (81.8%) and butyrate (153.9%) as compared to the wild type at pH 4.5 (Fig. 23). When considering the lower OD_{600} of the pSOL1-free mutant culture during growth at pH 4.5 (~2.5) as compared to the wild type (~3.8), the concentrations of both acetate and butyrate produced by the mutant were expected to be ~50% higher than those observed.

As discussed in section 4.1.2, it could not be determined so far whether the re-assimilation of acetic acid was present in a continuous culture (at pH 4.5). If it was absent, acetate concentration detected was dependent on how much it was produced. Concentrations of acetic acid in the wild type and the pSOL1-free mutant culture (at pH 4.5) were ~11 mM and

~20 mM, respectively. Therefore, the loss of the pSOL1 might promote the acetate production which is accompanied with ATP formation. In other words, genes located on the pSOL1 were probably involved in the control of acetate production. On the other hand, the re-assimilation of acetic acid relied on the acetone synthesis pathway (Jiang *et al.*, 2009; Lehmann *et al.*, 2012a) and pSOL1 contained the genes for key enzymes of this route (*ctfAB* and *adc*). As a result, loss of pSOL1 led to a defect in acetate uptake due to absence of genes for key enzymes for acetone formation. Furthermore, the concentration of acetate produced was equal to that detected in the mutant culture (~20 mM). All in all, during growth at pH 4.5 that triggered solventogenesis in the wild type culture, the pSOL1-free mutant could produce ~20 mM of acetic acid no matter whether acetate utilization was present in chemostat cultures, and pSOL1 was involved in the acetate metabolism.

Similarly, there are two conditions in terms of butyrate metabolism in the pSOL1-free mutant culture (at pH 4.5). If butyrate uptake was absent during growth at pH 4.5 in a continuous culture, the concentration of butyric acid detected depended on the amount that was produced. In the wild type culture, ~13 mM of butyrate was formed during solventogenic growth. Furthermore, ~33 mM of butyric acid was detected in the pSOL1-free mutant culture during growth at pH 4.5 which triggered solventogenesis in the wild type culture. Therefore, the loss of the pSOL1 megaplasmid might promote the production of butyric acid which was accompanied with the formation of ATP and regeneration of $NAD(P)^+$. Because the pSOL1 megaplasmid carried genes encoding key alcohol dehydrogenases (AdhE1/2 and CA_P0059) responsible for generation of alcohol, butanol production was completely abolished (Fig. 23) in the pSOL1-free mutant culture. The cell compensated the loss of pSOL1 by producing more butyrate to consume the surplus reducing equivalents. On the other hand, the key enzymes for butyrate utilization had not yet been identified. If there was butyrate utilization in a chemostat culture, the assimilated amount of butyrate in the pSOL1-free mutant culture was zero. The production of butanol might come from two routes, either direct synthesis via the C_4 pathway or the re-assimilation of butyric acid (Jang *et al.*, 2012). The direct production pathway might be blocked due to the absence of alcohol dehydrogenases whose genes were located on the pSOL1 megaplasmid. Accordingly no butanol was detected in the pSOL1-free mutant culture. Therefore, removal of the pSOL1 megaplasmid might abolish the butyrate utilization if it was present in a chemostat culture. This suggested that the pSOL1 might contain the key genes for the re-assimilation of butyric acid.

The possibility that pSOL1 might be responsible for the re-assimilation of butyric acid was an important insight. The results presented in this study suggested that the pSOL1 megaplasmid contained the genes for enzymes for butyrate uptake and thus considerably narrowed down the candidates. It also proved that the re-assimilation of butyric acid was independent of sporulation due to the characteristics of continuous cultures. The key genes for butyrate uptake might be so far unknown genes located on the pSOL1, or *adhE1/2* and/or *CA_P0059*. Loss of the pSOL1 led to absence of the alcohol dehydrogenase-coding genes. As a result, the inability to convert butyryl-CoA to butanol probably exerted effects on butyrate uptake. In other words, the re-assimilation of butyric acid might rely on the butanol biosynthesis. A potential supporting argument was that in the *ptb* mutant butyrate was not produced but its uptake remained operational, although butanol production was decreased (Lehmann *et al.*, 2012b).

4.4.2.4 Transcriptional characteristics of a pSOL1-free (*CA_P0175*) mutant as compared to the wild type during growth at pH 4.5

During growth at pH 4.5 that triggered solventogenesis in the wild type, the loss of the pSOL1 megaplasmid led to profound effects on chromosomal genes at the transcription level (Table 24-27). Genes involved in biosynthesis and transport of several amino acids (cysteine, arginine and methionine, etc.) were significantly up-regulated (Table 26). Arginine metabolism genes and the *aro* locus for formation of chorismate (a intermediate for synthesis of phenylalanine, tyrosine and tryptophan) were found to be up-regulated following butyrate stress, and genes associated with the biosynthesis and transport of cysteine and methionine were induced after acetate stress (Alsaker *et al*., 2010). The pSOL1-free mutant mainly produced ~33 mM butyrate and ~20 mM acetate during growth at pH 4.5 with lower (~33.7%) OD_{600} as compared to the wild type culture (Fig. 4, 23). Therefore, the pSOL1-free mutant probably suffered from a combined stress of acetate plus butyrate during growth at pH 4.5. It had been described that addition of 40 mM butyric acid into a batch culture was poisonous to *C. acetobutylicum* cells and resulted in a obvious decrease of the OD_{600} (Lehmann *et al.*, 2012b). Thus, as compared to the wild type, it seemed that the decreased OD_{600} of the pSOL1-free mutant culture resulted from increased concentrations of acids and that the amounts of acids accumulated in this mutant culture became stresses to cells.

The expression of genes related to the carbohydrate metabolism, especially the clustered genes *CA_C0910*-*CA_C0919* for a putative cellulosome (Lopez-Contreras *et al.*, 2003), was also strongly enhanced in the pSOL1-free mutant culture during growth at pH 4.5 as compared to the wild type (Table 26). This putative operon had been described to be significantly induced only during solventogenic growth (Janssen *et al.*, 2010; Grimmler *et al.*, 2011) and its transcript level was rather weak during acidogenesis or during the metabolic switch to solventogenesis (Grimmler *et al.*, 2011). It is known that *C. acetobutylicum* does not grow on cellulose (Lee *et al.*, 1985) and in this study glucose was used as the single carbon source during the whole fermentation process. Therefore, the significant induction of these genes involved in cellulose degradation (Nölling *et al.*, 2001) might respond to some events, which occurred during growth at pH 4.5 of the pSOL1-free mutant culture. It was suggested that the solvents generated at pH 4.5 trigger the high expression of this putative operon (Grimmler *et al.*, 2011). However, the pSOL1-free mutant did not produce any acetone and butanol during growth at pH 4.5, and ethanol formed during this phase was also decreased by 68.4% (~1.2 mM left) as compared to the wild type (Fig. 23). As a result, it seemed that solvents did not directly trigger the induction of this putative operon. During growth at pH 4.5, the pSOL1-free mutant synthesized excess acetate and butyrate as the predominant products. It is speculated that high levels of acetate and butyrate in the pSOL1-free mutant culture might be the main factor for the significant up-regulation of this cellulosome-like operon. In a word, the strong induction of the cellulosome-like operon might be a response to a combined stress of acetate and butyrate during growth at pH 4.5. It is important to mention that at pH 4.5 the transcript level of this cluster in the wild type was significantly induced as compared to that during acidogenesis of the wild type (Grimmler *et al.*, 2011), and the loss of the pSOL1 megaplasmid led to a further induction of this operon during growth at pH 4.5. The pSOL1-free mutant produced higher concentrations of acetate (81.8%) and butyrate (153.8%) than the wild type. It implied that ~11 mM acetate and ~13 mM butyrate in the wild type culture (at pH 4.5) were mild stresses for the cells, so that the expression of the cellulosome-like operon was increased. When the pSOL1 megaplasmid was removed from cells, higher concentrations of acids produced during growth at pH 4.5 made the stress more severe and the transcript level of this cluster was further enhanced as a

response.

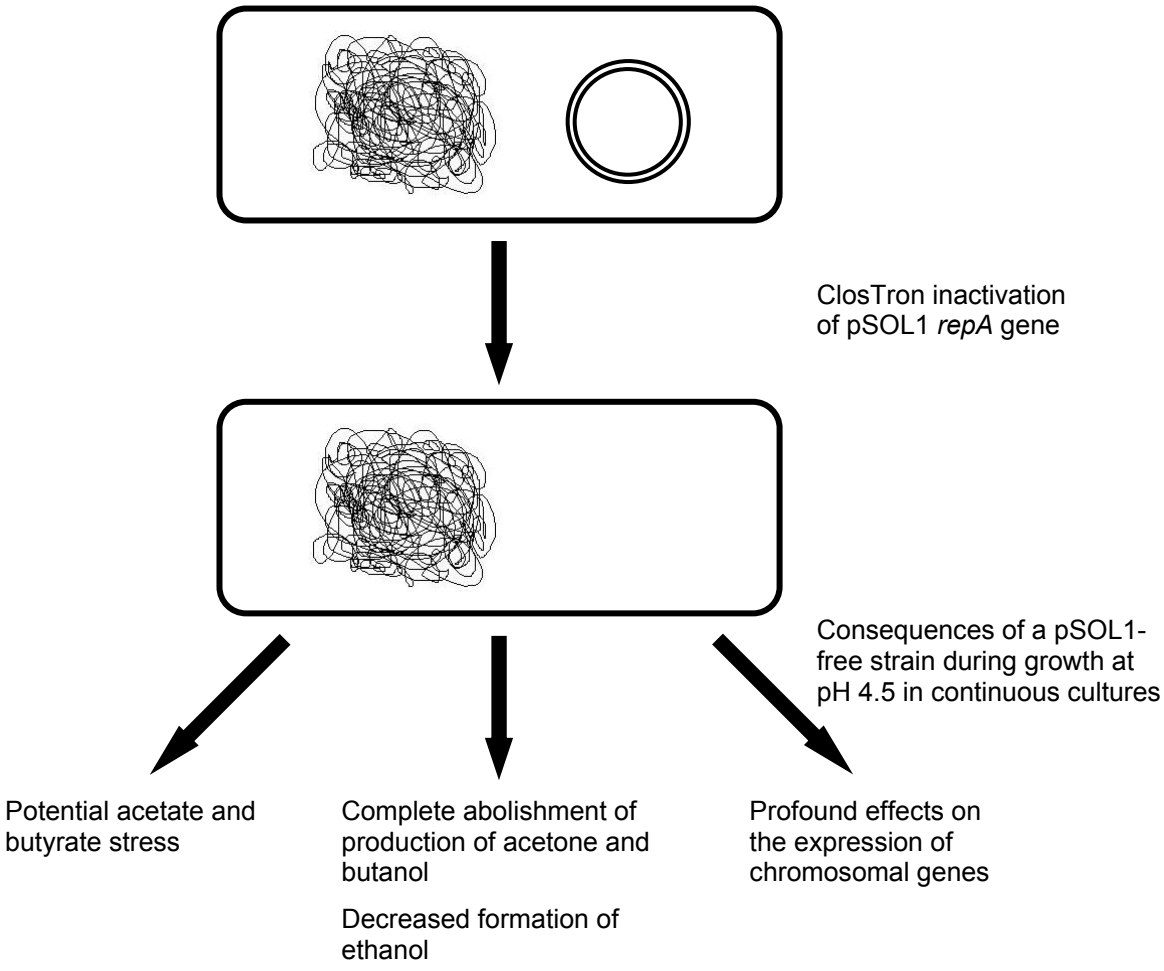

Fig. 31. Schematic diagram summarizing the consequences of absence of pSOL1 during growth at pH 4.5 in continuous cultures. The genome of *C. acetobutylicum* contains a chromosome and a pSOL1 megaplasmid. Knockout of the pSOL1 *repA* gene led to loss of the pSOL1 from the cells.

4.4.3 Physiological effects of the genes located on the pSOL1 megaplasmid

4.4.3.1 Physiological effects of the *adhE1* mutant during the steady-state acidogenic growth

During acidogenic growth of a continuous culture, acids were predominant products and the solvents acetone, butanol and ethanol were still slightly formed in the wild type (Fig. 4). During acidogenesis of the *adhE1* mutant culture, the production of acetone and butanol was strongly reduced as compared to the wild type, whereas ethanol and butyrate were generated at normal levels. The acetate concentration was slightly decreased (Fig. 29). These results suggested that the mutation of *adhE1* brought about positive effects on the production of acetone and butanol under acidogenic conditions.

The most remarkable expression pattern during acidogenic growth of the *adhE1* mutant culture was the induction of a huge cluster of genes related to fatty acid synthesis (*CA_C1988-CA_C2026*). But this has been discussed previously (section 4.4.1.4).

4.4.3.2 Physiological effects of the *adhE1* mutant during the steady-state solventogenic growth

Mutation of *adhE1* led to negligible generation of all three solvents and increased formation of acids under batch conditions (Cooksley *et al.*, 2012). In this study, an *adhE1* mutant was characterized in a continuous culture (Fig. 29). The results obtained further demonstrated that AdhE1 was an important enzyme for the production of butanol, but not obviously involved in ethanol formation. The concentration of ethanol during solventogenesis of the *adhE1* mutant was ~1.5 mM and the OD_{600} of the mutant culture was also decreased (~1.7) during this phase (in the wild type, ~3.8 mM ethanol/~3.8 OD_{600} was observed). The difference between both studies in terms of ethanol synthesis was likely attributed to the way of fermentation. A chemostat culture features separation of the two typical growth phases, i.e. acidogenesis and solventogenesis. This results in a solventogenic environment which is unaffected by acidogenesis. In the batch culture of the *adhE1* mutant, however, acid crash (Maddox *et al.*, 2000; Schuster *et al.*, 2001) might happen because of the accumulation of excess acids. During the steady-state solventogenic growth, the *adhE1* mutant produced only ~0.8 mM acetone. Inability to produce the wild type level of acetone was attributed to the simultaneous repression of *ctfAB* which formed a transcription unit together with *adhE1*. Down-regulation of *ctfAB* disturbed the synthesis of acetoacetate from acetoacetyl-CoA and the lack of these two enzymes led to a complete abolishment of acetone formation (Cooksley *et al.*, 2012; Lehmann *et al.*, 2012a).

During solventogenic growth of the *adhE1* mutant, the concentration of acetic acid was comparable to the wild type. It seemed that *adhE1* was not involved in acetate metabolism. As discussed previously, acetate uptake was not determined so far in a continuous culture (section 4.1.2). If it was absent, the *adhE1* mutant synthesized ~10 mM acetate under solventogenic conditions, which was similar to the wild type, suggesting that the mutation of *adhE1* did not exert an influence on the production of acetic acid. This was consistent with the unchanged expression levels of key genes (*pta* and *ack*) for acetate formation. On the other hand, the re-assimilation of acetic acid was interfered during the solventogenesis of the *adhE1* mutant culture, if acetate uptake was present. *adhE1* and *ctfAB* are part of the *sol* operon. The knock-out of *adhE1* led the simultaneous repression of *ctfAB* which is responsible for the acetate utilization (Lehmann *et al.*, 2012a; Cooksley *et al.*, 2012). Therefore, acetate uptake was blocked, if it was present, and the *adhE1* mutant only produced ~10 mM acetic acid. In a word, the *adhE1* mutant was able to synthesize ~10 mM of acetic acid during solventogenic growth no matter whether acetate uptake was present or not, and *adhE1* might affect the re-assimilation of acetic acid if the acetate uptake was present in a chemostat culture.

The concentration of butyric acid during solventogenesis of an *adhE1* mutant culture was similar to that of a pSOL1-free strain culture at pH 4.5 if the OD_{600} of the cultures was considered. At pH 4.5, ~33 mM butyrate was detected in the pSOL1-free mutant culture at an OD_{600} of ~2.5, and the *adhE1* mutant formed ~20 mM butyrate at an OD_{600} of ~1.7 (Fig. 23, 29). If butyrate uptake was absent in a continuous culture, the mutation of *adhE1* promoted the production of butyrate as compared to the wild type (~13 mM butyrate). If there was a butyrate utilization, the assimilated amount of butyric acid was negligible, because the butanol concentration detected during solventogenesis of the *adhE1* mutant was less than 3 mM. In other words, mutation of *adhE1* might affect butyrate uptake if it is present in a continuous culture. For the pSOL1-free mutant it was discussed that butanol production might be important for the butyrate uptake (section 4.4.2.3). That *adhE1* disruption resulted

in butyrate accumulation during solventogenesis further indicated that the re-assimilation of butyric acid might be dependent on butanol synthesis route.

4.4.3.3 Transcriptional characteristics of the *adhE1* mutant as compared to the wild type during the steady-state solventogenic growth

In the *adhE1* mutant culture, more than 200 genes were significantly regulated during both acidogenesis and solventogenesis (Table 34-37). This suggested that the mutation of *adhE1* had important influences on gene expression.

During solventogenesis of the *adhE1* mutant culture, *adhE2* was up-regulated by 9.1-fold, which revealed the negative correlation between these two genes coding for alcohol dehydrogenases (Table 36). This result was consistent with what was observed previously in a wild type continuous culture (Grimmler *et al.*, 2011) and Northern blots (Fontaine *et al.*, 2002), although *adhE2* was reported to be exclusively induced at high pH (pH 5.7 for acidogenesis and pH 6.50 for alcohologenesis) and *adhE1* was highly expressed only at pH 4.5. The result further indicated that *adhE1* negatively influenced the expression of *adhE2* during solventogenic growth. Moreover, the induction of *adhE2* during solventogenic growth of the *adhE1* mutant culture resulted in the production of a small amount of butanol (~2.8 mM) although *adhE1* was inactivated. This further demonstrated the importance of AdhE1 for butanol production. However, the expression patterns of *adhE2* was in fact complex. The expression of *adhE2* was repressed by 58% during acidogenesis of the *adhE1* mutant culture. This suggested that *adhE1* positively influenced *adhE2* transcript level at pH 5.7, which was different from their correlations during acidogenesis of a chemostat culture of the wild type (Grimmler *et al.*, 2011). In the wild type, *adhE2* was strongly induced during acidogenic growth, while *adhE1* was simultaneously repressed. The reason behind this difference could not be determined. Nevertheless, their expression patterns were consistent with the slight production of butanol during acidogenic growth of the continuous culture, i.e., ~4.6 mM butanol was produced in the wild type and in the *adhE1* mutant ~1.6 mM butanol was formed.

4.4.3.4 Physiological effects of a mutant in the predicted alcohol dehydrogenase CA_P0059

In addition to *adhE1* and *adhE2*, *CA_P0059* was the third alcohol dehydrogenase-coding gene located on the pSOL1 megaplasmid. The product of this gene had been suggested to be a key alcohol dehydrogenase for ethanol and butanol production (Papoutsakis, 2008) and only had 51% identity to a homologous counterpart in *Clostridium hylemonae* instead of other species of the genus *Clostridium* (Cooksley *et al.*, 2012). It was expected that inactivation of *CA_P0059* led to decreased production of all three solvents, but mutation of this gene resulted in elevated production of acetone, butanol and ethanol in a batch culture, for which authors could not give explanations (Cooksley *et al.*, 2012). In contrary, a chemostat culture of the *CA_P0059* mutant showed a completely different phenotype: The production of butanol and acetone were decreased by ~40% and the ethanol formation was declined by ~26% under solventogenic conditions (Fig. 30). This was probably attributed to the fermentation method and the medium used in this study. The CBM medium used in that study (Cooksley *et al.*, 2012) contained casein hydrolysate which might be favorable for the *CA_P0059* mutant. But the main reason might be the fermentation strategy. Continuous fermentation offered a constant environment for the cultivation and clear characterization of

acidogenesis and solventogenesis. Moreover, in a chemostat culture the pH was also stable and fresh medium kept feeding. Consequently, the observations described in this study was the authentic phenotype of the *CA_P0059* mutant during both acidogenesis and solventogenesis. Therefore, it could be argued that continuous culture is an optimal way for characterization of strains of *C. acetobutylicum*.

4.4.3.5 Physiological effects of a mutant in the glycogen-binding regulatory subunit of Serine/Threonine protein phosphatase I CA_P0129 (GbRs)

Acidogenic growth of a *CA_P0129* (*GbRs*) mutant culture resembled that of a wild type culture (Fig. 4, 28). During acidogenesis of the *GbRs* mutant, the expression of *adhE2* was elevated while *adhE1* was repressed, indicating they were both influenced by the *GbRs* gene. Again, the antagonistic correlation between *adhE1* and *adhE2* during acidogenesis was in agreement with an early report (Grimmler *et al.*, 2011). The down-regulation of *adhE1* and the induction of *adhE2* corresponded to the observation that butanol was produced at a slightly lower level (~3.4 mM) during this phase.

In addition, transcript levels of a gene cluster (*CA_C2086*-*CA_C2092*) coding for the stage III sporulation proteins (Nölling *et al.*, 2001) were significantly declined (Table 30) during acidogenic growth. This finding might be related to the phenotype that the *GbRs* mutant was unable to produce granulose on CBM agar plates (Fig. 27B-D). The stage III during sporulation features the production of granulose (Dürre, 2005).

During solventogenesis, the phenotype of the *GbRs* mutant was pretty much like that of the *CA_P0059* mutant (Fig. 28, 30): The production of solvents was decreased during solventogenic growth. The expression of a *pfor* (*CA_C2229*) was not changed when *GbRs* was inactivated (Table 28). This suggested that carbon flux was able to flow into C_4 pathways of the *GbRs* mutant without barriers. Moreover, the transcript levels of *thlA*, *hbd*, *crt* and *bcd*, the genes for the C_4 route, were all hardly altered. Nevertheless, it was observed for the *GbRs* mutant that the production of acetone and butanol was reduced by ~40% and glucose was consumed less than by the wild type. This suggested that the *GbRs* gene affected the production of acetone and butanol via a so far unknown pathway and by some unknown mechanisms the carbon flux through the C_4 route was changed. I speculate that during solventogenesis of the *GbRs* mutant, the significant induction of the *CA_P0037/36* operon (Janssen *et al.*, 2010) (Table 31) was probably involved in the reduced production of solvents. Because this operon also showed strong induction during solventogenic growth of the mutant of each gene of the *etfB-etfA-fcd* cluster (Table 11, 16, 21). In these three mutants, the production of solvents was decreased at pH 4.5 (Fig. 7, 10, 13), which resembled what was observed for the *GbRs* mutant. The *CA_P0037/36* operon was reported to be highly expressed during acidogenesis of continuous cultures of the wild type (Janssen *et al*., 2010; Grimmler *et al*., 2011) and its significant up-regulation during solventogenesis of these mutants generated in this study suggested that this operon might somehow be involved in inibition of solvent production. In other words, the stronger this operon was expressed during solventogenic growth, the less solvents might be produced. In addition, correlation of this transcriptional unit with sporulation was not reasonable. Because spores were washed out at the beginning of the continuous fermentation. The function of the *CA_P0037/36* operon during both acidogenesis and solventogenesis remains to be elucidated in future studies.

5 Summary

The rod-shaped, endospore-forming anaerobe bacterium *Clostridium acetobutylicum* produces butanol, acetone and ethanol during its fermentation. Biobutanol can be used as a regenerative fuel. In order to maximize the butanol yield, it is important to study the biochemistry of this bacterium. In this dissertation, eight mutants of *C. acetobutylicum* were generated using an intron-based ClosTron technology. The disrupted genes form an EtfA/B-dependent dehydrogenase system or are located on the pSOL1 megaplasmid. The resultant mutants, together with two mutants received from Prof. Nigel Minton (Nottingham University, UK), were characterized in phosphate-limited continuous cultures and by transcriptome analyses using DNA microarrays. The results obtained from the study of this set of ten mutants gave interesting new insights in the physiology of the solvent formation in *C. acetobutylicum*. The main results are as follows:

1. The clustered genes encoding the EtfA/B-Fcd dehydrogenase system are involved in the production of acetone, butanol and ethanol. The *etfB-etfA-fcd* gene cluster is able to affect carbon flux flowing through the C_4 pathways after glycolysis.

2. The *etfB-etfA-fcd* gene cluster probably possesses a self-regulation mechanism to control its own expression level.

3. Mutations in *etfA* and *etfB* of the *etfB-etfA-fcd* gene cluster exert stronger effects than *fcd* on acidogenic metabolism than on solventogenic physiology.

4. A mutation of the *bcd* gene that is part of the other EtfA/B-dependent dehydrogenase system EtfA/B-Bcd is probably lethal for *C. acetobutylicum*.

5. A gene coding for a heat-shock protein, *htpG*, does not influence the production of solvents and the concentrations of acetate and butyrate.

6. RepA and SpoOJ are responsible for the stable presence of the pSOL1 megaplasmid in *C. acetobutylicum*. Inactivation of either of the corresponding genes resulted in the loss of the pSOL1.

7. A pSOL1-free strain (the *repA* mutant) is able to grow in a continuous culture at pH 4.5 that triggers solventogenesis in the wild type. pSOL1 contains the potential key genes for the butyrate uptake, which considerably narrows down the candidates. Loss of pSOL1 leads to profound alteration of the expression of the chromosomal genes during both acidogenic and solventogenic growth, and results in potential acetate stress at pH 5.7 and a combined stress of acetate and butyrate at pH 4.5.

8. The production of acetone and butanol was completely abolished in a pSOL1-free strain (*repA* mutant) during the whole fermentation course. The defect may be largely attributed to the loss of the *sol* locus and *adc* located on the pSOL1.

9. Key genes responsible for ethanol formation do not reside on the pSOL1 megaplasmid but on the chromosome.

10. The gene encoding a glycogen regulator is indispensable for granulose formation, a typical event during the sporulation stage III. Deletion of this gene led to inability to

produce this storage substance. Moreover, a mutation of this regulator lowers solvent production.

11. The gene *adhE1* is the main alcohol dehydrogenase gene in *C. acetobutylicum*. This gene alters the expression of more than 200 (>5%) genes in acidogenic and solventogenic cells. It probably influences the re-assimilation of acetate and butyrate during solventogenic growth.

12. A mutation of the putative alcohol dehydrogenase CA_P0059 lowers the production of solvents.

13. Phosphate-limited continuous fermentations are a better strategy to characterize ClosTron mutants of *C. acetobutylicum* than traditional batch cultures.

14. The usage of the first generation ClosTron plasmid pMTL007 might result in insertions in second sites other than the target gene.

15. A DNA ligase-mediated PCR strategy was developed in this study. This method is timesaving and effective to determine the unknown insertion site of the intron on the chromosome.

16. The ClosTron system is reliable and reproducible for the generation of mutants of *C. acetobutylicum* and the Group II intron stays stably inserted during continuous fermentations.

6 Zusammenfassung

Das stäbchenförmige, Endosporen-bildende, anaerobe Bakterium *Clostridium acetobutylicum* bildet während des Gärungsstoffwechsels Butanol, Aceton und Ethanol. Biobutanol kann als regenerativer Kraftstoff verwendet werden. Für die Maximierung der Butanolausbeute ist es wichtig, die Biochemie dieses Bakteriums zu untersuchen. Im Rahmen der vorliegenden Arbeit wurden unter Einsatz der Intron-basierten ClosTron-Technik acht *C. acetobutylicum* Mutanten hergestellt. Die inaktivierten Zielgene stehen mit dem EtfA/B-abhängigen Dehydrogenasesystem im Zusammenhang oder befinden sich auf dem pSOL-Megaplasmid. Die generierten Mutanten wurden zusammen mit zwei Mutanten von Prof. Nigel Minton (Universität Nottingham, Vereinigtes Königreich) durch kontinuierliche Kultivierung und Transkriptomanalyse mit DNA-Microarrays charakterisiert. Die Resultate der Untersuchung dieses Satzes von 10 Mutanten führten zu interessanten neuen Erkenntnissen über die Physiologie der Lösungsmittelbildung in *C. acetobutylicum*. Die wesentlichen Ergebnisse können wie folgt zusammengefasst werden:

1. Die geclusterten Gene für das EtfA/B-Fcd Dehydrogenasesystem sind an der Bildung von Aceton, Butanol und Ethanol während des solventogenen Wachstums beteiligt. Das *etfB-etfA-fcd* Gencluster kann den Kohlenstoffflux durch die C_4-Wege im Anschluss an die Glykolyse beeinflussen.

2. Das *etfB-etfA-fcd* Gencluster besitzt vermutlich einen autoregulatorischen Mechanismus zur Kontrolle seiner Expression.

3. Mutationen in *etfA* und *etfB* des *etfB-etfA-fcd* Genclusters wirken sich stärker als *fcd* auf den acidogenenim Vergleich zum solventogenen Stoffwechsel aus.

4. Eine Inaktivierung des *bcd*-Gens, das für ein weiteres EtfA/B-abhängiges Dehydrogenasesystem codiert (EtfA/B-Bcd), ist vermutlich letal.

5. Ein Hitzeschock-Protein-kodierendes Gen, *htpG*, beeinflusst weder die Lösungsmittelbildung, noch die Konzentrationen von Acetat und Butyrat.

6. RepA und SpoOJ sind für die Stabilität des pSOL-Megaplasmids in *C. acetobutylicum* wesentlich. DieInaktivierung eines der korrespondierenden Gene führte zum Verlust von pSOL1.

7. Ein pSOL1-freier Stamm (die *repA*-Mutante) kann in kontinuierlicher Kultur auch bei pH 4,5, bei dem im Wildtyp Solventogenese ausgelöst wird, wachsen. pSOL1 trägt auch die potentiellen Schlüsselgene für die Butyrat-Aufnahme. Damit wird die Zahl von Kandidatengene dafür deutlich reduziert. Der Verlust von pSOL1 führt zu grundlegenden Änderungen in der Expression chromosomaler Gene während des acidogenen und solventogenen Wachstums und zu potentiellem Acetatstress bei pH 5,7 sowie kombiniertem Acetat- und Butyratstress bei pH 4,5.

8. Die Bildung von Aceton und Butanol war in einem pSOL1-freien Stamm (*repA*-Mutante) während des gesamten Fermentationsverlaufs vollständig unterbunden. Dieser Defekt wurde vermutlich vor allem durch den Verlust des *sol*-Locus und von *adc* auf pSOL1 verursacht.

9. Schlüsselgene für die Ethanolbildung sind nicht auf pSOL1 sondern chromosomal lokalisiert.

10. Das Gen für einen Glycogen-Regulator ist für die Granulosebildung, die typischer Weise während Sporulationsphase III auftritt, unverzichtbar. Eine Deletion dieses Gens führte zum Unvermögen, diesen Speicherstoff zu bilden. Der Glykogenregulatorwirkt sich auchpositiv auf die Lösungmittelbildung aus.

11. Das *adhE1*-Gen ist die Haupt-Alkoholdehydrogenase in *C. acetobutylicum*. Dieses Gen beeinflusst die Expression von über 200 (>5%) Genen in acidogenen und solventogenen Zellen. Vermutlich spielt es eine Rolle für die Assimilierung von Acetat und Butyrat während des solventogenen Wachstums.

12. Eine Mutation der putativen Alkoholdehydrogenase, CA_P0059, führt zur verminderten Bildung von Lösungsmitteln.

13. Phosphat-limitierte kontinuierliche Fermentationensind für die Charakterisierung von ClosTron-Mutanten von *C. acetobutylicum* besser geeignet als traditionelle *Batch*-Kulturen.

14. Die Verwendung des ClosTron-Plasmids pMTL007 der ersten Generation kann zu weiteren Insertionen, außer imim Zielgen führen.

15. In dieser Arbeit wurde eine DNA-Ligase-vermittelte PCR Strategie entwickelt. Diese zeitsparende und effektive Methode dient zum Nachweis der unbekannten Insertionsstelle des Introns auf dem Chromosom.

16. Das ClosTron-System war zuverlässig und reproduzierbar für die Herstellung von *C. acetobutylicum* Mutanten, und das Gruppe II Intron blieb während kontinuierlicher Fermentationen stabil integriert.

7 References

Alsaker KV and Papoutsakis ET (2005) Transcriptional Program of Early Sporulation and Stationary-Phase Events in *Clostridium acetobutylicum*. ***J Bacteriol***, 187(20):7103

Alsaker KV, Paredes C, Papoutsakis ET (2010) Metabolite stress and tolerance in the production of biofuels and chemicals: gene-expression-based systems analysis of butanol, butyrate, and acetate stresses in the anaerobe *Clostridium acetobutylicum*. ***Biotechnol Bioeng***, 105:1131-1147

Amador-Noguez D, Feng XJ, Fan J, Roquet N, Rabitz H, Rabinowitz JD (2010) Systems-level metabolic flux profiling elucidates a complete, bifurcated TCA cycle in *Clostridium acetobutylicum*. ***J Bacteriol***, 192:4452-4461

Andersch W, Bahl H, Gottschalk G (1983) Levels of enzymes involved in acetate, butyrate, acetone and butanol formation by *Clostridium acetobutylicum*. ***Eur J Appl Microbiol Biotechnol***, 18:327–332

Bahl H, Andersch W, Gottschalk G (1982) Continuous production of acetone and butanol by *Clostridium acetobutylicum* in a two-stage phosphate limited chemostat. ***Eur J Appl Microbiol Biotechnol***, 15:201-205

Bahl H, Gottwald M, Kuhn A, Rale V, Andersch W, Gottschalk G (1986) Nutritional Factors Affecting the Ratio of Solvents Produced by *Clostridium acetobutylicum*. ***Appl Environ Microbiol***, 52(1):169-72

Baldwin RL and Milligan LP (1964) Electron transport in *Peptostreptococcus elsdenii*. ***Biochim Biophys Acta***, 92:421-432

Bao G, Wang R, Zhu Y, Dong H, Mao S, Zhang Y, Chen Z, Li Y, Ma Y (2011) Complete genome sequence of *Clostridium acetobutylicum* DSM 1731, a solvent-producing strain with multireplicon genome architecture. ***J Bacteriol***, 193(18):5007-8

Bi C, Jones SW, Hess DR, Tracy BP, Papoutsakis ET (2011) SpoIIE is necessary for asymmetric division, sporulation, and expression of σ^F, σ^E, and σ^G but does not control solvent production in *Clostridium acetobutylicum* ATCC 824. ***J Bacteriol***, 193(19): 5130-5137

Boynton ZL, Bennet GN, Rudolph FB (1996) Cloning, sequencing, and expression of clustered genes encoding beta-hydroxybutyrylcoenzyme A (CoA) dehydrogenase, crotonase, and butyryl-CoA dehydrogenase from *Clostridium acetobutylicum* ATCC 824. ***J Bacteriol***, 178:3015–3024

Brockman HL Jr (1971) Doctoral dissertation, Michigan State University

Brückner R & Titgemeyer F (2002) Carbon catabolite repression in bacteria: choice of the carbon source and autoregulatory limitation of sugar utilization. ***FEMS Microbiol Lett***, 209: 141–148

Clark SW, Bennett GN, Rudolph FB (1989) Isolation and Characterization of Mutants of *Clostridium acetobutylicum* ATCC 824 Deficient in Acetoacetyl-Coenzyme A:Acetate/Butyrate:Coenzyme A-Transferase (EC 2.8.3.9) and in Other Solvent Pathway Enzymes. ***Appl Environ Microbiol***, 55(4):970-6

Cooksley CM, Zhang Y, Wang H, Redl S, Winzer K, Minton NP (2012) Targeted mutagenesis of the *Clostridium acetobutylicum* acetone-butanol-ethanol fermentation pathway. ***Metab Eng***, 14(6):630-41

Cornillot E, Nair RV, Papoutsakis ET, Soucaille P (1997) The genes for butanol and acetone formation in *Clostridium acetobutylicum* ATCC 824 reside on a large plasmid whose loss leads to degeneration of the strain. ***J Bacteriol***, 179(17):5442

Datta R and Zeikus JG (1985) Modulation of acetone-butanol-ethanol fermentation by carbon monoxide and organic acids. ***Appl Environ Microbiol***, 49:522-529

Desai RP, Harris LM, Welker NE, Papoutsakis ET (1999) Metabolic flux analysis elucidates the importance of the acid-formation pathways in regulating solvent production by *Clostridium acetobutylicum*. ***Metab Eng***, 1:206–213

Dong H, Zhang Y, Li Y (2010) Genetic modification systems for *Clostridium acetobutylicum*. ***Sheng Wu Gong Cheng Xue Bao***, 26(10):1372-8

Doremus MG, Linden JC, and Moreira AR (1985) Agitation and pressure effect on acetone butanol fermentation. ***Biotechnol Bioeng***, 27:852–860

Dürre P, Fischer RJ, Kuhn A, Lorenz K, Schreiber W, Sturzenhofecker B, Ullmann S, Winzer K, and Sauer U (1995) Solventogenic enzymes of *Clostridium acetobutylicum*: catalytic properties, genetic organization, and transcriptional regulation. ***FEMS Microbiol Rev***, 17:251–262

Dürre P (2005) Hankbook on clostridia. CRC Press

Dürre P (2007) Biobutanol: an attractive biofuel. ***Biotechnol J***, 2:1525–1534

Ehrenreich A (2006) DNA microarray technology for the microbiologist: an overview. ***Appl Microbiol Biotechnol***, 73:255-273

Engel PC (1981) Butyryl-CoA dehydrogenase from *Megasphaera elsdenii*. ***Methods Enzymol***, 71:359–366

Ezeji T, Blaschek H (2008) Fermentation of dried distillers' grains and solubles (DDGS) hydrolysates to solvents and value-added products by solventogenic Clostridia. ***Bioresource Technol***, 99, 5232-5242

Fitzpatrick JM, Johnston DA, Williams GW, Williams DJ, Freeman TC, Dunne DW, Hoffmann KF (2005) An oligonucleotide microarray for transcriptome analysis of *Schistosoma mansoni* and its application/use to investigate gender-associated gene expression. ***Mol Biochem Parasitol***, 141: 1-13

Fontaine L, Meynial-Salles I, Girbal L, Yang X, Croux C, Soucaille P (2002) Molecular characterization and transcriptional analysis of adhE2, the gene encoding the NADH-dependent aldehyde/alcohol dehydrogenase responsible for butanol production in alcohologenic cultures of *Clostridium acetobutylicum* ATCC 824. ***J Bacteriol***, 184(3):821-30

Gavard R and Milhaud G (1952) Ann. Inst. Pasteur Paris 82, 470-488

González-Pajuelo M, Meynial-Salles I, Mendes F, Andrade JC, Vasconcelos I, Soucaille P (2005) Metabolic engineering of *Clostridium acetobutylicum* for the industrial production of 1,3-propanediol from glycerol. ***Metab Eng***, 7(5-6):329-36

González-Pajuelo M, Meynial-Salles I, Mendes F, Soucaille P, Vasconcelos I (2006) Microbial conversion of glycerol to 1,3-propanediol: physiological comparison of a natural producer, *Clostridium butyricum* VPI 3266, and an engineered strain, *Clostridium acetobutylicum* DG1(pSPD5). ***Appl Environ Microbiol***, 72(1):96-101

Grimmler C, Held C, Liebl W, Ehrenreich A (2010) Transcriptional analysis of catabolite repression in *Clostridium acetobutylicum* growing on mixtures of D-glucose and D-xylose. ***J Biotechnol***, 150(3):315-23

Grimmler C., Janssen H., Krauße D., Fischer R. -J., Bahl H., Dürre P., Liebl W., Ehrenreich (2011) A Genome-Wide Gene Expression Analysis of the Switch between Acidogenesis and Solventogenesis in Continuous Cultures of *Clostridium acetobutylicum*. ***J Mol Microbiol Biotechnol***, 20:1–15

Harris LM, Welker NE, Papoutsakis ET (2002) Northern, morphological, and fermentation analysis of spo0A inactivation and overexpression in *Clostridium acetobutylicum* ATCC 824. ***J Bacteriol***, 184(13):3586-97

Hartmanis MGN and Gatenbeck S (1984a) Intermediary metabolismin *Clostridium acetobutylicum*: levels of enzymes involved in the formation of acetate and butyrate. ***Appl Environ Microbiol***, 47:1277–1283

Hartmanis MGN, Klason T, Gatenbeck S (1984b) Uptake and activation of acetate and butyrate in *Clostridium acetobutylicum*. ***Appl Microbiol Biotechnol***,20:66–71

Heap JT, Pennington OJ, Cartman ST, Carter GP, Minton NP (2007) The ClosTron: a universal gene knock-out system for the genus *Clostridium*. ***J Microbiol Methods***, 70(3):452-64

Heap JT, Cartman ST, Kuehne SA, Cooksley C, Minton NP (2010a) ClosTron-targeted mutagenesis. ***Methods Mol Biol***, 646:165-82.

Heap JT, Kuehne SA, Ehsaan M, Cartman ST, Cooksley CM, Scott JC, Minton NP (2010b) The ClosTron: Mutagenesis in *Clostridium* refined and streamlined. ***J Microbiol Methods***, 80(1):49-55

Herrmann G, Jayamani E, Mai G, Buckel W (2008) Energy conservation via electron-transferring flavoprotein in anaerobic bacteria. ***J Bacteriol***, 190(3):784-91

Hetzel M, Brock M, Selmer T, Pierik AJ, Golding BT, Buckel W (2003) Acryloyl-CoA reductase from *Clostridium propionicum*: An enzyme complex of propionyl-CoA dehydrogenase and electron-transferring flavoprotein. ***Eur J Biochem***, 270(5):902-10

Hillmann F, Döring C, Riebe O, Ehrenreich A, Fischer RJ, Bahl H (2009) The role of PerR in O_2-affected gene expression of *Clostridium acetobutylicum.* ***J Bacteriol,*** 191(19):6082-93

Ho SN, Hunt HD, Horton RM, Pullen JK, Pease LR (1989) Site-directed mutagenesis by overlap extension using the polymerase chain reaction. ***Gene***, 77:51–59

Hou X, Peng W, Xiong L, Huang C, Chen X, Chen X, Zhang W. (2013) Engineering *Clostridium acetobutylicum* for alcohol production. ***J Biotechnol***, 166(1-2):25-33

Hönicke D (2014) Doctoral dissertation. Technical University of Munich

Hu S, Zheng H, Gu Y, Zhao J, Zhang W, Yang Y, Wang S, Zhao G, Yang S, Jiang W (2011) Comparative genomic and transcriptomic analysis revealed genetic characteristics related to solvent formation and xylose utilization in *Clostridium acetobutylicum* EA 2018. ***BMC Genomics***, 12:93

Inui M, Suda M, Kimura S, Yasuda K, Suzuki H, Toda H, Yamamoto S, Okino S, Suzuki N, Yukawa H. (2008) Expression of *Clostridium acetobutylicum* butanol synthetic genes in *Escherichia coli*. ***Appl Microbiol Biotechnol***, 77(6):1305-16

Ireton K, Gunther NW, Grossman AD (1994) *spo0J* is required for normal chromosome segregation as well as the initiation of sporulation in *Bacillus subtilis*. ***J Bacteriol***, 176:5320–5329

Jang YS, Lee JY, Lee J, Park JH, Im JA, Eom MH, Lee J, Lee SH, Song H, Cho JH, Seung do Y, Lee SY. (2012) Enhanced butanol production obtained by reinforcing the direct butanol-forming route in *Clostridium acetobutylicum*. ***mBio***, 3(5):e00314-12

Janssen H, Döring C, Ehrenreich A, Voigt B, Hecker M, Bahl H, Fischer RJ (2010) A proteomic and transcriptional view of acidogenic and solventogenic steady-state cells of *Clostridium acetobutylicum* in a chemostat culture. ***Appl Microbiol Biotechnol***, 87:2209-2226

Janssen H, Grimmler C, Ehrenreich A, Bahl H, Fischer RJ (2012) A transcriptional study of acidogenic chemostat cells of *Clostridium acetobutylicum*-solvent stress caused by a transient n-butanol pulse. ***J Biotechnol***, 161(3):354-65

Jiang Y, Xu C, Dong F, Yang Y, Jiang W, Yang S (2009) Disruption of the acetoacetate decarboxylase gene in solvent-producing *Clostridium acetobutylicum* increases the butanol ratio. ***Metab Eng***, 11:284–291

Jones DT and Woods DR (1986) Acetone-butanol fermentation revisited. ***Microbiol Rev***, 50:484–524

Jones SW, Paredes CJ, Tracy B, Cheng N, Sillers R, Senger RS, Papoutsakis ET (2008) The transcriptional program underlying the physiology of clostridial sporulation. ***Genome Biol***, 9(7):R114

Jones SW, Tracy BP, Gaida SM, Papoutsakis ET (2011) Inactivation of σ^F in *Clostridium acetobutylicum* ATCC 824 blocks sporulation prior to asymmetric division and abolishes σ^E and σ^G protein expression but does not block solvent formation. ***J Bacteriol***, 193(10):2429-40

Junelles AM, Janiti-Idrissi R, Petitdemange H, Gay R (1988) Iron effect on acetone-butanol fermentation. ***Curr Microbiol***, 17:299–303

Kadoya R, Baek JH, Sarker A, Chattoraj DK (2011) Participation of chromosome segregation protein ParAI of *Vibrio cholerae* in chromosome replication. ***J Bacteriol***, 193(7):1504-14

Kelly DP, Kim JJ, Billadello JJ, Hainline BE, Chu TW, Strauss AW (1987) Nucleotide sequence of medium-chain acyl-CoA dehydrogenase mRNA and its expression in enzyme-deficient human tissue. ***Proc Nat Acad Sci***, 84:4068–4072

Kim BH, Bellows P, Datta R, and Zeikus JG (1984) Control of carbon and electron flow in *Clostridium acetobutylicum* fermentation: utilization of carbon monoxide to inhibit hydrogen production and to enhance butanol yields. ***Appl Environ Microbiol***, 48:764-770

Kim TS and Kim BH (1988) Electron flow shift in *Clostridium acetobutylicum* fermentation by electrochemically introduced reducing equivalent. ***Biotechnol Lett***, 10:123–128

Kuit W, Minton NP, López-Contreras AM, Eggink G (2012) Disruption of the acetate kinase (ack) gene of *Clostridium acetobutylicum* results in delayed acetate production. ***Appl Microbiol Biotechnol***, 94(3):729-41

Lambowitz AM and Zimmerly S (2011) Group II introns: mobile ribozymes that invade DNA. ***Cold Spring Harbor Perspect. Biol***, 3(8): a003616

Lee SF, Forsberg CW, Gibbins LN (1985) Cellulolytic activity of *Clostridium acetobutylicum*. ***Appl Environ Microbiol***, 50:220–228

Lee JY, Jang YS, Lee J, Papoutsakis ET, Lee SY (2009) Metabolic engineering of *Clostridium acetobutylicum* M5 for highly selective butanol production. ***Biotechnol J***, 4(10):1432-40

Lehmann D and Lütke-Eversloh T (2011) Switching *Clostridium acetobutylicum* to an ethanol producer by disruption of the butyrate/butanol fermentative pathway. ***Metab Eng***, 13(5):464-73

Lehmann D, Hönicke D, Ehrenreich A, Schmidt M, Weuster-Botz D, Bahl H, Lütke-Eversloh T. (2012a) Modifying the product pattern of *Clostridium acetobutylicum*: physiological effects of disrupting the acetate and acetone formation pathways. ***Appl Microbiol Biotechnol***, 94(3):743-54.

Lehmann D, Radomski N, Lütke-Eversloh T (2012b) New insights into the butyric acid metabolism of *Clostridium acetobutylicum*. ***Appl Microbiol Biotechnol***, 96(5):1325-39

Leonardo MR, Cunningham PR, and Clark DP (1993) Anaerobic regulation of the adhE gene, encoding the fermentative alcohol dehydrogenase of *Escherichia coli*. ***J Bacteriol***, 175:870–878

Li F, Hinderberger J, Seedorf H, Zhang J, Buckel W, Thauer RK (2008) Coupled ferredoxin and crotonyl coenzyme A (CoA) reduction with NADH catalyzed by the butyryl-CoA dehydrogenase/Etf complex from *Clostridium kluyveri*. ***J Bacteriol***, 190(3):843-50

Lin DC and Grossman AD (1998) Identification and characterization of a bacterial chromosome partitioning site. ***Cell***, 92(5):675-85

Lopez-Contreras AM, Martens AA, Szijarto N, Mooibroek H, Claassen PA, van der Oost J, de Vos WM (2003) Production by *Clostridium acetobutylicum* ATCC 824 of CelG, a cellulosomal glycoside hydrolase belonging to family 9. ***Appl Environ Microbiol***, 69:869–877

Maddox IS (1980) Production of n-butanol from whey filtrate using *Clostridium acetobutylicum* N.C.I.B. 2951. ***Biotechnol Lett***, 2:493-498

Maddox IS, Steiner E, Hirsch S, Wessner S, Gutierrez NA, Gapes JR, Schuster KC (2000) The cause of "acid-crash" and "acidogenic fermentations" during the batch acetone-butanol-ethanol (ABE-) fermentation process. ***J Mol Microbiol Biotechnol***, 2(1):95-100

Mao S, Luo Y, Zhang T, Li J, Bao G, Zhu Y, Chen Z, Zhang Y, Li Y, Ma Y (2010) Proteome reference map and comparative proteomic analysis between a wild type *Clostridium acetobutylicum* DSM 1731 and its mutant with enhanced butanol tolerance and butanol yield. ***J Proteome Res***, 9(6):3046-61

Mao S, Luo Y, Bao G, Zhang Y, Li Y, Ma Y (2011) Comparative analysis on the membrane proteome of *Clostridium acetobutylicum* wild type strain and its butanol-tolerant mutant. ***Mol Biosyst***, 7(5):1660-77

Matsubara, Y., J. Kraus, H. Ozasa, R. Glassberg, G. Finocchiaro, Y. Ikeda, J. Mole, L. E. Rosenberg, and K. Tanaka. (1987) Molecular cloning and nucleotide sequence of cDNAs encoding the entire precursors of rat liver medium chain acyl coenzyme A dehydrogenase. ***J Biol Chem***, 262:10104–10108

Matsubara Y, Indo Y, Naito E, Ozasa H, Glassberg R, Vockley J, Ikeda Y, Kraus J, Tanaka K (1989) Molecular cloning and nucleotide sequence of cDNAs encoding the precursors of rat long chain acyl-coenzyme A, short chain acyl-coenzyme A, and isovaleryl-coenzyme A dehydrogenases. ***J Biol Chem***, 264:16321–16331

Mendes FS, González-Pajuelo M, Cordier H, François JM, Vasconcelos I (2011) 1,3-Propanediol production in a two-step process fermentation from renewable feedstock. ***Appl Microbiol Biotechnol***, 92(3):519-27

Mermelstein LD, Papoutsakis ET, Petersen DJ, and Bennett GN (1993) Metabolic engineering of *Clostridium acetobutylicum* ATCC 824 for increased solvent production by enhancement of acetone formation enzyme activities using a synthetic acetone operon. ***Biotechnol Bioeng***, 42:1053– 1060

Meyer CL, Roos JW, Papoutsakis ET (1986) Carbon monoxide gasing leads to alcohol production and butyrate uptake without acetone formation in continuous cultures of *Clostridium acetobutylicum*. ***Appl Microbiol Biotechnol***, 24:159–167

Mills DA, Manias DA, McKay LL, Dunny GM (1997) Homing of a group II intron from *Lactococcus lactis* subsp. lactis ML3. ***J Bacteriol***, 179(19):6107-11

Mitchell WJ (1998) Physiology of carbohydrate to solvent conversion by clostridia. ***Adv Microb Physiol***, 39:31–130

Murray H and Errington J (2008) Dynamic control of the DNA replication initiation protein DnaA by Soj/ParA. ***Cell***, 135(1):74-84

Nair RV and Papoutsakis ET (1994) Expression of plasmid-encoded aad in *Clostridium acetobutylicum* M5 restores vigorous butanol production. ***J Bacteriol***, 176:5843–5846

Nair RV (1995) Ph.D. dissertation. Northwestern University, Evanston, Ill.

Naito E, Ozasa H, Ikeda Y, Tanaka K (1989) Molecular cloning and nucleotide sequence of complementary DNAs encoding human short chain acyl coenzyme A dehydrogenase and the study of the molecular basis of human short chain acyl-coenzyme A dehydrogenase deficiency. ***J Clin Invest***, 83:1605–1613

Nölling J, Breton G, Omelchenko MV, MakarovaKS, Zeng Q, Gibson R, Lee HM, Dubois J,Qiu D, Hitti J, Wolf YI, Tatusov RL, SabatheF, Doucette-Stamm L, Soucaille P, Daly MJ,Bennett

GN, Koonin EV, Smith DR (2001) Genomesequence and comparative analysis of thesolvent-producing bacterium *Clostridium acetobutylicum* . ***J Bacteriol***, 183: 4823–4838

O'Brien RW, Morris JG (1971) Oxygen and the growth and metabolism of *Clostridium acetobutylicum*. ***J Gen Microbiol***, 68:307–318.

O'Neill H, Mayhew SG, Butler G (1998) Cloning and analysis of the genes for a novel electron-transferring flavoprotein from *Megasphaera elsdenii*. Expression and characterization of the recombinant protein. ***J Biol Chem***, 273(33):21015-24

Papoutsakis ET (2008) Engineering solventogenic clostridia. ***Curr Opin Biotechnol***, 19(5):420-9

Paredes CJ, Alsaker KV, Papoutsakis ET (2005) A comparative genomic view of clostridial sporulation and physiology. ***Nat Rev Microbiol***, 3(12): 969–978

Peguin S, Delorme P, Goma G, and Soucaille P (1994a) Enhanced alcohol yields in batch cultures of *Clostridium acetobutylicum* using a three-electrode potentiometric system with methyl viologen as electron carrier. ***Biotechnol Lett***, 16:269–274

Peguin S, Goma G, Delorme P and Soucaille P (1994b) Metabolic flexibility of *Clostridium acetobutylicum* in response to methyl viologen addition. ***Appl Microbiol Biotechnol***, 42(4): 611-616

Peguin S and Soucaille P (1995) Modulation of carbon and electron flow in *Clostridium acetobutylicum* by iron limitation and methyl viologen addition. ***Appl Environ Microbiol***, 61(1):403

Perutka J, Wang W, Goerlitz D, Lambowitz AM (2004) Use of computer-designed group II introns to disrupt *Escherichia coli* DExH/D-box protein and DNA helicase genes. ***J Mol Biol***, 336(2):421-39

Rao G and Mutharasan R (1986) Alcohol production by *Clostridium acetobutylicum* induced by methyl viologen. ***Biotechnol Lett***, 8:893–896

Rao G and Mutharasan R (1987) Altered electron flow in continuous cultures of *Clostridium acetobutylicum* induced by viologen dyes. ***Appl Environ Microbiol***, 53:1232–1235.

Reed DW and Hartzell PL (1999) The *Archaeoglobus fulgidus* D-lactate dehydrogenase is a Zn^{2+} flavoprotein. ***J Bacteriol***, 181, 7580–7587

Reid SJ (2005) Genetic organization and regulation of hexose and pentose utilization in the clostridia. Handbook on Clostridia, pp. 133-153. Edited by P. Durre. Boca Raton, FL: CRC Press.

Rellos P, Ma J, Scopes RK (1997) Alteration of substrate specificity of *Zymomonas mobilis* alcohol dehydrogenase-2 using in vitro random mutagenesis. ***Protein Expr Purif***, 9:83–90

Ren C (2010) Identification and inactivation of pleiotropic regulator CcpA to eliminate glucose repression of xylose utilization in *Clostridium acetobutylicum*. ***Metab Eng***, 12:446–454.

Robson RL, Robson RM, Morris JG (1974) The biosynthesis of granulose by *Clostridium pasteurianum*. ***Biochem J***, 144(3):503-511

Rodionov DA, Mironov AA & Gelfand MS (2001) Transcriptional regulation of pentose utilisation systems in the *Bacillus/Clostridium* group of bacteria. ***FEMS Microbiol Lett***, 205:305– 314

Sambrook J (2001) *Molecular Cloning: A Laboratory Manual* Cold Spring Harbor Laboratory.

Sambrook J and Russell DW (2006) Purification of nucleic acids by extraction with phenol:chloroform. ***Cold Spring Harb Protoc***, doi:10.1101/pdb.prot4455

Satomura T, Kawakami R, Sakuraba H, Ohshima T (2002) Dye-linked D-proline dehydrogenase from hyperthermophilic archaeon *Pyrobaculum islandicum* is a novel FAD-dependent amino acid dehydrogenase. ***J Biol Chem***, 277:12861–12867

Schaffer S, Isci N, Zickner B, Dürre P (2002) Changes in protein synthesis and identification of proteins specifically induced during solventogenesis in *Clostridium acetobutylicum*. ***Electrophoresis***, 23:110–121

Schwarz KM, Kuit W, Grimmler C, Ehrenreich A, Kengen SW (2012) A transcriptional study of acidogenic chemostat cells of *Clostridium acetobutylicum*-cellular behavior in adaptation to n-butanol. ***J Biotechnol***, 161(3):366-77

Schuster KC, Goodacre R, Gapes JR, and Young M (2001) Degeneration of solventogenic *Clostridium* strains monitored by Fourier transform infrared spectroscopy of bacterial cells. ***J Ind Microbiol Biotechnol***, 27:314–321

Servinsky MD, Kiel JT, Dupuy NF, Sund CJ (2010) Transcriptional analysis of differential carbohydrate utilization by *Clostridium acetobutylicum*. ***Microbiology***, 156(11):3478-91

Sillers R, Chow A, Tracy B, Papoutsakis ET. (2008) Metabolic engineering of the non-sporulating, non-solventogenic *Clostridium acetobutylicum* strain M5 to produce butanol without acetone demonstrate the robustness of the acid-formation pathways and the importance of the electron balance. ***Metab Eng***, 10(6):321-32

Sonenshein A, Hoch J, and Losick R (ed.) (2002) *Bacillus subtilis* and its closest relatives: from genes to cells. ASM Press, Washington, D.C.

Steiner E, Dago AE, Young DI, Heap JT, Minton NP, Hoch JA, Young M (2011a) Multiple orphan histidine kinases interact directly with Spo0A to control the initiation of endospore formation in *Clostridium acetobutylicum*. ***Mol Microbiol***, 80(3):641-54

Steiner E, Scott J, Minton NP, Winzer K (2011b) An agr quorum sensing system that regulates granulose formation and sporulation in *Clostridium acetobutylicum*. ***Appl Environ Microbiol***, 78(4):1113-22

Tomas CA, Alsaker KV, Bonarius HP, Hendriksen WT, Yang H, Beamish JA, Paredes CJ, Papoutsakis ET (2003) DNA array-based transcriptional analysis of asporogenous, nonsolventogenic *Clostridium acetobutylicum* strains SKO1 and M5. ***J Bacteriol***, 185(15):4539-47

Tracy BP, Jones SW, Papoutsakis ET (2011) Inactivation of σ^E and σ^G in *Clostridium acetobutylicum* illuminates their roles in clostridial-cell-form biogenesis, granulose synthesis, solventogenesis, and spore morphogenesis. ***J Bacteriol***, 193(6):1414-26

Van Berkel WJ, Van den Berg WA, Müller F (1988) Large-scale preparation and reconstitution of apo-flavoproteins with special reference to butyryl-CoA dehydrogenase from *Megasphaera elsdenii*. Hydrophobic-interaction chromatography. ***Eur J Biochem***, 178(1):197-207

Vasileva D, Janssen H, Hönicke D, Ehrenreich A, Bahl H (2012) Effect of iron limitation and fur gene inactivation on the transcriptional profile of the strict anaerobe *Clostridium acetobutylicum*. ***Microbiology,*** 158(7):1918-29

Ventura JR, Hu H, Jahng D (2013) Enhanced butanol production in *Clostridium acetobutylicum* ATCC 824 by double overexpression of 6-phosphofructokinase and pyruvate kinase genes. ***Appl Microbiol Biotechnol***, 97(16):7505-16

Whyte JNC and Strasdine GA (1972) Carbohyd. Res. 25, 435-443

Xiao H, Gu Y, Ning Y, Yang Y, Mitchell WJ, Jiang W, Yang S (2011) Confirmation and elimination of xylose metabolism bottlenecks in glucose phosphoenolpyruvate-dependent phosphotransferase system-deficient *Clostridium acetobutylicum* for simultaneous utilization of glucose, xylose, and arabinose. ***Appl Environ Microbiol***, 77(22):7886-7895

Yang SY and Elzinga M (1993) Association of both coenzyme A hydratase and 3-hydroxyacyl coenzyme A epimerase with an active site in the aminoterminal domain of the multifunctional fatty acid oxidation protein from *Escherichia coli*. ***J Biol Chem***, 268:6588–6592

Yang XYH, Schulz H, Elzinga M, and Yang SY (1991) Nucleotide sequence of the promoter and fadB gene of the fadBA operon and primary structure of the multifunctional fatty acid oxidation protein from *Escherichia coli*. ***Biochemistry***. 30:6788–6795

Yerushaimi L and Volesky B (1985) Importance of agitation in acetone-butanol fermentation. ***Biotechnol Bioeng***, 27:1297–1305

Youngleson JS, Jones DT, Woods DR (1989) Homology between hydroxybutyryl and hydroxyacyl coenzyme A dehydrogenase enzymes from *Clostridium acetobutylicum* fermentation and vertebrate fatty-acid b-oxidation pathways. ***J Bacteriol***, 171:6800–6807

Zhang Y, Chen J, Yang Y, Jiao R (1996) Breeding of High-Ratio Butano Strains of *Clostridicum acetobutylicum* and Application to Industrial Production. ***Indust Microbiol***, 26:1–6

8 Appendix

Table 38. Primers for the ClosTron mutagenesis

Name	**Sequence** (5'→3')
EBS universal	CGAAATTAGAAACTTGCGTTCAGTAAAC
fcd-IBS	AAAAAAGCTTATAATTATCCTTAAATTTCACTCTAGTGCGCCC AGATAGGGTG
fcd-EBS1d	CAGATTGTACAAATGTGGTGATAACAGATAAGTCACTCTAAC TAACTTACCTTTCTTTGT
fcd-EBS2	TGAACGCAAGTTTCTAATTTCGGTTAAATTCCGATAGAGGAA AGTGTCT
*bcd*1-IBS	AAAAAAGCTTATAATTATCCTTAGTTGCCGATACTGTGCGCCC AGATAGGGTG
*bcd*1-EBS1d	CAGATTGTACAAATGTGGTGATAACAGATAAGTCGATACTTT TAACTTACCTTTCTTTGT
*bcd*1-EBS2	TGAACGCAAGTTTCTAATTTCGATTGCAACTCGATAGAGGAA AGTGTCT
*bcd*2-IBS	AAAAAAGCTTATAATTATCCTTATTTGCCGAAAATGTGCGCCC AGATAGGGTG
*bcd*2-EBS1d	CAGATTGTACAAATGTGGTGATAACAGATAAGTCGAAAATGA TAACTTACCTTTCTTTGT
*bcd*2-EBS2	TGAACGCAAGTTTCTAATTTCGGTTGCAAATCGATAGAGGAA AGTGTCT
*bcd*3-IBS	AAAAAAGCTTATAATTATCCTTAACTAACGCAGTAGTGCGCC CAGATAGGGTG
*bcd*3-EBS1d	CAGATTGTACAAATGTGGTGATAACAGATAAGTCGCAGTACA TAACTTACCTTTCTTTGT
*bcd*3-EBS2	TGAACGCAAGTTTCTAATTTCGATTTTAGTTCGATAGAGGAAA GTGTCT
etfA-IBS	AAAAAAGCTTATAATTATCCTTAGTTATCGATCAGGTGCGCCC AGATAGGGTG
etfA-EBS1d	CAGATTGTACAAATGTGGTGATAACAGATAAGTCGATCAGCT TAACTTACCTTTCTTTGT
etfA-EBS2	TGAACGCAAGTTTCTAATTTCGATTATAACTCGATAGAGGAA AGTGTCT
etfB-IBS	AAAAAAGCTTATAATTATCCTTATCTGCCCCTGCAGTGCGCCC AGATAGGGTG
etfB-EBS1d	CAGATTGTACAAATGTGGTGATAACAGATAAGTCCCTGCAAA TAACTTACCTTTCTTTGT
etfB-EBS2	TGAACGCAAGTTTCTAATTTCGGTTGCAGATCGATAGAGGAA AGTGTCT

Table 38. (continued)

Name	**Sequence** (5'→3')
htpG-IBS	AAAAAAGCTTATAATTATCCTTACACACCCAGTTTGTGCGCCC AGATAGGGTG
htpG-EBS1d	CAGATTGTACAAATGTGGTGATAACAGATAAGTCCAGTTTGT TAACTTACCTTTCTTTGT
htpG-EBS2	TGAACGCAAGTTTCTAATTTCGGTTGTGTGTCGATAGAGGAA AGTGTCT
repA-IBS	AAAAAAGCTTATAATTATCCTTAACTAACGTACAGGTGCGCC CAGATAGGGTG
repA-EBS1d	CAGATTGTACAAATGTGGTGATAACAGATAAGTCGTACAGAA TAACTTACCTTTCTTTGT
repA-EBS2	TGAACGCAAGTTTCTAATTTCGATTTTAGTTCGATAGAGGAAA GTGTCT
spoOJ-IBS	AAAAAAGCTTATAATTATCCTTACACTTCCATTCAGTGCGCCC AGATAGGGTG
spoOJ-EBS1d	CAGATTGTACAAATGTGGTGATAACAGATAAGTCCATTCATT TAACTTACCTTTCTTTGT
spoOJ-EBS2	TGAACGCAAGTTTCTAATTTCGGTTAAGTGTCGATAGAGGAA AGTGTCT
GbRs-IBS	AAAAAAGCTTATAATTATCCTTATATGGCCTATCAGTGCGCCC AGATAGGGTG
GbRs-EBS1d	CAGATTGTACAAATGTGGTGATAACAGATAAGTCCTATCATC TAACTTACCTTTCTTTGT
GbRs-EBS2	TGAACGCAAGTTTCTAATTTCGGTTCCATATCGATAGAGGAA AGTGTCT

Table 39. Gene-specific primers (GSP)

Name	**Sequence** (5'→3')
fcd-Forward	CCTATGGTTGCAGATTTTTC
fcd-Reverse	TGAGGATTTTAGCCATGATG
*bcd*1-Forward	TTTAGTTCTGTCAGTCATTG
*bcd*1-Reverse	ATACATCACTTTGTGCTTCA
*bcd*2-Forward	GCAAACCTTTGATAATTC
*bcd*2-Reverse	GTAAGACAGATGGTTAGAGA
*bcd*3-Forward	TCTCATCATTCTTTCAACTGGAT
*bcd*3-Reverse	TGGAAGAAGCCTTGACAA
etfA-Forward	CAGGAACTATTTCATATAAATCTC
etfA-Reverse	ATGGGAAAGTTAGTTATTAACGA

Table 39. (continued)

Name	**Sequence** (5'→3')
etfB-Forward	ATTTATCAGAAAGCTCTTTACCT
etfB-Reverse	TGGAAATATTGGTTTGCATC
htpG-Forward	CCTTAAATGCTGCCTTAATG
htpG-Reverse	TTTAGGTTTTGAAGCGGATG
*htpG*2-Forward	GAGGTTTTTCAAATCCAAAG
*htpG*2-Reverse	ATCGTTCACTCGTTGATACA
repA-Forward	TAATCCTCATCATCTTCCCAT
repA-Reverse	AGAAATTAGTAGCAATGCGTC
spoOJ-Forward	ACAAAGACTTGTAAACCTTACTG
spoOJ-Reverse	TATAATCAACGTTAAAGGTGGAG
GbRs-Forward	TAGTTGGAGCCAAAGTTGTTATC
GbRs-Reverse	ATCAGCAGGAAAAATTATTACTC
p0059-Forward	GGTCTTAGTTATTACAACTGCTG
p0059-Reverse	CCTGCCATTTGACTTACAC
adhE1-Forward	GAAGCTCAAAAAAAATTCTC
adhE1-Reverse	ATCTCACTTGTAAGAGGAAATC
adc-Forward	ATAACTTCAGCTCTAGGCAA
adc-Reverse	TAGCACGCCATTAACTTC
p0168-Forward	ACTTTAGGGACACTGCTC
p0168-Reverse	GGTATAGGTATGCCAGAT
0570-Forward	AAGATATTTGCCGTACTTCA
0570-Reverse	CAGCTTTCTCGGAATTTTTA
sigF operon-Forward	AAGCTTGTGGTTTCTATAATTG
sigF operon-Reverse	CTATTTGGTTAGTTTTTCCCTT
ftsAZ-Forward	ATCCAAGATTTGTATAGCATTAG
ftsAZ-Reverse	TTGTCTTCTTAAAAACGCAGGTA
atpB-Forward	ATGGAGCTAGGTGCAAAGAC
atpB-Reverse	GAACCCATGAAGAGGTACTG
atpH-Reverse	ACATCATCGCCAACTCTTAC

Table 40. Other primers

Name	**Sequence** (5'→3')
pMTL007check-Forward	GTCGAAGTGGGCAAGTTGAA
pMTL007check-Reverse	CAACAGGCTTACCCGTCTTACT
pMTL007CE2check-Forward	AGCCTGTGAAATAAGTAAGGAA
pMTL007CE2check-Reverse	TTAGGCATTCTTGTTTAGGGTA
Intron-specific primer (ISP)-Forward	AAACGAAAGCGATGCCGAGAA
Intron-specific primer (ISP)-Reverse	AAACTTACCCGCCATACCACA
Adaptor-*Eco*RV-primer	CATGCAAATGCTGAATGAG
Intron-Forward	CAGTCACAGTAATGTGAACA
Intron-Reverse	CTACTTGACTTAACACCCTA

Resume

XU, Zheng

May 1985	Born in Beijing, P. R. China
09/1991-06/1997	Study in a primary school in Beijing
09/1997-06/2003	Study in a middle school in Beijing
09/2003-06/2007	Study Biotechnology at Nanjing Forestry University, Jiangsu, P. R. China Bachelor's degree in Science
09/2007-06/2010	Study Developmental Biology at Beijing Normal University, Beijing, P. R. China Master's degree in Science
09/2010-08/2014	Pursue a Doctoral Study (Microbiology) at the Technical University of Munich, Freising Under the supervision of Prof. Dr. W. Liebl, in the group of Dr. A. Ehrenreich Financial support by China Scholarship Council (CSC)

Publications

1. **Zheng Xu**, Daniel Hönicke, Klaus Winzer, Nigel P. Minton, Wolfgang Liebl, Armin Ehrenreich. Influences of pSOL1 and pSOL1-borne genes for alcohol dehydrogenases on the metabolism of *Clostridium acetobutylicum* in continuous cultures. (In preparation)

2. **Zheng Xu**, Wolfgang Liebl, Armin Ehrenreich. The gene cluster encoding an EtfA/B-dependent dehydrogenase system affects the solvent formation of *Clostridium acetobutylicum* in continuous cultures. (In preparation)

Acknowledgement

I would like to express my sincere gratitude to my supervisor, Prof. Dr. Wolfgang Liebl, for giving me an opportunity to study in his department and for his instructive advice to the dissertation. I am deeply grateful to his help in the completion of this dissertation.

I also thank my group leader, Dr. Armin Ehrenreich, for providing great experimental instruction and happy smile. During my stay in Freising, I learnt a lot from him.

I acknowledge Prof. Dr. Erwin Grill and Prof. Dr. Rudi F. Vogel for reviewing this doctoral dissertation.

I would also like to thank China Scholarship Council (CSC) for the 4 years' financial support for the study.

Sincere thanks to my collegues, Huang C.-N., Li H., Liu Z., Benedikt, Björn, David, Desiree, Hedwig, Justyna, Lena, Markus, Michael, Milad and Trang. I thank Claudia, Helga and Johanna for the help for the GC and Daniel for operating microarray devices.

I thank you all from the bottom of my heart.